Habilitační práce

2005

RNDr. Dalibor Štys, CSc.

Struktura thylakoidních membrán – interakce proteinů na atomární úrovni: experiment a výpočet

RNDr. Dalibor Štys, CSc.

ústav fyzikální biologie, Jihočeská univerzita v Českých Budějovicích
Akademické a univerzitní centrum
Zámek 136
373 33 Nové Hrady

UNIVERZITNÍ KNIHOVNA
TECHNICKÉ UNIVERZITY V LIBERCI
3146088104

KES

TECHNICKÁ UNIVERZITA V LIBERCI
Univerzitní knihovna
Voroněžská 1329, Liberec 1
PSČ 461 17

U 490 M 68.1 [103 Ja. pů
Ob. lab.

Obsah:

5.2 Článek č. 2: Complex formation in plant thylakoid membranes. Competition studies on membrane protein interactions using synthetic peptide fragments Stys D., Stancek M., Cheng L. and Allen J.F., 1995, 44, 277-285.

5.3 Článek č. 3: Stacking and separation of photosystem I and photosystem II in plant thylakoid membranes: A physico-chemical view. Stys D., Physiol. Plant. 1995, 95, 651-657

5.4 Článek č. 4 Structure and magnesium binding of LHCII in its phosphorylated and unphosphorylated forms studied by multinuclear NMR. Stys D., Drakenberg T., Spangfort M.D., Forsen S. and Allen J.F., 1995, Photosysnthesis: from light to biosphere, Vol. I, 127-130.

5.5 Článek č. 5: Phosphorylation controls the three-dimensional structure of plant light harvesting complex II, Nilsson A., Stys D., Drakenberg T., Spangfort M.D., Forsen S. and Allen J.F., 1997, J. Biol. Chem. 1997, 272, 18350-18357.

5.6 Článek č. 6: The relation between changes in non-photochemical quenching, low temperature fluorescence emission, and membrane ultrastructure upon binding of polyionic compounds and fragments of light-harvesting complex 2, Stys D., Siffel P., Hunalova I. and Nebesarova J., 1999 Photosynthetica 37, 325-334

5.7 Článek č. 7: Studies of phospholipid binding to N-terminal domain of membrane protein light-harvesting complex II. Veverka V., Hrabal R., Durchan M. and Stys D., 2000, J. Mol. Struct., 523, 281-287.

5.8 Článek č. 8: The PsbH protein of photosystem 2. 2003, Komenda J., Stys D. and Lupinkova L., Photosynthetica, 41, 1-7.

5.9 Článek č. 9: Overexpression and purification of recombinant membrane protein PsbH in *Escherichia coli.* Halbhuber Z., Petrmichlova Z., Alexciev K., Thulin E. and Stys D., 2003, Prot. Expres. Purif., 32, 18-27.

5.10 Článek č. 10: Secondary structure estimation of recombinant psbH, encoding a photosynthetic membrane protein of cyanobacterium Synechocystis sp PCC 6803. Stys D., Schoefberger W., Halbhuber Z., Ristvejova J., Muller N. and Ettrich R., Photosynthetica 43, 421-424.

5.11 Článek č. 11: Molecular basis of a lipid-PsbH protein interaction: a structural and ab-initio computational study 2006, Stys D., Sovova Z., Halbhuber Z., Komenda J. and Ettrich R. (rukopis)

Poděkování:
Předem bych chtěl poděkovat všem, kteří mne na mé experimentální i teoretické dráze podporovali. Při mé kandidátské práci to byli můj školitel Petr Štrop, ale zejména kolegové, kteří mne odborně vedli v laboratoři NMR, Miloš Buděšínský a Jan Pelnář a ostatní kolegyně kolegové, kteří v té ve všech směrech převratné době okolo mne pracovali. Oponentem mé disertační práce byl, mimo jiné, Richard Hrabal, z čehož se vyvinulo dlouholeté osobní i profesionální přátelství. Jiří Soukup a jeho žena mi v roce 1991 pomohli s mou první profesionální zahraniční cestou a dnes, po letech, začínáme rozbíhat zajímavý odborný projekt.
Ve Švédsku to byli profesoři Sture Forsén a Torbjörn Drakenberg na Katedře fyzikální chemie 2 na univerzitě v Lundu, kteří mi dali důvěru po mé krátké stáži v roce 1992 a doporučili mne profesoru Johnu F. Allenovi z katedry biologie rostlinné buňky. Ten pak financoval mé vzdělávání ve fotosyntéze i všechny ne zcela standardní a kontroverzní experimenty, které jsem prováděl a jejichž výsledky jsem ho zásoboval. Přestože jsme se dodnes neshodli na interpretaci některých pozorování a dodnes máme velké koncepční neshody, dával mi po celou dobu prostor pro vlastní práci a umožnil mi mít vlastní studenty, což nebývá pro člověka v mé pozici zdaleka samozřejmé. A, v neposlední řadě, děkuji též všem kolegům z Univerzity v Lundu, kteří pomáhali mě i mé rodině při našem tříletém pobytu na tamní univerzitě. Jmenovitě tedy chci poděkovat Björnovi Walse, díky němuž jsme v počátcích bydleli tak, aby nás to neodradilo od dalšího snažení, a který nás uvedl do tamního studentského dění, a Evě Thulin, která byla dobrým klidným duchem celé katedry. Se všemi formálními otázkami nám významně pomohly Gunilla Håkansson a Carin Jarl-Sunesson, které navíc díky souběhu svých mateřství s mateřstvím mé manželky byly i velmi praktickými přítelkyněmi. Z doby lundského pobytu mi dodnes zbyla další osobní a profesionální přátelství s Cecilii Sundby a její rodinou a s Nilsem Ekelundem, s nímž dodnes pracujeme na společných projektech.
Další velký dík patří Dr. Ivanu Šetlíkovi, který stál za mým návratem a zaměstnáním v Třeboni, což nebylo vůbec triviální, a zaštítil svým jménem budování Laboratoře biomembrán v Českých Budějovicích. Díky němu jsme mohli využít prostředků z programu „Rozšíření vědy na vysokých školách". Pan doktor Šetlík zaštítil i náš další rozvoj v jižních Čechách a zasloužil se i o vznik výzkumného centra „Mechanismus, ekofyziologie a biotechnologie fotosyntézy", které pak dalo vzniknout ústavu fyzikální biologie Jihočeské univerzity v Nových Hradech. V dobrém i zlém jsem těmto projektům od svého návratu věnoval více času než vlastní vědecké práci.
Než budu děkovat svým kolegům, chtěl bych zmínit Alexandra Jegorova, s nímž se znám už dlouhá léta. Dá se i říci, že kdybych se více řídil jeho radami, možná bychom všichni byli i s naší vědou o něco dál. Byl to právě on, kdo mne v době, kdy jsem vážně pochyboval o smyslu našeho konání, přátelsky, ale rázně upozornil na sliby, které jsme na začátku učinili. Bez ohledu na to, že ostatní autoři podobných slibů na ně zapomněli okamžikem ukončení projektu, my jsme byli

schopni nabízené šance využít a objektivním vyjádřením toho je přes 30 kvalitních publikací v mezinárodních časopisech našeho ústavu v roce 2005.
Kolegové, kteří nám s projekty pomáhali, jsou z laboratoří v Třeboni, Ladislav Nedbal, který se mnou potom pokládal základy Akademického a univerzitního centra Nové Hrady, Jiří Masojídek a Jiří Kopecký, kteří vedou Laboratoř biotechnologie a na nichž spočívá největší tíha budování biotechnologického inkubátoru „Centrum biologických technologií" v Nových Hradech. Dále Josef Komenda, Ondřej Prášil, Michal Koblížek, Martin Tichý a celá řada studentů a dalších spolupracovníků.
Z Českých Budějovic musím opět připomenout tragicky zesnulého Pavla Šiffela, který, jako výjimečně tvrdohlavý experimentální fyzik, dovedl některé biologické problémy na hranici, která by mohla vést i ke skutečnému pochopení jejich podstaty. Věta „tomu já nerozumím" znamenala ve skutečnosti, „tak to teda opublikujte, ale já si ve skutečnosti nemyslím, že je to hotové". Bohužel naladění světové vědy takovým kolegům nepřeje a já si nejsem jist do jaké míry my se s jeho odkazem vyrovnáváme. Největší pomoc a oporu jsem po celou dobu měl v osobě Františka Váchy, o němž jsem vždy věděl, že mi, byť se stejně zaťatými zuby jako byly ty moje, bude pomáhat v řešení administrativních problémů, které měly často jen velmi vágní oporu v objektivní realitě. Z dalších kolegů musím poděkovat Janě Nebesářové, Ivaně Kuté Smatanové, která má největší podíl na vysoké kvalitě a mezinárodním uznání našeho vzdělávání na Nových Hradech, Michalovi Kutému a dále všem studentům a technickým pracovníkům kteří s námi spolupracovali.
Na Nových Hradech se částečně vytvořil tým zcela nový, částečně se na naší práci podíleli kolegové zmínění v předchozích odstavcích. Velkým organizačním dílem se na našich vzdělávacích aktivitách podílí Karel Roháček. Rüdiger Ettrich, který přišel později, je klíčovou osobou v rozvoji výpočetní chemie a především díky němu se naše centrum získalo opravdu mezinárodní význam a uznání. Martinu Žáčkovi, Jiřímu Plchovi, Petru Kohoutovi a Vitězslavu Březinovi patří zvláštní dík za podíl na vybudování technického zázemí centra.
Z blízkého zahraničí s námi po většinu cesty šel Norbert Müller z Univerzity v Linci, díky němuž už 8 let běží přeshraniční studijní obor Biofyzika. Přestože neustále čelíme více-méně politickému protitlaku na obou stranách hranice, položili jsme spolu základ něčemu, co se dále různými směry rozvíjí a má snad budoucnost.
Pokud jde o vědeckou stránku věci, můj největší dík patří určitě mým studentům, Martinu Stančekovi z Bratislavy, který byl mým studentem v Lundu, Julii Benešové a Kristině Ničkové, které pracovaly na projektech s biotechnologickým zaměřením, ale zejména Zbyňkovi Halbhuberovi a Zdeňce Petrmichlové, kteří mají velký podíl na výsledcích, uvedených v této práci. V její poslední fázi se na ní podíleli i Michael Green z univerzity v Princetonu a Žofie Sovová.
Samozřejmě se omlouvám všem, kteří nebyli explicitně jmenováni.

Za „politickou“ záštitu děkuji zejména Michalovi Markovi a bývalému rektoru Jihočeské univerzity Františku Střelečkovi, kteří nám poskytli nebývalý prostor pro náš rozvoj.

Poděkování mým přátelům a rodině bych chtěl zahájit u Jiřího Bryndy, který mou odbornou práci už po 28 (!!!) let, tedy od doby střední průmyslové školy chemické, sleduje a trefně a kriticky ji glosuje. Je velká otázka, zda je tento člověk dnes více mým nejbližším přítelem nebo profesionálním kolegou, nejspíše ale nějakou kombinací obojího a k tomu ještě bratra, kterého si člověk nevybírá ale je mu souzen.

Na mou profesionální dráhu mě nasměrovali moji rodiče, kteří mne v ní finančně podporovali a navíc mi dali šanci v té době zcela výjimečného praktického jazykového výcviku, z něhož dodnes těžím. Můj bratr se mnou sdílí podobný způsob humoru i jistou skepsi k svému okolí i sobě samým.

Nejdůležitější část mé profesionální kariéry a s ní spojeného osobního neklidu a neustálého stěhování se mnou sdílí moje manželka Naďa. Vzala si mne i přes varování svých rodičů, že ji se mnou čeká zajímavý, pestrý, ale náročný život. Nezbývá mi než doufat, že ji toto naše společné směřování alespoň občas uspokojuje. Každopádně bez ní by nic z toho, co se popisuje v této práci, nikdy nevzniklo. Zvláštní dík jí patří za čas a úsilí, které věnovala výchově našich dětí Dalibora Kašpara a Kryštofa-Mikuláše, kterým se také musím omluvit za časté neplnění role otce.

1. Objekt studia – thylakoidní membrány a jejich klíčové proteiny

Thylakoidní membrány jsou tím místem fotosyntetických organismů, kde je energie fotonů zachycených fotosyntetickými pigmenty přeměněna na redukovanou formu nikotinamidadenindinukleotidfosfátu (NADPH) a na gradient elektrochemického potenciálu protonů přes membránu. Fotosyntetické pigmenty jsou vázány na proteinové komplexy fotosystému I a fotosystému II. Další malé organické molekuly, jako chinony a molekuly hemu, se účastní transportu elektronů (viz obr. 1.1).

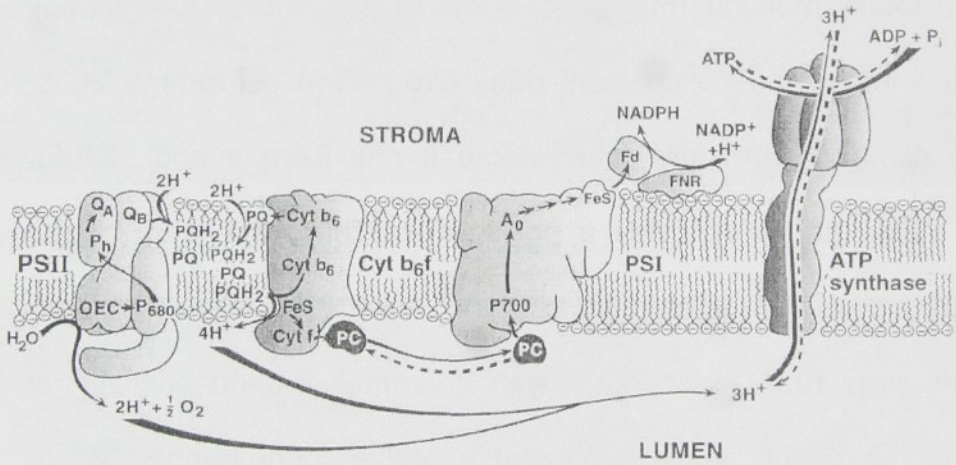

Obr. 1.1 Schematický diagram přenosu elektronů v kyslíkové fotosyntéze. Energie zachycená anténními systémy je přenesena do reakčního centra fotosystému 2. Tam dojde k rozdělení náboje. Vzniklý elektrochemický potenciál je tak vysoký, že postačuje k oxidaci kyslíku z vody na molekulární kyslík. Zároveň jsou uvolňovány protony na lumenální straně membrány. Uvolněné elektrony jsou transportovány po spádu elektrochemického gradientu až na molekulu chinonu, která se redukuje na chinol za přijetí dvou protonů ze stromální strany membrány. Protony jsou předány membránově vázaným cytochromům, které elektron přenesou na lumenální stranu membrány, kde jsou předány plastochinonu za dalšího uvolnění protonů. Plastochinon je pak oxidován fotosystémem 1, který opět zužitkovává energii zachycenou svými anténními systémy. Konečným příjemcem elektronu je molekula NADP+, která reaguje s elektronem a protonem a vytváří redukovanou

formu NADPH. Vzniklý gradient protonů je pak využit k produkci ATP. (Upraveno podle Ort a Yocum 1996)

Vzniklý elektrochemický potenciál protonů se využívá k syntéze energetického přenašeče adenosintrifosfátu –(ATP) z adenosindifosfátu (ADP) za katalýzy enzymem ATP synthetázou.

Funkce thylakoidní membrány byla studována celou řadou přímých i nepřímých metod po dobu posledních nejméně 40 let (Ort a Yocum 1996). Podstata funkce na úrovni molekul a atomů je však mnohem méně známá.

Mezitím se objevily první proteinové struktury, na nichž bylo možno studovat detaily molekulárních mechanismů jejich funkce (přehledený článek o fotosystému I z poslední doby Grotjohann a Fromme 2005, poslední článek o struktuře fotosystému II pak Kern a spol. 2005), metody studia se zpřesňovaly a posléze umožnily i navržení metod molekulární dynamiky (přehledně o vývoji molekulové dynamiky např. van Gunsteren 1998), které za jistých podmínek mohou přiblížit i ty proteinové struktury, jež jsou experimentálně nepřístupné. V této kapitole se snažím krátce přiblížit objekt studia s důrazem na experimentálně studované a modelované objekty.

1.1 Principy formování architektury thylakoidních membrán

Architekturou thylakoidních membrán rozumíme jejich prostorové uspořádání na dlouhé vzdálenosti. Tento pojem není užíván pro jiné biologické membrány, protože v nich nebyly nikdy pozorovány podobné komplexní struktury (obr. 1.2), kdy část membránových lamel je velmi

těsně navzájem naskládána (tzv. grana) a další část je volná ve formě standardních lipidových dvojvrstev (tzv. lumen).

Obr. 1.2

(a)

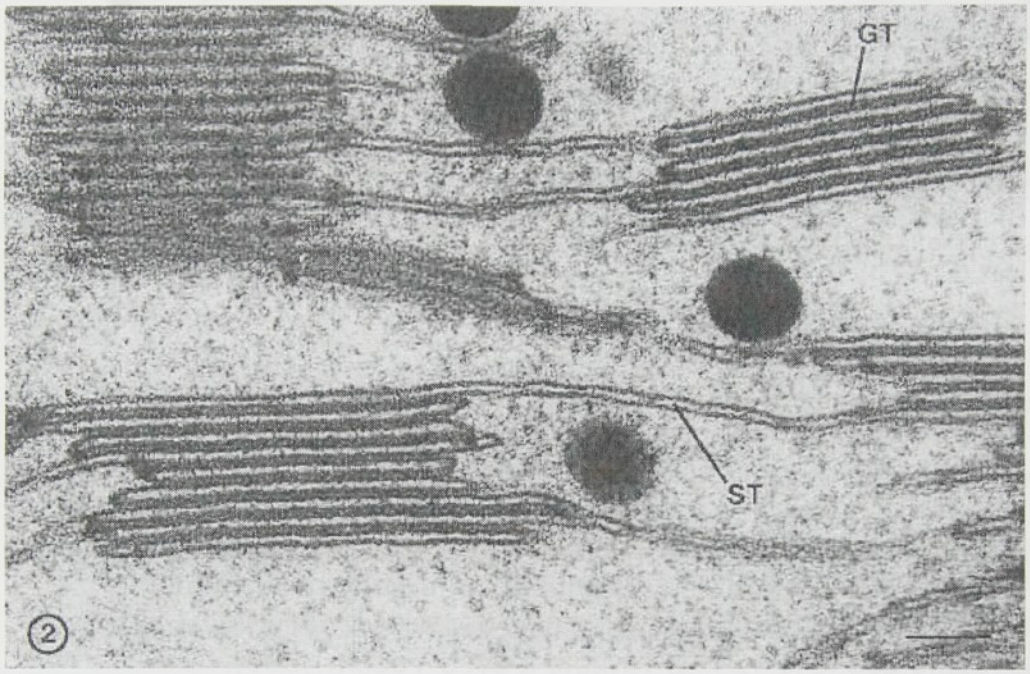

(b)

(c)

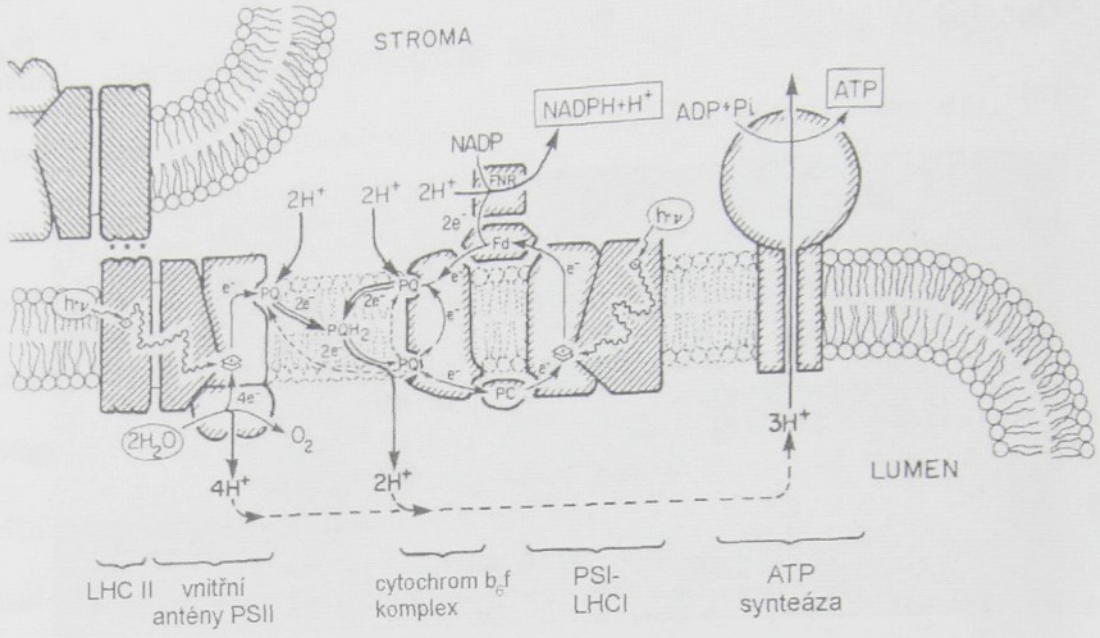

Obr. 1.2 (a) ultratenký řez chloroplastem tabáku zobrazený metodou elektronové mikroskopie. Dvě obalové membrány (envelope membrane – EM) ohraničují stroma chloroplastu (S). V thylakoidní membráně lze rozlišit naskládaná grana (GT) a volné stromální lamely (ST). Velikost rozlišovacího úseku je 1μm. (Převzato z Ort a Yocum 1996).
(b) elektronový mikrogram thylakoidních membrán získaný metodou mrazového lámání z jednotlivého grana thylakoidů hrachu. Struktura membránových lamel se zdá naznačovat, že nahloučená grana se organizují do spirál propojených stromálními lamelami. (Upraveno podle Ort a Yocum 1996)
(c) Představa o funkční organizaci thylakoidních membrán. (Upraveno podle Ort a Yocum 1996) Zobrazeny jsou pozice hlavních enzymů spojených elektronovým transportem, vznikem protonového gradientu a jeho využitím pro fixaci energie. Jedná se o světlosběrný komplex II (LHCII), vnitřní antény a reakční centrum fotosystému II (PSII), komplex cytochromu b_6f, fotosystém I (PSI) a ATP synthetáza. Experimentálními metodami bylo zjištěno, že proteinové i lipidové složení jednotlivých oblastí je různé a že tato laterální heterogenita má funkční význam (historický přehled např. Staehelin 2003).

Architektura thylakoidních membrán se dá studovat celou řadou metod (review například Albertsson 2001). Nejpřímější pozorování je možné metodou *elektronové mikroskopie*. Z těchto experimentů pochází terminologie jako nahloučená grana (grana stacks), stromální lamela a podobně. Využitím metody mrazového lámání (freeze etching) bylo

možno pozorovat i laterální strukturu thylakoidních membrán a bylo tak poprvé zjištěno, že biologické membrány nejsou vždy homogenní „fluidní mozaikou", ale že se mohou skládat z oddělených a dobře definovaných lipid-proteinových oblastí. Podobnou informaci, navíc se zahrnutím dílčího funkčního měření, dává mikroskopie atomárních sil (Kaftan a spol., 2002).

Bližší přiblížení ke složení a funkci thylakoidních membrán přinesly separační metody. Ty lze provádět s využitím detergentů, kdy se využívá faktu, že stromální lamely jsou pro detergent přístupnější a tudíž se v něm rychleji rozpouští (přehled z poslední doby například Bricker a spol. 2001) než nahloučená grana. Mnohem reprezentativnější je však metoda mechanické fragmentace, v podstatě lámání, pomocí sonikace a následné separace mezi dvě vodné fáze. Při tom nedochází k rozpouštění částí membrány a výsledné částice jsou pro původní části membrány reprezentativní (Albertsson a spol. 1994). Jakékoliv kvantitativní vyjádření výsledků bývá zatíženo velkou experimentální chybou, i když výsledky Albertssonovy skupiny (Albertsson 2001) se zdají být vnitřně konzistentní a ukazují, že v granách se nachází jak fotosystém II, tak fotosystém I a že v nich probíhá lineární elektronový transport. Ve stromálních lamelách je pak fotosystém II přinejmenším nefunkční a probíhá v nich cyklický elektronový transport okolo fotosystému I.

Zdá se, že všechna měření podporují hypotézu, že vznik oddělených oblastí v membránách je analogií fázového rozdělení ve směsích o mnoha složkách (Stys 1995 – článek 3) z poslední doby například

Engelman (2005). Biochemická měření v separovaných oblastech je tedy nutno posuzovat s výhradou, že v nehomogenní směsi jiného složení dojde posléze k jiné separaci. Pokud jde ovšem o vlastní složení thylakoidních membrán a jejich domén, zejména metoda separace mezi dvě vodné fáze je jistě reprezentativní. Thylakoidní membrány jsou tak nejzajímavějším objektem pro studium principů formování biologických membrán jako takových.

1.2 Interakce formující thylakoidní membrány

Dominantním proteinem thylakoidních membrán rostlin, ve skutečnosti evolučně nejúspěšnějším membránovým proteinem vůbec, je světlosběrný komplex II (LHCII). Proto se také většina modelových úvah o struktuře a organizaci thylakoidních membrán opírá o dílčí experimenty s tímto proteinem. Struktura LHCII je poměrně dobře známa (Liu a spol., 2004, Kühlbrandt a Wang 1991) mimo nejzajímavější oblast, která obsahuje specifické vazebné místo pro lipidy (Nussberger a spol. 1993, Veverka a spol. 2000 – článek 7) a místo, kde dochází k proteinové fosforylaci (Allen 1992). Struktura této klíčové oblasti byla studována metodou NMR spektroskopie a dalšími strukturními metodami (Veverka a spol. 2000 – článek 7, Nilsson a spol., 1997 – článek 5), které vedly k identifikaci některých specifických funkčních míst. Neexistuje však žádná experimentální metoda, která by v plné míře popsala trojrozměrnou strukturu této interagující oblasti. To je pro poznání thylakoidní membrány velmi nepříznivé, protože se stále více ukazuje, že vzájemné přeměny organizovaných struktur LHCII

různých řádů jsou pro strukturu thylakoidní membrány klíčové (Kühlbrandt a Standfuss 2004, Páli a spol. 2003 a články v nich citované).

Ve věci funkčního významu regulace založené na fosforylaci N-koncové domény LHCII existují dvě filozoficky odlišné koncepce. Koncepce Barbera (1982) i Allena (1992) sdílí představu, že existují dvě více-méně stabilní domény – chemicky dvě oblasti různého lipidového a proteinového složení – mezi nimiž regulované molekuly migrují na základě afinity k těmto doménám. Jelikož fosforylace LHCII je považována za masivní jev (Allen, 1992b), vedl by tento mechanismus k rozsáhlým změnám v architektuře thylakoidní membrány. Ty však nebyly experimentálně pozorovány (Stefánsson a spol 1995). Druhou koncepcí, která se zdá být konzistentnější s experimentem, je koncepce Garabovy skupiny. Ta za rozhodující pro architekturu thylakoidní membrány považuje lipid proteinové interakce (Páli a spol. 2003). Tím se problém migrace komplexů a změn architektury do značné míry vytrácí, protože pro vlastnosti proteinu a jeho okolí, a tím i pro jeho umístění v jednotlivé fázi při využití různých separačních metod, jsou zodpovědny společně fyzikálně-chemické vlastnosti proteinů i lipidů. Fakt, že nedochází k makroskopicky pozorovatelným změnám pod vlivem fosforylace, může být nejspíše způsoben tím, že rozsah fosforylace LHCII je za skutečných podmínek, při nichž je experiment prováděn, fakticky mnohem menší než se předpokládá, což poprvé naznačily výsledky Štyse a spolupracovníků (Štys a spol., 1995 článek 2), dále pak i Aro a spolupracovníků (Rintamaki a spol. 1997). Zcela

opomenut v této souvislosti zůstal poznatek, že vazebná konstanta pro hořečnaté ionty na fosfátovou skupinu je přibližně o řád vyšší, než vazebná konstanta v běžných fosfátových skupinách vázaných na lipidové nebo cukerné zbytky (Štys a spol 1995b - článek č. 4). Tím se zcela neguje původní hypotéza o negativně nabité fosfátové skupině jako zdroji odpuzování mezi membránovými lamelami. Právě naopak, její zavedení může vést i ke zvýšení pozitivního náboje na povrchu membrány na úroveň vyšší než je rovnovážná úroveň předpokládaná na základě coulombických interakcí.

Vedle LHCII se zdá být hlavním proteinem, jehož chování je rozhodující pro formování struktury thylakoidních membrán, protein PsbH (Komenda a spol. 2003 – článek 9). Tento protein se vyskytuje v thylakoidních membránách jak vyšších rostlin, tak všech nižších rostlin i sinic. Je, na rozdíl od většiny ostatních proteinů, přítomen i v etiolovaných listech rostlin rostoucích ve tmě, kde není chlorofyl a lipidy se místo v lipidových dvojvrstvách vyskytují ve formě kapalných krystalů v kubické fázi. V posledních letech (Komenda 2005, Komenda a spol. 2005, Bumba a spol. 2005) byla ověřena klíčová role PsbH ve formování jádra fotosystému II (photosystem II core), který je tvořen reakčním centrem a systémem vnitřních antén. V nepřítomnosti PsbH se jádro fotosystému II buď netvoří vůbec a organismus není schopen fotosyntézy (rostliny), nebo je stabilita jádra snížena a organismus je velmi citlivý na světlo (sinice). Protein PsbH navíc zřejmě hraje roli i v obměně proteinu D1, jehož dynamická výměna v proteinovém komplexu probíhá nejméně o řád rychleji než formování komplexů *de*

novo (Komenda a spol. 2005). Přitom protein D1 se nachází uprostřed jádra a je obklopen dalšími proteiny. Při jeho obměně tedy musí dojít buď k otevření jádra, nebo k jeho výměně ze strany kolmo na membránu a zároveň musí dojít k rychlému navázání kofaktorů. Také tento proces je v nepřítomnosti PsbH velmi omezený (Komenda a spol., 2005). Protein PsbH byl pozorován též v množství vyšším než stechiometrickém vzhledem k jádru fotosystému II za podmínek obecného stresu, při němž dochází k biosyntéze stresových membránových proteinů jako jsou malé anténní proteiny apod. (Komenda a spol. zasláno). Tato data naznačují, že kromě specifické funkce v jádře fotosystému II (Komenda a spol., 2003) by protein PsbH mohl i méně specifickým způsobem asistovat při rychlém sbalování membránových proteinů.

Abychom takovou funkci mohli posoudit, potřebujeme vědět, jak protein PsbH interaguje s membránou ve své volné formě. Tím ovšem úkol nabývá na vysoké teoretické zajímavosti, protože jakkoliv se o lipid-proteinových interakcích široce diskutuje (viz. kapitola 2.2), ab-initio výpočet formováni struktury – sbalování proteinu s jedním helixem a jeho interakce s lipidy se zahrnutím všech atomů - doposud nebyl proveden. Jediný výpočet tohoto typu (Venturoli a spol. 2005) využíval potenciálové funkce, která explicitně nezahrnuje všechny atomy a ani proteinový model nebyl reálný. První výsledky simulace interakce proteinu PsbH s lipidovou dvojvrstvou, v nichž je zároveň výsledek porovnán s experimentem, jsou popsány v článku 10, který je součástí tohoto spisu.

1.3 Fyzikální principy interakcí v biologických membránách

Fyzikální základy interakcí specifických pro thylakoidní membrány rostlin jsou popsány v článku Stys 1995 (článek 3). Autorův příspěvek k nim je pak popsán v komentáři k přiloženým článkům v části 5 této práce. Pokrok, který od doby napsání článku nastal, se netýká žádných informací, jež by byly specifické právě pro tyto membrány, spíše naopak, zdá se, že některé experimenty jsou opakovány, aniž by se četly a byly citovány experimenty autorů předchozích prací, obsahující téměř identické výsledky (např. Kim a spol. 2005 versus Stys a spol 1999 a dokonce Hager 1966). V oblasti formování lipid-proteinových domén jsou stále klíčové hypotézy o hydrofobním přizpůsobování (hydrophobic matching) a coulombickém charakteru repulzí mezi mimomembránovými částmi lipidových molekul a jejich odstínění ionty při tvorbě domén (Sackmann 1990, Jönsson a Wennerström 1983, v poslední době například Tanaka a Sackmann 2005). Tento stav je na jedné straně způsoben nedostatkem nových experimentálních informací a na druhé straně výpočetní náročností všech modelů, které zahrnují více než pouze bodové náboje a membránu simulovanou jako planární těleso. Detailnější modely začínají být dostupné přibližně od roku 2000 (Lindahl a Edholm 2000 a, b), do roku 2003 probíhala optimalizace výpočetních systémů a modelů a teprve od této doby jsou všeobecně využitelné. Přesto některé skupiny (Venturoli a spol. 2005) stále pracují na zjednodušování modelů, které se zdá být nezbytné pro výpočty, jež se budou týkat tvorby lipid-proteinových domén. Celkově shrnuto,,

domníváme se, že pro organizaci membrán jsou klíčové interakce mezi proteinovými mimomembránovými oblastmi a lipidovými skupinami, které se nacházejí na přechodu mezi hydrofobní a vodnou fází. Tyto oblasti jsou v obou případech polární, někdy nesou i elektrický náboj. Podle charakteru se tak mohou přitahovat nebo odpuzovat. Přídavek iontů pak vede k odstínění tohoto odpuzování a promíšení lipidů (v rovině membrány) nebo, u rostlinných thylakoidních membrán, též k přitahování mezi lipidovými vrstvami.

Podstatný pokrok nastal při posuzování specifických lipid-proteinových interakcí, kdy se na proteinu nachází natolik silné vazební místo, že v něm lipid zůstane vázán i po extrakci komplexu detergentem. Různých struktur vysokého rozlišení, které umožňují detailní posouzení takových interakcí, je známo méně něž 20 (Marsh and Páli 2004, nové struktury jsou pak v databázi proteinových struktur). Diverzita lipidových molekul, které jsou ve strukturách pozorovatelné, ve spojení s možností tvorby artefaktů způsobenou různým vlivem entropické složky při interakcích v rovině membrány a v prostoru, dává jen málo prostoru pro jakákoliv zobecnění. Je možné ale porovnávat výsledky získané pomocí výpočtů s výsledky strukturních studií a následně zlepšovat simulační prostředí (viz kap. 3).

2. Struktury proteinů a metody jejich stanovování

2.1 Principy organizace proteinových struktur

Jako *primární struktura proteinů* je označována sekvence aminokyselinových zbytků v proteinové makromolekule.

Aminokyselinové zbytky jsou navzájem vázány peptidovou vazbou (viz obr. 2.1) a liší se mezi sebou postranními řetězci.

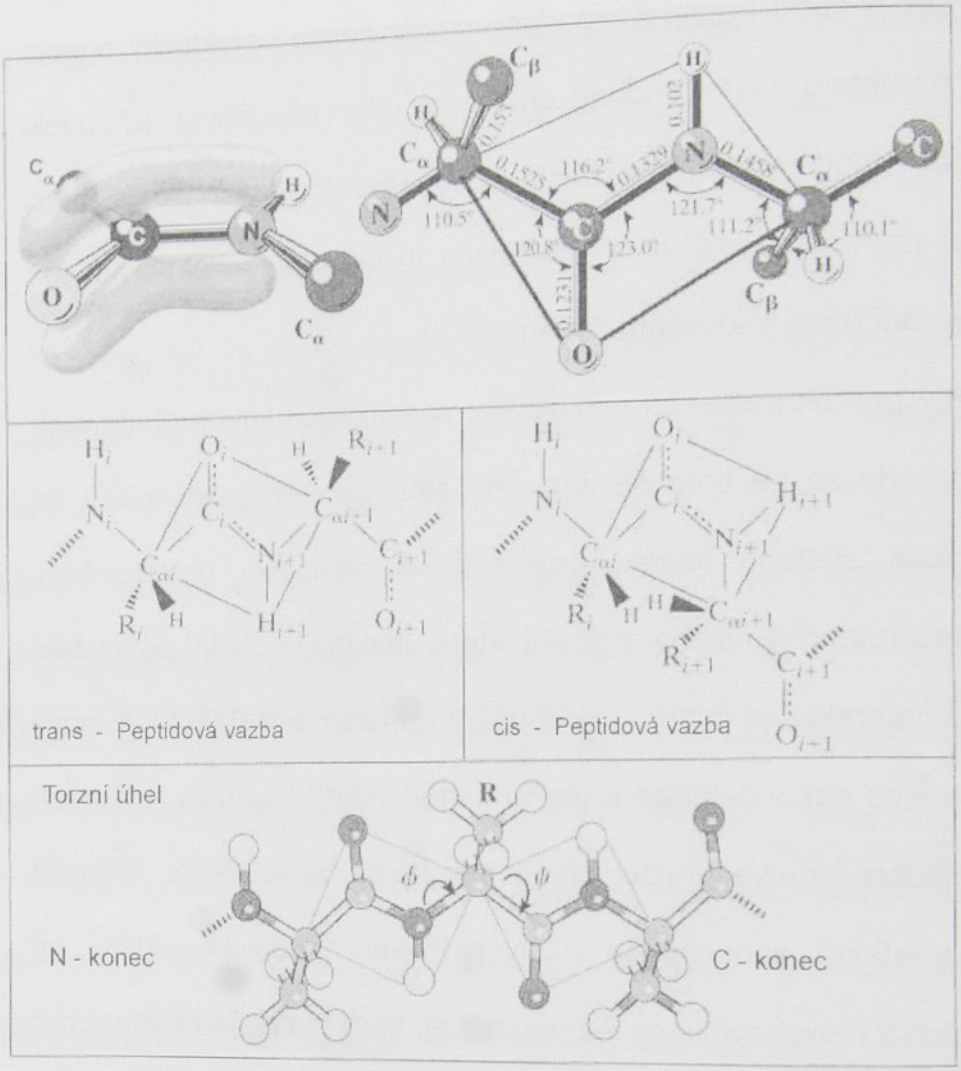

Obr. 2.1 peptidová vazba chemicky spojuje dva aminokyselinové zbytky podél peptidového řetězce a vazba C-N je amidovou vazbou (upraveno podle van der Holde a spol. 2006). Vazba vykazuje částečný charakter dvojné vazby, kdy π elektrony pocházejí z volných elektronových párů kyslíku a dusíku a jsou rozptýleny mezi kyslík, dusík i uhlík karbonylu hlavního řetězce. Tato vazba proto volně nerotuje a zůstává planární – rovinná. Vazba je přednostně v konfiguraci trans, ve výjimečných případech může zaujímat též konfiguraci cis. Pro definici konformace v rámci jednoho aminokyselinového zbytku tak postačují dva torzní úhly, ϕ a ψ. Ty představují rotaci okolo vazby N-C_α respektive C_α-karbonylový uhlík. Tato situace jednak výrazně snižuje počet možných konformací (níže Levinthalův paradox) a jednak umožňuje reprezentovat konformaci hlavního řetězce peptidu pouze pomocí poloh uhlíků C_α. Tak vznikají nejznámější přehledná zobrazení peptidových konformací.

Podle vlastností postranních řetězců se aminokyseliny dělí na nepolární, aromatické, nenabité, záporně nabité a kladně nabité (viz obr. 2.2).

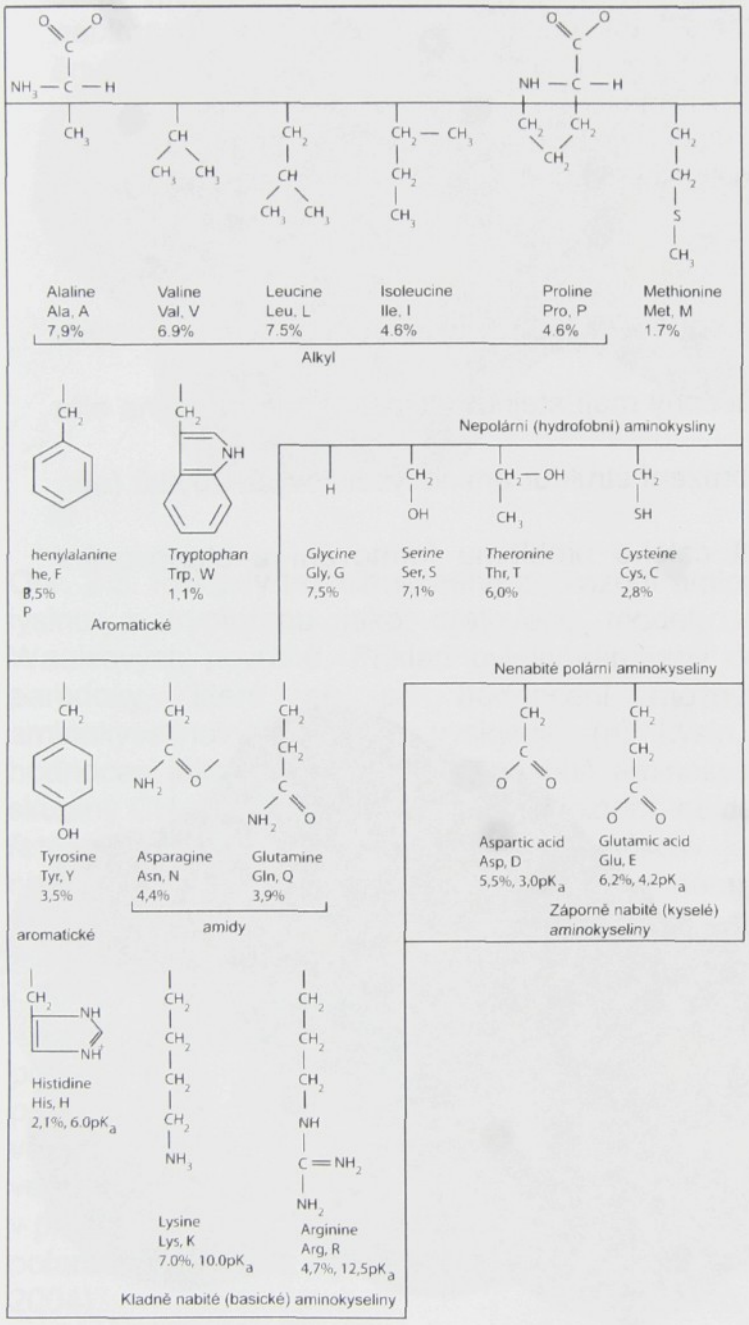

Obr. 2.2 Dvacet běžných aminokyselin. Ve všech živých organismech se vyskytuje těchto dvacet aminokyselin a to v chirální konformaci L na uhlíku C_α. Podle postranních řetězců se aminokyseliny dělí na nepolární – hydrofobní, nenabité polární a nabité polární aminokyseliny. Podskupinu v rámci jak nepolárních, nenabitých i nabitých polárních, aminokyselin tvoří aminokyseliny s aromatickými postranními řetězci.

Polární nabité postranní řetězce vstupují zejména do interakcí typu solných můstků – iontových interakcí. V kontextu tohoto článku je třeba upozornit na tvorbu solných můstků mezi fosfátovými skupinami lipidů a nabitými aminokyselinami, která je zřejmě zodpovědná za velmi silné vazby, jež jsme nalezli v článcích 7 a 11 diskutovaných v této práci. Ostatní polární skupiny na postranních řetězcích vstupují typicky do interakcí typu vodíkových vazeb, které, podle našich poznatků, vytvářejí většinu interakcí mezi proteinem a membránou. Mnohem hůře postižitelné jsou hydrofobní interakce pro jejich entropický charakter, který de-facto není současnými výpočetními metodami správně reprezentován (kap. 3). Aromatické aminokyselinové zbytky se pak, díky své polarizabilitě, často vyskytují na površích membrán. Také postižení tohoto typu interakcí pomocí výpočetních metod si vyžádá další vývoj.

Aminokyselin, z nichž jsou vystavěny všechny proteiny v živých organismech, je 20 a všechny mají stejnou chirální konformaci na alfa uhlíku. Trojrozměrné zobrazení struktur aminokyselinových zbytků (obr. 2.3) naznačuje složitost celého problému formování a stanovování struktur proteinů.

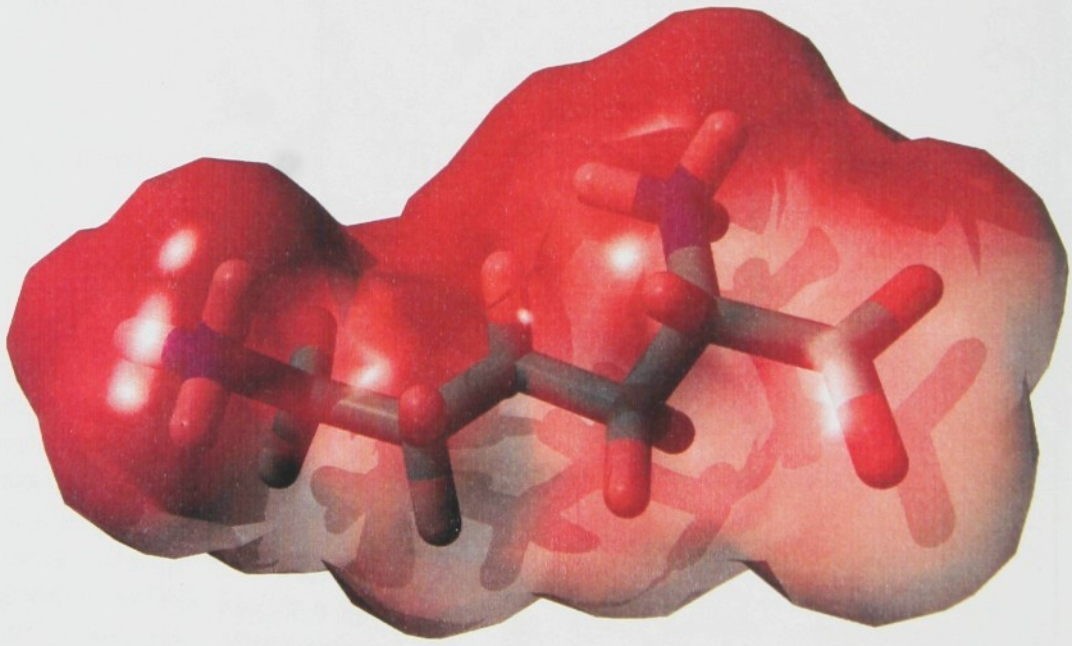

(a)

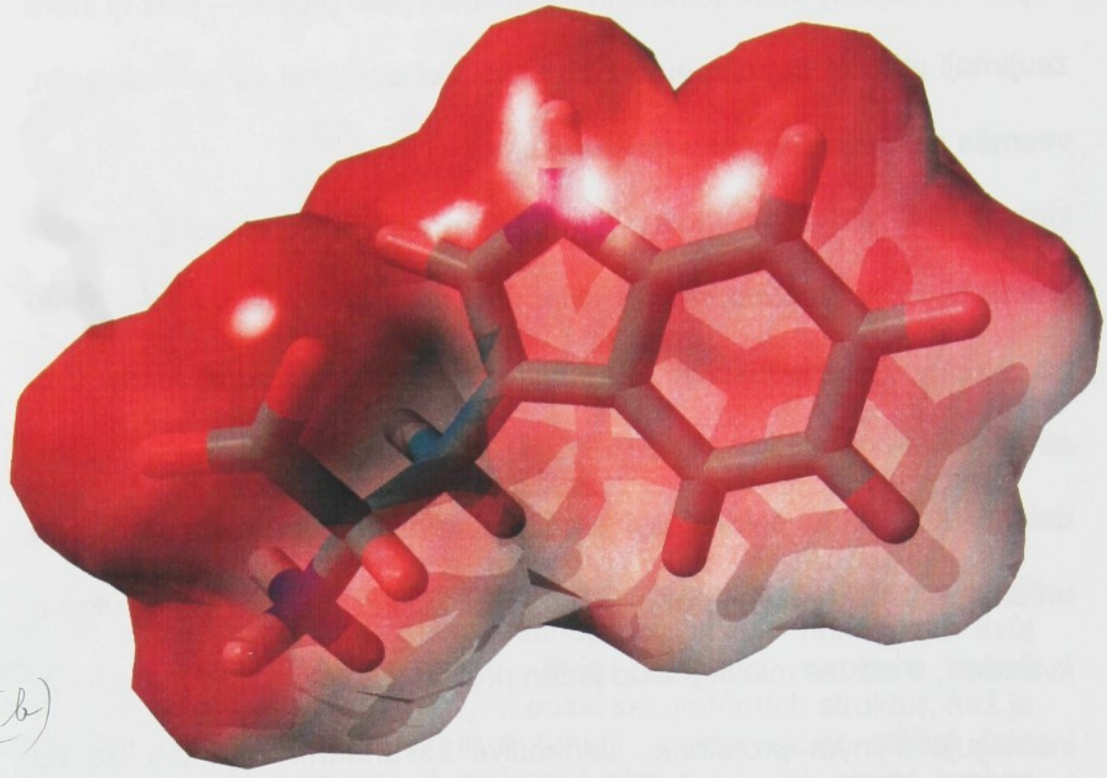

Obr. 2.3. Příklady trojrozměrného zobrazení aminokyselinových zbytků lysinu a tryptofanu jako drátového modelu a modelu van der Waalsových povrchů. Příklad byl vybrán, aby demonstroval některé paradoxy, které se při hodnocení možných interakcí mezi aminokyselinovými zbytky vyskytují. (a) Lysin, který bývá běžně hodnocen jako typická pozitivně nabitá aminokyselina, obsahuje čtyři skupiny CH_2 a vytváří tak, spolu s argininem, nejdelší lineární nepolární řetězce mezi všemi aminokyselinami. Ačkoliv je tedy zdánlivě lysin nutno hledat na povrchu proteinu exponovaném vodě, pokud má být struktura stabilní, musí pozici lysinu vždy zároveň doprovázet hydrofobní interakce jeho nepolárního řetězce. Voda v okolí nabité skupiny způsobuje stínění náboje (hydrataci) a proto nejsou solné můstky v proteinech tak silné jako by byly ve vakuu. V membránových proteinech uvnitř hydrofobní části membrány, v nepřítomnosti vody, se pak mohou vytvářet solné můstky podstatně silnější než v přítomnosti vody. (b) Tryptofan, typická nepolární aromatická aminokyselina, může velmi snadno vystupovat jako polární nenabitá aminokyselina, zejména v přechodné oblasti na povrchu membrány, kde dochází k částečné polarizaci. Obrázek byl vytvořen v programu Yasara ((Krieger a spol., 2004)

Na příkladu dipeptidu složeného ze dvou velmi jednoduchých aminokyselin (obr.2.1) lze demonstrovat rozsah vzájemně odlišných konformací, v nichž se i tento velmi jednoduchý systém může nacházet.

Nejmenší objekty které je možno kvalifikovat jako protein – totiž ty které zaujímají stabilní trojrozměrnou strukturu - však mívají 40 aminokyselin, vesměs jsou však proteiny mnohem větší.

Úrovně, na nichž se studují struktury proteinů v prostoru, se dělí hierarchicky na *sekundární strukturu*, kterou charakterizují dvojice úhlů na po sobě následujících alfa uhlících (obr. 2.1), *supersekundární strukturu* neboli anglicky fold (obr 2.4), která určuje vzájemnou polohu delších segmentů sekundární struktury, *terciární strukturu* v níž jsou určeny pozice všech postranních řetězců (obr. 2.5) a strukturu *kvartérní*, o níž lze mluvit pokud jeden protein jako chemické individuum interaguje s jiným proteinem. Jednotlivé sekundární struktury lze od sebe rozeznat jejich zařazením do takzvaného Ramachandranova diagramu (obr. 2.6), který je také první kontrolou správnosti proteinové struktury, ať už ji stanovujeme experimentálně nebo výpočtem.

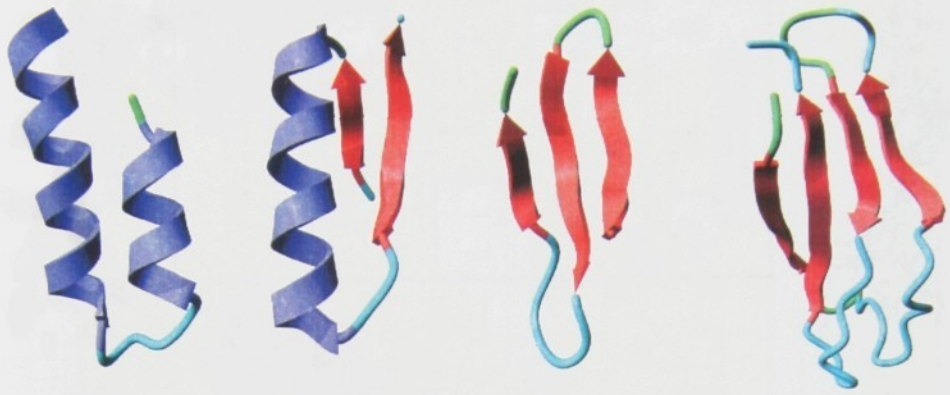

Obr. 2.4 Supersekundární struktura proteinu neboli fold. Výše zmíněný fakt, že strukturu proteinů dobře definují polohy alfa uhlíků, má svůj odraz i ve strukturách proteinů. Bylo nalezeno mnohem méně rozdílných vzájemných prostorových pozic sekundárních struktur, než je rozdílných proteinových struktur a funkcí. Jinými slovy, stejný fold v žádném případě neznamená stejnou funkci a naopak stejná funkce může být nalezena v různých foldech. Jakou roli mají foldy při sbalování proteinů a co je vlastně vede k jejich vzniku, když identita aminokyselinových sekvencí je často blízká náhodnosti a naopak záměna jedné klíčové aminokyseliny vede k úplně jinému foldu, je jednou z klíčových otázek modelování proteinových struktur.
Typické foldy byly vybrány takto (v pořadí zprava doleva) alfa-alfa: Fructose-bisphosphate aldolasa A (1ALD), beta-alfa-beta: Nitrit reduktáza (1ET7), beta hairpin: Hlavní cold shock protein z Bacillus subtilis (1CSP), greek key: SAM doména z lidského EphB2 receptoru 1B4F. Reprezentace struktur byly vytvořeny v programu Yasara (Krieger a spol., 2004)

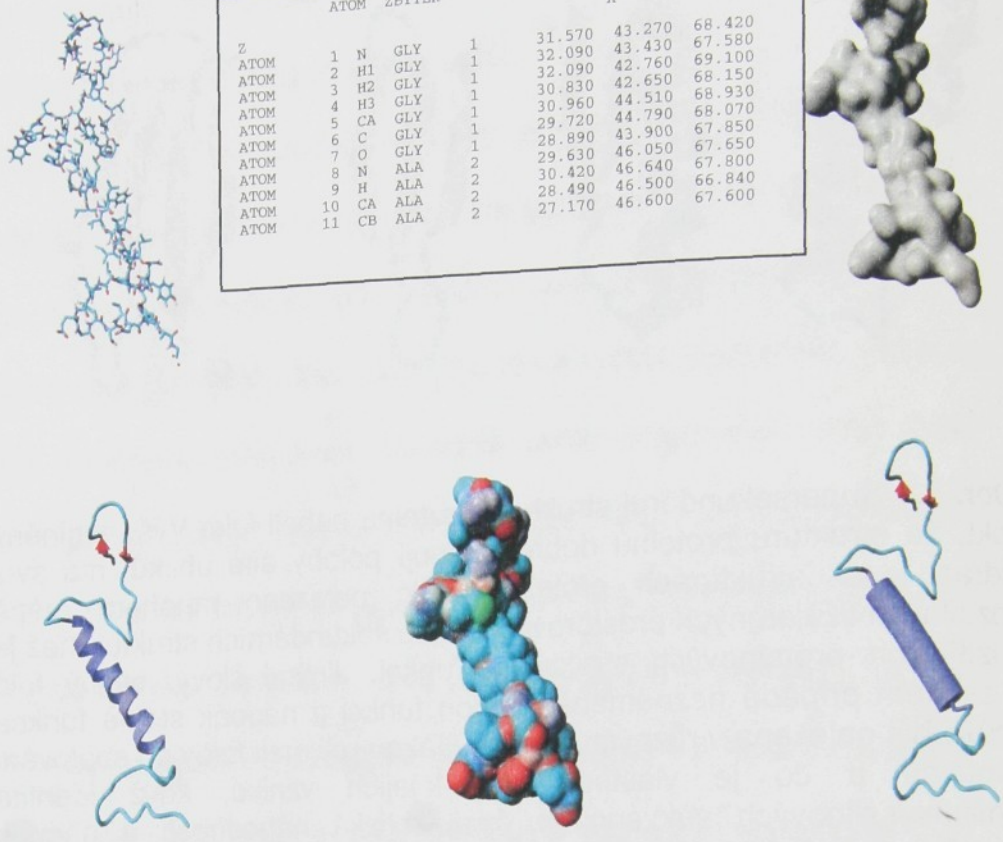

Obr. 2.5 Reprezentace struktury proteinové molekuly. Struktura makromolekuly je seznam souřadnic jejích atomů. Tyto hodnoty mohou být interpretovány tak, že vznikne (a) drátový model, (b) model CPK nebo model van der Waalsových povrchů, který přibližně reprezentuje povrch proteinu na určité hladině významnosti z hlediska pravděpodobnosti výskytu elektronového obalu, (c) stuhový - *Ribbon* model, (d) model povrchu dostupného rozpouštědlu a (e) zjednodušený nákres proteinu. Jedná se o reprezentace struktury proteinu psbH diskutovaného v této práci vytvořené v programu Yasara (Krieger a spol., 2004)

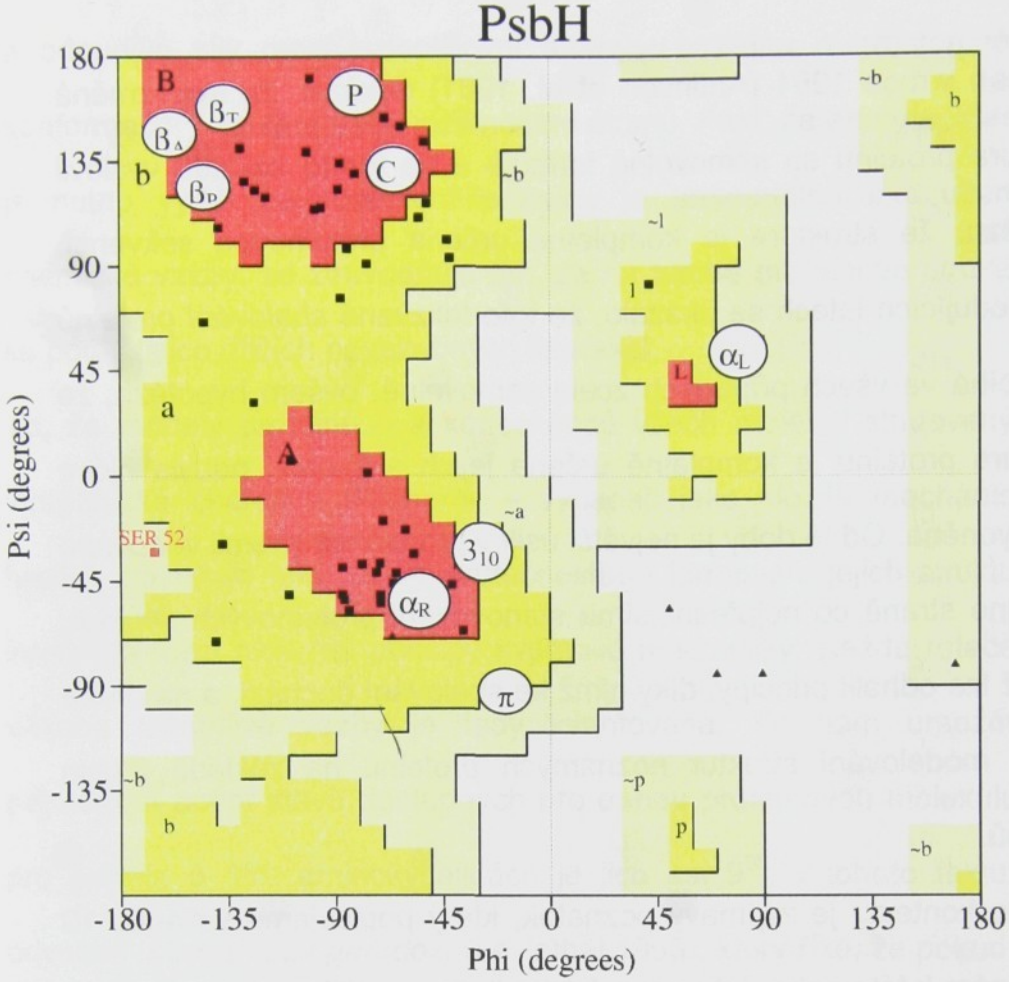

Plot statistics

Residues in most favoured regions [A,B,L]	39	73.6%
Residues in additional allowed regions [a,b,l,p]	13	24.5%
Residues in generously allowed regions [~a,~b,~l,~p]	1	1.9%
Residues in disallowed regions	0	0.0%
Number of non-glycine and non-proline residues	53	100.0%
Number of end-residues (excl. Gly and Pro)	0	
Number of glycine residues (shown as triangles)	8	
Number of proline residues	3	
Total number of residues	64	

Obr. 2.6 Ramachandranův diagram modelu struktury proteinu PsbH. Van der Waalsovy energie v aminokyselinovém zbytku (v tomto případě alaninu) mohou být, v případě alaninu dokonce do značné míry jednoznačně, vyneseny proti úhlům ϕ a ψ. Diagram ϕ a ψ ukazuje oblasti, které jsou stericky povolené (tmavé oblasti), oblasti které jsou částečně povolené, neboli jejichž zaujetí je v proteinech časté, ale vyžaduje dodávku energie jinými interakcemi (šedé oblasti), a oblasti zakázané. Křívky procházející grafem ukazují na možnosti cyklického opakování struktury – tvorby šroubovice neboli helixu příslušného opakování. Každá povolená oblast odpovídá struktuře určitého názvu jako je pravotočivý α-helix (α_R), levotočivý alfa helix (α_L), 3_{10} helix, paralelní β skládaný list (β_P), antiparalelní β skládaný list (β_A), β ohyb (β_T), polyprolin (P) a kolagen (C). Výsledek je výstupem programu procheck (Laskowski a spol., 1993).

Anfinsen v roce 1961 (Anfinsen et al. 1961) dokázal, že trojrozměná struktura proteinů se samovolně formuje a na tomto základě vyslovil hypotézu, že struktura je kompletně určena proteinovou sekvencí. V následujících letech se ukázalo, že toto takzvané *sbalování* proteinů neprobíhá ve všech případech zcela samovolně, ovšem hypotéza, že struktura proteinů je kompletně určena jejich sekvencí, nebyla ničím zpochybněna. Od té doby je největší úsilí v proteinové chemii věnováno na jedné straně co nejpřesnějšímu stanovování proteinových struktur, z nichž lze odhalit principy, díky nimž ke sbalování dochází, a na druhé straně modelování struktur neznámých proteinů na základě těchto principů.

V tomto kontextu je zajímavý poznatek, který popisujeme v článku 10 přiloženém k této práci, kdy jsme dokázali, že v určitém detergentovém prostředí se správně sbaluje i membránová doména malého membránového proteinu PsbH. Doposud se totiž předpokládalo, že sbalování membránových proteinů je těsně spjato s jejich aktivním transportem přes membránu nebo je závislá na vazbě kofaktorů. Souhrn o těchto poznatcích a experimentální potvrzení faktu, že tomu tak nemusí vždy být, lze nalézt například v článku (Roosild a spol. 2005). Náš článek č 10 procházel redakcí souběžně.

Chemická struktura proteinu je dána. V průběhu sbalování se vytvářejí pouze takzvané S-S můstky oxidací sousedních –SH skupin na aminokyselině cysteinu. Obecně se však soudí, že S-S můstky spíše stabilizují již zformovanou strukturu, než aby ji vytvářely. Pro formování struktur jsou rozhodující nevazebné interakce, na jedné straně přitažlivé

a odpudivé síly mezi jednotlivými atomy v proteinu a prostorová a konformační omezení daná vlastnostmi atomů. Fakt, že energie, kterou je nutno vydat na rozbalení proteinu je srovnatelná s roztržením chemické vazby, se zdůvodňuje tím, že na tvorbě proteinové struktury se podílí tisíce dílčích nevazebných interakcí.

To, že modely proteinů – a koneckonců všech molekul studovaných v organické chemii a biochemii – vypadají jako složité mechanické hračky, zastiňuje fakt, že ve skutečnosti se formování jejich struktur i interakce mezi nimi řídí principy kvantové mechaniky. Každá rotace a vibrace jednotlivé vazby je tedy kvantována. To nám umožňuje odhadnout počet stavů dostupných pro danou proteinovou molekulu – pro protein o 100 aminokyselinách je jich asi 9^{98}. Z tohoto faktu je odvozen *Levinthalův paradox,* (Levinthal 1968), který říká, že pokud by pro sbalení proteinové struktury bylo nutno vzorkovat celý konformační prostor, protein by se nikdy nesbalil. Například pokud by vzorkování jedné konformace trvalo 1ps, vzorkování všech konformací by trvalo 10^{74} let. Přítom řada pohybů detekovaných experimentálně v proteinech se odehrává v mnohem delších časových škálách (tab. 2.1).

Tab. 2.1 Časové škály molekulových procesů v proteinech (podle Cammon a Harvey 1987)

Proces	Časová škála
Vibrace vázaných atomů	10-100 fs
Elastické vibrace globulárních oblastí	1-10 ps
Torzní librace ponořených skupin	10 ps-1 ns
Relativní pohyby vzájemně volně vázaných globulárních domén	10 ps-100 ns
Allosterické přechody	10 μs-1 s
Místní denaturace	10 μs-1 s
Rotace povrchových postranních řetězců	10-100 ps
Rotace středně velikých řetězců uvnitř proteinů	0.1 ms – 1 s

Pochopit, čím se řídí proces sbalování proteinů, ale koneckonců i jejich funkce, lze tedy nejspíše pouze v konfrontaci tvorby modelů proteinů a stále přesnějšího experimentálního stanovení jejich struktur. Díky vhodnému modelu, který se zdá představovat právě protein PsbH, se tohoto výzkumu účastníme i my (viz článek 11). Dokonce se z naší, zatím relativně omezené zkušenosti zdá, že pro některé klíčové malé membránové proteiny jsou výpočty struktur jednodušší, než pro stejně velké proteiny rozpustné ve vodě.

2.2 Metody stanovení proteinových struktur s rozlišením na úrovni atomů

Informace o struktuře proteinů na vysokém rozlišení dávají převážně pouze dvě rozšířenější metody: rentgenová krystalografie monokrystalů proteinů a NMR spektroskopie vysokého rozlišení v roztoku.

Podmínkou pro úspěšný experiment při stanovení struktury proteinu pomocí *rentgenové difrakce (X-ray struktury)* je právě získání kvalitního

proteinového monokrystalu (přehled z poslední doby například Blundell 2005). Ten je pak umístěn v difraktometru a měří se rozptyl světla na jednotlivých atomech v něm. Pro účely této diskuse jsou podstatné následující závěry: Výsledkem měření není struktura proteinu, ale mapa elektronové hustoty, která udává hustotu elektronového obalu atomů, vytvářejících strukturu proteinů (obr. 2.7).

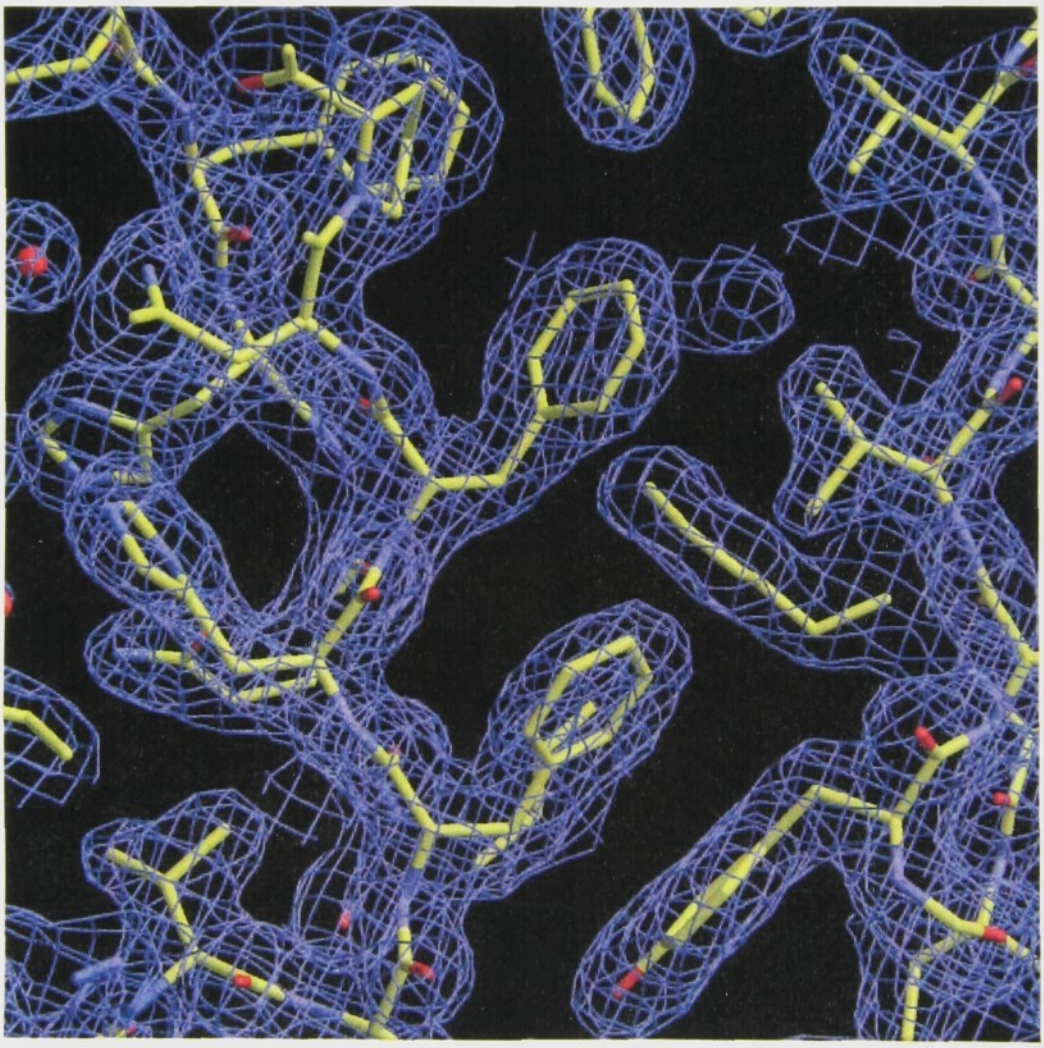

Obr. 2.7 Mapa elektronové hustoty s rozlišením 2.1Å s vloženým drátovým modelem proteinové struktury. Jedná se o doposud nepublikovanou strukturu CRD1 domény galectinu 4 v komplexu s laktózou (poskytnutou laskavě Dr. Jiřím Bryndou před zasláním k publikaci).

Kvalita této mapy je dána kvalitou difrakčního obrazce, z nějž se mapa rekonstruuje. Jen ve strukturách s nejlepším rozlišením je možné identifikovat elektronovou hustotu příslušející některým atomům vodíku. Přitom právě atomy vodíku jsou klíčem pro tvorbu vodíkových můstků – klíčových nevazebných interakcí, které stabilizují proteinové struktury (viz. kap. 3).

Základem pro interpretaci proteinové funkce z X-ray difrakce je model vytvořený na základě difrakční mapy. Tento model je vytvořen kombinací ručního zpracování, kdy se identifikují jednotlivé, především velké, aminokyselinové zbytky a z nich pak i celé části proteinového řetězce, a počítačového zpřesňování většinou metodami molekulové mechaniky. Přitom se řeší minimalizace potenciální energie, přičemž při přiblížení hranicím mapy elektronové hustoty hodnota potenciálové funkce vysoce vzrůstá. Výsledkem je model struktury proteinu, který je pak uložen v databázi proteinových struktur (Berman a spol. 2000). Při následném modelování, jehož cílem je, například, interpretace funkce proteinů, se často na fakt, že sama struktura uložená v databázi je vlastně modelem, zapomíná. To vede k občasnému zpochybňování těchto interpretací experimentátory, a to jak ze strany řešitelů krystalových struktur, vesměs kvalifikovaně, tak ze strany biochemiků, zde často neoprávněně.

Pro objasnění funkce proteinu jsou velmi důležité případy, kdy se podaří makromolekulu vykrystalovat se substrátem nebo jeho analogem. Fakt, že tyto systémy lze často získat už pouhým sycením monokrystalů roztokem substrátu nebo inhibitoru, demonstruje další

důležitý poznatek: monokrystaly proteinů mají vysoký obsah vody. Ta je většinou neuspořádaná, což na jednu stranu samozřejmě snižuje dosažitelné rozlišení, na druhou stranu ukazuje, že značná část proteinu je obalena vodou stejně jako v přirozeném prostředí uvnitř buňky.

Obecně lze shrnout, že přesnost stanovení krystalových struktur je experimentálně omezena naší schopností odečíst a správně kvantifikovat difrakční obraz u difrakcí vyššího řádu. Přesný vztah mezi dosaženým rozlišením, počtem reflexí a počtem atomů v molekule není tedy možno jednoduše definovat. Pro ilustraci složitosti problému uvádím tabulku převzatou z práce Jabri a spol. 1995 (Tab. 2.2).

Tab.2.2 Krystalografická data a výsledky pro ureázu (podle Jabri a spol. 1995)

Krystal	Rozlišení dat	Počet unikátních reflexí	Konečný R faktor	Nevodíkové proteinové atomy	Molekuly rozpouštědla
Nativní protein	2 Å	58 336	18,5%	6002	215
Apoenzym	2,8 Å	20 532	18,4%	5944	157
$HOHgC_6H_4CO_2Na$	3.3 Å	11 027			
$EuCl_2$	3.3 Å	12 210			
$Hg_2(CH_3COO)_2$	2,5 Å	28 709			
$C(HgOOCCH_3)_4$	2,4 Å	29 672			
$(CH_3)_3Pb(CH_3COO)$	2,4 Å	23 486			
Se-Met	3.0 Å	20 332			

Druhou metodou pro stanovení detailní struktury proteinu je NMR spektroskopie vysokého rozlišení (Evans 1995). Velkou výhodou této metody je možnost práce s proteiny v roztoku. Odpadá tudíž často velmi obtížná příprava monokrystalů a je možná celá řada manipulací

jako změny pH, teploty, přídavky substrátů a inhibitorů. NMR spektroskopie navíc poskytuje velké množství snadno čitelných informací, jako jsou údaje o chemických vazbách mezi atomy, vzdálenostech mezi atomy, dynamice jednotlivých částí molekuly, vodíkových vazbách, disociačních konstantách apod. Naproti tomu je velikost molekul měřitelných pomocí NMR spektroskopie omezena velikostí molekuly, teoreticky asi do 40 000 Da i více, ve skutečnosti však většinou do 20 000 Da, tedy asi 200 aminokyselin. Zvyšování molekulové váhy vede k rozšiřování spektrálních linií a zvyšující se komplikovanosti a tudíž zhoršené interpretovatelnosti spektra.

Příklad vícerozměrných NMR spekter je v článcích 7 a 10, které jsou přiloženy k této práci. U těchto spekter jsme však nedělali kompletní a rigorózní analýzu, protože výsledky experimentů ukázaly, že bychom nebyli schopni získat dostatek dat pro stanovení trojrozměrné struktury. Interpretace NMR spekter se odehrává v několika krocích. Prvním je přiřazení (assignment) jednotlivých signálů jednotlivým protonům. V nejjednodušších, proton-protonových spektrech, se využívá čtení dvou typů experimentů – experimentu, který ukazuje sousedství atomů na chemických vazbách a druhého, který ukazuje sousedství atomů v prostoru. První typ spekter nám definuje aminokyselinové zbytky a druhý ukazuje jejich vzájemnou polohu v prostoru. V dobře rozlišeném spektru lze tak principiálně „číst" proteinovou sekvenci.

Jakmile je přiřazení hotovo, začíná se stanovováním struktur. K tomu jsou dostupné dva typy informací (a) informace o vzdálenostech mezi protony a (b) informace o konformacích na jednotlivých vazbách. Obě

informace jsou zatíženy významnými chybami, které pramení jak z podstaty metody NMR spektroskopie, tak z dynamiky proteinu, jež způsobuje rozšiřování spektrálních linií a fluktuaci vzdáleností. Navíc dosah stanovení vzdáleností je maximálně 5,5 Å. Vzájemná poloha vzdálenějších atomů tak není vůbec určena. Struktura proteinů se stanovuje optimalizací modelu, který vyhovuje všem známým poznatkům a je tak často významně ovlivněna vlastním modelovacím prostředím.

Velkou výhodou NMR spektroskopie, kterou jsme právě využívali v pracech popsaných v publikacích 7 a 10, je získání detailních poznatků o změnách v proteinové struktuře způsobených interakcemi. To nám umožnilo identifikovat ty atomy, které se účastní specifické vazby N-koncové domény světlosběrného komplexu II s fosfatidylglycerolem (Veverka a spol. 2000 – článek 7) a ujistit, že při přídavku lipidů k detergentovému roztoku proteinu PsbH dochází k tvorbě velkých komplexů, jejichž velikost přesahuje předpokládaný komplex PsbH-jedna lipidová molekula (Štys a spol. 2005 – článek 10).

2.3 Studium struktur membránových proteinů

Vše, co bylo řečeno v předchozí kapitole, se jen velmi omezeně týká membránových proteinů. Jejich přirozeným prostředím je lipidová dvojvrstva z obou stran obklopená prostředím vody a iontů (obr. 2.8).

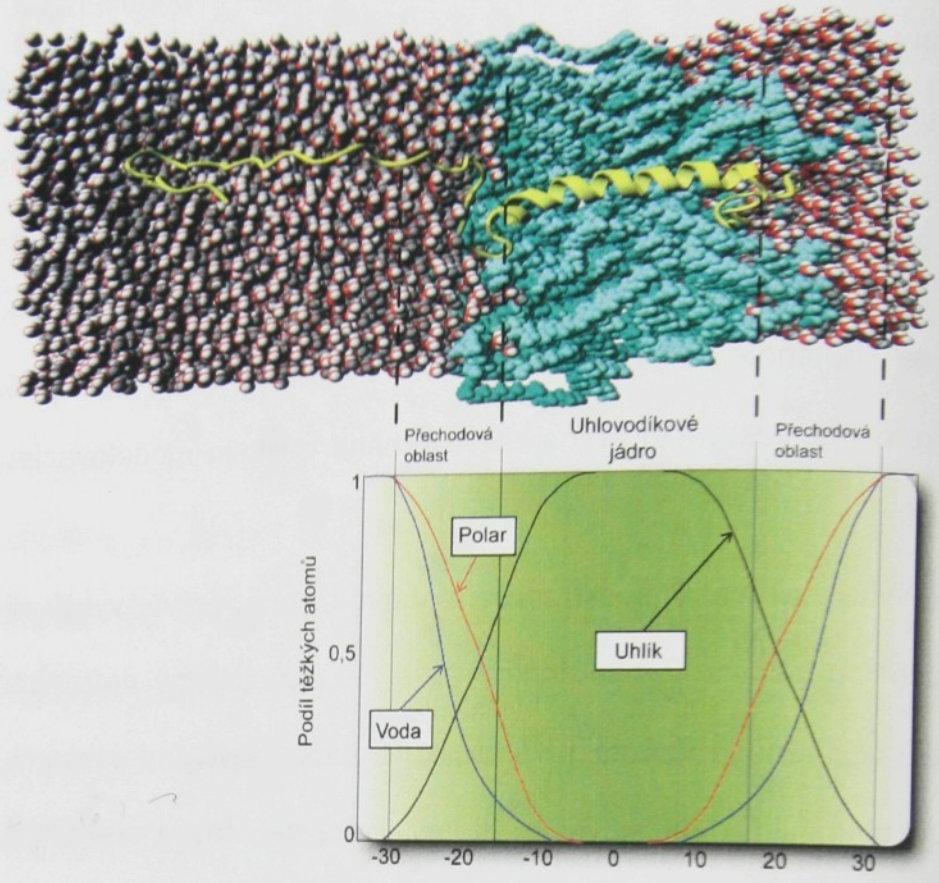

Obr. 2.8 (a) Membránový protein je zanořen do lipidové dvojvrstvy svou hydrofobní částí, mimomembránové části interagují s hydrofilními částmi lipidových molekul prostřednictvím solných můstků, vodíkových vazeb a ne zcela detailně popsanými interakcemi závislými na polarizabilitě postranních řetězců aromatických aminokyselin. Modelovací prostředí zatím není schopno plně postihnout ani fluktuace tloušťky membrány, ani tvorbu domén. *Vlastní nepublikovaný výsledek Ettrich, Sovová a Štys.* (b) Přechodná vrstva mezi vodným prostředím a hydrofobní částí membrány tvoří až ½ její celkové tloušťky. Toto anisotropní prostředí proměnné tloušťky výrazně ovlivňuje interakce, naše výsledky (článek 11), například naznačují, že dochází k postupné stabilizaci solných můstků na poměrně krátkou vzdálenost, což může naznačovat, že uvnitř přechodné oblasti mohou tyto typy interakcí hrát větší roli než ve vodném prostředí. Většina interakcí je ale tvořena vodíkovými můstky.

Z tohoto prostředí jsou proteiny extrahovány detergenty, v jejichž nepřítomnosti denaturují, srážejí se a ztrácejí aktivitu. V několika případech se podařilo získat trojrozměrné struktury membránových proteinů pomocí analýzy jejich monokrystalů, vyrostlých z roztoků

proteinů v micelách detergentu. Pomocí NMR spektroskopie zatím skutečná trojrozměrná struktura membránového proteinu, která by dávala detailní informaci o pozici funkčně významných skupin, stanovena nebyla. Struktur membránových proteinů s rozlišením pod 2,5 Á, z nichž by bylo možno odvodit nové přesné poznatky o funkci proteinů, bylo stanoveno o čtyři řády méně než struktur proteinů rozpustných.

Navíc, i když je už struktura membránového proteinu známa, o jeho funkci vypovídá jen ta část, kde se neočekává interakce s lipidovou dvojvrstvou. Tedy uvnitř komplexu a v jeho mimomembránových doménách. O interakcích s lipidovou dvojvrstvou a s okolními proteiny v ní nevíme experimentálně téměř nic. Jak již bylo zmíněno v kapitole 1 této práce, interakce mezi proteiny a lipidy při formování struktury thylakoidní membrány, ale i jiných membrán, je rozhodující pro jejich funkci. Jediný přístup je tedy modelování.

V této práci uvádím dva pokusy, kdy jsme se snažili získat informace o interakcích mezi proteinem a lipidovou dvojvrstvou na úrovni jednotlivých atomů.

3. Modely proteinových struktur, proteinová dynamika a interakce

(Notace a pořadí diskuse je shodné s van der Holde a spol 2006.)

3.1 Problémy modelování proteinových struktur

Jak už bylo řečeno v kapitole 2.1, síly formující struktury lze přesně popsat pouze metodami kvantové chemie. Je tomu tak zcela samozřejmě, uvědomíme-li si rozměry objektů, se kterými pracujeme, pro něž je adekvátní jednotka Ångström Å - 10^{-10} M (např. obr. 2.7). Jinak řečeno, konformační prostor, který při modelování proteinových struktur vzorkujeme, není kontinuální ani z hlediska prostorového uspořádání, ani z hlediska dynamiky dovolených pohybů. Ani u poměrně malých organických molekul (několik desítek atomů) však takové výpočty v úplnosti není možno provést. Proto se využívá metod aproximativních, takzvaných empirických potenciálů, které pak umožňují využívat pro modelování metod klasické newtonovské fyziky.

I při tomto zjednodušeném přístupu je modelování proteinů extrémně komplikované. Například insulin, velmi malý protein s 51 aminokyselinami a tudíž na spodní hranici velikosti nutné pro stabilní konformaci, má 760 atomů, z nichž 400 je nevodíkových. Když zahrneme molekuly vody, které jsou samozřejmě asociovány s každou molekulou proteinu, systém se stává nezpracovatelným. Například jediná molekula proteinu v koncentraci 10^{-3}mol/l interaguje s přibližně 10^{8} molekulami vody.

Všechny zúčastněné molekuly jsou velmi dynamické. To se netýká jen prostředí, ale i makromolekul samotných, které rotují a pohybují se jako celek a zároveň se na jejich povrchu i uvnitř pohybuje celá řada atomů a skupin postranních i hlavních řetězců. Jinými slovy, všechny molekuly mají velké množství stupňů volnosti. Jedinou možností jak systém modelovat je zjednodušit ho.

Zjednodušující předpoklady, které bývají zaváděny, vycházejí především z předpokladu, že *průměrné chování celého systémů odpovídá chování jedné jeho reprezentativní části.* Jako reprezentativní část se vybírá jedna makromolekula obklopená molekulami vody v kubickém prostoru - krabici (obr. 2.8). Je-li jedna molekula v této krabici skutečně dynamická, tedy nikoliv, například, vázána na protein, za určitou dobu bude vzorkovat celý konformační prostor, který je pro systém dostupný. Pokud tento přístup periodicky opakujeme, krabice položíme vedle sebe a necháme každou molekulu nebo její část, která krabici opouští, vstoupit do krabice sousední (fakticky, při výpočtu, do původní krabice z druhé strany), koncentrace zůstávají neměnné. Tento předpoklad je klíčový, protože vlastnosti proteinů včetně stability jejich struktur kriticky závisí na koncentrací vody i jiných molekul (ionty, malé organické molekuly apod.). Velkým problémem tohoto druhu modelování je vytvořit krabici tak velkou, aby správně simulovala systém včetně chování okolního rozpouštědla.

Naproti tomu se dnes objevují metody (pro námi studované systémy přehledný článek například Vácha a spol., 2005), které umožňují studium funkce jednotlivých molekul. Zatím ale tato měření nepřinesla

dostatek dat, pomocí nichž by se dala ověřovat validita výpočetních metod.

Druhým hlavním předpokladem je, že *nativní konformace je konformací s nejnižší potenciální energií*, přičemž dynamika systému se ignoruje.

3.2 Molekulová mechanika

Při tomto přístupu popisujeme formování proteinové struktury jako pohyb v potenciálovém poli přístupy klasické mechaniky. Definujeme tedy celkovou energii E systému jako součet kinetické energie K a potenciální energie V

$$E = K + V \quad (3.1)$$

Za kinetickou energii považujeme energii vyvolanou pohybem všech atomů v systému. Potenciální energie je součtem všech potenciálů jednotlivých atomů a může být reprezentována multidimenzionálním povrchem pro každou jednotlivou konformaci tohoto pohybu. Řez tímto povrchem představuje například i Ramachandranův diagram v podobě, jak je zobrazen na obr. 2.6 s tím, že v případě aminokyselinového zbytku zabudovaného do proteinu by se energetické hodnoty v jednotlivých oblastech lišily od hodnot pro jednotlivý dipeptid.

Na základě druhého Newtonova zákona pak můžeme napsat vztah mezi silou **F** podél molekulární trajektorie (vektor vzdálenosti **r**), zrychlením **a** a hmotností m.

$$\mathbf{F} = m.\mathbf{a} \quad (3.2)$$

Pro zjednodušení diskuse budeme uvažovat pouze pohyb podél osy x. Povrch se pak zjednoduší na energetický profil. Síla podél trajektorie r je pak

$$F = -\frac{\partial V}{\partial r} \quad (3.3)$$

jinými slovy, síla závisí na tom, jak se potenciál mění podél molekulární trajektorie. Místní gradient potenciální energie definuje *silové pole* v molekulové mechanice. Pro molekulovou mechaniku byla vyvinuta celá řada silových polí. Každé silové pole má své výhody a nevýhody a žádné se nedá použít univerzálně. Proto se v další diskusi omezím na to, co je všem silovým polím společné.

Speciální případ, který hledáme, je systém v rovnováze kdy F=0 a tedy $-\frac{\partial V}{\partial r} = 0$. Hledáme tedy energetické minimum a tyto metody molekulové mechaniky se proto často nazývají též minimalizace energie.

Pokud zahrneme též kinetickou energii danou vyvolanou rychlostí **v** respektive hybností **p**, (při odvození opět uvažujeme jen složky ve směru jedné osy)

$$K = \frac{1}{2}mv^2 = \frac{1}{2}\frac{p^2}{m} \quad (3.4)$$

jedná se o metody molekulové dynamiky, kdy sledujeme dynamickou změnu v pozici atomu v každém čase t.

3.3 Molekulové potenciály

Návrh molekulových potenciálů do značné míry vychází z tradičních (předkvantových) představ o chemických vazbách a nevazebných interakcích. Vývoj potenciálů stále probíhá, ovšem slabinou celého tohoto přístupu je fakt, že se jedná pouze o metodu aproximativní, která nezohledňuje kvantově-mechanickou podstatu problému. Často se ukazuje, že potenciály vhodné pro jeden systém nejsou použitelné pro systém jen mírně odlišný.

Naproti tomu probíhají neustále pokusy o vytvoření zjednodušeného potenciálového pole, které by zohledňovalo vlastnosti několika atomů najednou (Grubmüller a Tavan 1994). Takové sjednocené potenciály by umožňovaly, například, výpočty ab-initio sbalování proteinů. Tyto potenciály se vytvářejí pro jednotlivé případy (např. Venturoli a spol. 2005) tak, aby odrážely určité vlastnosti simulovaného systému, ale zároveň probíhá snaha i o jejich využití pro ab-initio sbalování proteinů. Tato snaha je tažena úsilím o pochopení principů sbalování proteinů neboli otázkou, proč se proteiny sbalují přesto, že platí Levinthalův paradox.

Základní představou je tedy, že celková vnitřní potenciální energie molekuly V_{total} se dá popsat jako součet všech vazebných interakcí (= energií všech chemických vazeb) $V_{bonding}$ a všech nevazebných interakcí $V_{nonbonding}$. Neboli:

$$V_{total} = \sum_{i}^{N} (V_{bonding} + V_{nonbonding}) \quad (3.5)$$

pro N atomů v molekule proteinu. V_{total} je tedy funkcí koordinát jednotlivých atomů. Předpokládá se, že k hodnotě V_{total} významně přispívají pouze interakce s malou skupinou sousedních atomů. Mohou

to být vzájemně chemicky vázané nebo chemicky nevázané atomy nebo jejich skupiny.

Vazebná energie je definována jako energie, kterou je nutno dodat k roztržení kovalentní chemické vazby. Nevazebné interakce zahrnují například elektrostatické interakce, dipól-dipólové interakce, sterická omezení a podobně.

3.3.1 Vazebné potenciály

Vazebné potenciály přirozeně dominují potenciálové funkci, protože představují energii 150-1000 kcal/mol (obr 3.1).

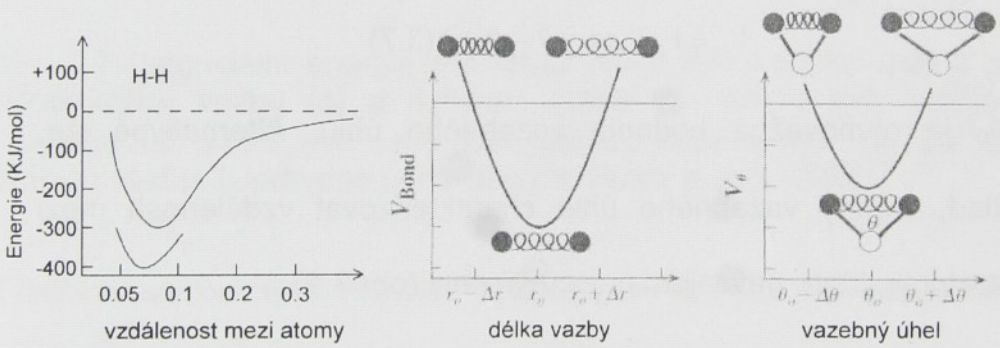

Obr. 3.1 Potenciální energie vodíkové vazby a energie deformace vazebného úhlu (upraveno podle van der Holde a spol. 2006). Potenciální energie počítaná pomocí kvantové mechaniky (horní křivka) je porovnána s vazebnou energií posuzovanou modelem pružiny a s experimentálními hodnotami pro vodíkovou vazbu (dolní křivka). Deformace spojené s délkou vazby jsou modelovány, v nejjednodušším případě, jako pružina s danou pružinovou konstantou pro natahování a kompresi vazby o vazebné délce r. Pružinový model především nadhodnocuje natahování vazby pro velká kladná Δr. Deformace vazebného úhlu θ mohou být podobně modelovány jako deformace pružiny mezi dvěma atomy vázanými na společného vazebného partnera.

To zohledňuje fakt, že v rámci výpočtu nepředpokládáme roztržení chemické vazby ani její zásadní deformaci. Nejjednodušší model pro zjednodušený popis vazby je v zásadě modelem pružiny tedy:

$$V_{bond} = V_{0,bond} + k_{bond}(r - r_0)^2 \quad (3.6)$$

kde $V_{0,\,bond}$ je délka vazby v rovnovážném stavu a funkce popisuje změnu energie při odchylce délky vazby od rovnovážné polohy r_0. k_{bond} je fakticky konstanta pružnosti a celá rovnice je jednoduchá harmonická funkce. Ve skutečnosti takto popsaný potenciál neodráží ani naše empirické představy o chemické vazbě, ale pro malé odchylky od rovnováhy, které lze v proteinech předpokládat, do značné míry vyhovuje.

Pro vibrace vazebných úhlů lze například napsat podobnou rovnici

$$V_\theta = V_{0,\theta} + k_\theta(\theta - \theta_0)^2 \quad (3.7)$$

kde θ_0 je rovnovážná hodnota vazebného úhlu. Alternativně lze, například, změny vazebného úhlu charakterizovat vzdáleností mezi dvěma atomy, které navzájem nejsou vázány (obr 3.1).

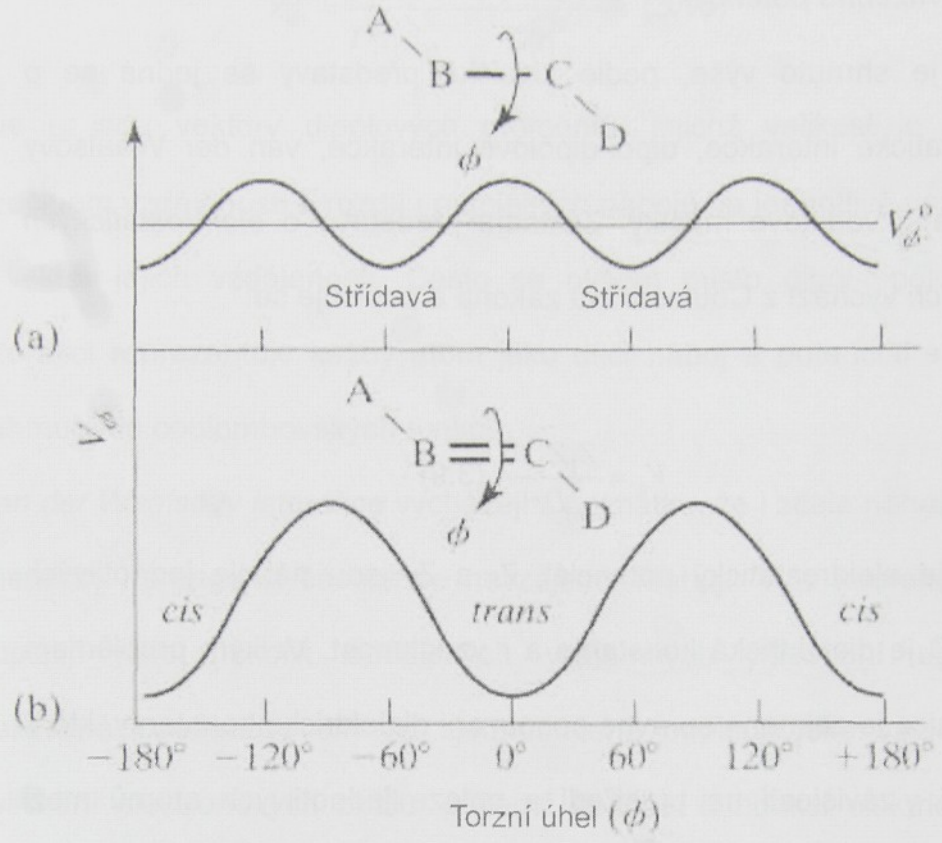

Obr. 3.2 Potenciální energie pro rotaci okolo dihedrálního úhlu ϕ pro jednoduchou vazbu (a) a dvojnou vazbu (b). Křivky byly počítány z rovnice 3.8. s n=3, γ=0°, pro jednoduchou vazbu a n=2, γ=-180° pro dvojnou vazbu. (Upraveno podle van der Holde a spol. 2006).

Z dalších uvažovaných interakcí je důležité se zmínit o interakcích mezi čtyřmi atomy vzájemně vázanými třemi vazbami (obr. 3.2). Taková interakce se charakterizuje takzvaným torzním úhlem ϕ a nejjednodušší přiblížení k jejímu popisu představuje rovnice

$$V_\phi = V_{0,\phi} + V_n \cos(\gamma - \frac{\phi}{n}) \quad (3.8)$$

kde V_n je torzní síla, n počet minim a γ úhel v němž leží minimum

Samozřejmě pokud atomy na vazbě nejsou ekvivalentní, musí být rovnice složitější.

3.3.2 Nevazebné potenciály

Jak už je shrnuto výše, podle klasické představy se jedná se o elektrostatické interakce, dipól-dipólové interakce, van der Waalsovy interakce a vodíkové můstky. Základní představa o *elektrostatických interakcích* vychází z Coulombova zákona a popisuje se:

$$V_e = \frac{Z_1 Z_2 e^2}{Dr} \quad (3.9)$$

kde V_e je elektrostatický potenciál, Z_1 a Z_2 jsou náboje jednotlivých atomů, D je dielektrická konstanta a r vzdálenost. Velkým problémem této rovnice je zejména správné posouzení dielektrické konstanty, která se mění v závislosti na prostředí a poloze jednotlivých atomů mezi jednotlivými náboji. Přístupů je několik. Například lze dielektrickou konstantu považovat za funkci vzdálenosti, kdy se předpokládá, že v okolí náboje se vyskytuje více polarizovatelných atomů a se vzdáleností jejich počet klesá. Alternativně se například může dielektrická konstanta považovat za lokální funkci závisející na hustotě atomů proteinu v daném místě. Zde se předpokládá, že prostor, v němž se nenacházejí atomy samotného proteinu, je vyplněn vodou a D je v tomto místě rovna D vody. Každé další zpřesnění nad tyto (a podobné) jednoduché předpoklady bohužel vede k vysokému nárůstu náročnosti výpočtu.

Dipól-dipólové interakce vznikají mezi polarizovanými vazbami, v zásadě vazbami mezi nestejnými atomy. Díky tomu mají tyto interakce vektorový charakter a klasicky se popisují rovnicí:

$$V_{dd} = \frac{\boldsymbol{\mu}_1 \boldsymbol{\mu}_2}{D|\mathbf{r}|^3} - \frac{3(\boldsymbol{\mu}_1 .\mathbf{r})(\boldsymbol{\mu}_2 .\mathbf{r})}{D|\mathbf{r}|^5} \quad (3.10)$$

kde μ_i jsou vektory dipólových momentů, jejichž velikost je dána součinem vzdálenosti a rozdílu parciálních nábojů na jednotlivé vazbě a **r** vektor jejich vzdálenosti. Často se ovšem místo dipól-dipólových interakcí reprezentuje každý atom jako dílčí náboj a potenciál se tak zahrnuje do coulombovských funkcí.

Van der Waalsovy interakce vycházejí z poznatku, že i zcela nenabité a chemicky nereagující částice se navzájem přitahují. Tyto interakce se popisují jako několik oddělených vzájemných působení atomů. Takzvané Londonovy síly se zjednodušeně popisují jako vzájemné ovlivnění elektronových obalů, přičemž dochází k indukci elektrických dipólů, které spolu následně interagují. Van der Waalsův potenciál pro Londonovy síly V_L je popsán rovnicí

$$V_L = -\frac{3I\alpha_1\alpha_2}{4r^6} \quad (3.11)$$

kde I je ionizační energie, α_i jsou polarizability jednotlivých atomů.

Druhá významná interakce, takzvaná repulzivní síla V_r, v zásadě zohledňuje fakt, že atomy mají nenulový objem a nemohou se k sobě tedy přiblížit nekonečně blízko. Nejjednodušším přiblížením je model pevné koule, kdy při přiblížení na určitou vzdálenost funkce nabývá nekonečnou hodnotu. Obvykle se ale tato interakce aproximuje funkcí

$$V_R = \frac{k}{r^m} \quad (3.12)$$

kde m se stanoví mezi 6 a 12 a k je empirická konstanta.

Někdy se tyto dvě síly dohromady sčítají jako van der Waalsovy interakce. Pokud se m=12, jedná se o takzvaný *Lennart-Jonesův potenciál.*

Vodíkové vazby jsou fakticky interakce, které lze popsat pouze na základě kvantově-mechanických představ o chemické vazbě. Jsou pozorovány mezi vodíkem a těmi atomy první periody, které mají volné elektronové páry. Pokud se takový pár atomů přiblíží na dostatečně malou vzdálenost (0,26-0,3 nm), vznikne takzvaná koordinačně-kovalentní vazba. Je zřejmé, že se jedná jak o problém vzdálenosti, tak o problém geometrický. Aniž bych se pouštěl do hlubšího rozboru této síly, lze shrnout, že bývá popisována součtem atraktivní a repulsivní komponenty jako

$$V_{HB} = \frac{C}{r^{12}} - \frac{D}{r^{6}} \quad (3.13)$$

kde C a D jsou konstanty charakterizující jednotlivé vazebné partnery. Vodíková vazba je, vzhledem k počtu takových potenciálních párů, pro tvorbu proteinových struktur velmi významná.

3.4 Simulace makromolekulárních struktur a pochopení sil, které struktury formují

Simulace struktur biologických makromolekul v sobě tedy nese celou řadu problémů, jejichž společným jmenovatelem je komplexnost, která neumožňuje jejich korektní řešení v rámci současného poznání.

Nejjednodušší *molekulárně mechanické* výpočty jsou založeny na hledání minima potenciálové funkce v rámci molekulárního potenciálu definovaného v předchozí kapitole. Vychází se z toho, že Newtonovy

rovnice jsou deterministické, a proto se dá použít metody nejstrmějšího klesání, kdy měníme polohu jednotlivého atomu o malý příspěvek a sledujeme, zda energie klesá nebo stoupá. Tím získáme trajektorii, která vede nejrychlejší cestou k minimu, na jehož svahu se výchozí konformace nachází. Nikoliv tedy k minimu celkovému.

Metoda *molekulové dynamiky* řeší nejen potenciální, ale celkovou energii systému. Hybnost atomů je vztažena k síle působící na atom a potenciální energií vztahem

$$F = \frac{\partial p}{\partial t} = -\frac{\partial v}{\partial r} \quad (3.14)$$

Jinými slovy, kinetická energie je vztažena k funkci potenciální energie dané silovým polem. Použijeme-li první dva členy Taylorova rozvoje, můžeme pro změnu pozice atomu z polohy v čase t do polohy v čase t+Δt napsat:

$$x(t+\Delta t) = x(t) + \left[\frac{dx(t)}{dt}\right]\Delta t + \left[\frac{d^2x(t)}{dt^2}\right]\frac{\Delta t}{2} + ... \quad (3.15)$$

přičemž $\left[\frac{dx(t)}{dt}\right]$ je rychlost, která je rovna $v=(2K/m)^{1/2}$ a $\left[\frac{d^2x(t)}{dt^2}\right]$ zrychlení a=F/m. Ačkoliv Taylorův rozvoj je možno expandovat do nekonečna, pro molekulovou dynamiku se využívají pouze první dva členy. Jinými slovy, pro danou hmotnost je poloha atomu definována jako funkce potenciální a kinetické energie. Kinetická energie je vztažena ke stavu systému rovnicí

$$K = 3k_B T \quad (3.16)$$

kde k_B je Boltzmannova konstanta a faktor 3 zohledňuje 3 stupně volnosti pohybu atomu. Jelikož potenciální energie V nezávisí na teplotě, je teplotně závislá pouze kinetická energie. Za nízkých teplot je poloha atomu závislá hlavně na potenciální energii, za vysokých hlavně na kinetické.

Molekulová dynamika předpokládá, že soubor atomů v makromolekule se z hlediska rozdělení rychlostí chová v souladu s Maxwell-Boltzmannovým rozdělením a tedy platí:

$$P(v)\partial V = \left[\frac{m}{2\pi k_B T}\right]^{3/2} \exp\left(-mv^2 / 2k_B T\right) 4\pi v^2 \partial v \quad (3.17)$$

kde P(v) je pravděpodobnost, že hmota má rychlost v a teplotu T. Pravděpodobnost g, že určitý atom bude mít rychlost v ve směru osy x má tedy gaussovské rozdělení. Protože krok Δt musí být velmi malý, je omezena i délka výpočtu. Například počet jednotlivých výpočtů energie systému při sledování trajektorie v čase 1 ps je asi 10^6. Tato výpočetní náročnost je dalším hlavním omezením velikosti systémů, které je možno studovat.

Prakticky se nejčastěji používá simulace pomocí takzvaného simulovaného žíhání (simulated annealing). Jedná se o opakovaný simulovaný ohřev a ochlazování sytému. Je to jedna z metod, jak obcházet nebezpečí, že systém sklouzne do lokálního minima. Z čistě termodynamického hlediska (tzv. ergodický teorém, Birkoff 1931) bychom si však mohli být jisti, že jsme dosáhli globálního minima až po nekonečně dlouhé simulaci.

Až do tohoto okamžiku byla diskutována v zásadě pouze energetika sbalování. Nejedná se tedy o výpočet Gibbsových volných energií ale pouze entalpického příspěvku k nim. V systému, který obsahuje makromolekulu, je třeba odlišit dva druhy *entropického* přípěvku. Konformační entropii makromolekuly a entropii rozpouštědla. Počet různých konformací W může být odhadnut na základě počtu možných konformací g aminokyselinového zbytku o n atomech jako:

$$W = g^{(n-2)} \quad (3.18)$$

Například pro řetězec 100 různých aminokyselin s průměrným g=9 je počet různých izomerů $9^{98} \cong 3x10^{93}$. Rozdíl ΔS mezi entropií nativní struktury S_N a entropií všech možných náhodných struktur je pak

$$\Delta S = S_N - S_R = k_B[\ln(1) - \ln(W)] = k_B(n-2)\ln g \quad (3.19)$$

V tomto výpočtu ΔS= asi –2KJ/molK. To je jedno z možných odvození Levinthalova paradoxu zmíněného v části 2.1.

Levinthalovu paradoxu bychom se mohli vyhnout pokud platí, že sbalování prochází jen určitou sadou konformací. To je princip sbalování prostřednictvím zformování „roztaveného klubka" (molten globule). Pro existenci takového intermediátu existuje řada experimentálních indicií, jako jsou nalezené intermediáty při sbalování proteinů in vitro nebo molekuly zvané „chaperony" (přehledný článek např Baram a Yonath 2005) které, jak se zdá, rozvolňují špatně sbalené intermediáty a dovolují jejich další korektní sbalení.

Za proces tažený entropií se všeobecně považuje i hydrofobní efekt. Jedná se v principu o známý jev oddělení fází ve směsi dvou nemísitelných rozpouštědel. Při energetickém přístupu k simulaci

makromolekul jsou vzájemné atrakce respektive repulze hydrofobních a hydrofilních částic skryty v parametrech potenciálového pole. Pokud se ale skutečně jedná o entropický jev, tento přístup by neměl být dostatečný. Za současného stavu poznání a (možná především) při možnostech výpočetních kapacit se ale při hodnocení hydrofobního efektu omezujeme fakticky na hodnocení velikosti povrchů přístupných nebo nepřístupných rozpouštědlu a pro vlastní simulaci se jich nevyužívá.

K získání *Gibbsovy volné energie* G, což je hodnota běžně měřená chemickým experimentem, z výpočtu se může přistoupit několika způsoby. Například můžeme posuzovat rozdíl mezi volnou energií nativní konformace G_N a rozbalené (unfolded) konformace G_U. To lze z výpočtu odvodit například tak, že spočteme energie velkého množství konformací a ty pak statisticky vyhodnotíme. Pro výpočet G bylo navrženo několik postupů, z nichž ovšem všechny bez výjimky narážejí na naši neschopnost konformace dostatečně vzorkovat – Levinthalův paradox.

Přes to všechno se proteiny v reálném čase sbalují, nejspíše tedy je v našich úvahách nějaká zásadní chyba. Potvrdilo se však, že vycházíme-li ze struktury jen málo odlišné od struktury nativní, molekulárně dynamická simulace vede k očekávanému výsledku. Úspěch předpovědi struktury především závisí na dobré znalosti výchozí konformace.

3.5 Simulace lipidových dvojvrstev a lipid-proteinových interakcí

Jak bylo řečeno v kapitole 2.3, studium biologických membrán, které by poskytovalo údaje o interakcích jednotlivých atomů, je experimentálně nepřístupné. Velké úsilí tedy bylo věnováno tomu, aby simulace potvrzovaly výsledky, které tyto interakce popisují nepřímo. Jsou jimi různá měření lipidové dynamiky a orientace lipidových molekul ve dvojvrstvě. Edholm a Lindahl ve spolupráci s dalšími skupinami (Lindahl a Edholm 2000) dokázali, že při vhodně zvoleném potenciálu lze lipidovou dvojvrstvu úspěšně simulovat standardními metodami molekulové dynamiky v přítomnosti vody.

V dalších letech byl tento systém úspěšně aplikován též na interakce membránových proteinů známé struktury s lipidovou dvojvrstvou. Postupovalo se tak, že se v první fázi výpočtu vytvořil v membráně otvor velikosti studovaného proteinu (Faraldo-Gómez a spol. 2002) tím, že se z daného prostoru vyňaly všechny molekuly lipidu, které se v něm nacházely celé. Dále se na systém aplikoval další potenciál tvaru podobnému potenciálu tuhých koulí, kdy přítomnost atomu v oblasti vyčleněné pro protein je vysoce energeticky penalizována. Tak vznikl v membráně otvor, do nějž byl zasazen protein a simulace mohla proběhnout. Z hlediska proteinové funkce nebo lipid-proteinových interakcí však tyto simulace nepřinesly zásadní poznatky.

V poslední době se objevilo několik simulací konformace peptidu povrchově vázaného na biologickou membránu. Doposud nikdy ale nebyl popsán případ, kdy by bylo studováno, jak malý membránový protein ovlivňuje funkci membrány jako celku. Ten popisujeme poprvé v článku 11 přiloženém v této práci.

4. Reference

Albertsson P.A., 2001. A quantitative model of the domain structure of the photosynthetic membrane. Trends in Plant Science 6 (8): 349-354

Allen J.F., 1992. Molecular structural effects of protein-phosphorylation in regulation of photosynthesis. Photosynthesis Research 34 (1): 118-118

Allen J.F., 1992. Protein-phosphorylation in regulation of photosynthesis. Biochimica et Biophysica Acta 1098 (3): 275-335

Anfinsen C.B., Haber E., Sela M. a White F.H., 1961. The kinetics of formation of native ribonuclease during oxidation of reduced polypeptide chain, Proc. Natl.Acad. Sci. U.S.A., 47, 1309-1314.

Baram D., Yonath A., 2005. From peptide-bond formation to cotranslational folding: dynamic, regulatory and evolutionary aspects. FEBS Letters 579 (4): 948-954 Sp. Iss. SI

Barber J., 1982. Influence of surface-charges on thylakoid structure and function. Annual Review of Plant Physiology and Plant Molecular Biology 33: 261-295

Berman H.M., Westbrook J., Feng Z., Gilliland G., Bhat T.N., Weissig H., Shindyalov I.N., Bourne P.E., 2000. The Protein Data Bank. Nucleic Acids Research , 28 pp. 235-242

Birkhoff G.D., 1931. Proof of the ergodic theorem. Proceedings of the National Academy of Sciences USA, 17: 656-660

Blundell T.L., 2005. The developing art of protein crystallisation: new advances from improved knowledge automation and miniaturisation. Progress in Biophysics & Molecular Biology 88 (3): 283-284

Bond P.J., Faraldo-Gomez J.D., Sansom M.S.P., 2002. OmpA: A pore or not a pore? Simulation and modeling studies. Biophysical Journal 83 (2): 763-775

Bricker T.A., Prevost M., Vu. V., Laborde S., Womack J., Frankel L.K., 2001. Isolation of lumenal proteins from spinach thylakoid membranes by Triton X-114 phase partitioning. Biochimica et Biophysica Acta-Bioenergetics 1503 (3): 350-356

Bumba L., Tichy M., Dobakova M., Komenda J., Vacha F., 2005. Localization of the PsbH subunit in photosystem II from the Synechocystis 6803 using the His-tagged Ni-NTA Nanogold labeling. Journal of Structural Biology 152 (1): 28-35

Engelman D.M., 2005. Membranes are more than fluid mosaics. Nature, 486, 578-580

Evans J.N.S, 1995. Biomolecular NMR spectroscopy, Oxford University Press.

Grotjohann I., Fromme P., 2005. Structure of cyanobacterial Photosystem I. Photosynthesis Research 85 (1): 51-72

Grubmüller H., Tavan P., 1994. Molecular dynamics of conformational substates for a simplified protein model. *J. Chem. Phys.* 101:5047-5057

Hager A., 1996. Die Zusammenhänge zwischen lichtinduzierten Xantophyll- Umwandlungen und Hill Reaktion. Ber. deutsch botan. Gesell. 79:94-107

Jabri E., Carr M.B., Hausinger R.P., Karplus P.A., 1995. The crystal-structure of urease from klebsiella-aerogenes. Science 268 (5213): 998-1004

Jönsson B., Wennerström B., 1983. Image-charge forces in phospoholipid bilayer systém, J. chem. Soc Faraday Trans. II. :19-35

Kaftan D., Brumfeld V., Nevo R., Scherz A., Reich Z., 2002. From chloroplasts to photosystems: in situ scanning force microscopy on intact thylakoid membranes. EMBO Journal 21 (22): 6146-6153

Kern J., Loll B., Zouni A., Saenger W., Irrgang K.D., Biesiadka J., 2005. Cyanobacterial Photosystem II at 3.2 angstrom resolution - the plastoquinone binding pockets. Photosynthesis Research 84 (1-3): 153-159

Kim E.H., Chow W.S., Horton P., Anderson J.M., 2005. Entropy-assisted stacking of thylakoid membranes. Biochimica et Biophysica Acta-Bioenergetics 1708 (2): 187-195

Komenda J., 2005. Autotrophic cells of the Synechocystis psbH deletion mutant are deficient in synthesis of CP47 and accumulate inactive PSII core complexes. Photosynthesis Research 85 (2): 161-167

Komenda J., Stys D., Lupinkova L., 2003. The PsbH protein of photosystem 2. Photosynthetica 41 (1): 1-7

Komenda, J., Tichý, M., Eichacker, L.A., 2005. The PsbH protein is associated with the inner antenna CP47 and facilitates D1 processing and incorporation into Photosystem II in the cyanobacterium Synechocystis PCC 6803. Plant Cell Physiol. 46, 1477–1483

Krieger E., Darden T., Nabuurs S. Finkelstein B.A., Vriend G., Making optimal use of empirical energy functions: force-field parametrisation in crystal space. Proteins: Struct. Funct. Bioinform. 57: 678-683, 2004

Kuhlbrandt W., Wang D.N., Fujiyoshi Y., 1994. Atomic model of plant light-harvesting complex by electron crystallography. Nature 367 (6464): 614-621

Laskowski R.A., MacArthur M-W., Moss D.S. and Thornton J.M. Procheck – a program to check the stereochemical quality of protein structures, J. Appl. Crystal. 26, 283-291, 1993.

Levinthal, 1968. Are there pathways for protein folding? J. Chim. Phys. 65, 44-45

Lindahl E., Edholm O., 2000. Mesoscopic undulations and thickness fluctuations in lipid bilayers from molecular dynamics simulations. Biophysical Journal 79 (1): 426-433

Lindahl E., Edholm O., 2000. Spatial and energetic-entropic decomposition of surface tension in lipid bilayers from molecular dynamics simulations Journal of Chemical Physics 113 (9): 3882-3893

Liu Z.F., Yan H.C., Wang K.B., Kuang T.Y., Zhang J.P., Gui L.L., An X.M., Chang W.R., 2004. Crystal structure of spinach major light-harvesting complex at 2.72 angstrom resolution. Nature 428 (6980): 287-292

Marsh D., Pali T., 2004. The protein-lipid interface: perspectives from magnetic resonance and crystal structures. Biochimica et Biophysica Acta-Biomembranes 1666 (1-2): 118-141

McCammon J.A. a Harvey S.C., 1987. Dynamics of proteins and nucleic acids, Cambridge University Press, Cambridge, UK.

Nilsson A., Stys D., Drakenberg T., Spangfort M.D., Forsen S., Allen J.F., 1997. Phosphorylation controls the three-dimensional structure of

plant light harvesting complex II. Journal of Biological Chemistry 272 (29): 18350-18357

Nussberger S., Dorr K., Wang D.N., Kuhlbrandt W., 1993. Lipid-protein interactions in crystals of plant light-harvesting complex. Journal of Molecular Biology 234 (2): 347-356

Ort D.R. and Yocum C.F., 1996, Oxygenic Photosynthesis: The Light reaction, Kluwer Acad. Publ. ISBN 0-7923-3684-4.

Pali T., Garab G., Horvath L.I., Kota Z., 2003. Functional significance of the lipid-protein interface in photosynthetic membranes. Cellular and Molecular Life Sciences 60 (8): 1591-1606

Rintamaki E., Salonen M., Suoranta U.M., Carlberg I., Andersson B., Aro E.M., 1997. Phosphorylation of light-harvesting complex II and photosystem II core proteins shows different irradiance-dependent regulation in vivo - Application of phosphothreonine antibodies to analysis of thylakoid phosphoproteins. Journal of Biological Chemistry 272 (48): 30476-30482

Roosild T.P., Greenwald J., Vega M., Castronovo S., Riek R., Choe S., 2005. NMR structure of Mistic, a membrane-integrating protein for membrane protein expression. Science 307 (5713): 1317-1321

Sackmann E., 1990. Molecular and global structure and dynamics of membranes and lipid bilayers. Canadian Journal of Physics 68 (9): 999-1012

Staehelin L.A., 2003. Chloroplast structure: from chlorophyll granules to supra-molecular architecture of thylakoid membranes. Photosynthesis Research 76 (1-3): 185-196

Standfuss J., Kuhlbrandt W., 2004. The three isoforms of the light-harvesting complex II - Spectroscopic features, trimer formation, and functional roles. Journal of Biological Chemistry 279 (35): 36884-36891

Stefansson H., Wollenberger L., Yu S.G., Albertsson P.A., 1995. Phosphorylation of thylakoids and isolated subthylakoid vesicles derived from different structural domains of the thylakoid membrane from spinach chloroplast. Biochimica et Biophysica Acta-Bioenergetics 1231 (3): 323-334

Stys D., 1995. Stacking and separation of photosystem I and photosystem II in plant thylakoid membranes: A physico-chemical view. Physiologia Plantarum 95 (4): 651-657

Stys D., Siffel P., Hunalova I., Nebesarova J., 1999. The relation between changes in non-photochemical quenching, low temperature fluorescence emission, and membrane ultrastructure upon binding of polyionic compounds and fragments of light-harvesting complex 2. Photosynthetica 37 (2): 325-334

Stys D., Stancek M., Cheng L.L., Allen J.F., 1995. Complex-formation in plant thylakoid membranes - competition studies on membrane-protein interactions using synthetic peptide-fragments. Photosynthesis Research 44 (3): 277-285

Tanaka M., Sackmann E., 2005. Polymer-supported membranes as models of the cell surface. Nature 437 (7059): 656-663

Vacha F., Bumba L., Kaftan D., Vacha M., 2005. Microscopy and single molecule detection in photosynthesis. Micron 36 (6): 483-502

van der Holde K.E., Johnson W.C., Ho P.S., 2006. Principles of Physical Biochemistry, Pearson Prentice Hall

van Gunsteren W.F., Mark A.E., 1998. Validation of molecular dynamics simulation. Journal of Chemical Physics 108 (15): 6109-6116

Venturoli M., Smit B., Sperotto M.M., 2005. Simulation studies of protein-induced bilayer deformations, and lipid-induced protein tilting, on a mesoscopic model for lipid bilayers with embedded proteins. Biophysical Journal 88 (3): 1778-1798

Venturoli M., Smit B., Sperotto M.M., 2005. Simulation studies of protein-induced bilayer deformations, and lipid-induced protein tilting, on a mesoscopic model for lipid bilayers with embedded proteins. Biophysical Journal 88 (3): 1778-1798

Veverka V., Hrabal R., Durchan M., Stys D., 2000. Studies of phospholipid binding to N-terminal domain of membrane protein light-harvesting complex II Journal of Molecular Structure 523: 281-287

5. Shrnutí článků přiložených k této práci

Články shrnují jednu z experimentálních linií, jíž jsem se v posledních letech věnoval. Cílem bylo objasnění interakcí, které vedou k formování architektury thylakoidních membrán. V letech 1993-1995 jsme s kolegy na Katedře biologie rostlinné buňky na Univerzitě v Lundu zkoumali regulace funkce thylakoidních membrán proteinovou fosforylací. Cílem bylo zjistit, jaké změny struktury vyvolává fosforylace v nejvýznamnějších proteinech, které se na regulaci podíleji, světlosběrném komplexu 2 a PsbH. Jinými slovy, cílem bylo zjistit, jaké interakce se mění při této vazbě. První krok byl udělán s využitím biochemických metod, kdy jsme studovali vliv N-koncové domény LHCII na aktivitu specifických enzymů: kinázy, která katalyzuje vazbu fosfátové skupiny na protein, a fosfatázy, která naopak fosfátovou skupinu odštěpuje.

Článek č. 1 - Cheng a spol. 1995, - popisuje získání základních materiálů pro další práci, chemickou syntézu N-koncového peptidu z proteinu LHCII ve fosforylované a nefosforylované formě. Dále jsou zde popsány základní experimenty, které ukazují nespecificitu enzymu fosfatázy. Dokázali jsme experimentálně, že pokud syntetický peptid o sekvenci stejné jako má N-koncová doména LHCII fosforylujeme pomocí izolovaných thylakoidních membrán, tento peptid může sloužit jako substrát pro fosfatázu vázanou na membránu. Takto fosforylovaný peptid byl defosforylován mnohem pomaleji než jednotlivé proteiny vázané v membráně. Naproti tomu syntetický peptidový analog N-koncové domény LHCII zpomaloval defosforylaci všech membránových

fosfoproteinů. To ukazovalo, že membránově vázaná fosfatáza nebo fosfatázy nemá nebo nemají specificitu pro určitou proteinovou sekvenci. (Na tomto článku se autor podílel jako jeden ze dvou hlavních experimentátorů a přispěl významně i k jeho sepsání, 35%)

Článek č. 2 – Štys a spol. 1995, ukazuje, že proteiny LHCII a PsbH se podílejí na dvou odlišných regulačních procesech. Původním cílem studie publikované v tomto článku bylo zjistit, zda peptid, který obsahuje sekvenci odpovídající fosforylačnímu místu LHCII, může blokovat zpětnou vazbu LHCII do membránových komplexů. Proto byly navozeny podmínky, za nichž dochází k fosforylaci LHCII a sledovalo se, jak se mění tvar spekter nízkoteplotní fluorescence. Touto metodou lze relativně citlivě sledovat změny ve složení komplexů v thylakoidní membráně, jen obtížně však lze tyto dílčí změny přiřadit jednotlivým proteinům a jejich komplexům. Přesto se podařilo dokázat, že při zablokování vazebných míst peptidovým analogem LHCII se ve spektru objevuje mnohem výraznější zastoupení maxima při 715 nm. Toto maximum bývá připisováno volnému LHCII, vyskytuje se však i v různým způsobem poškozených membránách. V případě našich experimentů se kontrolní vzorky chovaly jako nepoškozené membrány, čímž se pravděpodobnost naší identifikace tohoto maxima zvýšila. Mnohem zajímavější však byl poznatek, který byl v tomto článku získán více-méně jako okrajový. Snažili jsme se zjistit, jak probíhá fosforylace LHCII a dalších proteinů v časových škálách, v nichž jsme pracovali. Ukázalo se, že za všeobecně akceptovaných podmínek, za nichž se provádí většina experimentů, dochází k rychlému nárůstu fosforylace

všech proteinů v prvních dvaceti minutách. To jsou časy, při nichž se zastavuje většina běžných experimentů. Po této době začala fosforylace LHCII klesat, fosforylace většiny proteinů se zastavila – zřejmě díky saturaci – a stoupala jedině fosforylace PsbH. Je tedy zřejmé, že role LHCII a PsbH v regulaci struktury a funkce thylakoidních membrán je odlišná a dokonce, že v časech delších než 20 minut za námi nastavených podmínek, není ani klíčová. Tento poznatek byl v dalších letech potvrzen mnoha autory, dodnes však nikdo nepátral po možných molekulárních principech této odlišnosti zejména proto, že nastal odklon od biochemického přístupu k problému a převážilo jeho studium v intaktních buňkách *in vivo*. Dále se ukázalo, že v zásadě nikdo se nikdy nezabýval otázkou, jaká je efektivní koncentrace druhého substrátu fosforylační reakce (vedle proteinu), totiž ATP. Tyto experimenty jsem provedl a ukázalo se, že právě koncentrace ATP limituje rychlost fosforylace LHCII. Bohužel se mi již tyto výsledky nepodařilo zopakovat a publikovat, protože jsem svůj pobyt na univerzitě v Lundu ukončil a v Třeboni pro tyto experimenty nebyly podmínky. (Na této práci jsem se podílel jako hlavní experimentátor spolu se studentem bakalářského studia Martinem Stančekem z Bratislavy, práci jsem celou sepsal, 80%).

Článek č. 3 - Štys 1995a, shrnuje dosavadní znalosti o možných principech regulace struktury a funkce membrán na molekulární úrovni. Hlavním cílem tohoto přehledového článku bylo zdůraznit (tehdy) poslední experimentální výsledky a konfrontovat je s hypotézami, které byly rozvíjeny v tehdy začínajícím směru studia membránových raftů,

fázových rozhraní v lipidových směsích a interakcí v rámci membránové lamely. Bylo konstatováno, že mechanismus na jehož základě dochází k formování membránových lamel, je studován již od roku 1982, kdy byla Barberem navržena hypotéza, která vycházela z klasické teorie DLVO, popisující chování koloidních částic. Proti ní byla postavena hypotéza specifických interakcí vyslovená Allenem 1992. Z experimentů však bylo zřejmé, že vliv iontů není možné vyloučit. Dosavadní hypotézy úplně opomíjely vliv protein-lipidových interakcí na rozdělení lipid-proteinových domén a možný vliv sterického omezení pro přiblížení membránových lamel dostatečně blízko, aby mohlo dojít ke vzniku jejich atrakce vlivem iontů nebo van der Waalsových sil. Bylo navrženo několik experimentů, které by navržené hypotézy mohly vyvrátit, čímž byl více-méně stanoven další experimentální plán. (Na článku jsem jediným autorem a je 100% mou autorskou prací.)

Článek č. 4, Štys a spol. 1995b, kromě analýzy strukturních změn způsobených fosforylací N-koncové domény LHCII obsahuje také jinde nepublikovanou titraci fosforylovaného peptidového fragmentu N-koncové domény LHCII hořečnatými ionty. Vazba byla sledována málo užívanou metodou NMR spektroskopie hořečnatých iontů, kdy se využívá sledování změn tvaru spektra kvadrupolárního jádra. Zjistili jsme, že vazebná konstanta má hodnotu 110 M^{-1}. To je sice méně než například u kaseinu nebo jiných fosfát-vážících peptidů (250-25000 M^{-1}), tam se jedná o vazbu do specifického vazebného místa s řadou fosfátových skupin, ale je to přibližně o řád více než u fosfátových skupin vázaných na lipidy nebo peptidy. Tím se zcela mění pohled na

roli fosfátové skupiny při vazbě na LHCII. Na rozdíl od běžného pohledu založeného na vzniku elektrostatického odpuzování, způsobeného vnesenou nabitou fosfátovou skupinou nebo konformační změnou (která je ovšem samozřejmá), může jít i o vznik specifického vazebného místa pro iont. To pak může ovlivnit jak specifickou vazbu proteinu na další proteiny, tak nespecifickou atrakci zprostředkovanou iontovými silami. (Výsledky uvedené v práci jsme experimentálně vytvořili s Torbjornem Drakenbergem, ostatní spoluautoři přispívali k diskusi výsledků, 60%)

Článek č. 5 Nilsson et al. 1997, již dává první přiblížení k strukturnímu základu regulace. Klíčovým poznatkem bylo že N-koncová doména má ve fosforylovaném stavu tendenci k agregaci. Experimenty byly prováděny na peptidu, který obsahoval pouze fosforylační místo a to ve fosforylovaném a nefosforylovaném stavu. Používali jsme metody strukturního stanovení a to pomocí spektroskopie cirkulárního dichroismu a NMR spektroskopie. V NMR spektroskopii se ukázaly jasné rozdíly ve struktuře nefosforylovaného peptidu – ta odpovídala volnému peptidu v roztoku bez tendence zaujímat specifickou konformaci – a fosforylovaného peptidu, kde se objevovalo mnohem více signálů, než by bylo možno přiřadit peptidu o 15 aminokyselinách. Zároveň se ukazovalo, že přinejmenším určitá část peptidu zaujímá velmi přesně definovanou a dlouhodobě stabilní konformaci, což dokonce komplikovalo navržení optimálních experimentů pro NMR spektroskopii. V době, kdy se experimenty prováděly, byl tento výsledek obtížně vysvětlitelný. S rostoucí znalostí struktur fosforylovaných

proteinů se ukázalo, že velká a nabitá fosfátová skupina po zavedení do proteinu vždy vytváří vazbu se sousedními NH skupinami hlavního řetězce. Tím je také možno vysvětlit, proč je fosfátová skupina velmi často využívána v různých regulačních procesech. V našem případě se ukázalo, že nejpravděpodobnějším, i když úplně nepotvrzeným, vysvětlením pro strukturní změnu mezi fosforylovaným a nefosforylovaným peptidem je zvýšení agregace v případě fosforylované formy. Pro vlastní vysvětlení mechanismu měl tento výsledek jen dílčí význam. (Podílel jsem se na přípravě a měření všech experimentů s výjimkou infračervených spekter a napsal jsme i podstatnou část článku, 30%).

V další etapě jsem se snažil oddělit a experimentálně charakterizovat od sebe jednotlivé jevy, jejichž vliv na formování thylakoidních membrán jsem předpokládal.

Článek č. 6 Štys a spol. 1999 experimentálně dokazuje odlišnosti ve vlivu polyiontů a specificky interagujících N-koncových peptidů na organizaci thylakoidních membrán. Hlavním cílem bylo zjistit, jakou část změn v thylakoidní membráně představují specifické interakce mezi LHCII a ostatními proteiny a jakou část lze připsat nespecifické atrakci způsobené vazbou polyiontu. Dalším experimentálním testem bylo použití alifatických diaminů různé délky uhlíkového řetězce, které měly objasnit, zda při adhezi membránových lamel hraje roli vzdálenost mezi lamelami. Byly využity tři metody detekce stavu membrán: elektronová mikroskopie, nizkoteplotní fluorescenční spektroskopie a nefotochemické zhášení. Bylo zjištěno, že vazba peptidů na membránu

je specifická a že chování membrán je odlišné i při přídavku různých diaminů. (Provedl jsem sám převážnou část experimentů kromě elektronové mikroskopie a článek jsem sám sepsal, 80%).

Článek č. 7 Veverka a spol. 2000 představuje nejzazší experimentální přiblížení k pochopení interakce N-koncové domény LHCII s lipidovou dvojvrstvou. Byly experimentálně identifikovány ty protony, které se přímo podílejí na interakci s fosfatidylglycerolem. Rychlost výměny mezi vázanou a volnou formou však neumožnila stanovení trojrozměrné struktury vázané formy. (Navrhl jsem většinu experimentů, podílel se na jejich provádění i zpracování dat, článek jsem z větší části sám sepsal, 40%).

Článek 8 Komenda a spol. 2003 je shrnutím poznatků o proteinu PsbH, přičemž je poprvé vyslovena hypotéza, že PsbH je zodpovědný za správné sestavování komplexů fotosyntetických reakčních center. Obsah této práce se do značné míry shoduje s příslušnou kapitolou úvodu této práce. (25% podíl).

Článek 9, Halbhuber a spol. 2003 popisuje novou metodu získávání membránových proteinů heterologní expresí v bakterii *E. coli* a jeho využití pro produkci proteinu PsbH. Metoda je založena na spojení malého membránového proteinu do jednoho genového konstruktu s velkým rozpustným proteinem glutathion transferázou. Vzniklý fúzní protein se pak chová jako velký rozpustný protein, který se jen z velmi malé části integruje do membrány hostitelského organismu. Díky tomu není buňka okamžitě po indukci produkce proteinu poškozena ve svých funkcích, jak je tomu v případě, kdy se membránový protein produkuje

samotný a integruje se do membrány. (Konstrukt byl navržen a realizován K. Alexcievem, biochemická izolace byla navržena E.Thulin, další experimenty jsme prováděli a optimalizovali s mými studenty Z. Halbhuberem a Z. Petrmichlovou, vlastní práce asi 25%.)

Článek 10, Štys a spol. 2005 popisuje model struktury PsbH v detergentovém roztoku. Struktura byla vypočítána pomocí molekulové dynamiky a odpovídá experimentálnímu stanovení struktury proteinu pomocí cirkulárního dichroismu. V článku se popisuje příprava proteinu značeného izotopem ^{15}N, který má spinové kvantové číslo ½ a může být tedy využit v klasických experimentech, které dávají spektra vysokého rozlišení. Dále se popisují výsledky spektroskopie CD detergentového roztoku proteinu, kdy se ukázalo, že protein se sbaluje autonomně a že k jeho sbalení není třeba ani aktivní integrace do membrány, ani přítomnost dalších proteinů. Spektrum NMR také ukázalo, že v proteinu je možno jednotlivě identifikovat každý aminokyselinový zbytek, což ukázalo, že se jedná o unikátní konformaci proteinu, který se nachází v monomerním stavu. Tyto experimentální údaje byly podkladem pro výpočet struktury proteinu, který byl veden jako výpočet struktur samotné C-koncové a N-koncové mimomembránové domény. Tyto domény byly následně napojeny na model transmembránového helixu připravený metodou molekulového nahrazování na základě známé struktury transmembránového helixu stejné délky. Vypočtené hodnoty byly ve shodě s experimentem CD. (Podílel jsem se na přípravě proteinu, návrhu experimentů i jejich vyhodnocování a přípravě dat k výpočtu - 30%)

Článek 11 Štys a spol. 2006 (rukopis) popisuje simulaci reálné struktury PsbH v lipidové membráně, tvořené jiným než vlastním lipidem. Cílem této simulace bylo posoudit tu část lipid-proteinové interakce, která není specifická pro daný protein. V článku jsou zahrnuta i další měření metodou cirkulárního dichroismu, kdy se ukázalo, že při pokusech o rekonstituci proteinu do lipidové dvojvrstvy dochází k tvorbě struktur většího rozsahu. Takové struktury byly pozorovány i ve směsi detegentu a lipidového extraktu z celých thylakoidních membrány a byly doprovázeny vznikem anomálního signálu v nízkoteplotní fluorescenci chlorofylu. Nebyly však nikdy pozorovány ve směsi detergentu a jednotlivého separovaného lipidu. Byly však pozorovány ve spektrech liposomů obsahujících PsbH a jednotlivé lipidy, které vytvářejí dvojvrstvy. Jedná se s největší pravděpodobností o vznik lipidových struktur, které vznikají ve směsích lipidů při určitém poměru složek ve směsi a jejichž formování je indukováno i proteinem PsbH. Měření metodou NMR při rekonstituci ukazovalo, že při přídavku lipidů nevznikají žádné komplexy lipid-protein, které by ukazovaly na stechiometrii mezi 1:1 až 1:15. Ve spektrech se vždy vyskytovaly pouze signály odpovídající proteinu v roztoku a ty se při překročení určité koncentrace lipidu začaly ztrácet. Tento výsledek ukazoval na tvorbu agregátů vysoké molekulové hmotnosti, které jsou pro velkou šíři spektrálních čar nepozorovatelné. To je vysvětlitelné pouze tím, že PsbH nevytváří žádné specifické pevné komplexy s lipidy, které by existovaly v micelách v nepřítomnosti membrány, ale že s největší pravděpodobností ve všech lipidových dvojvrstvách vytváří domény,

které se pak projevují dlouhovlnným signálem v spektru CD. Pro vysvětlení těchto jevů bylo nutno přistoupit k simulaci proteinu v membránovém prostředí. K tomu byl využit model popsaný v článku 10. V připravené lipidové membráně byl vytvořen otvor o velikosti, která právě odpovídala helixu PsbH a do něj byl tento helix vložen. Molekulárně dynamická simulace ukázala, že mimomembránové domény proteinu se velmi rychle integrují do lipid-proteinové dvojvrstvy a po určité době se ustálí i určitý počet lipidů, které těsně obklopují protein ponořený do membrány. Zdá se, že tento modelový experiment naznačuje, že navržená hypotéza, že protein PsbH indukuje tvorbu lipidových domén, je pravděpodobná. (Podílel jsem se na přípravě proteinu, návrhu experimentů i jejich vyhodnocování a přípravě dat k výpočtu a jeho vyhodnocování - 35%)

PHYSIOLOGIA PLANTARUM 93: 173–178. 1995
Printed in Denmark – all rights reserved

Copyright © Physiologia Plantarum 1995
ISSN 0031-9317

Effects of synthetic peptides on thylakoid phosphoprotein phosphatase reactions

Läling Cheng, Dalibor Stys and John F. Allen

Cheng, L., Stys, D. and Allen, J. F. 1995. Effects of synthetic peptides on thylakoid phosphoprotein phosphatase reactions. – Physiol. Plant. 93: 173–178.

A synthetic peptide analogue of the phosphorylation site of LHC II, when phosphorylated by thylakoid membranes, served as a substrate for the thylakoid phosphoprotein phosphatase. The phosphopeptide became dephosphorylated at a low rate, comparable to that of the 9 kDa phosphoprotein. Phospho-LHC II itself became dephosphorylated much more rapidly, at a rate unaffected by endogenous phosphorylation of the peptide. Endogenous phosphorylation of the peptide was also without effect on other thylakoid protein phosphorylation and dephosphorylation reactions. In contrast, dephosphorylation of many thylakoid phosphoproteins was inhibited by addition of a pure, chemically-synthesised phosphopeptide analogue of phospho-LHC II. This result suggests that at least one thylakoid phosphoprotein phosphatase exhibits a broad substrate specificity. The results indicate that any one of a number of amino acid sequences can give a phosphoprotein configuration that is recognised by a single phosphatase.

Key words – Chloroplast thylakoids, LHC II, molecular recognition, phosphoprotein phosphatase, protein kinase, synthetic phosphopeptide.

L. Cheng, D. Stys and J. F. Allen (corresponding author), Plant Cell Biology, Lund Univ., Box 7007, S-220 07 Lund, Sweden.

This paper is part of the contributions to a Plant Cell Biology Workshop on Thylakoid Protein Phosphorylation, held at Lund University, Sweden, 27–29 March, 1994.

Introduction

Reversible protein phosphorylation regulates protein function in many aspects of prokaryotic and eukaryotic metabolism, gene expression and response to environmental change (Edelman et al. 1987). Protein phosphorylation is catalysed by protein kinases and dephosphorylation by protein phosphatases. In plants, a number of protein phosphorylation systems have been found (Ranjeva and Boudet 1987). One of these is the chloroplast thylakoid system that regulates photosynthesis (Bennett 1991, Allen 1992). Phosphorylation of thylakoid proteins is stimulated by light (Bennett 1979) and when phosphorylated material is then placed in the dark, it becomes dephosphorylated (Bennett 1980). The phosphatase that catalyses dephosphorylation of thylakoid phosphoproteins is membrane bound (Bennett 1980) and redox-independent (Silverstein et al. 1993). The enzyme was found to be inhibited by classical phosphatase inhibitors fluoride (Bennett 1980) and molybdate (Owens and Ohad 1982) but not by okadaic acid (Mackintosh et al. 1991, Sun and Markwell 1992), an inhibitor of specific mammalian phosphatases (Cohen et al. 1990).

A central question is how protein kinases and phosphatases recognise their diverse protein substrates. Since structural information is available for only a handful of protein substrates (Johnson and Barford 1993), synthetic peptides have played an important role in assessing the specificity and recognition features of protein kinases and phosphatases (Kemp and Pearson 1990, Kennelly and Krebs 1991). Synthetic phosphopeptides have been used to distinguish different protein phosphatases (Donella-Deana et al. 1990, 1991) and as model substrates to investigate their specificity (Agostinis et al. 1987, 1990),

Received 27 June, 1994; revised 26 August, 1994

providing clues to sequence requirements for protein phosphatase recognition. For the thylakoid phosphoprotein phosphatase, synthetic phosphopeptides mimicking the N-terminal phosphorylation site of the LHC II have been shown to act as substrates of a phosphoprotein phosphatase. Dephosphorylation of phosphopeptides by thylakoid membranes was similar to dephosphorylation of endogenous LHC II in its pH-dependence profile, in its sensitivity to inhibitors, and in its divalent cation requirement (Sun et al. 1993). To test further the regulatory properties of thylakoid phosphoprotein phosphatase and the structural requirements of its substrates, we used both unphosphorylated and phosphorylated synthetic peptides. Our results demonstrate that dephosphorylation of a phosphopeptide that has been phosphorylated by a thylakoid-bound protein kinase proceeds at a much lower rate than that of phospho-LHC II. We also show that the presence of endogenously phosphorylated peptide has no effect on the dephosphorylation of LHC II or other thylakoid phosphoproteins. However, the corresponding chemically-synthesised phosphopeptide exhibits an inhibitory effect on all phosphoprotein phosphatase reactions. We suggest that any one of a number of amino acid sequences can give a phosphoprotein configuration that is sufficient for recognition of the phosphoprotein by a single phosphatase. However, the configuration of other domains in the native protein, remote from the phosphorylation site, may also be essential for efficient catalysis. The possible regulatory role of molecular recognition between thylakoid phosphoprotein phosphatase and its substrates is discussed.

Abbreviations – Chl, chlorophyll; CP43, PS II (psbC) polypeptide; D1 and D2, 31 (psbA) and 32 (psbD) kDa PS II reaction centre polypeptides; DCC, dicyclohexylcarbodiimide; HF, hydrogen fluoride; HOBt, 1-hydroxybenzotriazole; LHC II, light harvesting complex II; 9 kDa, PS II (psbH) polypeptide; PQ, plastoquinone; PS I and II, photosystem I and II; SDS-PAGE, sodium dodecyl sulphate-polyacrylamide gel electrophoresis.

Materials and methods

Plant material

Pea seedlings (*Pisum sativum* L. cv. Sockerärt de grace) were grown at 20°C with a 12 h light period. Leaves were harvested during the light period 14–16 days after sowing.

Preparation of the synthetic peptide

A 15 amino-acid synthetic peptide corresponding to an N-terminal fragment of pea LHC II (RKSATTKKVASSGSP) and its phosphorylated form (RKSAT[PO_4]TKKVASSGSP) were synthesised by a solid phase, t-Boc strategy according to Barany and Merrifield (1980) and Grehn et al. (1987). The phosphopeptide was synthesized using the standard Boc-protocol on an ABI 430A solid phase peptide synthesizer. In place of phosphorylated threonine in the synthetic peptide, a Boc-Thr[$OPO(OPh)_2$] was incorporated. Boc-Thr[$OPO(OPh)_2$] was obtained by phosphorylating Boc-Thr-OBn with diphenylphosphochloridate according to Perich (1991) and then hydrogenated using 5% Pd/C in ethyl acetate:acetic acid (25:1) for 2 h. The phosphothreonine was coupled twice for 3 h using DCC and HOBt. The peptide was cleaved from the resin with HF:Anisol (9:1) for one hour at −5°C. After washing the resin with ether and extracting the peptide with 30% acetic acid, the peptide was lyophilized. The product was then hydrogenated in the solution containing 200 mg peptides, 185 mg platinum oxide (PtO_2) in H_2 at twice atmospheric pressure in 12 ml 80% acetic acid for 4 days. The product was purified on a 250 × 20 mm Kromasil 5 µm, C8 column with 1% TFA-acetonitrile gradient. The purity of the phosphopeptide was >90% as revealed by HPLC and mass spectroscopy (not shown). The correct mass according to mass spectroscopy was 1585.5 Da (theoretical mass: 1584.7 Da). High specific activity [γ-^{32}P]ATP was obtained from Amersham. Other chemical reagents were purchased from Sigma (St. Louis, MO, USA).

In vitro phosphorylation and dephosphorylation

Thylakoid membranes were isolated from pea chloroplasts by the method described in Harrison and Allen (1991) and then stored on ice in darkness for 60 min prior to radiolabelling. Phosphorylation of thylakoid membrane proteins and of the synthetic peptide was carried out by incubation of purified thylakoids at 0.2 mg Chl ml^{-1} together with 334 µ*M* synthetic peptide in a medium containing 0.1 *M* sorbitol, 50 m*M* HEPES (pH 7.6) and $MgCl_2$, NaCl, NH_4Cl, all at 5 m*M* and [γ-^{32}P]ATP (0.2 m*M*) at a molar activity of 3.7 TBq mol^{-1} at 22°C (Allen and Findlay 1986) and by illuminating the samples for 10 min with a desk-lamp giving a light intensity ~ 130 µmol m^{-2} s^{-1}. Dephosphorylation was obtained by incubation of the ^{32}P-labelled samples in darkness from 10 to 180 min with or without chemically-synthesised phosphopeptide (final concentration 167 µ*M*). Dephosphorylation time-courses were started by switching off the light, and samples (100 µl) were withdrawn at intervals and immediately precipitated by mixing with 0.8 ml acetone (pre-cooled at −20°C). The sample at zero time served as the control (100% phosphorylation). The acetone suspension was stored on ice for at least 30 min before centrifugation at 13 000 *g* for 2.5 min. The protein pellets were prepared for gel electrophoresis as described below.

Polyacrylamide-gel electrophoresis

Samples were solubilized in 62.5 m*M* Tris-HCl (pH 6.8) buffer, containing 12% glycerol, 5% 2-mercaptoethanol, 4.5% SDS, and 0.01% bromophenolblue by vortexing and incubation at room temperature for 2 h until the pellets were dissolved. The samples were heated to 70°C for 5 min, and centrifuged at 13 000 *g* for 5 min before loading on the slab gel. SDS-PAGE was performed on

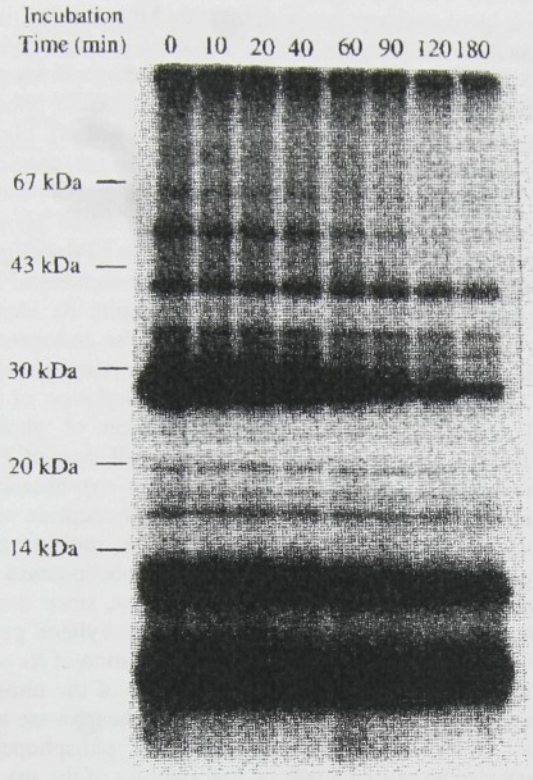

Fig. 3. SDS-PAGE phosphorimage of the time-course of dephosphorylation of both endogenously phosphorylated peptide and pea thylakoid phosphoproteins in presence of exogenous phosphopeptide. The ^{32}P labelled samples were incubated with 167 μM of exogenous phosphopeptide in darkness for 0, 10, 20, 40, 60, 90, 120 and 180 min. Stained gels for all the samples are identical (not shown). Tracks were loaded with protein equivalent to 2 µg chlorophyll.

protein in solution. Competition of a membrane protein with a soluble protein for the same binding site is incompletely understood. Nevertheless, other factors may be responsible for less efficient catalysis of the endogenously phosphorylated peptide by the thylakoid phosphoprotein phosphatase. These factors could include absence of other domains in the native protein, remote from the phosphorylated site, or a low stability of the proper configuration on the phosphopeptide.

The presence of endogenously phosphorylated peptide did not interfere with the dephosphorylation of phospho-LHC II. Similar results were observed on the dephosphorylation of most other thylakoid phosphoproteins (Fig. 2). The results show that the thylakoid phosphoprotein phosphatase is activated not only by its native substrates, but also by an exogenous product of the kinase reaction. On the other hand, although the total concentration of the phosphopeptide is higher than those of the phosphoproteins (Fig. 1, Lane time 0), it does not compete significantly with them for the phosphatase. The difference between the phosphoproteins and the phosphopeptide in recognition by the phosphoprotein phosphatase may be responsible for their different rates of dephosphorylation.

Figure 3 shows a phosphorimage of SDS-PAGE fractionation of the time-course of dephosphorylation of both endogenously phosphorylated peptide and thylakoid phosphoproteins in presence of the chemically-synthesised phosphopeptide (RKSAT[PO_4]TKKVASSGSP). The chemically-synthesised phosphopeptide acts as a competitive inhibitor not only of phospho-LHC II, but also of all the thylakoid phosphoproteins (Cheng et al. 1994). By addition of the same phosphopeptide in the system with the endogenously phosphorylated peptide present, the dephosphorylation of most thylakoid phosphoproteins was inhibited (Fig. 4). The inhibitory effects are stronger on the rapidly dephosphorylated phosphoproteins such as LHC II and 56 kDa phosphoprotein compared to those slowly dephosphorylated phosphoproteins such as 9 kDa and endogenously phosphorylated peptide, the dephosphorylation of which were hardly detectable. However, the inhibitory effects of the chemically-synthesised phosphopeptide on the dephosphorylation of thylakoid phosphoproteins in the presence of endogenously phosphorylated peptide are slightly less compared with the dephosphorylation of thylakoid phosphoproteins in the absence of endogenously phosphorylated peptide. We have measured the concentration of the phosphorylated peptide in the solution of the endogenous peptide by HPLC. The chromatographic peak of the phosphopeptide was not detectable although the phosphorylated and unphosphorylated peptides were clearly

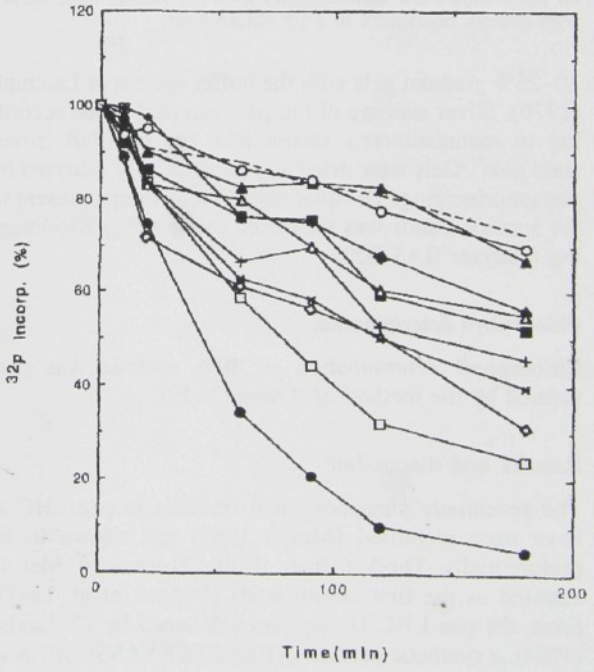

Fig. 4. Quantification of the ^{32}P labelling in specific bands of phosphorimage shown in Fig. 3. The sample incubated at zero time served as 100% ^{32}P incorporation. Peptide (- - -), LHC II (●), 9 kDa (○), CP43 (■), 56 kDa (□), 12 kDa (◇), 20 kDa (△), 18 kDa (▲), 16 kDa (◆), D1 (+), D2 (×).

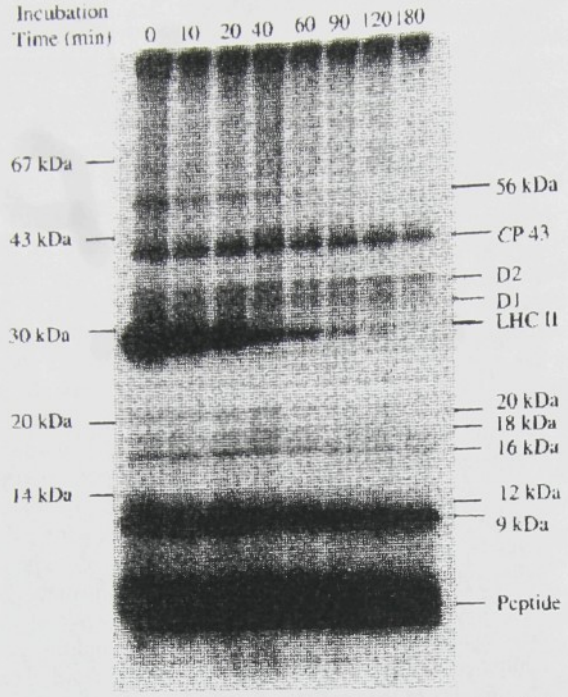

Fig. 1. SDS-PAGE phosphorimage of the time-course of dephosphorylation of both endogenously phosphorylated peptide and pea thylakoid phosphoproteins. Purified pea thylakoid membranes were incubated with the unphosphorylated peptide in a reaction medium with [γ-^{32}P]ATP, illuminated for 10 min. The ^{32}P labelled samples were subsequently incubated in darkness for 0, 10, 20, 40, 60, 90, 120 and 180 min. Stained gels for all the samples are identical (not shown). Tracks were loaded with protein equivalent to 2 µg chlorophyll.

10–25% gradient gels with the buffer system of Laemmli (1970). Silver staining of the gels was performed according to manufacturer's instructions for Bio-Rad 'silver stain plus'. Gels were dried and subsequently analysed by phosphorimaging. The quantity of radioisotope present in the specific bands was measured using a Fuji Bio-Imaging analyzer BAS 2000.

Chlorophyll determination

Chlorophyll determination in 80% acetone was performed by the method of Arnon (1949).

Results and discussion

The potentially phosphorylated residues in pea LHC II have been identified (Mullet 1983) and shown to be preferentially Thr-5 (Thr-6 if the N-terminal Met is counted as the first amino acid) (Bennett et al. 1987). From the pea LHC II sequences deduced by Cashmore (1984), a synthetic peptide (RKSATTKKVASSGSP) analogue of an N-terminal segment of LHC II and its phosphorylated form (RKSAT[PO$_4$]TKKVASSGSP) were synthesised. The unphosphorylated synthetic peptide was phosphorylated by a thylakoid protein kinase simultaneously with native thylakoid proteins when the peptide was incubated together with thylakoid membranes illuminated in the presence of [γ-^{32}P]ATP. Dephosphorylation of this phosphopeptide (here termed 'endogenously phosphorylated peptide') and of the other thylakoid phosphoproteins started when the light was switched off. Figure 1 is a phosphorimage of an SDS-PAGE gel showing a typical time-course of dephosphorylation of endogenously phosphorylated peptide and thylakoid phosphoproteins. The relative quantities of the ^{32}P-labelling in specific bands of the phosphorimage are shown in Fig. 2. As can be seen in Figs 1 and 2, despite its identical sequence with a fragment of LHC II, the endogenously phosphorylated peptide was dephosphorylated slowly, at a rate comparable to that of dephosphorylation of the 9 kDa phosphoprotein. Dephosphorylation of phospho-LHC II was much more rapid, with a half-time of 7 min, in agreement with results obtained in the absence of peptide (Cheng et al. 1994). The phosphopeptide served as a weak substrate for the phosphatase, indicating that the recognition features required by the phosphatase were present in the phosphopeptide. However, since dephosphorylation of the endogenously phosphorylated peptide was slow compared to the dephosphorylation of its parent protein LHC II, some structural feature of the phosphopeptide must be unfavourable for the phosphatase activity. Slower dephosphorylation of the phosphopeptide may also be caused either by low stability of the structure of the phosphopeptide or by a higher probability that membrane proteins interact with each other than with a

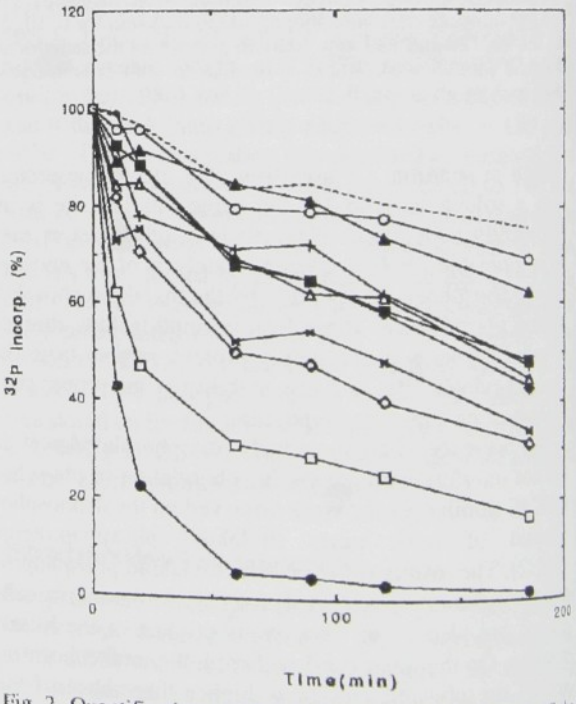

Fig. 2. Quantification of ^{32}P-labelling in specific bands of the phosphorimage shown in Fig. 1. The sample incubated at zero time served as 100% ^{32}P incorporation. Peptide (- - -), LHC II (●), 9 kDa (○), CP43 (■), 56 kDa (□), 12 kDa (◇), 20 kDa (△), 18 kDa (▲), 16 kDa (◆), D1 (+), D2 (×).

segment which regulates membrane adhesion (grana stacking) in chloroplasts. – J. Biol. Chem. 258: 9941–9948.
Owens, G. & Ohad, I. 1982. Phosphorylation of *Chlamydomonas reinhardtii* chloroplast membrane proteins in vivo and in *vitro*. – J. Biol. Chem. 93: 712–718.
Perich, J. W., Alewood, P. F. & Johns, R. B. 1991. Synthesis of casein-related peptides and phosphopeptides. VII* The efficient synthesis of ser(P)-containing peptides by the use of Boc-ser(PO_3R_2)-OH derivatives. – Aust. J. Chem. 44: 233–252.
Ranjeva, R. & Boudet, A. M. 1987. Phosphorylation of proteins in plants: regulatory effects and potential involvement in stimulus/response coupling. – Annu. Rev. Plant Physiol. 38: 73–93.
Silverstein, T., Cheng, L. & Allen, J. F. 1993. Chloroplast thylakoid protein phosphatase reactions are redox-independent and kinetically heterogeneous. – FEBS Lett. 334: 101–105.
Sun, G. & Markwell, J. 1992. Lack of types 1 and 2A protein serine (P)/threonine (P) phosphatase activities in chloroplasts. – Plant Physiol. 100: 620–624.
– , Sarath, G. & Markwell, J. 1993. Phosphopeptides as substrates for thylakoid protein phosphatase activity. – Arch. Biochem. Biophys. 304: 490–495.

Edited by C. H. Bornman

resolvable on the control assay (data not shown). The concentration of the phosphopeptide in the solution containing endogenously phosphorylated peptide is therefore negligible compared to that of the unphosphorylated peptide. This again supports the conclusion that the phosphopeptide is a weak substrate compared to the membrane phosphoproteins and is able to inhibit the phosphatase only at high concentration. We cannot exclude very limited feedback control of the phosphatase by the concentration of the substrate but our experiments make such control less probable.

In summary, our results show that the presence of the endogenously phosphorylated peptide served only as a weak substrate of the phosphatase, with a dephosphorylation rate similar to that of the 9 kDa phosphoprotein, which has a sequence at the phosphorylation site unrelated to that of LHC II (Michel and Bennett 1987) and the phosphopeptide. When the chemically-synthesised phosphopeptide was present at a concentration much higher than that of the endogenously phosphorylated peptide, it acted as a competitive inhibitor of the phosphatase, not only for dephosphorylation of LHC II but also for dephosphorylation of other thylakoid phosphoproteins. The results are in agreement with our previous observation and support the conclusion that at least one phosphoprotein phosphatase in thylakoid membranes exhibits a broad substrate specificity. The results indicate that any one of a number of amino acid sequences can give a phosphoprotein configuration that is sufficient for recognition of the phosphoprotein by a single phosphatase. However, the configuration of other domains remote from the phosphorylated site of the substrate are likely to be essential for efficient catalysis. The availability of phosphopeptides creates the possibility of using an artificial structure for specific detection and assay the thylakoid phosphoprotein phosphatase. Future experiments involving structural and enzymological characterisation of synthetic phosphopeptide analogues of the phosphorylation site of other thylakoid phosphoproteins as substrates for the thylakoid phosphoprotein phosphatase should clarify the general structural features required for substrate recognition.

Acknowledgments – We thank Dr Ivo Bláha for the unphosphorylated synthetic peptide and Dr Henry Franzén for the synthetic phosphopeptide. We also thank the Swedish Natural Science Research Council (NFR) and Per-Eric and Ulla Schyberg Foundation for research grants and NFR and Federation of European Biochemical Societies for fellowships to D.S.

References

Agostinis, P., Goris, J., Waelkens, E., Pinna, L. A., Marchiori, F. & Merlevede, W. 1987. Dephosphorylation of phosphoproteins and synthetic phosphopeptides. – J. Biol. Chem. 262: 1060–1064.

– , Goris, J., Pinna, L. A., Marchiori, F., Perich, J. W., Meyer, H. E. & Merlevede, W. 1990. Synthetic peptides as model substrates for the study of specificity of the polycation-stimulated protein phosphatases. – Eur. J. Biochem. 189: 235–241.

Allen, J. F. 1992. Protein phosphorylation in regulation of photosynthesis. – Biochim. Biophys. Acta 1098: 275–335.

– & Findlay, J. B. C. 1986. Amino acid composition of the 9 kDa phosphoprotein of pea thylakoids. – Biochem. Biophys. Res. Commun. 138: 146–152.

Arnon, D. I. 1949. Copper enzymes in chloroplasts. Polyphenoloxidases in *Beta vulgaris*. – Plant Physiol. 24: 1–15.

Barany, G. & Merrifield, R. B. 1980. Special methods in peptide synthesis. – *In* The Peptides (E. Gross and J. Meienhofer, eds), Vol. 2, pp. 1–284. Academic Press, New York, NY. ISBN 0-12-304202-X.

Bennett, J. 1979. Chloroplast phosphoproteins. The protein kinase of thylakoid membranes is light-dependent. – FEBS Lett. 103: 342–344.

– 1980. Chloroplast phosphoproteins. Evidence for a thylakoid-bound phosphoprotein phosphatase. – Eur. J. Biochem. 104: 85–89.

– 1991. Protein phosphorylation in green plant chloroplast. – Annu. Rev. Plant Physiol. Plant Mol. Biol. 42: 281–331.

– , Shaw, E. K. & Bakr, S. 1987. Phosphorylation of thylakoid proteins and synthetic peptide analogs. – FEBS Lett. 210: 22–26.

Cashmore, A. R. 1984. Structure and expression of a pea nuclear gene encoding a chlorophyll *a/b*-binding polypeptide. – Proc. Natl. Acad. Sci. USA 81: 2960–2964.

Cheng, L., Spangfort, M. D. & Allen, J. F. 1994. Substrate specificity and kinetics of thylakoid phosphoprotein phosphatase reactions. – Biochim. Biophys. Acta (In press).

Cohen, P., Holmes, C. F. B. & Tsukitani, Y. 1990. Okadaic acid: a new probe for the study of cellular regulation. – Trends Biochem. Sci. 15: 98–102.

Donella-Deana, A., Mac Gowan, C. H., Cohen, P., Marchiori, F., Meyer, H. E. & Pinna, L. A. 1990. An investigation of the substrate specificity of protein phosphatase 2C using synthetic peptide substrates; comparison with protein phosphatase 2A. – Biochim. Biophys. Acta 1051: 199–202.

– , Meyer, H. E. & Pinna, L. A. 1991. The use of phosphopeptides to distinguish between protein phosphatase and acid/alkaline phosphatase activities: opposite specificity toward phosphoseryl/phosphothreonyl substrates. – Biochim. Biophys. Acta 1094: 130–133.

Edelman, A. M., Blumenthal, D. K. & Krebs, E. G. 1987. Protein serine/threonine kinases. – Annu. Rev. Biochem. 56: 567–613.

Grehn, L., Fransson, B. & Ragnarsson, U. 1987. Synthesis of substrates of cyclic AMP-dependent protein kinase and use of their protected precursors for the convenient preparation of phosphoserine peptides. – J. Chem. Soc. Perkin Trans. I 529–535.

Harrison, M. A. & Allen, J. F. 1991. Light-dependent phosphorylation of photosystem II polypeptides maintains electron transport at high light intensity: separation from effects of phosphorylation of LHC-II. – Biochim. Biophys. Acta 1058: 289–296.

Johnson, L. N. & Barford, D. 1993. The effects of phosphorylation on the structure and function of proteins. – Annu. Rev. Biophys. Biomol. Struct. 22: 199–232.

Kemp, B. E. & Pearson, R. B. 1990. Protein kinase recognition sequence motifs. – Trends Biochem. Sci. 15: 342–346.

Kennelly, P. J. & Krebs, E. G. 1991. Consensus sequences as substrate specificity determinants for protein kinases and protein phosphatases. – J. Biol. Chem. 266: 15555–15558.

Laemmli, U. K. 1970. Cleavage of structural proteins during the assembly of the head of bacteriophage T4. – Nature 227: 680–685.

Mackintosh, C., Coggins, J. & Cohen, P. 1991. Plant protein phosphatases. – Biochem. J. 273: 733–738.

Michel, H. & Bennett, J. 1987. Identification of the phosphorylation site of an 8.3 kDa protein from photosystem II of spinach. – FEBS Lett. 212: 103–108.

Mullet, J. E. 1983. The amino acid sequence of the polypeptide

Photosynthesis Research 44: 277–285, 1995.
© 1995 *Kluwer Academic Publishers. Printed in the Netherlands.*

Regular paper

Complex formation in plant thylakoid membranes. Competition studies on membrane protein interactions using synthetic peptide fragments

Dalibor Stys, Martin Stancek[1], Luling Cheng & John F. Allen

Plant Cell Biology, Lund University, Box 7007, S-220 07 Lund, Sweden; [1]*Department of Molecular Genetics, Comenius University, Mlynská dolina B2, SK-842 15 Bratislava, Slovakia*

Received 13 October 1994; accepted in revised form 27 April 1995

Key words: light harvesting complex II, membrane proteins, macromolecular recognition, protein phosphorylation, excitation energy transfer, energy quenching, psb H

Abstract

Thylakoid membranes of pea were used to study competition between extra-membrane fragments and their parental membrane-bound proteins. Phosphorylated and unphosphorylated fragments of light harvesting complex II (LHC II) from higher plants were used to compete with LHC II for interactions with itself and with other thylakoid protein complexes. Effects of these peptide fragments of LHC II and of control peptides were followed by 80 K chlorophyll fluorescence spectroscopy of isolated thylakoids. The phosphorylated LHC II fragment competes with membrane-bound phosphoproteins in the phosphatase reaction. The same fragment accelerates the process of dark-to-light adaptation and decreases the rate of the light-to-dark adaptation when these are followed by fluorescence spectroscopy. In contrast, the non-phosphorylated LHC II peptide does not affect the rate of adaptation but produces results consistent with inhibition of formation of a quenching complex. In this quenching complex we propose that LHC II remains inaccessible to the LHC II kinase, explaining an observed decrease in LHC II phosphorylation in the later stages of the time-course of phosphorylation. The most conspicuous protein which is steadily phosphorylated during the time-course of phosphorylation is the 9 kDa (psbH) protein. The participation of the phosphorylated form of psbH in the quenching complex, where it is inaccessible to the phosphatase, may explain its anomalously low dephosphorylation. The significance of the proposed complex of LHC II with phospho-psbH is discussed.

Abbreviations: LHC II – light harvesting complex II; PS II – Photosystem II; PS I – Photosystem I

Introduction

Adaptation of chloroplast thylakoid membranes to changes in light intensity and light quality is accompanied by phosphorylation or dephosphorylation of several thylakoid proteins (Allen 1992). Most of these belong to Photosystem II (PS II). Membrane fractionation studies (Anderson and Andersson 1982; Kyle et al. 1984) are consistent with lateral movement of light harvesting complex II (LHC II) from PS II to PS I upon phosphorylation, but the productive binding of LHC II to PS I has not been consistently observed (Allen 1992). While most thylakoid protein kinase reactions are redox-dependent (Silverstein et al. 1993a), thylakoid protein phosphatase reactions are redox-independent and kinetically heterogeneous (Silverstein et al. 1993b). LHC II is dephosphorylated more rapidly than other proteins. The 9 kDa protein exhibits an extremely low rate of dephosphorylation (Allen and Findlay 1986; Cheng et al. 1994). Other phosphoproteins are dephosphorylated at various rates between these two extremes (Cheng et al. 1994). It has been shown by Demming et al. (1987) that changes in chlorophyll fluorescence are not in a simple relation to LHC II phosphorylation. The adaptation of thylakoid membranes by protein phosphorylation to changes in light conditions may then be a more complex process

than simple movement of LHC II proteins between PS II- and PS I-enriched domains.

Here we present results of low-temperature fluorescence spectroscopy which are consistent with formation of a quenching complex in which LHC II participates in its unphosphorylated form. Phosphorylation of LHC II reaches its maximum in an early stage after which LHC II becomes dephosphorylated and protected against further phosphorylation. This dephosphorylation of LHC II is accompanied by increasing phosphorylation of the 9 kDa phosphoprotein whereas the majority of other thylakoid phosphoproteins maintain a constant degree of phosphorylation. We therefore suggest that the quenching complex is formed between 9 kDa phosphoprotein in its phosphorylated form and LHC II in its unphosphorylated form.

Materials and methods

Peptide synthesis

Peptides were synthesized by a solid phase, t-Boc strategy (Barany and Merrifield 1980). The peptides RKSATTKKVASSGSP and SRPLSDQEKRKQISVRGLAGVENV were supplied by the Dr. Ivo Blaha group in the Institute of Organic Chemistry and Biochemistry, Prague. The phosphorylated peptide RKSA[T(PO_3)]TKKVASSGSP was synthesized by the same methods. In place of phosphorylated threonine, Boc-Thr[OPO($OPh)_2$] was incorporated and a deprotection step carried out as described by (Grehn et al. 1987). This peptide was supplied by Dr. Henry Franzén from the Biomedical Unit at Lund University.

Thylakoid preparation

Thylakoid membranes were isolated from pea (Pisum sativum). Peas were grown at 20 °C in a 12-hour light and 12-hour dark cycle. Leaves were harvested from 14–16-day-old seedlings towards the end of the dark phase of the cycle. Thylakoids were prepared by the method described in (Harrison and Allen 1991). Thylakoids were stored on ice in darkness for at least 60 minutes before the measurements. Results were independent of the age of thylakoid preparation up to 6 hours after isolation.

Dark-to-light adaptation

Thylakoid membranes were suspended to give the
concentration of 5 μg Chl ml^{-1} in the suspending
um given by (Harrison and Allen 1991) to which
and peptides were added to give final concentration
mM ATP and 2 mM peptides. A peptide-free thyla
suspension was used for the control experiment.
ples were illuminated with a fluorescent strip lamp
ing a light intensity of 5 μmol $m^{-2} \cdot s^{-1}$ while wor
with the phosphorylated peptide and 8.5 μmol m^{-2}
while working with the non-phosphorylated pep
Samples were pipetted at different time intervals
the suspension into the fluorescence cuvette and fr
immediately in darkness to the temperature of li
nitrogen. Fluorescence spectroscopy was carried
using a Perkin-Elmer LS-5 luminescence spectro
ter.

Light-to-dark adaptation

Fully light-adapted thylakoids after 2.5 hours of
mination in a suspension of concentration 10 μg C
ml^{-1} with the light intensity 8.5 μmol $m^{-2} \cdot s^{-1}$
suspended in an equal volume of solution containi
mM peptide in darkness. The samples for fluoresce
measurements were taken in the same way as for
dark-to-light adaptation.

Phosphorylation measurements

For measurement of the amount of ^{32}P incorpora
into membrane proteins during the phosphorylati
we prepared a suspension containing [γ-^{32}P] ATP
concentration of 0.1 mM at a specific activity 2.4
$\cdot$ ml^{-1}. The concentration of thylakoid membra
was 0.2 mg Chl $\cdot$ ml^{-1}. Samples were taken at t
intervals from 15 seconds to 2 hours. At each t
interval a sample (100 μl) of suspension was w
drawn and precipitated in Eppendorf tubes contain
0.9 ml of acetone pre-cooled to −20 °C. Tubes w
placed on ice for 30 minutes and centrifuged at 13
rpm for 2.5 minutes. The pellets were redissolved
2% SDS sample buffer at 70 °C for one hour,
which SDS-PAGE (Laemmli 1970) and autoradiog
phy were performed. Measurement of the ^{32}P-labell
of the protein bands was performed by phosphorima
ing with a Molecular Dynamics PhosphorImager
Background labelling was subtracted for each lane.

Results

Isolation of thylakoids

Thylakoids were isolated from pea leaves harvested before the light was switched on in the growth chamber. Isolation of chloroplasts and their lysis were performed in low light. The isolated thylakoids were incubated in darkness for several hours. We have found no difference in behavior between thylakoids incubated for 1 and 6 hours and it may be concluded that in the freshly isolated thylakoids the complete oxidation of the plastoquinone pool does not take more than 1 hour.

Fluorescence measurements

The light-do-dark and dark-to-light adaptation was followed by measurement of emission spectra at 80 K of samples withdrawn at the times indicated and frozen in liquid nitrogen. The light intensity was chosen in order to keep the depletion of PS II fluorescence in the presence of peptides in the time scale which may be followed by the experimental arrangement used. Differences in the range of up to 15% of the total fluorescence intensity were observed both for the initial values and for the kinetics of adaptation between various preparations of thylakoids.

As a result of dark-to-light adaptation, the PS II emission band of isolated thylakoid membranes becomes depleted in the chlorophyll b (Chl b) as may be seen from the loss of the 473 nm excitation component in excitation spectra of fluorescence emission 685 and 695 nm (Fig. 1). No subsequent increase in the Chl b component was observed in the excitation spectra of PS I at 735 nm (Fig. 1C) and no rise of a separate emission peak for the free antenna systems (AS) was observed (Fig. 2). The reversibility of the light-dependent depletion of Chl b absorption was also checked. The fully light-adapted thylakoids (2.5 hours after the beginning of the adaptation) were put into darkness and the fluorescence changes were followed. In about 30 minutes the fluorescence of PS II increased by about 25% but no further increase was observed in the next 18 hours (Fig. 3, control). In all the procedures, the control experiment was performed under the same conditions in absence of ATP. A decrease of up to 5% in the relative fluorescence intensity of fluorescence emission at 686 to 735 nm was observed after 2.5 hours of illumination in the absence of ATP. Incubation in darkness had no influence on the fluorescence spectrum.

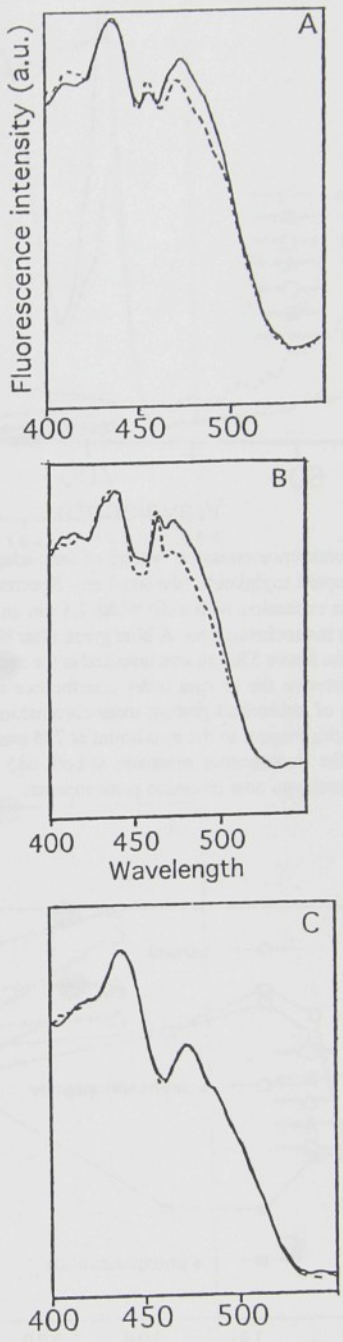

Fig. 1. Superposition of fluorescence excitation spectra of dark adapted (solid line) and fully light adapted thylakoids (dashed line) at 685 (Fig. 1A), 695 (Fig. 1B) and 735 (Fig. 1C). Spectra were obtained using slit width 2.5 nm on both excitation and emission monochromators. Spectra were normalised with respect to the maximum at 435nm. The depletion of chlorophyll b component in the spectrum at 685 and 695 nm may be clearly seen from the decrease of the intensity at 473 nm. No such effect was observed in the excitation spectrum at 735 nm. The symmetrical maximum seen at 460 nm in Fig. 1A and at 466 nm in Fig. 1B are most likely second order interference artefacts arising from the use of unblocked grating monochromators.

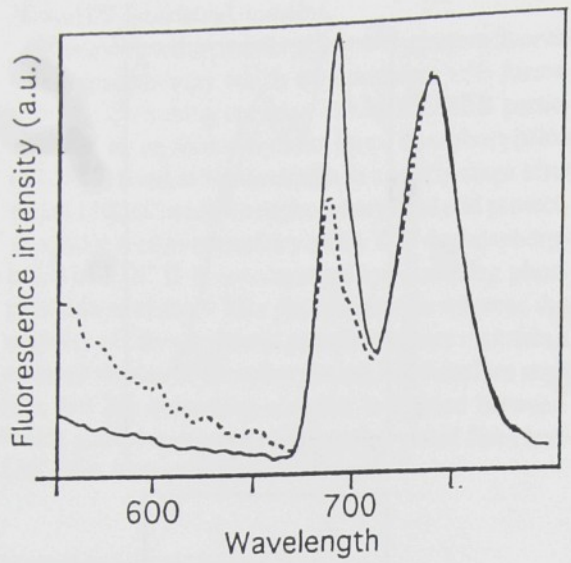

Fig. 2. Fluorescence emission spectra of dark-adapted (solid line) and light-adapted thylakoids (dashed line). Spectra were obtained using 480 nm excitation with a slit width 2.5 nm on both excitation and emission monochromators. A blue green filter blocking all light of wavelengths above 530 nm was installed in the excitation pathway in order to remove the second order interference artefacts arising from the use of unblocked grating monochromators. Spectra were normalised with respect to the maximum at 735 nm. A decrease in intensity of the fluorescence emission at both 685 and 695 nm is observed whereas no new emission peak appears.

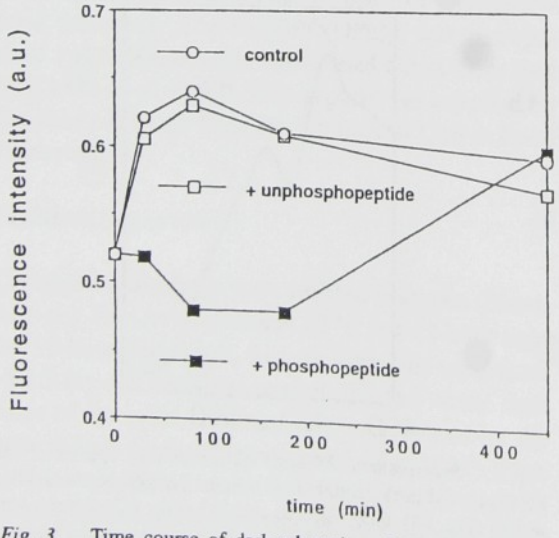

Fig. 3. Time course of dark adaptation of fully light adapted thylakoids. Value on the y axis represents the ratio of fluorescence intensity at 685 nm to 735 nm (F_{685}/F_{735}). The slowdown of the adaptation in presence of the phosphorylated peptide is apparent. The original F_{685}/F_{735} in the dark adapted thylakoids before the light adaptation was 1.2.

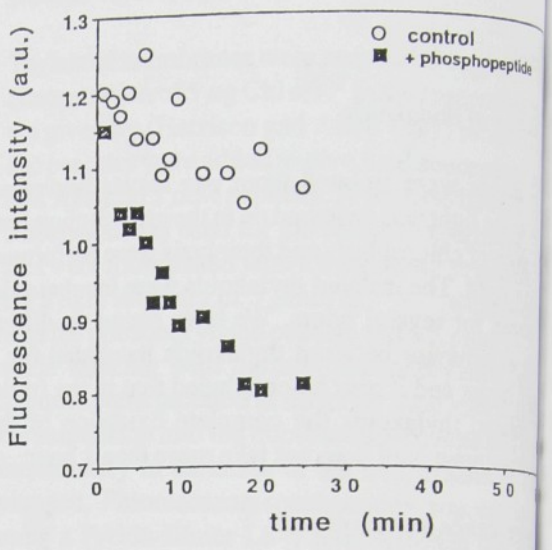

Fig. 4. Time course of light-adaptation of dark adapted thylak
Value on the y axis represents the ratio of fluorescence intens
685 nm to 735 nm (F_{685}/F_{735}). Significant acceleration of adapt
in the presence of phosphorylated peptide is observed.

In the next series of experiments we followed
influence of the phosphorylated peptide fragment
LHC II on the rate of the dark-to-light adaptat
If the main consequence of adaptation is discon
tion of LHC II from PS II by its phosphorylat
and subsequent binding of phosphorylated LHC I
antenna system of PS I, we would expect comp
tion of the phosphopeptide in this process. The a
tion of the phosphorylated peptide fragment of LH
leads to acceleration of the adaptation (Fig. 4) wh
may be explained by its competition with membr
phosphoproteins in the phosphatase reaction (Ch
et al. 1994). This explanation is supported by the
that addition of the phosphorylated peptide marke
decreased the rate of dark adaptation of fully lig
adapted thylakoids (Fig. 3). The phosphorylated p
tide itself had no effect on either the emission or
excitation spectra of thylakoids at various stages
adaptation (data not shown).

In the presence of high concentrations of n
phosphorylated peptide the depletion of PS II in
b was not significantly accelerated (data not show
However, major changes were observed in the em
sion spectrum, where a new peak at 697 nm appe
(Fig. 5). A shift of the emission maximum of PS I fr
735 nm to 731 nm also occurred. The new peak at
nm and the blue shift of PS I were not observed
the presence of phosphorylated peptide or at advan
stages of light adaptation of thylakoid membranes

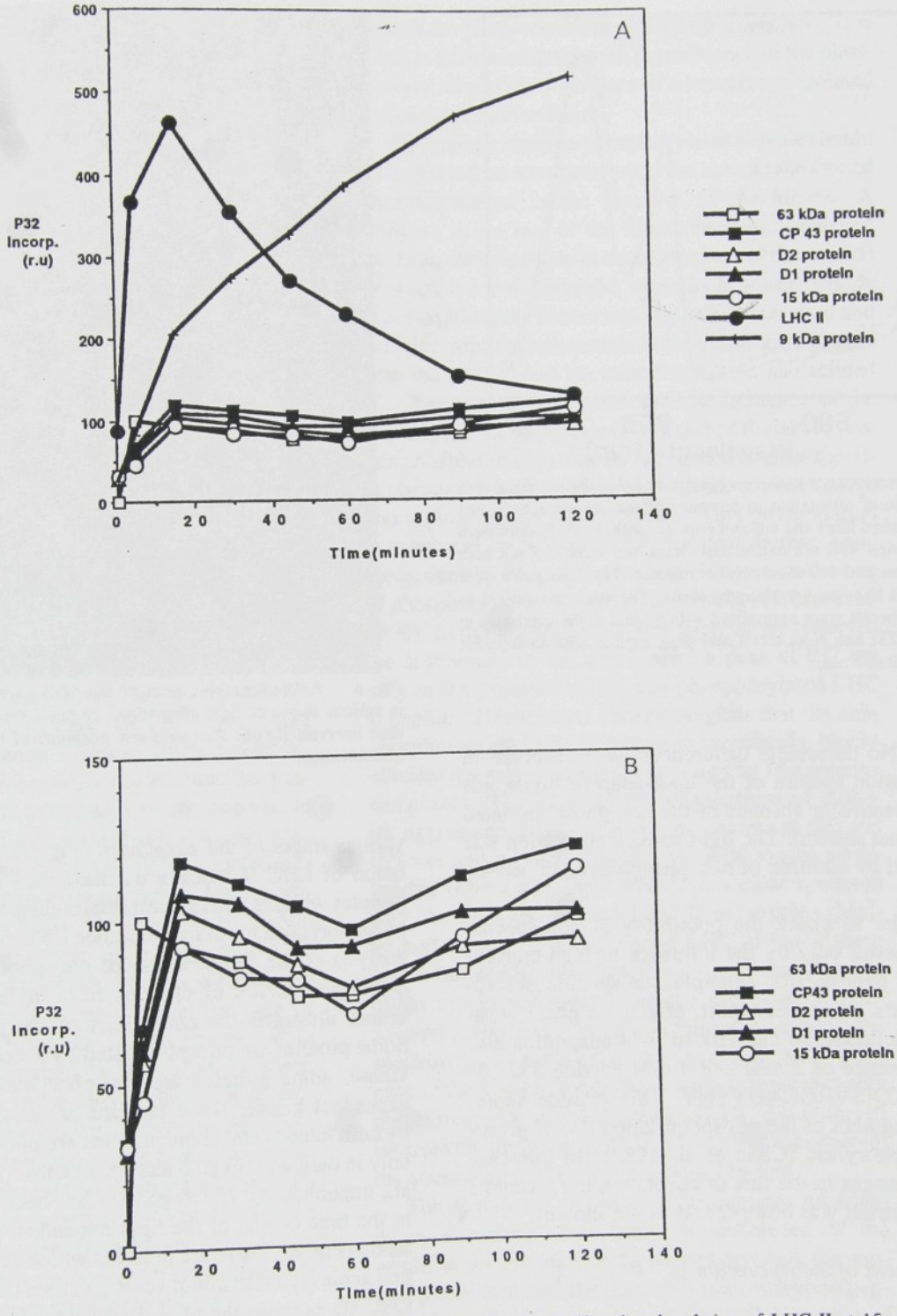

Fig. 7. Time course of ^{32}P incorporation into the thylakoid membrane proteins. The phosphorylation of LHC II at 15 minutes largely exceeds that of other phosphoproteins. The majority of phosphoproteins maintain a constant level of phosphorylation (Fig. 7B), whereas the phosphorylation of LHC II decreases with time and the phosphorylation of the 9 kDa protein increases.

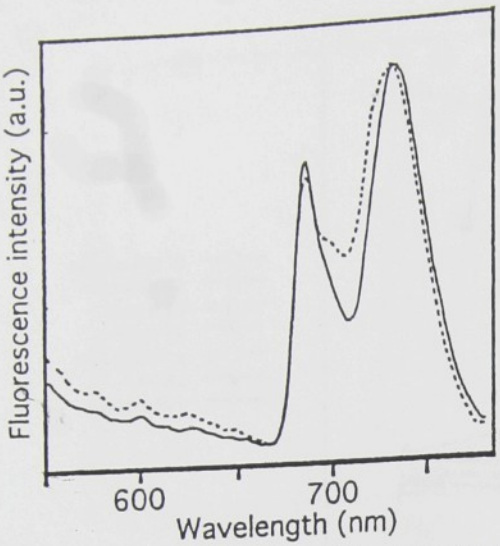

Fig. 5. Fluorescence emission spectra of light adapted thylakoids after 60 min of adaptation in presence of the non-phosphorylated peptide (dashed line) and without peptide (solid line). Spectra were obtained using 480 nm excitation with a slit width 2.5 nm both on excitation and emission monochromator. The blue green filter blocking all light on wavelengths above 530 nm was installed as in Fig. 2. Spectra were normalised with respect to the maximum at 735 nm or 731 nm. Note that a new peak appears with an apparent maximum at 697 nm.

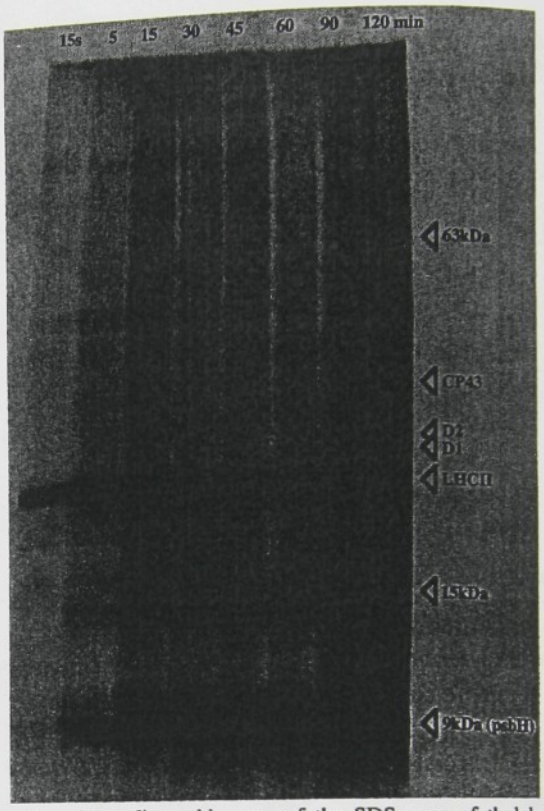

Fig. 6. Autoradiographic scan of the SDS page of thylakoids at various stages of light adaptation. Samples were taken at the time intervals shown. Arrows show positions of bands used for quantification.

shown). No detectable differences were observed in the excitation spectra of the light-adapted thylakoids in the presence or absence of the non-phosphorylated peptide (not shown). The light-to-dark adaptation was unaffected by addition of non-phosphorylated peptide (Fig. 3).

In order to check the possibility of non-specific effects caused only by the influence of high concentration of peptide (for example non-specific absorption, effects on ion transport, effects on phase separation) we measured the dark-to-light adaptation also in the presence of 2 mM and 4 mM peptide SRPLSDQEKRKQISVRGLAGVENV. This peptide represents a fragment of the phosphorylation site of glycogen phosphorylase (Chan et al. 1982). In this case neither changes in the rate of adaptation nor a change in the spectrum was observed (data not shown).

Measurement of incorporation of ^{32}P

The time course of incorporation of ^{32}P into various phosphoproteins in the thylakoid membrane was followed for 2 hours (Fig. 6). The phosphorylation of LHC II and of the 9 kDa phosphoproteins exceeds that of the other phosphoproteins by several times at various stages of the adaptation (Fig. 7). Phosphorylation of LHC II reaches its maximum in about 15 minutes whereas 9 kDa phosphoprotein is increasingly phosphorylated for at least another 1.5 hours. Detailed analysis of the times course of phosphorylation and dephosphorylation of proteins from thylakoid membranes illustrates the complexity of the phenomena. Some proteins are phosphorylated by a steadily active kinase, some proteins are phosphorylated by light-dependent kinase, some proteins are phosphorylated by both kinases and some proteins are phosphorylated only in darkness (Figs. 6 and 7), and also (L. Cheng et al., unpublished). Heterogeneity has been found also in the time course of the light-dependent phosphorylation (Fig. 6). There are proteins whose phosphorylation achieves a maximum value and then declines (e.g. LHC II), proteins the phosphorylation level of which is constant, and proteins which are increasingly phosphorylated during the time-course (e.g. 9 kDa). As a control we measured the level of phosphorylation of several other membrane phosphoproteins whose maximal level of ^{32}P incorporation was achieved within 15

minutes and did not increase further with time. In order to eliminate the possibility that we observed a kinetic difference in the phosphatase reaction when the kinase reaction becomes limited by depletion of ATP, we performed two control experiments. In the first, a fresh mixture of ATP was added to the system after 15 minutes of adaptation. In the second, after 15 minutes of adaptation membranes were spun down, a new batch of dark adapted thylakoids was added, and their phosphorylation was followed. In all cases the phosphorylation of membranes followed the same time course as seen in Fig. 7A (data not shown).

Conclusions

The dark-to-light adaptation of thylakoid membranes consists mainly of depletion of PS II in chlorophyll b (Chl b)-containing antenna systems. Such a mechanism has been proposed by (Kyle et al. 1984). The fact that this depletion is not accompanied by an increase in the corresponding antenna component of PS I or by the appearance of a new fluorescence emission peak for the free antenna system shows that there is an efficient quenching mechanism for the Chl b-containing component of the antenna systems. Such a quenching mechanism does not completely exclude the possibility of migration of minor part of the antenna to the PS I. The fact that this mechanism does not lead to immediate quenching of all the PS II fluorescence suggests that the antenna systems are no longer productively connected to PS II. In the purple bacterium *Rhodospillium rubrum*, where the energy difference between the chlorophylls of the antenna systems and the photosystem is much higher than in the case of plant PS II, about 25% of the energy transferred to the photosystem is detrapped by the antenna systems (Timpman et al. 1993). In the case of plants, the detrapping rate should be even higher. Formation of a tight complex between the reaction centre and antenna system is necessary for productive energy transfer to PS II. As the random contacts between the proteins in the membrane are very frequent (Grasberger et al. 1986), the free antenna systems must quench very efficiently in order to prevent energy transfer to PS II.

Analogues of the N-terminus of LHC II are known to be substrates for the LHC II kinase (Bennett et al. 1987; Michel and Bennett 1989) and phosphatase (Sun et al. 1993). Recent results from our group (Cheng et al. 1994) show that the phosphorylated form of the LHC II N-terminal fragment may compete efficiently with the phosphoprotein phosphatase reaction. This result is quite consistent with the influence of the phosphorylated peptide on the rate of adaptation of isolated thylakoids described here.

By analogy, the non-phosphorylated peptide should be expected to compete with the membrane-bound phosphoproteins in the reaction of the kinase. A decrease in the rate of the kinase reaction, however, has been observed only at concentrations of the peptide between 0.5 and 1.34 mM, whereas at lower peptide concentrations the kinase was apparently activated and at higher peptide concentrations the phosphorylation of both the peptide and the membrane proteins declined (L. Cheng et al., unpublished). The influence of the unphosphorylated peptide on the rate of thylakoid protein phosphorylation may be interpreted as an unspecific phenomena related to changes in the surface charge and ionic strength in the solution. This interpretation is supported by the influence of a peptide that is not recognized by the membrane bound kinase on the rate of phosphorylation of membrane proteins (White et al. 1990). In our experiments, nevertheless, we observed the appearance of the new emission peak at 697 nm only in the presence of the non-phosphorylated LHC II peptide. This spectral change suggests that the non-phosphorylated LHC II fragment specifically blocks efficient quenching of energy captured by free antenna complexes. The 77 K emission spectrum of isolated, aggregated LHC II shows two maxima at 680 and 697 nm and a broad shoulder towards longer wavelengths (Moya and Tapie 1984). A similar spectrum was observed for isolated LHC II in vesicles (Mullet and Arntzen 1980). Diluted LHC II has a sharp maximum at 680 nm. Superposition of the spectrum of the aggregated antenna on the spectrum of light-adapted thylakoids gives a spectrum equivalent to the spectrum found in our experiments (Fig. 5). In the presence of the non-phosphorylated peptide most probably the fluorescence of free aggregated LHC II is observed whereas the depletion of PS II in LHC II is not affected: the quenching mechanism has been blocked.

The specificity of influence of peptides on adaptation is clearly seen from the difference of the results in the presence of the phosphorylated, the non-phosphorylated and the glycogen-phosphorylase peptides. In a diluted solution in which ATP forms one of the negatively-charged ions, the concentration of ATP in the proximity of the membrane surface is to a large extent dependent on the charge on the surface (Cevc 1990). The membrane surface charge itself would be changed by non-specific binding of positively charged

peptides (Sackmann 1994). The experiments involving phosphorylated peptide represent a special case because the phosphorylated peptide is dephosphorylated by a membrane bound phosphatase (Cheng et al. 1995) and therefore binds to a class of binding sites on the membrane inaccessible to unphosphorylated peptides. The influence of the phosphorylated peptide on the concentration of ions in the membrane-solution interface may therefore be different from that of the other peptides (Cevc 1990). One should concentrate on qualitative changes in the spectrum rather than on the changes in the rate of adaptation.

On the basis of our results we propose a two-step mechanism for light adaptation. As a first step LHC II is liberated from its binding site at PS II by partial phosphorylation. Free, partially phosphorylated LHC II immediately forms the quenching complex with other proteins. These proteins are either constantly present in the membrane or also released from their original position by phosphorylation. Alternatively, based on our knowledge of rapid dephosphorylation of LHC II, the quenching complex may be built around the completely dephosphorylated LHC II.

The mechanism proposed here predicts that phosphorylation of LHC II will reach a maximum and then decline or stay constant at constant illumination. Among the proteins of the thylakoid membrane, LHC II reaches its maximum phosphorylation in approximately 15 minutes, and subsequently its phosphorylation declines (Figs. 6 and 7). The majority of other phosphoproteins, including known phosphoproteins CP43, D1 and D2, reach their maximum of phosphorylation within 15 minutes and then stay steadily phosphorylated (Fig. 7). In contrast, the 9 kDa phosphoprotein becomes increasingly phosphorylated for 2 hours. The decline of LHC II phosphorylation excludes the simple mechanism according to which LHC II fluorescence is quenched solely by LHC II migration outside the PS II region of the membrane, since this predicts a steady level of phosphorylation of LHC II in the final stage of adaptation. More likely a quenching complex is built in which one of the other phosphoproteins of thylakoid membranes participates. A necessary requirement for this mechanism is that either the second component of the quenching complex has higher affinity for the liberated antenna than PS II or the PS II binding site for the LHC II is modified, or both. In each case, if a single introduced phosphate group per unit of liberated LHC II is expected, the total number of phosphate groups introduced either to the second component of the quenching complex or to the modified LHC II binding protein should be equal to the total amount of phosphate groups introduced to LHC II. The total number of phosphate groups introduced to LHC II is difficult to examine as the level of its phosphorylation at any time is a result of both the kinase and the phosphatase reactions, the nature of which in many important aspects unknown. Nevertheless, it is clear from the phosphorylation pattern seen on Figs. 6 and 7, that only the number of phosphate groups introduced to the 9kDa phosphoprotein may possibly equal the number of phosphate groups introduced to LHC II in the maximum of its phosphorylation. The 9 kDa protein may be expected to form the second main component of the quenching mechanism.

The 9 kDa protein has been isolated from oxygen-evolving PS II particles (Farchaus and Dilley 19[illegible]) and it may be considered that phosphorylation of the 9 kDa phosphoprotein may be responsible for alteration of the PS II binding site for LHC II. A weak sequence similarity of the 9 kDa phosphoprotein with LHC II has been reported (Hind et al. 1986; Allen and Findlay 1986). The difficulties in isolation of the 9 kDa from the light harvesting proteins when both are specifically extracted from oxygen-evolving PS II particles (Farchaus and Dilley 1986) may indicate that phospho-9 kDa protein forms a complex with LHC II and itself forms the component responsible for LHC II quenching. Analogously to protection of LHC II in its unphosphorylated form from the kinase reaction by its binding to the quenching complex, the anomalously slow dephosphorylation of the 9 kDa phosphoprotein may be a consequence of its protection from the phosphatase reaction in the quenching complex. The psbH protein may itself be a pigment binding protein (Allen and Findlay 1986) on the pathway of excitation energy transfer from LHC II to PS II reaction centers (Allen and Holmes 1986). In possible contrast to mechanisms based on formation of a single, tight complex are the results of membrane fractionation experiments (Stefánsson et al. 1994) which show that the stroma fraction in thylakoid membranes phosphorylated in 15 minutes at conditions similar to those used in this article becomes enriched in LHC II but not in PS II proteins, including the 9 kDa. No data are, nevertheless, available at present about the changes in protein composition at later stage of phosphorylation. The results described here suggest that phosphorylation of psbH initiates non-photochemical radiationless excitation decay, thereby deflecting excitation energy from the path to PS II photochemistry. Whether the site

this decay lies in LHC II or
to be determined.

Acknowledgements

The authors thank Dr Ivo Bla
for the peptides used in th
supported by the Swedish N
Council (J.F.A.) and Kunglig
in Lund (D.S.) by research
fellowship from Swedish Na
Council and M.S. a studentsh
program.

References

Ell JF (1992) Protein phosphorylat
thesis. Biochim Biophys Acta 109
JF and Holmes NG (1986) A g
photosynthetic unit function by pr
Lett 202: 175–181
JF, Bennett J, Steinback KE an
light protein phosphorylation coup
redistribution of excitation energy b
301: 25–29
JF and Findlay JBC (1986) An
9 kDa phosphoprotein of pea thylak
Commun 136: 146–152
son JM and Andersson B (1982
synthetic membranes: lateral and tra
Biochem Sci 7: 288–292
ey G and Merrifield RB (1980) Th
New York
ent I, Shaw EK and Bakr S (1987) P
proteins and synthetic peptide analog
25
ann BJ and Engelman DM (1992)
association in oligomerization and
Rev Biophys Biomol Struct 21
G (1990) Membrane electrostati
(3): 311–382
L FJ, Hurst MO and Graves DJ (1
specificity. J Biol Chem 257: 3655–3
ng L, Spangfort MD and Allen JF (
and kinetics of thylakoid phosphopro
Biochim Biophys Acta 1188: 151–15
ng L, Sys D and Allen JF (1995) Ef
in thylakoid protein phosphatase re
73–178
son B, Cleland RE and Björkman
F, chlorophyll fluorescence quenc
of the light-harvesting complex of Ph
376–385
son I and Dilley RA (1986) Purific
of the Mr 10,000 phosphoprotein from
Biochem Biophys 244: 94–101

this decay lies in LHC II or in phospho-psbH remains to be determined.

Acknowledgements

The authors thank Dr Ivo Blaha and Dr Henry Franzén for the peptides used in the study. The work was supported by the Swedish Natural Sciences Research Council (J.F.A.) and Kungliga Fysiografiska Sällskapet in Lund (D.S.) by research grants. D.S. received a fellowship from Swedish Natural Sciences Research Council and M.S. a studentship from the EC TEMPUS program.

References

Allen JF (1992) Protein phosphorylation in regulation of photosynthesis. Biochim Biophys Acta 1098: 275–335

Allen JF and Holmes NG (1986) A general model for regulation of photosynthetic unit function by protein phosphorylation. FEBS Lett 202: 175–181

Allen JF, Bennett J, Steinback KE and Arntzen CJ (1981) Chloroplast protein phosphorylation couples plastoquinone redox state to distribution of excitation energy between photosystems. Nature 291: 25–29

Allen JF and Findlay JBC (1986) Amino acid composition of the 9 kDa phosphoprotein of pea thylakoids. Biochem Biophys Res Commun 136: 146–152

Anderson JM and Andersson B (1982) The architecture of photosynthetic membranes: lateral and transverse organization. Trends Biochem Sci 7: 288–292

Barany G and Merrifield RB (1980) The Peptides. Academic Press, New York

Bennett J, Shaw EK and Bakr S (1987) Phosphorylation of thylakoid proteins and synthetic peptide analogues. FEBS Lett 210 (1): 22–26

Bormann BJ and Engelman DM (1992) Intramembrane helix-helix association in oligomerization and transmembrane signalling. Annu Rev Biophys Biomol Struct 21: 233–242

Cevc G (1990) Membrane electrostatics. Biochim Biophys Acta 1031 (3): 311–382

Chan K-FJ, Hurst MO and Graves DJ (1982) Phosphorylase kinase specificity. J Biol Chem 257: 3655–3658

Cheng L, Spangfort MD and Allen JF (1994) Substrate specificity and kinetics of thylakoid phosphoprotein phosphatase reactions. Biochim Biophys Acta 1188: 151–157

Cheng L, Stys D and Allen JF (1995) Effects of synthetic peptides on thylakoid protein phosphatase reactions. Physiol Plant 93: 173–178

Demmig B, Cleland RE and Björkman O (1987) Photoinhibition, 77 K chlorophyll fluorescence quenching and phosphorylation of the light-harvesting complex of Photosystem II. Planta 172: 378–385

Farchaus J and Dilley RA (1986) Purification and partial sequence of the Mr 10,000 phosphoprotein from spinach thylakoids. Arch Biochem Biophys 244: 94–101

Giardi MT (1993) Phosphorylation and disassembly of the photosystem II core as an early stage of photoinhibition. Planta 190: 107–113

Grasberger B, Minton AP, DeLisi C and Metzger H (1986) Interactions between proteins localized in membranes. Proc Nat Acad Sci USA 83: 6258–6262

Grehn L, Fransson B and Ragnarsson U (1987) Synthesis of substrates of cyclic AMP-dependent kinase and use of their precursors for convenient preparation of phosphoserine peptides. J Chem Soc Perkin Elmer I: 529–535

Harrison MA and Allen JF (1991) Light-dependent phosphorylation of photosystem II polypeptides maintains electron transport at high-light intensity: Separation from effects of phosphorylation of LHC II. Biochim Biophys Acta 1058: 289–296

Hind SM, Dyer TA and Gray JC (1986) The gene for the 10 kDa phosphoprotein of Photosystem II is located in chloroplast DNA. FEBS Lett 209: 181–186

Kyle DJ, Kuang T-J, Watson JL and Arntzen CJ (1984) Movement of a sub-population of the light harvesting complex from grana to stroma lamellae as a consequence of its phosphorylation. Biochim Biophys Acta 765: 89–96

Laemmli UK (1970) Cleavage of structural proteins during the assembly of the head of bacteriophage T4. Nature 227: 680–685

Michel H and Bennett J (1989) Use of synthetic peptides to study substrate specificity of a thylakoid protein kinase. FEBS Lett 254: 165–170

Moya I and Tapie P (1984) Lifetime studies by phase fluorimetry in isolated light-harvesting complexes (LHC): Dependence on the aggregation state. In: Sybesma C (ed) Advances in Photosynthetic Research, pp 103–106. Martinus Nijhoff/ Dr W. Junk Publishers, The Hague

Mullet JE and Arntzen CJ (1980) Simulation of grana stacking in a model membrane system. Biochim Biophys Acta 589: 100–117

Sackmann E (1994) Membrane bending energy concept of vesicle- and cell-shapes and shape transitions. FEBS Lett 346: 3–16

Silverstein T, Cheng L and Allen JF (1993a) Redox titration of multiple protein phosphorylations in pea chloroplast thylakoids. Biochim Biophys Acta 1183: 215–220

Silverstein T, Cheng L and Allen JF (1993b) Chloroplast thylakoid protein phosphatase reactions are redox independent and kinetically heterogeneous. FEBS Lett 334: 101–105

Stefánsson H., Wollenberger L. and Albertsson P.-Å. (1994) Fragmentation and separation of the thylakoid membrane. Effect of light-induced protein phosphorylation on domain composition. J. Chromatogr. A, 668: 191–200

Sun G, Sarath G and Markwell J (1993) Phosphopeptides as substrates for thylakoid protein phosphatase activity. Arch Biochem Biophys 304: 490–495

Timpman K, Zhang FG, Freiberg A and Sundström V (1993) Detrapping of excitation energy from the reaction centre in the photosynthetic purple bacterium *Rhodospillium rubrum*. Biochim Biophys Acta 1183: 185–193

White IR, O'Donnell PJ, Keen JN, Findlay JBC and Millner PA (1990) Investigation of the substrate specificity of thylakoid protein kinase using synthetic peptides. FEBS Lett 269: 49–52

PHYSIOLOGIA PLANTARUM 95: 651–657. 1995
Printed in Denmark – all rights reserved

Copyright © Physiologia Plantarum 1995
ISSN 0031-9317

Minireview

Stacking and separation of photosystem I and photosystem II in plant thylakoid membranes: A physico-chemical view

Dalibor Stys

Stys, D. 1995. Stacking and separation of photosystem I and photosystem II in plant thylakoid membranes: A physico-chemical view. – Physiol. Plant. 95: 651–657.

The main objective of this article is to highlight important experimental findings and discuss current theories on photosystem segregation and stacking in thylakoid membranes. The facts are put in a framework of recent theoretical developments in the field of membrane biochemistry and biophysics. Some important experiments not considered by the currently accepted theories are discussed. Modifications of these theories in order to incorporate new results are proposed. The currently accepted theories on formation of membrane domains (probably responsible for segregation of photosystem I and II) and on interlamellar interactions (stacking) are discussed. Finally, a scheme is put forward summarising the forces which are responsible for organisation of functional structure of thylakoid membranes.

Key words – Domain formation, ion-membrane interactions, membrane organisation, photosystem segregation, stacking.

D. Stys, Plant Cell Biology, Lund Univ., Box 7007, S-220 07 Lund, Sweden.

Introduction

Thylakoid membranes from green plants contain the two-photosystem photosynthetic apparatus. In all higher plants and many algae, thylakoid membranes form special regions called grana stacks and stroma lamella. It is known from membrane fractionation studies (Anderson and Andersson 1982) that photosystem I (PSI) is enriched in stroma lamellae and photosystem II (PSII) in grana stacks. Stacking of grana lamellae is induced by addition of cations, and the absence of cations leads to mixing of photosystems and quenching of PSII fluorescence (Murata 1969). The relative efficiency of PSI and PSII is regulated by protein phosphorylation (Allen 1992a, for a recent review). The evidence of unstacking upon state transitions (Bennoun and Jupin 1974) and evidence of phosphorylation dependence of state transitions (Allen et al. 1981) led to the proposition of coupling between the phosphorylation-induced regulation and stacking of thylakoid membranes.

The mechanism by which photosystems separate and membranes stack has been under dispute during the last 20 years. Two main theories dominate the field. Barber (1982) proposed that surface charge has a key role in stacking (surface-charge theory, SC). According to SC, two membrane lamellae are attracted by van der Waals' type forces and repulsed by electrostatic forces (Fig. 1). The repulsive electrostatic force is shielded by counterions, which finally results in the prevalence of the attractive, van der Waals' force. This theory is essentially an application of the DLVO (Deryagin and Landau 1945, Verwey and Overbeek 1948) theory of colloid aggregation. A recent detailed and clear analysis of the phenomenon of cation-induced shielding of electrostatic repulsion between two surfactant bilayers is given by Dubois et al. (1991). In this paper experimental evidence is also given for the validity of the DLVO theory and the limits of DLVO are explored.

The segregation of PSI and PSII is, according to SC, a cooperative effect of lipid and proteins which creates regions of low surface charge in which proteins contribute to the increase in van der Waals' attraction. Phosphorylation of membrane proteins then increases the negative charge on their surface, and phosphoproteins migrate out of the stacked regions or, in other words, create additional unstacked regions.

Allen (1992b) proposed an alternative hypothesis mainly based on molecular recognition between proteins

Received 31 May, 1995; revised 26 July, 1995

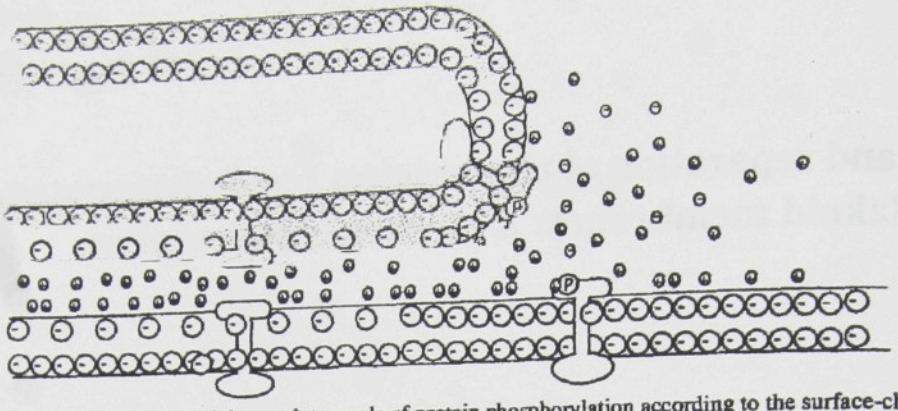

Fig. 1. Schematic view of thylakoids and the regulatory role of protein phosphorylation according to the surface-charge theory (SC, Barber 1982). The white transmembrane objects in the lamellae are the membrane proteins. Membrane lamellae are attracted by van der Waals' forces and repelled by electrostatic forces. Electrostatic repulsion is shielded by cations. The surface charge is lower in appressed than in unappressed regions. Phosphorylated proteins are driven from appressed to unappressed regions by electrostatic repulsion between the negative charge on the phosphate group and the negative charge on the membrane surface.

(MR). According to the MR, thylakoid membranes consist of complexes of PSII and its antenna systems and those of PSI and its antenna systems (Fig. 2). PSII with its antenna systems mainly occupies the stacked regions of thylakoids. Stacking of grana is achieved by specific interactions between proteins. A similar hypothesis with respect to stacking was proposed by Mullet and Arntzen (1980) who proposed that stacking is achieved specifically by binding of the N-terminal domains of light-harvesting complex II (LHCII). The MR does not specify the protein responsible for stacking, but quite generally phosphorylation of membrane proteins will alter their structure and consequently change the binding specificity of antenna complexes from PSII to PSI. At the same time phosphorylation will also cause a structural change of another protein specifically involved in stacking and this causes unstacking. In contrast to SC, MR is an application of observations on the interaction of soluble proteins with membrane proteins.

The main objective of this article is to highlight important experimental findings and discuss the established theories in the light of recent theoretical developments in the field of membrane biochemistry and biophysics. In the first part I will discuss important experiments not considered by SC and MR.

(1) Webb et al. (1988) and Menikh and Fragata (1993) observed aggregation between micelles of digalactosyldiacylglycerol (DGDG) caused by formation of specific complexes.

(2) Wollmann and Diner (1980) showed that stacking of thylakoids and segregation of photosystems are two independent phenomena caused by two different ion-dependent mechanisms.

In the second part I will discuss progress in the field of ion-membrane interactions: the ion induced segregation in lipid and lipid-protein mixtures caused by raising of the critical demixing temperature (Sackmann 1990, 1994) and the ion-dependent attractive correlation forces (Gulbrandt et al. 1984).

Abbreviations – DGDG, digalactosyldiacylglycerol; DLVO, Deryaging, Landau, Verwey and Overbeek theory; LHCII, light-harvesting complex II; MR, molecular recognition theory; PC, phosphatidylcholine; PG, phosphatidylglycerol; PSI, photosystem I; PSII, photosystem II; SC, surface-charge theory.

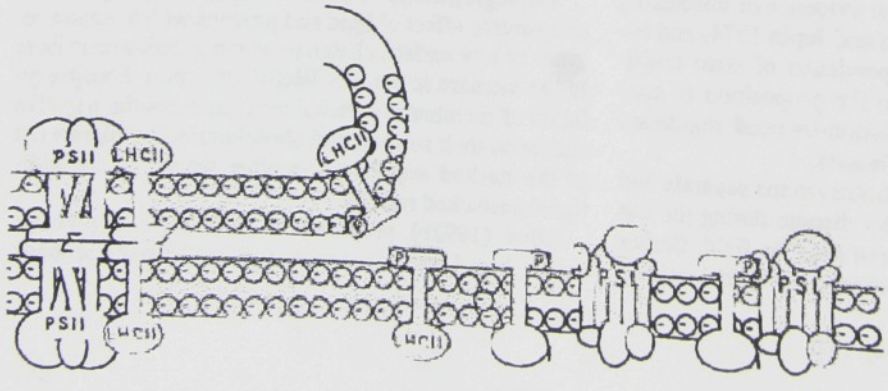

Fig. 2. Schematic view of thylakoids and the regulatory role of protein phosphorylation according to the molecular recognition theory (MR, Allen 1992b). Specific recognition between proteins is responsible for formation of complexes between antenna proteins (LHCII) and photosystems (PSI, PSII) as well as for stacking. Phosphorylation changes the structure of the binding site of LHCII on PSII. Phosphorylated membrane proteins lose their affinity for PSII and are driven, by diffusion, away from the stacked regions and bind to PSI.

in the review of Tocanne et al. (1994). It is, however, generally accepted that the formation of domains is mainly facilitated by the segregation of lipids according to their classes that is induced by the presence of proteins.

In thylakoids, the presence of ions will increase the critical demixing temperature, and this will mainly favour lipid-mediated protein-protein interactions. The strong hysteresis of the ion dependence of photosystem segregation (Wollman and Diner 1980) supports phase separation rather than gradual shielding of charge by increasing ion concentration. The experiments involving isolation of membrane compartments by detergent extraction clearly show that certain regions of thylakoid membranes behave as large complexes (e.g. Hipkins and Baker 1986, for a textbook).

The relative lipid composition of the various compartments in thylakoid membranes varies mainly for charged and zwitterionic lipids (Murata et al. 1990): phosphatidylglycerol (PG) accumulates in the region containing PSII and phosphatidylcholine (PC) in the region containing PSI. However, the differences in composition are not striking. Differences were found in the fatty acid composition of PSII particles and the rest of the membrane. In PSII particles, saturated and short-chain fatty acids in all lipids dominate, with the exception of DGDG. The experiments on lipid composition by Murata et al. (1990) support the hypothesis that PSII particles are lipid-protein domains whose stability is dependent on special properties of fatty acid chains. In general thylakoid membranes appear to form an exception to the generally accepted hypothesis that lipid segregation according to their headgroups plays a primary role in formation of membrane domains. It seems likely that lipid segregation may play a role, at a microscopic scale, in formation of membrane complexes, but forces driving the large-scale organisation have yet to be explored.

The observed dominance of protein-protein and lipid-protein interactions are consistent with the SC theory. At the same time, partial non-specific reversal of segregation caused by phosphorylation implies specific changes in protein-lipid and protein-protein affinities rather than a general change in surface charge that leads to a decrease in ion concentration in the interface, a decrease in critical demixing temperature and a subsequent and more pronounced mixing of domains. It appears that some degree of specificity is involved both in ion-induced segregation between photosystems and in all regulatory events. Thus, in the light of proper physicochemical analysis, the seemingly sharp border between SC and MR is smeared.

Ion-induced attractive and repulsive forces in lamellar liquid crystals

Lamellar liquid crystals of lipids consist of stacks of parallel lamellae of lipid bilayers. Most of the data on the structure of lipid bilayers have been obtained with lamellar liquid crystals (e.g. Petty 1993, for a recent textbook). Over a wide range of lipid-to-water ratios, the lamellar structure exists as a single-phase system. In most cases, when the critical concentration of water (maximum swelling) is achieved, another phase, of pure water, appears. In some systems, however, several distinct phases in the system may be observed (e.g. Dubois et al. 1991). Swelling of crystals may be diminished in the presence of ions. Such an observation, however, would be predictable in bilayers of negatively charged lipids for which the classical DLVO theory considers the existence of classical van der Waals' attraction forces and repulsive electrostatic forces between surfaces of the same charge. A detailed analysis (Dubois et al. 1991) shows that the repulsion between lamellae may be analysed by a comparison of the chemical potentials in the interlamellar space and in the outer solution. In the presence of salts, the salt concentration is considerably lower in the interlamellar space than in the outside solution, which leads to the equilibration of chemical potentials and thus to the decrease in repulsion. In sufficiently high salt concentration, the repulsive electrostatic force is lower than the attractive van der Waals' force and the lamellae do not swell. However, swelling is observed even in bilayers of zwitterions, whose surface is uncharged (Parsegian 1967). This observation cannot be explained by the DLVO theory.

The main limitation of the applications of DLVO theory to lipid bilayers is that it does not consider the influence of ions on each other and on the interacting lamellae. The lamellae are treated as surfaces with uniformly smeared charge which is not affected by the ions. There is no simple approach to overcome this limitation. Jönsson and Wennerström (1983) developed a model in which a border between regions of different dielectric properties (dielectric discontinuum) is a charged lipid surface, and ions from one side of this discontinuum induce formation of complementary charges on the other side of the discontinuum (image charges). This approach, called image-charge model, is a construction that extends the original model described by DLVO. Over the last few years the image-charge model has been successfully applied to explain electrostatic effects in ion-colloid and polyion-colloid interactions (Gulbrand et al. 1984, Granfeld et al. 1991, Woodward et al. 1994) in which predictions based on the classical DLVO theory would be incorrect.

In the same way as Barber (1982) used the classical DLVO theory for description of stacking of thylakoid membranes, one can use the current considerations on the influence of ions on colloids for an improved evaluation of possible stacking forces. The main differences between predictions by the image charge model and predictions by the classical theories as described by Gulbrand et al. (1984) are as outlined below.

(1) Ion-ion correlations are taken into account. This leads to prediction of higher concentrations of the counterions at the charged surface, which in turn reduces the

overlap between electric double layers and, consequently, reduces repulsion.

(2) Correlated fluctuations in the ion cloud lead to an additional attractive force of van der Waals' type, in a way similar to that by which correlated fluctuations in electron clouds lead to classical van der Waals' attraction. Using realistic values of parameters for the calculation, an attraction between two charged lamellae may be predicted.

Grana stacks in thylakoid membranes strongly resemble lamellar liquid crystals of lipids. The attractive force caused by correlation between cation clouds at the interface of neighbouring lamellae may provide an additional attractive force, non-specific and independent of other membrane properties except for surface-charge density. The analyses of the behaviour of lipid bilayers should, therefore, be fully applicable to grana stacks. It appears that it is fully legitimate to consider the dominance of electrostatic effects in the interlamellar interactions as considered by SC, although the detailed analysis has yet to be done.

The contribution of correlative forces, an ion-dependent force as well as non-specific van der Waals' attractions, may be completely negated by steric hindrances caused by proteins which prevent sufficiently close contact between membranes. The tertiary structure of the majority of membrane proteins belonging to stacked regions is not known. LHCII (Kühlbrandt 1994, Kühlbrandt et al. 1994) is unusually flat on the stromal side of the membrane. On the other hand, the structure of PSI (Krauss et al. 1993) shows a number of subunits stretching far from the membrane. It is possible that steric hindrance is an additional factor that prevents stacking in the PSI region. For the ion-induced correlative forces the steric hindrance may be overcome at high ion concentrations. The calculations considering this possibility have yet to be done.

Conclusions

The purpose of this article is to discuss some recent experiments on the properties of thylakoid membranes in relation to various physico-chemical experiments and calculations on model systems. The surface-charge hypothesis (SC, Barber 1982) was developed on the basis of the classical DLVO theory (Deryagin and Landau 1945, Verwey and Overbeek 1948). The novel experimental observations and theoretical conclusions cited in this article, namely (a) the involvement of specific interactions in the segregation of photosystems, (b) the existence of separate mechanisms for stacking and for photosystem segregation, (c) the existence of an attractive force caused by electrostatic interactions between ion clouds and (d) specific complex formation between the headgroups of uncharged lipids, require necessary adjustments of the SC theory. In fact, the source hypothesis for SC (DLVO; Deryagin and Landau 1945, Verwey and Overbeek 1948), is at present not accepted in its original

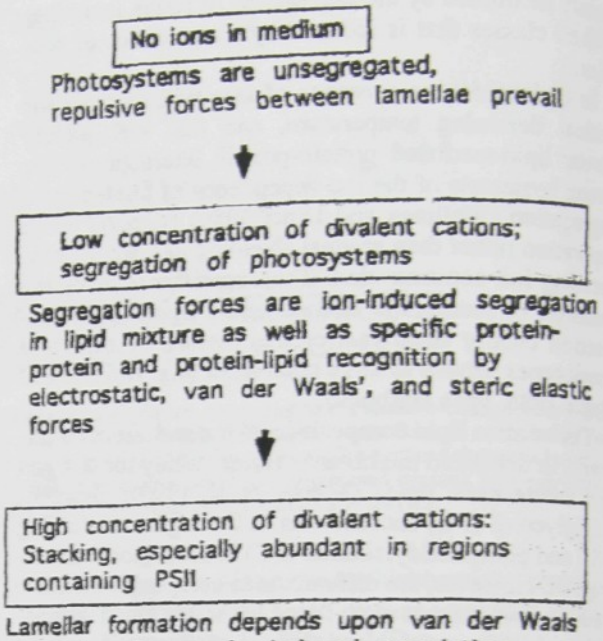

Fig. 5. Schematic overview of ion-induced events and forces which may operate in thylakoid membranes.

form. The attractive and repulsive forces in thylakoid membranes, as well as the events which may be involved in regulation, are summarised in Fig. 5.

The molecular recognition hypothesis (MR, Allen 1992b) was developed in order to explain a new observation regarding the phosphorylation-dependent adaptation of thylakoids. The MR does not attempt to explain the ion-dependent events in stacking and photosystem segregation. However, it appears that the ion-induced segregation of photosystems is also a process dependent on specific protein-protein and lipid-protein interactions. The role of specific interactions in both the segregation and the adaptation mechanisms seems to be a primary one while the stacking may be fully explained by unspecific electrostatic and van der Waals' forces. The possibility of contribution of interactions between lipid headgroups to the attractive force cannot be excluded. Thus, when the distinction between the segregation of photosystems and regulation of harvesting of energy on one side and stacking on the other side (Wollmann and Diner 1980) is accepted, only the MR and SC hypotheses together are able to explain properties of thylakoid membranes.

Acknowledgments – I thank Prof. Anders Kylin for encouraging me to write this article and for his critical reading and also Prof. John F. Allen for his critical reading of the manuscript and for many important suggestions. I especially thank Dr Bo Jönsson, from the Dept of Physical Chemistry 2, Lund Univ., who pa-

Important experiments not considered by SC and MR

Lipid-based stacking

Webb et al. (1988) observed ion-induced adhesion between digalactosyldiacylglycerol (DGDG) vesicles. This observation was confirmed and extended by Menikh and Fragata (1993), who found that adhesion between DGDG vesicles is most probably a consequence of the formation of specific complexes between lipid headgroups and cations. The efficiency of divalent cations for induction of adhesion was 10–20 times higher than that of monovalent cations. Apart from specific protein-protein interactions (as proposed by MR) and non-specific van der Waals' attractions (as proposed by SC), specific lipid-lipid interactions induced by ions should be considered as an additional attraction force, which may contribute to stacking. Both theories need only slight modification to account for this.

Disparity between stacking and segregation of photosystems

Wollmann and Diner (1980) followed the ion-dependence of photosystem segregation (monitored by total fluorescence intensity) and stacking (monitored by light scattering as compared to changes observed by electron microscopy). Different relative efficiencies of monovalent as compared to divalent cations were found for stacking and for segregation between photosystems. Full segregation of photosystems was achieved in a 2 m*M* solution of $MgCl_2$, whereas attempts to achieve a similar degree of segregation by KCl lead to precipitation of membranes at about half of the maximum achievable fluorescence yield. In the initial part of the titration curve of fluorescence versus ion concentration, the molar ratio of KCl to $MgCl_2$ at which the same effect was achieved was 110. The titration curve showed sharp hysteresis. In contrast, stacking increased uniformly during the whole titration curve, up to 25 m*M* $MgCl_2$. The titration by KCl led to precipitation when 80% of maximal stacking was achieved. This is a clear indication that ion-induced stacking and fluorescence are two different events. Wollman and Diner (1980) interpret their results by postulating the existence of two regions of different surface-charge density, one in which ion-induced fluorescence changes occur, and a second in which stacking is achieved.

An additional observation reported by Wollman and Diner (1980) is that fluorescence quenching of PSII by PSI does not occur in a mutant lacking the antenna systems of PSI. The authors conclude that there is a specific binding site for PSII antenna on antenna systems of PSI.

The SC basically considers a two-event mechanism, formation of a region with low surface-charge density and then stacking in this region. According to SC segregation of photosystems and stacking occur at the same time and have the same ion-dependence. This is inconsistent with the observations of Wollman and Diner (1980). The most obvious simple adjustment to SC is the separation between photosystem segregation and stacking, in which segregation is the primary event, creating the region of low surface-charge density, and stacking is the secondary event. Such a two-step mechanism predicts quantitatively different effects on stacking for monovalent as compared to divalent cations. In the case of divalent cations, segregation is complete at an early stage and the concentration dependence of scattering is simple. In the case of monovalent cations the curve reflects not only build-up of regions with low surface-charge but also stacking, the relative influence of monovalent and divalent cations will, therefore, change with the relative influence of these two events. Close examination of the data of Wollman and Diner (1980) shows that for monovalent cations the course of stacking is dominated by the segregation mechanism, and for divalent cations by the stacking mechanism. Although there is no doubt about the involvement of two mechanisms, more data, mainly using mixtures of ions and triple-charged ions, should be accumulated to distinguish between the mechanism predicting photosystem segregation as the primary event and stacking as the secondary event and a mechanism predicting two independent events.

The MR theory does not discuss the ion-dependence of stacking. It considers the situation that will occur in fully stacked membranes with completely segregated photosystems. However, according to Wollmann and Diner (1980), stacking is a continuous process, and the extent of stacking steadily increases with increasing concentration of ions. If stacking is dependent on specific binding between proteins, then such a protein should be uniformly distributed over the thylakoid membranes or several proteins contribute to this binding. Another possibility is that specific lipid-ion complexes are involved. DGDG, which is evenly distributed over all thylakoid membrane compartments (Murata et al. 1990), appears as a primary candidate for such specific recognition. Then, however, the regulation of stacking by phosphorylation will no longer be specific but rather caused by phosphorylation-induced changes in ion concentration at the membrane-solution interface.

A physico-chemical model for ion-induced events in membranes

Cation-induced phase separation in protein-containing lipid mixtures

Cation-induced separation of phases in a mixture of phosphatidylcholine and phosphatidic acid was demonstrated by Knoll et al. (1986). To avoid experimental difficulties in direct measurement of membrane composition, the gramicidin channel was reconstituted into the lipid mixture and current relaxation after a voltage jump was measured. At low Ca^{2+} concentration only a single population of channels was observed. With increasing Ca^{2+} concentration, the properties of the channels

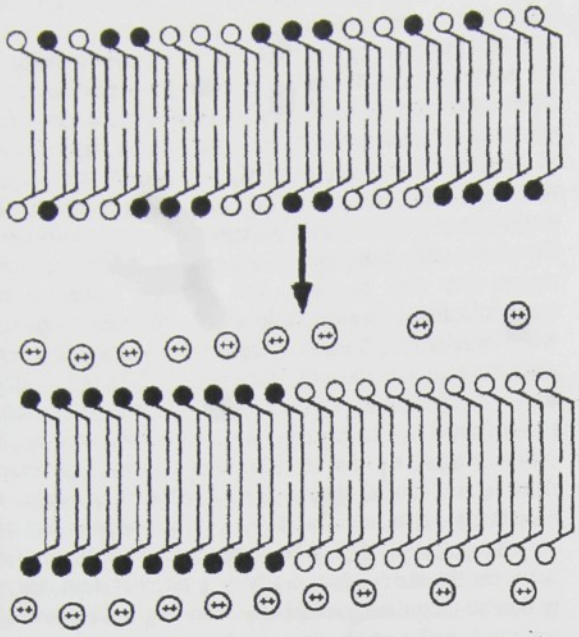

Fig. 3. Ion-induced separation of phases in a mixture of lipids as observed by Knoll et al. (1986). The mixed lipid bilayer contains phosphatidylcholine (lipids with white headgroups) and phosphatidylglycerol (lipids with black headgroups). Binding of cations to the membrane surface changes the electrostatic properties of lipids and increases the critical demixing temperature. Two phases of different lipid composition arise in a previously homogeneous mixture. The precise analysis of the composition of each of the phases was, however, beyond the possibilities of the experimental setting.

changed and finally two different populations of channels appeared. The properties of the two different populations corresponded to properties of channels in different lipid environments. In presence of ions there are two different regions in the lipid bilayer which have different lipid composition. Similar segregation may be achieved in many binary systems by lowering the temperature below the critical demixing temperature. Sackmann (1994) concluded that phase separation in lipid mixtures is a consequence of a decrease in the critical temperature of demixing in lipid mixtures. Ion-induced demixing of lipids is schematically shown in Fig. 3, which represents demixing in a mixture of lipids with different polar headgroups. Although there is no doubt about involvement of unspecific electrostatic interactions between lipid headgroups, some degree of specificity will play a role in each particular case.

According to most widely accepted theories, the major protein-lipid interactions (Sackmann 1990, 1994, Tocanne et al. 1994) are based on electrostatic interactions between lipid headgroups and hydrophilic parts of proteins, and on steric elastic mechanisms, perturbation of membrane thickness by interactions of hydrophobic parts of proteins with hydrophobic parts of lipids (Fig. 4). Lipids with negatively charged headgroups accumulate in the region occupied by proteins with positively charged extra-membrane regions, and lipids with short or more elastic fatty acid chains accumulate in the region containing proteins with shorter transmembrane helices and vice versa. In favourable cases the steric elastic mechanism would lead to segregation of lipids and proteins with matching hydrophobic regions (hydrophobic mismatch, Mouritsen and Bloom 1993) and formation of membrane domains (Welti and Glaser 1994, for a recent review).

Sackmann (1990) predicts that lipid-mediated, long-range protein-protein interactions play a role mainly close to the critical demixing temperature of a lipid-protein mixture. The critical demixing temperature may be increased by addition of cations. The distance between interacting proteins in segregated regions may be much larger than in regular protein complexes whereas the domains formed on the basis of these interactions retain the character of complexes (i.e. stay intact in certain detergent extraction procedures).

Recent results from Kühlbrandt's group (Nußberger et al. 1993) show that specific lipid-protein interactions exist between LHCII and an uncharged lipid DGDG. In this case the specific recognition is clearly of non-electrostatic origin. Nußberger et al. (1993) also found that only a limited amount of DGDG is necessary to facilitate crystallisation of LHCII. This is in agreement with theoretical predictions and with experimental observations that specific interactions between proteins and lipid headgroups are restricted on the first layer of lipids surrounding the protein (Newton 1993, for a recent review). Various types of protein-protein and protein-lipid interactions are systematically classified and evaluated

Fig. 4. Protein-lipid interactions in biological membranes. The big objects in the membrane are the membrane proteins. The hydrophilic parts of proteins are white, the hydrophobic transmembrane region is dashed. Black dots represent lipid-binding sites. Lipids differ in the charge of their headgroup, in their affinity for proteins as symbolised by the colour of their headgroups, and in the length and compressibility of their fatty acid chains. Lipids with specificity for proteins (black headgroups) bind specifically to binding sites on proteins (protein with large, hydrophilic, extra-membrane regions) by electrostatic (Sackmann 1990) or other specific interactions (Newton 1993, Nußberger et al. 1993). Lipids with shorter and/or more compressible fatty acid chains are driven by steric elastic forces to regions containing proteins with shorter hydrophobic transmembrane regions even though there is no other specific interaction between these proteins and lipids (Sackmann 1990, Mouritsen and Bloom 1993). Under favourable conditions, mainly close to the critical demixing temperature, proteins and lipids with mutual affinity segregate to form lipid-mediated protein-protein complexes. The critical demixing state may also be caused by the presence of cations.

tiently lead me towards an understanding of surface-ion interactions, and other colleagues who commented critically on the manuscript.

References

Allen, J. F. 1992a. Protein phosphorylation in regulation of photosynthesis. – Biochim. Biophys. Acta 1098: 275–335.

– 1992b. How does protein phosphorylation regulate photosynthesis? – Trends Biochem. Sci. 17: 12–17.

– , Bennett, J., Steinback, K. E. & Arntzen, C. J. 1981. Chloroplast protein phosphorylation couples plastoquinone redox state to distribution of excitation energy between photosystems. – Nature 291: 21–25.

Anderson, J. M. & Andersson, B. 1982. The architecture of photosynthetic membranes: lateral and transverse organisation. – Trends Biochem. Sci. 7: 288–292.

Barber, J. 1982. Influence of surface charges on thylakoid structure and function. – Annu. Rev. Plant Physiol. 33: 261–295.

Bennoun, P. & Jupin, H. 1974. The relationship between thylakoid stacking, state I and state II phenomena in whole cells and cation effects in chloroplasts of *Chlamydomonas reinhardtii*. – *In* Proceedings of the 3rd International Congress of Photosynthesis (M. Avron, ed.), pp. 163-169. Elsevier Amsterdam.

Deryagin, B. & Landau, L. 1945. A theory of the stability of strongly charged lyophobic sols and the coalescence of strongly charged particles in electrolytic solution. – Acta Physicochim. URSS. 14: 663.

Dubois, M., Zemb, T., Belloni, L., Delville, A., Levitz, P. & Setton, R. 1991. Osmotic pressure and salt exclusion in electrostatically swollen lamellar phases. – J. Chem. Phys. 96: 2278–2286.

Granfeld, M. K., Jönsson, B. & Woodward, C. E. 1991. A Monte Carlo simulation of the interaction between charged colloids carrying adsorbed polyelectrolytes. – J. Chem. Phys. 95: 4819–4826.

Gulbrand, L., Jönsson, B., Wennerström, H. & Linse, P. 1984. Electrical double-layer forces. A Monte-Carlo study. – J. Chem. Phys. 80: 2221–2228.

Hipkins, M. F. & Baker, N. R. 1986. Photosynthesis Energy Transduction. A Practical Approach. – IRL Press, Oxford. pp. 18–26. ISBN 0-947946-51-9.

Jönsson, B. & Wennerström, B. 1983. Image-charge forces in phospholipid bilayer systems. – J. Chem. Soc. Faraday Trans. II. 79: 19–35.

Knoll, W., Apell, H.-J., Eibl, H. & Miller, A. 1986. Direct evidence for Ca^{++}-induced lateral phase separation in black membranes of lipid mixtures by the analysis of gramicidin A single-channels. – Eur. Biophys. J. 13: 187–193.

Krauss, N., Hinrichs, W., Witt, I., Fromme, P., Pritzkow, W., Dauter, Z., Betzel, C., Wilson, K. S., Witt, H. & Saenger, W. 1993. Three-dimensional structure of system I of photosynthesis at 6Å resolution. – Nature 361: 326–331.

Kühlbrandt, W. 1994. Structure and function of the plant light-harvesting complex, LHCII. – Curr. Opin. Struct. Biol. 4: 519–528.

– , Wang, D. N. & Fujiyoshi, Y. 1994. Atomic model of plant light-harvesting complex by electron crystallography. – Nature 367: 614–621.

Menikh, A. & Fragata, M. 1993. Fourier-transform infrared spectroscopic study of ion-binding and intramolecular interactions in the polar head of digalactosyldiacylglycerol. – Eur. Biophys. J. 22: 249–258.

Mouritsen, O. G. & Bloom, M. 1993. Models of lipid-protein interactions in membranes. – Annu. Rev. Biophys. Biomol. Struct. 22: 145–171.

Mullet, J. E. & Arntzen, C. J. 1980. Simulation of grana stacking in a model system. Mediation by purified light-harvesting pigment-protein complex from chloroplasts. – Biochim. Biophys. Acta 589: 100–117.

Murata, N. 1969. Control of excitation transfer in photosynthesis. II. Magnesium ion dependent distribution of excitation energy between two pigment systems in spinach chloroplasts. – Biochim. Biophys. Acta 189: 171–181.

– , Higashi, S.-I. & Fujimura, Y. 1990. Glycerolipids in various preparations of photosystem II from spinach chloroplasts. – Biochim. Biophys. Acta 1019: 261–268.

Newton, A. C. 1993. Interactions of proteins with lipid headgroups. – Annu. Rev. Biophys. Biomol. Struct. 22: 1–25.

Nußberger, S., Dörr, K., Wang, D. N. & Kühlbrandt, W. 1993. Lipid-protein interactions in crystals of plant light-harvesting complex. – J. Mol. Biol. 234: 347–356.

Parsegian, V. A. 1967. Forces between lecithin bimolecular leaflets are due to a disordered surface layer. – Science 156: 939.

Petty, R. H. 1993. Molecular Biology of Membranes. – Plenum Press, New York, NY. pp. 7–352. ISBN 0-306-44429-1.

Sackmann, E. 1990. Molecular and global structure and dynamics of membranes and lipid bilayers. – Can. J. Phys. 68: 999–1012.

– 1994. Membrane bending energy concept of vesicle- and cell-shapes and shape transitions. – FEBS Lett. 346: 3–16.

Tocanne, J. F., Cézanne, L., Lopez, A., Piknova, B., Schram, V., Tournier, J.-F. & Welby, M. 1994. Lipid domains and lipid-protein interactions in biological membranes. – Chem. Phys. Lipids 73: 139–158.

Verwey, E. J. W. & Overbeek, J. Th. G. 1948. Theory of the Stability of Lyophobic Colloids. – Elsevier, New York, NY.

Webb, M. S., Tilcock, C. P. S. & Green, B. R. 1988. Salt-mediated interactions between vesicles of the thylakoid lipid digalactosyldiacylglycerol. – Biochim. Biophys. Acta 938: 323–333.

Welti, R. & Glaser, M. 1994. Lipid domains in model and biological membranes. – Chem. Phys. Lipids 73: 121–137.

Wollman, F.-A. & Diner, B. 1980. Cation control of fluorescence emission, light scatter, and membrane stacking in pigment mutants of *Chlamydomonas reinhardii*. – Arch. Biochem. Biophys. 201: 646–658.

Woodward, C. E., Åkesson, T. & Jönsson, B. 1994. Forces between polyelectrolyte coated surfaces in the presence of electrolyte. – J. Chem. Phys. 101: 2569–2576.

Edited by P. Böger and J. S. van Rensen

STRUCTURE AND MAGNESIUM BINDING OF PEPTIDE FRAGMENTS OF LHCII IN ITS PHOSPHORYLATED AND UNPHOSPHORYLATED FORMS STUDIED BY MULTINUCLEAR NMR.

Dalibor Stys[1], Torbjörn Drakenberg[2], Michael D. Spangfort[3], Sture Forsén[2] and John F. Allen[1].

[1]Plant Cell Biology, Box 7007, Lund University, S-220 07 Lund, Sweden, [2]Physical Chemistry 2, and [3]Biochemistry, Lund University, Box 124, S-221 00 Lund, Sweden

1. Introduction

It is believed that upon phosphorylation, some LHCII complexes move towards unappressed regions of the thylakoid and act as light-harvesting antennae for photosystem I [1,2,3]. A structure at 3.4 Å resolution has been described for the major part of non-phosphorylated LHCII [4] but gives no information regarding the N-terminal domain that contains the phosphorylation site. Attempts to isolate pure phosphorylated LHCII have so far been unsuccessful.

Appression of thylakoid membranes, also called "stacking", is induced by the presence of cations. For a long time there has been a dispute about the involvement of specific and non-specific interactions in this process [1,2,3,5,6]. Barber [1] suggested the dominance of unspecific electrostatic interactions in both stacking and lateral segregation of proteins, Mullet and Arntzen [8] considered dominance of protein-protein interactions involving LHCII in stacking and Allen [3] proposed dominance of protein-protein interactions in both stacking and lateral segregation. If unspecific, electrostatic shielding of electrostatic repulsion between lamellae in the presence of salts induces appression, then the salt concentration may be several orders of magnitude lower in the interlamellar space than in the rest of the solution [7]. This prediction is in clear disagreement with experimental evidence from thylakoids, where the membranes, although sometimes highly appressed, are more enriched in cations than it would be needed for compensation of the surface charge. The electrostatic equilibrium concentration may be restored by EDTA treatment, by which tight complexes may be disrupted. An alternative hypothesis could thus be proposed by which the interlamellar interactions in stacking are dominated by specific binding of ions rather than by purely electrostatic effects.

It is known that LHCII has a strong tendency to aggregate[5]. The three-dimensional structure of the stromal part of LHCII [4,8] is relatively flat and contains a number of carboxylic acid groups. It may also contain a phosphatidylglycerol (PG) headpiece which is known to be tightly bound to LHCII [9]. Several molecules of digalactosyldiacylglycerol (DGDG) are necessary for proper crystallisation of LHCII [8]. Carboxylic acids, phosphate groups and saccharides are known to bind cations.

A number of laboratories have produced data on the relative effectiveness of mono- and di-valen cations in cation-dependent processes in thylakoid membranes and in lipid vesicles. There is an apparent similarity of the effectiveness of Mg^{2+} relative to monovalent cations for stacking of thylakoids [10], for aggregation of LHCII [5], and for association of PG vesicles [11]. Such similarity may be just coincidental and the whole phenomena needs proper analysis.

P. Mathis (ed.), Photosynthesis: from Light to Biosphere, Vol. I, 127–130.
© 1995 *Kluwer Academic Publishers. Printed in the Netherlands.*

In systems containing a number of non-equivalent binding sites, the occupancy of binding site is determined by the local activity of ions [11]. The local activity is determined by electrostatics, by the affinity of neighbouring specific binding sites and by the position of individual binding sites on the surface [11]. However, in equilibrium conditions, the activity of cations should be the same all over the whole sample. In the case of thylakoids, a strong ion binding site is introduced when a phosphate group is attached to a membrane protein. We may well assume non-equlibrium conditionsin thylakoid memebranes, as it is known from fractionation experiments that it takes at least 30 min for the membrane to equilibrate for new conditions. Thus, a timescale for the equilibration exceeds that of phosphorylation-induced chages and local non-equilibrium conditions may be expected.

In the few known examples of magnesium binding to phosphate groups on protein [12,13] the binding constants are always of the order of few hundreds to thousands M^{-1}, largely exceeding the binding constant of the phosphate group of lipids [11,14]. Here we describe results obtained with small synthetic peptide fragments of the LHCII phosphorylation site. In any case the incorporation of the phosphate group into a protein a the membrane surface will significantly affect the binding of ions at weaker sites.

2.Results

2.1 Comparison of NMR spectra of the phosphorylated and non-phosphorylated LHCII fragments

Major differences between the spectra of the non-phosphorylated and phosphorylated peptides are clearly observed at all pH values (Figure 1). We will therefore concentrate th discussion to the spectra at pH 5.3, where the assignment of resonances was least complicated by spectral overlap and by exchange of NH protons.

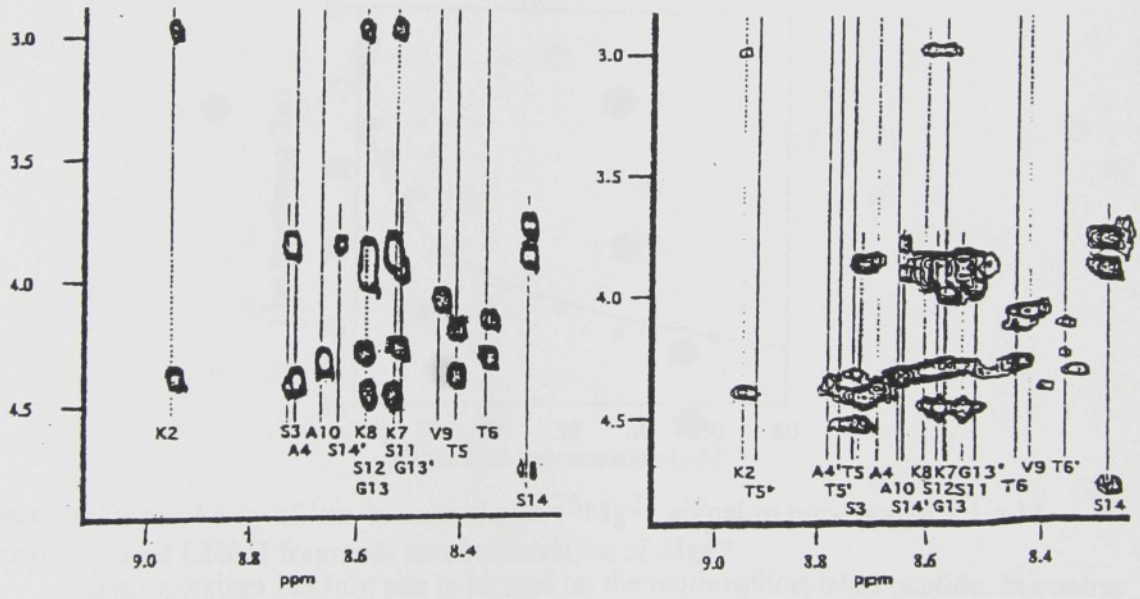

Figure 1. Segments of ^{1}H NMR TOCSY spectrum of unphosphorylated LHCII fragment and of phosphorylated LHCII fragment at pH 5.3

Both the non-phosphorylated and phosphorylated forms of the peptide RKSAT(PO3)TKKVASSGSP show non-random-coil chemical shifts for most of the protons (Figure 1). Major differences in chemical shifts between the two forms of the peptide are observed for protons of Thr 5 and 6, and these can be attributed to changes in

covalent structure and bond properties. In addition, changes in chemical shifts are greater in the region Ser 3 - Lys 8 than in the C-terminal part of the molecule. This indicates that changes in structure (or stabilisation of one prevalent structure) occur in the N-terminal part of the molecule upon phosphorylation. Further strong evidence for the existence of a different preferred structure in each form of the peptide is the observed doubling of the resonances of Ser 14 and Gly 13 in the non-phosphorylated form and in those of Ala 4, Thr(PO_3) 5 and Thr 6 in addition to Ser 14 and Gly 13 in the phosphorylated form. This doubling is most likely caused by cis/trans isomerism around the peptide bond between Ser 14 and Pro 15. The doubling of resonances for residues 4 to 6 shows that there exists at least one more populated conformation in which the C-terminus is sufficiently close to residues 4 to 6 to affect their chemical shifts. In addition, several non-sequential mainchain-to-sidechain NOE crosspeaks are seen in the spectrum of the phosphorylated peptide whereas in the non-phosphorylated peptide NOESY crosspeaks are observed only between the sidechains of Lys 7 or Lys 8 and Ser 14 NH. There is, however, a clear indication of a preferred tertiary structure in the non-phosphorylated peptide between residues 7 and 15, and of extension of such a structure right up to the N-terminus of the phosphorylated peptide.

The pH-dependent changes in the spectrum were consistent with pKa's of 4.5 an 5.9 for the single and double protonations, respectively, of the phosphate group, consisten with previous data on the protonation of the phosphate group of various phosphoproteins given in [15].

2.2 Magnesium binding to peptides

The binding constant of Mg^{2+} ions to both phosphorylated and unphosphorylated peptide was determined from the concentration dependence of line broadening of the ^{25}Mg NMR signal at 25°C (Fig.2).

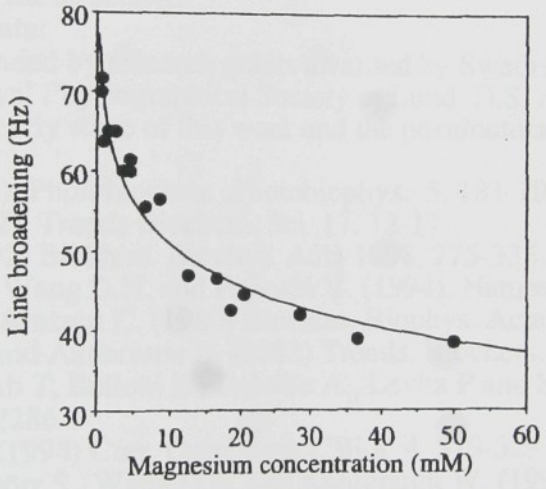

Figure 2. Dependency of line broadening of $^{25}Mg^{2+}$ signal in presence of 2.1 mM phosphorylated LHCII fragment on concentration of Mg^{2+}.

No magnesium binding site is located on the unphosphorylated peptide. In contras the phosphorylated peptide binds magnesium. The calculation of the binding constant of Mg^{2+}-phosphopeptide complex gives a value of 110 M^{-1}. The binding constant is low in comparison to known binding constants of phosphate group which are between 250 and 25000 M^{-1} in casein and casein-derived peptides [12] where the magnesium binding is to cluster of serine phosphates. The binding constants to phosphate groups on lipids and sugars are, however, of the order of 5-20 M^{-1}.

Proton NMR spectroscopy was performed in 8 mM solution of the phosphorylatec peptide in concentrations of $MgCl_2$ that were increased stepwise up to 150 mM. Small differences were found for the chemical shifts of the NH protons. The differences in chemical shift were uniform in direction, varying between 0.04 and 0.01. In the work of Wahlgren et al. [13] changes in chemical shifts were found also for the α protons surrounding the metal-binding phosphoserines. These changes [13] were one order of magnitude larger than those found in our work, indicating that the magnesium-induced change in the structure is very small, if any.

3. Conclusions

The proton NMR spectra of the phosphorylated as well as the unphosphorylated peptide gave indications of the existence of a preferred structure in solution. Marked differences between the proton NMR spectra of the phosphorylated and unphosphorylatec fragments were observed. These differences may be interpreted either as a change in preferred structure or as a stabilisation of one of the preferred conformations of the N-terminal part of the peptide. The structure of the peptide furthermore varied with changes in the protonation of the phosphate group.

The phosphate group on proteins is known to be one of the strongest magnesium binding groups in biochemical systems[14]. The hypothesis [16] that stacking of thylakoi membranes is determined to a large extent by binding of magnesium to lipids seems to have some experimental support [5,9,11]. The binding constant of 110 M^{-1} for magnesium to the phosphopeptide is almost one order of magnitude higher than the value 12 M^{-1} found in the literature for PG [11]. In phosphorylated LHCII will the phosphate group at the N-terminus favourably compete with the sites on lipids unless the phosphate group is buried in the structure..

Acknowledgements:
This work was funded by research grants awarded by Swedish Natural Research Council (NFR) and by Royal Physiographical Society in Lund. D.S. received a FEBS short term fellowship in the early stage of this work and the postdoctoral fellowship from NFR.

4. References:

1 Barber, J. (1983). Photobiochem .Photobiophys. 5, 181-190.
2 Allen, J.F. (1992). Trends Biochem. Sci. 17, 12-17.
3. Allen, J.F. (1992) Biochim. Biophys. Acta 1098, 275-335.
4 Kühlbrandt W., Wang D.N. and Fujioshi Y. (1994). Nature, 367, 614-621.
5 Mullet J.E. and Arntzen C. (1980) Biochim. Biophys. Acta 589, 100-117
6 Anderson J.M. and Andersson B. (1982) Trends. Biochem. Sci. 7, 288-292
7 Dubois M., Zemb T, Belloni L., Delville A., Levitz P and Setton R. (1992) J. Chem. Phys. 96, 2278-2286
8 Kühlbrandt W. (1994) Curr. Opin. Struct. Biol. 4, 519-528
9 Nußberger S., Dörr S., Wang D.N. and Kühlbrandt W. (1993) J. Mol. Biol. 234, 347-56
10 Wollman F.A. and Diner B. (1980) Arch. Biochem. Biophys.
11 Cevc G. Biochim. Biophys. Acta (1990) 1031-3, 311-382
12 Wahlgren N.M., Leonil J., Dejmek P. and Drakenberg T. (1993) Biochim. Biophys. Acta 1202, 121-128.
13 Wahlgren Wahlgren N.M., Dejmek P., Drakenberg T., J. (1990) Dairy Res. 57, 355-364.
14 Cowan J.A. (1995) The Biological Chemistry of Magnesium. VCH publishers, New York.
15 Ho, C., Magnusson, J.A., Willson, J.B., Magnusson, N.F., Curland, R.G. (1969). Biochemistry, 8, 2074-2082.
16 Menikh, A. and Fragata, M. (1993), Eur. Biophys. J., 22, 249-258.

THE JOURNAL OF BIOLOGICAL CHEMISTRY
© 1997 by The American Society for Biochemistry and Molecular Biology, Inc.
Vol. 272, No. 29, Issue of July 18, pp. 18350–18357, 1997
Printed in U.S.A.

Phosphorylation Controls the Three-dimensional Structure of Plant Light Harvesting Complex II*

(Received for publication, February 25, 1997, and in revised form, April 30, 1997)

Anders Nilsson‡, Dalibor Stys‡§, Torbjörn Drakenberg¶, Michael D. Spangfort§‖, Sture Forsén¶, and John F. Allen‡‡‡**

From ‡Plant Cell Biology, Box 7007, Lund University, S-220 07 Lund, ¶Physical Chemistry 2, Box 124, Lund University, S-221 00 Lund, and ‖Biochemistry, Box 124, Lund University, S-221 00 Lund, Sweden

The most abundant chlorophyll-binding complex in plants is the intrinsic membrane protein light-harvesting complex II (LHC II). LHC II acts as a light-harvesting antenna and has an important role in the distribution of absorbed energy between the two photosystems of photosynthesis. We used spectroscopic techniques to study a synthetic peptide with identical sequence to the LHC IIb N terminus found in pea, with and without the phosphorylated Thr at the 5th amino acid residue, and to study both forms of the native full-length protein. Our results show that the N terminus of LHC II changes structure upon phosphorylation and that the structural change resembles that of rabbit glycogen phosphorylase, one of the few phosphoproteins where both phosphorylated and non-phosphorylated structures have been solved. Our results indicate that phosphorylation of membrane proteins may regulate their function through structural protein-protein interactions in surface-exposed domains.

Light harvesting complex II (LHC II)[1] is a major chlorophyll-containing protein complex that accounts alone for half of the pigments involved in photosynthesis in plants. It is located mainly in appressed regions of the thylakoid membrane where it acts as the light-harvesting antenna for photosystem II (PS II). Reversible phosphorylation of LHC II is an established mechanism for redistribution of absorbed light energy between PS II and PS I. Phosphorylation of LHC II (giving LHC II(P)) is triggered by conditions where the plastoquinone pool of the photosynthetic electron transport chain becomes reduced (1). The kinase responsible for the phosphorylation of LHC II is not yet identified, although it is suggested that it is located in the core of photosystem II (2) or in contact with the cytochrome b_6f complex (3, 4). LHC II(P) is found in the unappressed regions of the chloroplast thylakoid membrane and there acts as a light-harvesting antenna for photosystem I (PS I) (5–7). From electron crystallography of 2-dimensional crystals, a structure for the major part of non-phosphorylated LHC II has been described at 3.4-Å resolution (8). This structure reveals no information regarding the N-terminal domain that contains the phosphorylation site at position 5 (Thr); the protein backbone was traced only to residue 26 where it ends up close to the lipid membrane, consistent with the fact that the sequence between residues 21 and 29 (RVKYLGPF) (9) consists mainly of hydrophobic, aromatic, or charged amino acids. Aromatic residues are located at the membrane surface in structures of membrane proteins (10–13), and residues Trp-16 and Tyr-17 of LHC II may also then form a point of contact with the membrane. LHC II has been shown to lose its ability to trimerize when more than the first 15 amino acids are removed from the apoprotein (14). At this site, specific lipid-protein interactions between the amino side chains and the lipid *phosphatidylglycerol* are involved in stabilization of the trimers (15), which implies that only the first 15 amino acid residues at the N terminus may be free of competing interactions with the membrane. This sequence (RKSAT*TKKVASSGSP, where * denotes the phosphorylation site, Thr-5) contains numerous positive charges, which may be compensated by the negative charge introduced by phosphorylation. To see whether a structural change occurs within the N-terminal domain itself, we have studied a synthetic peptide with the N-terminal sequence normally found in pea (9) with and without Thr-5 synthetically phosphorylated. We have also studied native LHC II/LHC II(P) from pea to see if there exists a structural analogy between the peptides and the native protein. Our results show that phosphorylation causes a structural change both in the model peptide and at the N terminus of LHC II itself, together with dissociation of the trimer aggregate. Specific changes in structure-dependent protein-protein as well as lipid-protein interactions must therefore be the basis of the mechanism by which phosphorylation controls the functional interactions of LHC II *in vivo*.

EXPERIMENTAL PROCEDURES

Peptide Synthesis and Protein Purification—The synthetic peptides RKSATTKKVASSGSP (1585.5 Da) and the corresponding phosphorylated form RKSAT(PO_3)TKKVASSGSP (1664.5 Da) were synthesized as described earlier (16). For the Fourier transform infrared (FTIR) and circular dichroism (CD) measurements, full-length proteins of LHC II were isolated from pea leaves (*Pisum sativum* L.) according to standard protocols (17, 18). Normally 100 g of pea leaves were harvested, and each batch of thylakoids was then divided into two; one, giving phospho-LHC II, was then illuminated (130 μmol m^{-2} s^{-1} for 20 min) in the presence of 0.4 mM ATP (Sigma) and 25 mM NaF (Sigma). The same purification protocol was followed for both samples, except that all buffers contained 10 mM NaF in the purification yielding phospho-LHC II. This preparation contained a mixture of both phosphorylated and non-phosphorylated LHC II; the proportion of LHC II(P) was determined by mass spectroscopy to be approximately 10%. For simplicity the phosphorylated preparation will from herein be denoted as LHC II(P).

* This work was supported by the Swedish Natural Sciences Research Council (NFR), Eric and Ulla Schyberg Foundation, the EC DG XII SCIENCE program, and Federation of European Biochemical Societies. The costs of publication of this article were defrayed in part by the payment of page charges. This article must therefore be hereby marked "*advertisement*" in accordance with 18 U.S.C. Section 1734 solely to indicate this fact.

§ Present address: Institute of Microbiology, Academy of Science of the Czech Republic, CZ-379 01 Trebon, Czech Republic.

** ALK Labs, Bøge Allé 10–12 DK-2970 Hørsholm, Denmark.

‡‡ To whom correspondence should be addressed. Tel.: 46-46 2227788; Fax: 46-46 2223684; E-mail: john.allen@plantcell.lu.se.

[1] The abbreviations used are: LHC II, light harvesting complex II; PS II, photosystem II; PS I, photosystem I; LHC II(P), phosphorylated light harvesting complex II; FTIR, Fourier transform infrared; ATR, attenuated total reflection; NOE, nuclear Overhauser effect; standard 1- and 3-letter abbreviations for the amino acid residues.

This paper is available on line at http://www.jbc.org

UV Absorption Measurements—Static solvent perturbation UV absorption measurements of LHC II(P) and LHC II were performed on a double-beam Hitachi U-3000 (Hitachi Ltd, Japan); equal concentrations dissolved in 20 mM Tris buffer (pH 8.0) or H_2O were used as sample and reference, respectively. Ethanol was then added to give up to 10% (v/v) in both sample and reference, and difference spectra were measured between 200 and 300 nm at a resolution of 0.1 nm. All difference spectra showed zero absorbance in the region 200–600 nm, before ethanol addition. The difference spectrum is the average of five individual, but nearly identical, difference spectra, each from one sample preparation (five non-phosphorylated and five phosphorylated), and the resulting spectra were then co-added and averaged. Standard spectra of L-tyrosine and L-tryptophan (Sigma) solutions in Tris buffer or H_2O with additional ethanol were used to confirm the origin of the increase in absorbance at 280 nm upon solvent perturbation. Identical solutions in the sample and reference cuvettes were used to check the samples for inhomogeneity; no spectral difference between samples was then seen either before or after addition of ethanol.

CD Measurements—The circular dichroism (CD) spectra were obtained on a JASCO 720 (Japan Spectroscopic Co. Ltd, Tokyo, Japan) spectrophotometer at 25 °C, using an 8.0 mM, 0.1 mM, or 0.8 μM protein solution in a quartz cuvette with an optical path length of 1 mm. The scan velocity was 1 nm s^{-1} in the frequency range between 180 and 250 nm, and each spectrum consists of eight scans. The spectra shown are the average of four, each from an individual sample, and with the water background subtracted. The relative contribution of each secondary structural motif was calculated with software supplied with the spectrophotometer (19). Solutions of LHC II and LHC II(P) were measured between 350 and 750 nm to determine the oligomeric state (20) but were otherwise under the same conditions as those described above.

FTIR Measurements—FTIR spectra were recorded at a Bruker IFS 66 (Karlsruhe, Germany) spectrometer using a liquid N_2 cooled MCT detector. 2000 scans were collected and Fourier transformed to obtain a spectral resolution of 2 cm^{-1} in the spectral region 4000–600 cm^{-1}. The spectra were measured using a horizontal attenuated-total-reflection (ATR)-crystal (45°) (ZnSe). Peptide solution (approximately 75 μl, 0.8 μM (pH 5.2)) was spread out on the internal reflection crystal and then the sample holder was sealed to avoid evaporation of water. All peptides were washed repeatedly with either H_2O or D_2O (Sigma), followed by rotary evaporation using a Speedvac (Savant Industries, Farmingdale, NY) to dry the peptide between washes, to remove traces of the trifluoroacetic acid used during peptide purification. The H_2O/D_2O exchange of LHC II was performed on a dried sample by addition of 70 μl of D_2O to the protein film. The exchange was followed by sequential measurements of 100 scans (30 s) during a period of 2 h. The film was then repeatedly dried and rehydrated with D_2O to obtain full H_2O/D_2O exchange. All the difference spectra are the average of eight individual spectra, each from one sample preparation (four non-phosphorylated and four phosphorylated), and each individual spectrum is the signal average of 2000 scans. Spectral deconvolution (LabCalc-Galactic Industries Corp., Salem, NH) and derivation were performed. The number of bands and the peak positions thereby obtained were used to calculate (PeakFit-Jandel Scientific Software, San Rafael, CA) a curve fit that is composed of Lorenzian bands for the original IR absorbance band. In the case of H_2O, an interactive spectral subtraction was performed to remove the spectral influence of the δ-mode of bulk water, positioned at 1645 cm^{-1}. All FTIR measurements were performed at 22 °C.

NMR Measurements—All nuclear magnetic resonance (NMR) spectra were acquired at 500 MHz on a GE Omega 500 spectrometer (General Electric, Fremont, CA). Spectra were obtained of aqueous peptide solutions (8 mM). pH was established by addition of small volumes of HCl or NaOH solution in the case of measurements in H_2O or of deuterium chloride or sodium deuteroxide in D_2O for measurements in deuterated solution; the peptide solutions were self-buffering. All NMR spectra were recorded at 2 °C. To obtain a temperature dependence of the NH chemical shift for the phosphorylated peptide at pH 5.2, TOCSY spectra were recorded at 5, 17, and 25 °C. TOCSY spectra were acquired using the MLEV sequence (21) with a mixing time of 120 ms, at 2048 data points with 16 repetitions and 256 τ_1 values. ROESY spectra (22) were acquired with a mixing time of 200 ms, at 2048 or 4096 data points with 32 repetitions and 256 τ_1 values. Nuclear Overhauser enhancement spectroscopy spectra (23) were acquired with a mixing time of 500 ms, at 2048 data points with 32 repetitions and 256 τ_1 values. Sequential assignment was carried out by methods of Wüthrich (24). One-dimensional spectra were recorded for both peptides at concentrations 8.0, 2.0, 0.5, and 0.1 mM, and no changes were observed in line shape or line position.

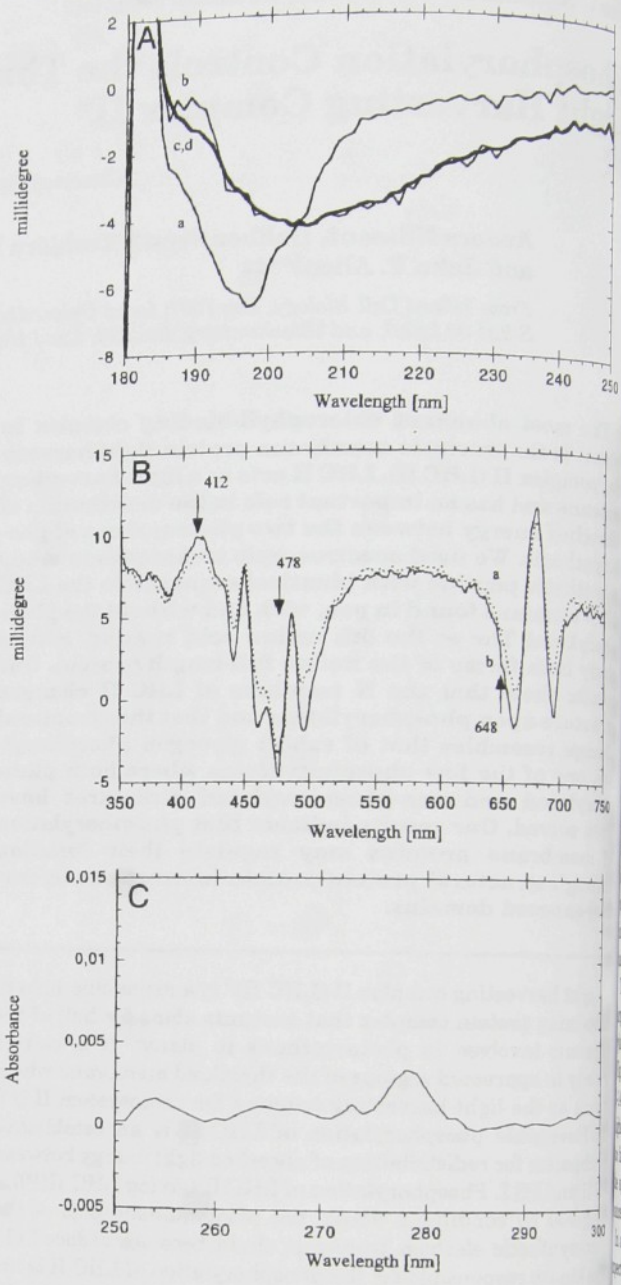

FIG. 1. **UV-visible spectra.** *Panel A* shows CD spectra of the phosphorylated (*a*) and the non-phosphorylated peptide (*b*) at 0.8 μM and at 8 mM (*c* and *d*) in the wavelength region 180–250 nm. *Panel B* shows CD spectra of LHC II(P) (*trace a, dotted line*) and LHC II (*trace b, solid line*) in the wavelength region 350–750 nm. The shoulder characteristic of the trimeric form of LHC II is found at 648 nm (20). *Panel C* shows the solvent pertubation difference spectrum of LHC II(P)/LHC II in the region 250–300 nm. The proteins are resuspended in 20 mM Tris buffer (pH 8.0), and ethanol is added to give a final concentration of 10% (v/v). Further details are given under "Experimental Procedures."

RESULTS

CD, NMR, and FTIR Spectroscopy of LHC II Peptides—All three spectroscopic methods revealed distinct differences between the non-phosphorylated and phosphorylated forms of a 15-residue peptide corresponding to the N-terminal phosphorylation site of LHC II. CD spectra clearly show differences in conformation between the two peptides in monomeric solution (0.8 μM) (Fig. 1*A*). The phosphorylated peptide contains α-helix, a structural type that is absent from the non-phosphorylated form (see Table I). The α-helix content of 12%, which corresponds to only 2 amino residues, in the phosphorylated peptide

TABLE I

Showing the calculated relative amount or relative area representing the different classes of secondary protein structures

The results are from the nonphosphorylated 15-mer peptide and the phosphorylated 15-mer peptide, presented above in that order.

Peak assignment	CD-calculated relative amount	FTIR relative peak area	FTIR peak position
	%	%	cm^{-1}
Aggregated strand	56/15	52/54	1620–1630
α-Helix	0/12	2/23	≈1655
β-Sheet	20/25	38/19	1670–1680
β-Turn	21/19	7/3	1698

is not sufficient to form a complete α-helical turn. The β-structure content is constant at around 45% for the two peptides, but the random coil content is decreased in the phosphorylated peptide by the same amount (12%) as the increase in α-helix. CD measurements made at the same concentration range (8.0–0.1 mM) as the NMR spectra (see below) show almost identical spectra (Fig. 1*A*) for the two peptides, both being rather similar to the spectrum of the non-phosphorylated peptide at lower concentrations. These spectra indicate mainly random coil structures with some β-structure contribution. The difference between the two sets of concentrations indicates that the peptides aggregate at higher concentrations, and intermolecular interaction is thereby introduced.

Most of the NMR spectra were taken of an 8 mM self-buffering solution, under conditions in which the CD spectra of both the phosphorylated and non-phosphorylated peptides were identical. Upon stepwise dilution down to 0.1 mM, neither the position of the resonances nor the line shape changed, which indicates that the structure remains unchanged and the eventual aggregates remain intact.

The NMR spectra of the non-phosphorylated peptide are largely independent of pH, whereas the spectra of the phosphorylated peptide change significantly in the pH range 4.0–7.5 (Fig. 2). We analyzed the spectra corresponding to residues 2–14 taken at pH values 4–5.6 and residues 3–14 at pH 6.2. At higher pH, the exchange rate of the backbone NH protons was too fast to enable analysis of the spectrum other than to assign the spin systems on the basis of their analogy with the resonances in the spectrum taken at lower pH.

In all NMR spectra, the number of spin systems exceeds the expected number deduced from the primary structure. In the non-phosphorylated peptide (Fig. 3*A*), doubling occurred of the spin system of Gly-13, whose NH protons appear at 8.45 and 7.9 ppm. In the corresponding ROESY spectrum, a strong sequential cross-peak for Gly-13(8.45)-αH-Ser-14-NH is present, whereas only a Gly-13(7.9)-NH Ser-14-NH cross-peak can be observed, and not the corresponding αH-NH cross-peak. The Lys-7(8)βH-Ser-14-NH cross-peak can also be identified for the non-phosphorylated peptide.

For the phosphorylated peptide we confine our discussion to the spectra measured at pH 6.2, the highest pH at which a spectrum could reasonably be interpreted (Fig. 3*B*) and the pH closest to the physiological value (pH 8). In addition, the spectra at pH values in the range 4.2–5.6 are complicated by the existence of a number of minor spin systems that probably arise from minor structures in slow exchange. Many spectral features of the non-phosphorylated peptide are seen also for the phosphorylated peptide. A new position appeared for the Gly-13 spin system resonances which is indicated by the cross-peak with coordinates 8.12 and 3.45. We could observe only a weak Gly(8.12)-NH-Ser-14-NH sequential cross-peak in the non-phosphorylated peptide. Distinct differences were found, not surprisingly, for the residues Thr-5 and Thr-6.

The NMR spectra of the phosphorylated peptide contained

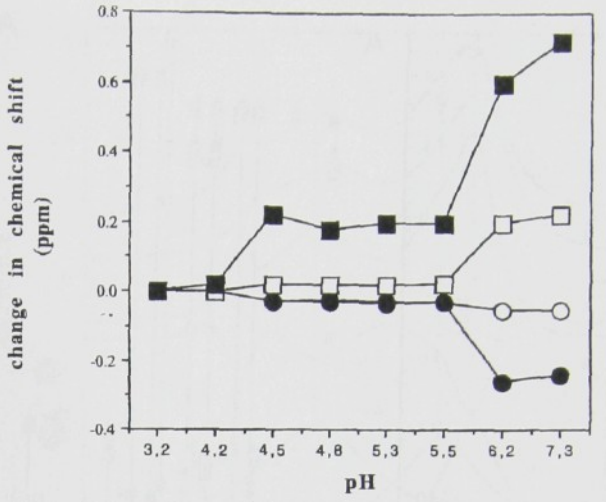

FIG. 2. **pH dependence of the chemical shifts.** The chemical shift of the residues Thr-5 and Thr-6 in the phosphorylated peptide as a function of pH is shown. The proton chemical shifts of the more populated structures are shown. ○, αH Thr-6; ●, αH Thr-5; □, NH Thr-6; ■, NH Thr-5.

many unique cross-peaks. These are difficult to assign unambiguously, since the peptide obviously adopted more than one conformation (Fig. 4).

Fig. 5 shows the FTIR spectral region of the C=O stretch vibration of the peptide backbone, normally denoted as the amide I band (1580–1750 cm^{-1}) or amide I′ when studies are performed in deuterated solvent. The dihedral angles of the peptide backbone determine the geometry of the backbone. Different backbone geometries thus imply different lengths and strengths of the hydrogen bonds involving C=O groups. The different characteristic amide I frequencies arise from the variation in length and direction of these hydrogen bonds correlated with the different structures. Different peak positions have been assigned through both empirical and theoretical work to different structural motifs of the peptide backbone (25). Bands located around 1650–1658 cm^{-1} correspond to α-structures (26) or, as found in some cases, loops (27), whereas bands centered around 1620–1640 and 1680–1689 cm^{-1} are due to β-structures (28, 29), and those at around 1690–1700 cm^{-1} are due to β-turns (30). Fig. 5 shows the FTIR spectra of the non-phosphorylated (*panel A*) and phosphorylated (*panel B*) peptide (*trace a* in H_2O, *trace b* in D_2O), together with the 2nd derivative spectrum (*trace c*), the Fourier self-deconvoluted spectrum (*trace d*), and the individual spectral components (*traces e*) from the curve fitting procedure, respectively. As can be seen, deuterated and H_2O-subtracted spectra are in a very good agreement. Furthermore, both the Fourier self-deconvoluted and the 2nd derivative spectra indicate identical numbers of bands and band positions. Table I lists the relative band areas and peak positions obtained for the different spectral components and their correspondence to different structural classes. The relative area of an infrared absorption band can, as a first approximation, be assumed to be a measure of the relative amount of that particular component. However, this assumption does not take into account absorption by amino acid side chains, or the slightly different extinction coefficients of different structural motifs (31–33). The most conspicuous difference between the FTIR spectra of the phosphorylated and the non-phosphorylated peptides is that the phosphorylated peptide contains a definite contribution from α- structure that is absent from that of the non-phosphorylated form (Table I). Furthermore, the large contribution of β-turn structure in the non-phosphorylated peptide is much lower in the phosphoryl-

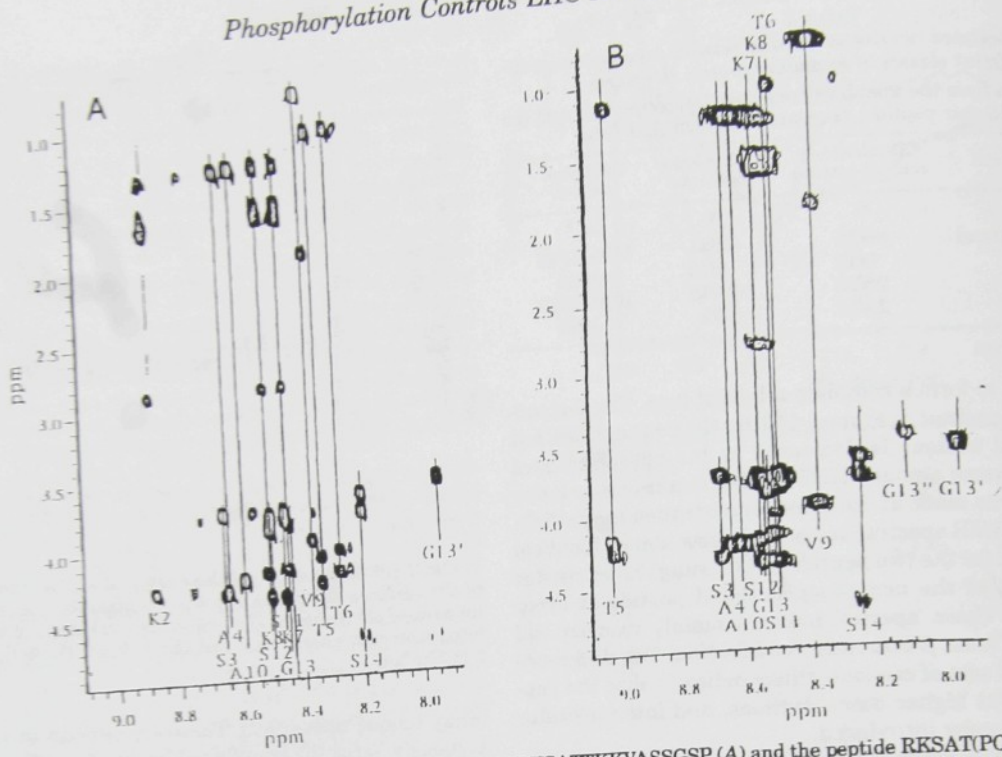

FIG. 3. **Detail of the 500-MHz TOCSY spectra.** Spectra of the peptide RKSATTKKVASSGSP (*A*) and the peptide RKSAT(PO$_3$)TKKVASSGSP (*B*) at pH 5.3. Only those spin systems that may be clearly assigned to the main or minor conformation are indicated. *Prime* indicates the spin systems belonging to the less populated conformation. *T5** is probably the spin system of the double charged phosphorylated threonine residue. This assignment is based solely on the comparison to spectra at higher pH.

ated form.

Structural Effect of Phosphorylation of LHC II by FTIR, CD, and UV Solvent Perturbation Spectroscopy—In addition to information obtained from synthetic peptides corresponding to the LHC IIb N terminus, we have performed studies of the native protein. Fig. 6 shows the amide I band region of the ATR-FTIR spectra of LHC II and LHC II(P), together with the difference spectrum. These absorbance bands are the sum of absorbances from each amino acid in the protein, and the first 15 amino acid residues of the N terminus contribute only as a part of the full structure of 234 amino acids. The main absorbance band is located at 1653 cm^{-1}, indicating mainly an α-helical structure, which is in agreement with the model based on electron diffraction (8). A second band is also shown in the figure at around 1550 cm^{-1} and is assigned to the delocalized amide II vibration. This band has a more complex origin and is therefore not interpreted here. Even though the individual spectra seem to be identical, the difference spectrum shows significant changes. The positive peaks in the difference spectrum reflect structures more abundant in the non-phosphorylated protein than in the phosphorylated protein, and vice versa. For the samples measured in H_2O, the positive band located at around 1625 cm^{-1} is assigned to β-strand structures, whereas the negative bands at 1678 cm^{-1} and 1652 cm^{-1} are assigned to β-turns and α-helices, respectively. H_2O/D_2O exchange experiments (Fig. 6*B*) confirm that the 1652-cm^{-1} band originates from an α-like structure and not from a random or unordered structure (25), since deuteration has no effect on this band even after 2 h, indicating no direct contact with the surrounding solvent. Furthermore, the deuteration effect on the amide II band (delocalized C—N—H bending mode) at 1550 cm^{-1} confirms the assumption that part of LHC II is exposed to the surrounding medium and is not embedded in the membrane. After exposure to D_2O for only 5 min, approximately 25% of the total area of that band is shifted to 1465 cm^{-1}, corresponding to 25% of the protein accessible for rapid H/D exchange. The hydrophobic segments inside the membrane and coiled structures outside the membrane are prevented from such exchange, and only a minor increase of exchanged protons can be found even after 2 h exposure. Interestingly, the negative 1652 cm^{-1} band in the D_2O difference spectrum is the only one of the three major bands found in H_2O difference spectrum that remains at the same positions in both solvents. The absolute area of the difference bands in this region is approximately 4% of the total area in the absorbance spectrum.

The FTIR results demonstrate that LHC II(P) has a higher content of α- and β-turn structures and a lower content of β-stranded structures than the non-phosphorylated form of LHC II. The protein segments that cause the 1625- and 1678-cm^{-1} bands are located outside the membrane domain of non-phosphorylated LHC II. The protein segment that causes the 1652-cm^{-1} band originates from an α-structure present only in LHC II(P). The total number of amino acid residues participating in these changes is in the order of 5–10 amino residues.

CD in the wavelength region 350–750 nm has been suggested as an assay for the oligomeric state of native protein (20): the trimeric form of LHC II has a characteristic negative shoulder in the CD spectrum at 648 nm, and further but less significant differences were found at 412 and 478 nm between the monomeric and trimeric forms of LHC II. LHC II(P) CD spectra measured here have a less pronounced shoulder at 648 nm than the LHC II spectra (Fig. 1*B*) together with spectral features typical for the monomeric form of LHC II at the other two wavelengths. Studies of the minor light-harvesting chlorophyll-*a*/*b*-binding protein CP 29 (Lhc b4) have shown that increased chlorophyll *b* content will enhance a negative signal at 648 nm in the CD spectrum (34). Our findings thus indicate that dissociation of the trimer and phosphorylation may perturb the chlorophyll b_2 or b_3 (8) in the same way. This suggests that phosphorylation induces dissociation of LHC II trimers. The samples here denoted LHC II(P) contain around 90% of non-phosphorylated LHC II (see "Experimental Procedures") and would therefore be expected to show only 10% of the decrease of the 648 nm signal of LHC II, as observed (Fig. 1*B*).

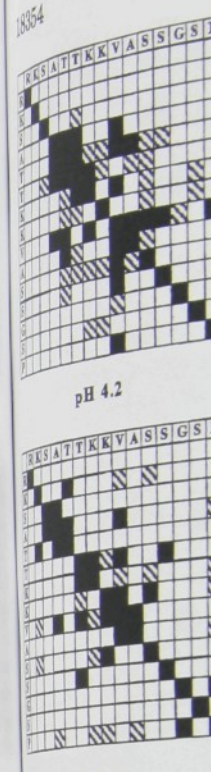

FIG. 4. **Summary of the st**
NMR spectroscopy. The NOE
tic peptide at pH 4.2, 5.3, and
at 5.3 for the non-phosphorylat
dicates that one or more N
protons of the residue defined
Hatched square indicates ambig
chain-to-backbone constraints a
(9)-γH to Val-9-γH NOE at p
assigned to the more populated

Aromatic amino acid res
light in the UV region. The
urbed by change in the p
ading glycerol or ethanol.
turned, residues will, how
egree by changes in the
was used here to study th
romatic residues between
addition of 10% (v/v) ethan
1.2) at equal concentratio
ifference spectrum LHC I
2). Both Tyr and Trp grou
on when dissolved in eth
his implies that the phos
ore aromatic amino acid
edium than the non-phos

D

Other studies of subunit
dies (35–43) have shown l
norylation in some cases
he chlorophyll protein 2
ated to LHC II. There i
ational change upon ph
9 (43). Previous structu
roduced no direct structu
ation site. Indirectly, it
ional of the first 8 amino
merization of LHC II b
herefore been proposed (
(the N terminus is diso

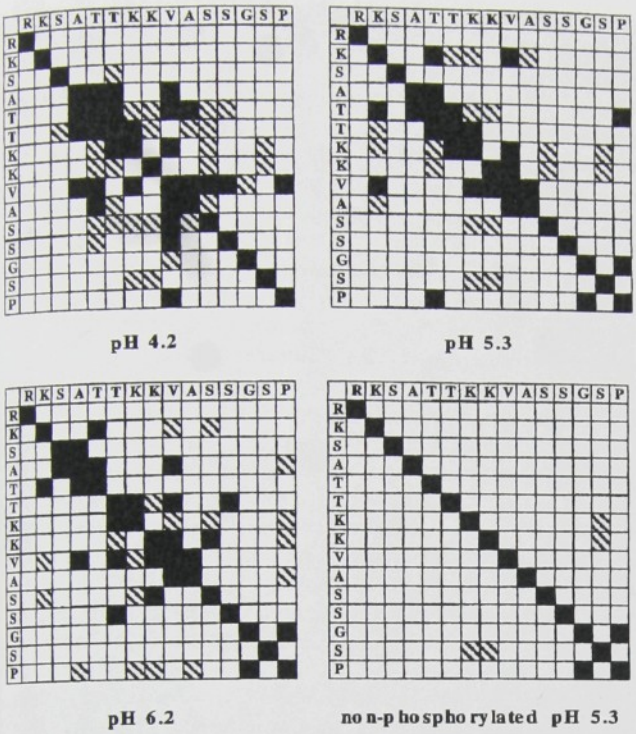

FIG. 4. **Summary of the structural information obtained by NMR spectroscopy.** The NOE constraints observed in the spectra of the peptide at pH 4.2, 5.3, and 6.2 for the phosphorylated form and at pH 5.3 for the non-phosphorylated peptide. A *filled square* in the figure indicates that one or more NOE constraints was observed between protons of the residue defined by the coordinates in the scheme. A *hatched square* indicates ambiguous assignment. In all cases only side chain-to-backbone constraints are observed, with the exception of Lys-7(8) γH to Val-9γH NOE at pH 6.2. Only those constraints that are assigned to the more populated structure are taken into account.

Aromatic amino acid residues (Trp, Phe, and Tyr) absorb light in the UV region. Their absorption spectra may be perturbed by change in the polarity of the environment, *e.g.* by adding glycerol or ethanol. Membrane-embedded, or otherwise buried, residues will, however, not be affected to the same degree by changes in the solvent. Such solvent perturbation was used here to study the differences in number of buried aromatic residues between the LHC II and LHC II(P). After an addition of 10% (v/v) ethanol, to samples of LHC II and LHC II(P) at equal concentrations, a positive peak is found in the difference spectrum LHC II(P)/LHC II at around 280 nm (Fig. 1*C*). Both Tyr and Trp groups have stronger absorbance at 280 nm when dissolved in ethanol than when dissolved in H_2O. This implies that the phosphorylated samples of LHC II have more aromatic amino acid residues exposed to the surrounding medium than the non-phosphorylated samples.

DISCUSSION

Other studies of subunits of phosphoproteins or phosphopeptides (35–43) have shown local structural alteration upon phosphorylation in some cases but not in others. Of these examples, the chlorophyll protein 29 subunit of PS II is most closely related to LHC II. There is independent evidence for a conformational change upon phosphorylation of chlorophyll protein 29 (43). Previous structural studies of LHC II (8, 44) have produced no direct structural information about the phosphorylation site. Indirectly, it has been found that proteolytic removal of the first 8 amino acid (44) residues does not affect the trimerization of LHC II but removal of the first 49 does. It has therefore been proposed (44) that the segment of 8 amino acids at the N terminus is disordered and has no structural role of

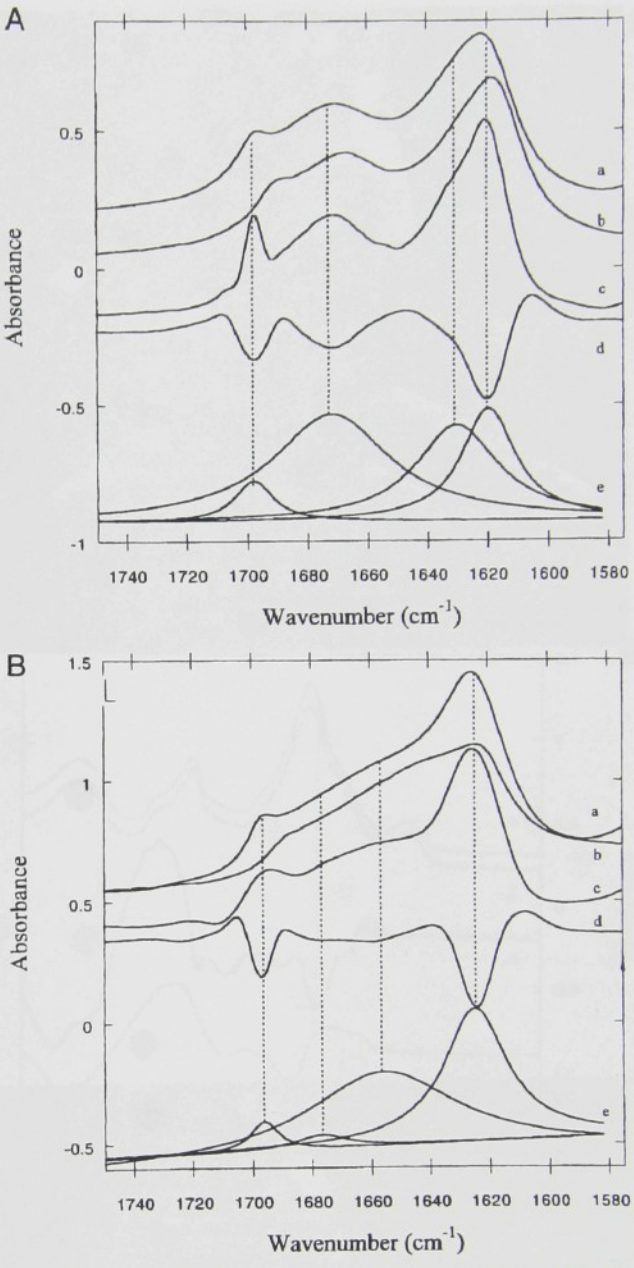

FIG. 5. **The FTIR spectra of the peptide in the amide I region.** ATR-FTIR spectra of the non-phosphorylated peptide (*panel A*), and the phosphorylated peptide (*panel B*). In both panels, *trace a* is the spectrum measured in H_2O after interactive subtraction of bulk water, and *trace b* is the spectrum obtained when the peptide is dissolved in D_2O and no subtraction is performed. *Trace c* is the Fourier self-deconvoluted H_2O spectrum (66), using a *k* value of 2.4 and (*d*) is the 2nd derivative of the H_2O spectrum. The *e traces* are the results of a curve fit performed on the original IR band measured in H_2O, using the number of bands and peak positions obtained from *traces c* and *d* as initial starting values.

the formation of trimers. However, the study was carried out only on LHC II and not on LHC II(P). LHC II(P) has not so far been found in the trimeric state, which is the only state that has been crystallized. The formation of two-dimensional and three-dimensional crystals has been shown (44) to depend on specific lipid-protein interactions. Specifically, the region around residue 16 (Pro-**Trp**-Tyr-Gly-Pro) has been shown to interact with the lipids phosphatidylglycerol (14, 15), monogalactosyl diacylglycerol, and digalactosyl diacylglycerol. Crystal formation is also dependent on the relative concentra-

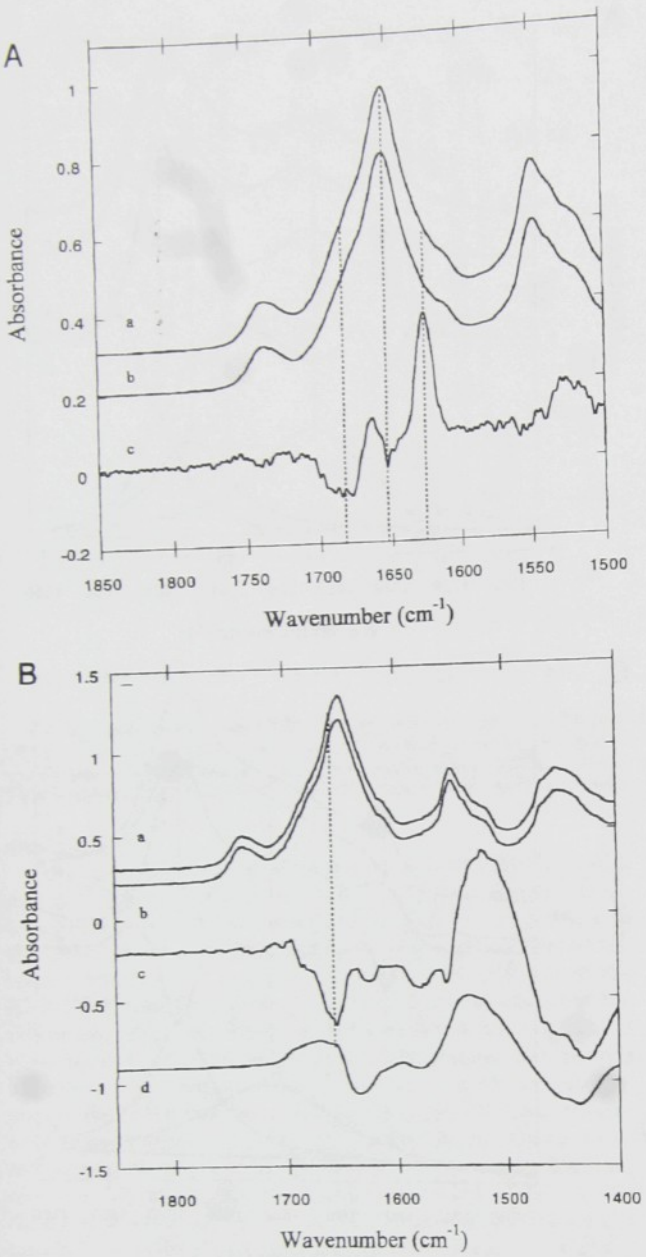

FIG. 6. **The FTIR spectra of LHC II/LHC II(P) in the amide I region.** ATR-FTIR spectra of LHC II (*trace a*)/LHC II(P) (*trace b*) in H_2O (*panel A*) and in D_2O (*panel B*). The difference spectra (*trace c*) were obtained by subtracting the LHC II(P) spectrum from that of LHC II and is scaled 50 times compared with the absolute absorbance spectra (*a* and *b*). In *panel B*, *trace d* is the H/D difference spectrum of LHC II, showing the effect of the H/D exchange on the amide I and II bands.

tion of the last two lipids. Monogalactosyl diacylglycerol is a non-lamellar phase-triggering lipid (for review of this area, see Ref. 45), whereas digalactosyl diacylglycerol forms bilayers or reversed hexagonal phases depending on the acyl chain composition. Furthermore, modification of the C-terminal end of LHC II (46) has been shown to be important for stabilization of the protein, particularly of the pigment-protein complex.

Our results clearly show that peptides corresponding to the N terminus of LHC II and LHC II(P) have non-random tertiary structure although the backbones are mostly extended. Furthermore, we found that the peptides can form stable dimers, and the NMR data indicate that the phosphate group of Thr-5 forms a hydrogen bond to the NH proton of Thr-6. In glycogen phosphorylase (47), a similar hydrogen bond between the phosphate group on Ser-14 and backbone NH of Val-15 is observed. Surprisingly, other protons in the N-terminal region of the peptide were affected only marginally. We also have an indication from the other spectroscopic techniques that the phosphate group interacts with surrounding amino acid residues and thereby alters the structure. The phosphate group also decreases the tendency of the peptides to aggregate. The discrepancy between the amount of the secondary structural motif, particularly the lower values of β-structure and higher content of random coil obtained from the CD compared with the FTIR measurements (see Table I), is similar to that described for other proteins (27, 28, 48) and may be attributed to the different sensitivities of the different methods and problems with structural classification of very small peptide segments. The CD spectrum actually reflects the asymmetric conformation of the single L-amino acid peptide backbone, whereas the FTIR spectrum reflects the environmental effects on the C=O bond of the peptide backbone. We conclude that the full-length LHC II exhibits structural differences between its phosphorylated and non-phosphorylated forms that are similar to those of the model peptide; upon phosphorylation of LHC II, an extended structure is replaced by a short, helix-like structure and by a β-turn. These changes are confined to parts of the protein extrinsic to the membrane.

The band at 1652 cm^{-1}, which is characteristic of a helix, may be assigned to the local structure around Thr-5, in agreement with our findings that the phosphorylated peptide has such a structure around its phosphorylation site. Such a structural change is similar to that seen in the crystal structures of rabbit glycogen phosphorylase in its non-phosphorylated and phosphorylated forms (47). The structural information obtained from the peptides in this investigation may not reflect a totally accurate protein backbone conformation. In the case of glycogen phosphorylase (47) the change in local structure induces a global structural change involving subunit interaction and cofactor binding. Our findings of enhanced β-turn content in LHC II(P) may thus indicate a similar global structural change upon phosphorylation of LHC II. Furthermore, our solvent perturbation measurements show that LHC II has a higher number of aromatic amino acid residues associated with the hydrophobic membrane domain than LHC II(P). Residue 16 is Trp and residue 17 is Tyr. It is therefore plausible to assume that these aromatic amino acid residues are the ones that are shielded by the lipids in the non-phosphorylated LHC II, whereas upon phosphorylation of the N terminus, they are exposed to the surrounding medium. Thus, a good candidate for the β-turn site is the same region as that at which the phosphatidylglycerol interaction has been shown to take place. There are two prolines located at positions 15 and 19. Prolines are able to *cis-trans*-isomerize, and a total isomerization of these two prolines would induce a complete turn of the protein backbone. Proline groups are also known to induce hinges in different proteins (49–51). Such relocation of the negatively charged phosphate group can move it closer to the highly positively charged region around the helix-membrane interface (see Fig. 7). This model would then also explain why LHC II(P) is not found as trimers and hence does not crystallize. The interaction between phosphatidylglycerol and the region around residue 16 was shown to be of importance for trimerization and thereby crystal formation. In LHC II(P) this lipid-protein interaction is broken by structural and interactional changes.

The Functions of LHC II and LHC II(P)—As discussed above, our results imply a quaternary and tertiary structural change upon phosphorylation of LHC II. We propose a model, shown in Fig. 7, describing the events of phosphorylation and protein

FIG. 7. **Schematic struc**
of LHC II. The structural r
of the loops and the propose
of the normal of the memb
phosphorylated protein in
phosphorylation of LHC II
protein (57), the probabili
stacked than in stacked

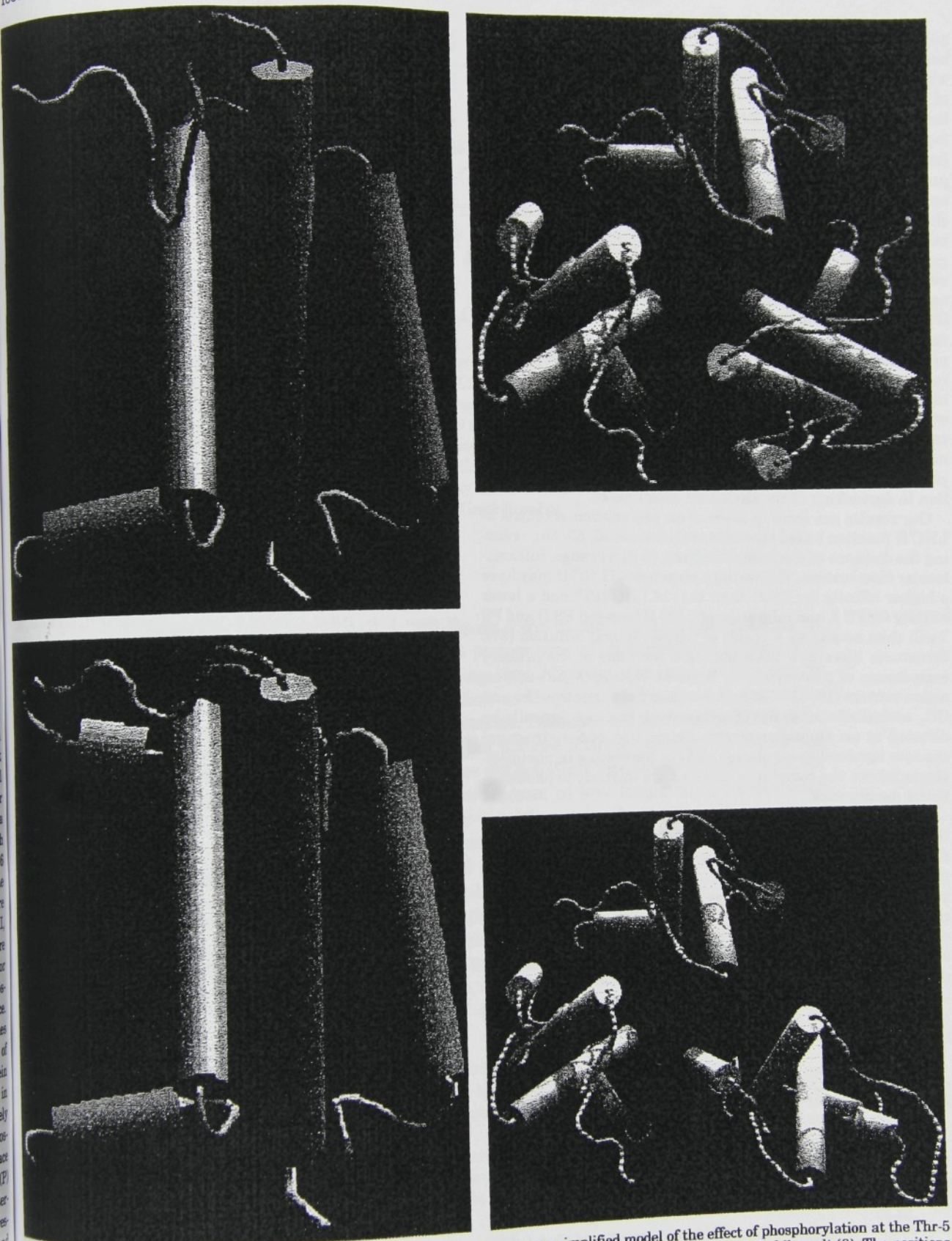

FIG. 7. **Schematic structural models of LHC II/LHC II(P).** The figure shows a simplified model of the effect of phosphorylation at the Thr-5 of LHC II. The structural model is based on coordinates of the helix-α-carbon in LHC II, kindly given to us by W. Kühlbrandt (8). The positions of the loops and the proposed new structure around the phosphorylation site are arbitrary. The *left panel* shows the protein viewed perpendicular to the normal of the membrane in two different rotations around the y axis, with the non-phosphorylated protein in the *upper half* and the phosphorylated protein in the *lower half*. The *right panel* shows a top view of the proposed effect of dissociation of the trimers by the phosphorylation of LHC II whereby LHC II/LHC II(P) becomes free to diffuse. Since unstacking of thylakoids will enhance the diffusion rate of proteins (57), the probability of finding the phosphorylated form of the protein, with its lower affinity for the trimer and PS II, is higher in nonstacked than in stacked thylakoids. See "Discussion" for further details.

migration. The tight complex between LHC II and PS II is based on specific protein-protein/protein-lipid interactions, which include the phosphorylation site. The regulatory effects of phosphorylation of LHC II are decoupling of adjacent thylakoids, destacking of the membranes, and migration and docking of LHC II(P) with PS I (5). Dephosphorylation of LHC II(P) has the opposite effects. These effects have previously been proposed to depend mainly on simple electrostatic repulsion and/or attraction (52), where the addition of the negatively charged PO_4 group induces a repulsive force between opposing, stacked thylakoids and, to reduce that force, LHC II(P) migrates laterally into unappressed regions of membrane. However, earlier it has been shown that photosystem segregation and membrane stacking are separate events (53). Furthermore, it has been shown that importing LHC II into stacked and unstacked thylakoid membranes causes the LHC II in the unstacked regions to migrate toward the PS II-rich stacked regions and not in the opposite direction toward regions with high density of PS I complexes (54). This result is in agreement with LHC II and LHC II(P) having different affinities for the two photosystems. The findings of dimer formation by the non-phosphorylated peptide and dissociation of the dimer by phosphorylation may help to explain the role of phosphorylation in destacking of the thylakoid membranes.

Our results are more in favor of an explanation of control of LHC II function based on structural changes (5, 55, 56), reducing the distance of electrostatic effects to short range, intramolecular interactions. The tertiary structure of LHC II may have a higher affinity for PS II than that of LHC II(P) and a lower affinity for PS I, and migration of LHC II between PS II and PS I will then be simply a result of normal lateral diffusion (57). Structures have now been obtained for some of the primary components of photosynthetic light harvesting (8, 58–60), reaction centers (10, 61–63), and secondary electron transfer and CO_2 assimilation (64, 65). Further work can now logically be directed at an atomic resolution description of the structural changes involved in regulation of light harvesting in photosynthesis, where the complexes involved are intrinsic to photosynthetic membranes.

Conclusions—The results presented here imply that regulation of light-harvesting by means of phosphorylation of chloroplast LHC II can be understood in terms of effects of the phosphate group on protein structure and on molecular recognition. This conclusion removes a conceptual barrier between regulation of ligand binding in soluble proteins and regulation of the function of membrane proteins, where, in photosynthesis at least, emphasis has been placed on the effect of protein phosphorylation on net membrane surface charge. Our results indicate that understanding regulation of photosynthesis will likewise depend on a full three-dimensional structural description of effects of post-translational, covalent modification.

Acknowledgments—We thank Drs. H. Franzén and I. Blaha for the synthetic peptides used, Dr. L. Cheng for the help with preparation of LHC II and LHC II(P), and Dr. P.-O Arvidsson for drawing Fig. 7.

REFERENCES

1. Ghanotakis, D. F., Demetriou, D. M., and Yocum, C. F. (1987) *Biochim. Biophys. Acta* **891**, 15–21
2. Race, H. L., and Hind, G. (1996) *Biochemistry* **35**, 13006–13010
3. Gal, A., Herrmann, R. G., Lottspeich, F., and Ohad, I. (1992) *FEBS Lett.* **298**, 33–35
4. Vener, A. V., van Kan, P. J. M., Gal, A., Andersson, B., and Ohad, I. (1995) *J. Biol. Chem.* **270**, 25225–25232
5. Allen, J. F. (1992) *Biochim. Biophys. Acta* **1098**, 275–335
6. Allen, J. F., Bennett, J., Steinback, K. E., and Arntzen, C. J. (1981) *Nature* **291**, 25–29
7. Larsson, U. K., Jergil, B., and Andersson, B. (1983) *Eur. J. Biochem.* **136**, 25–29
8. Kühlbrandt, W., Wang, D. N., and Fujiyoshi, Y. (1994) *Nature* **367**, 614–621
9. Cashmore, A. R. (1984) *Proc. Natl. Acad. Sci. U. S. A.* **81**, 2960–2964
10. Deisenhofer, J., Epp, O., Miki, K., Huber, R., and Michel, H. (1985) *Nature* **318**, 618–624
11. Weiss, M. S., and Schulz, G. E. (1992) *J. Mol. Biol.* **227**, 493–509
12. Henderson, R., Baldwin, J. M., Ceska, T. A., Zemlin, F., Beckman, E., and Downing, K. H. (1990) *J. Mol. Biol.* **213**, 899–929
13. Tsukihara, T., Aoyama, H., Yamashita, E., Tomizaki, T., Yamaguchi, H., Shinzawa-Itoh, K., Nakashima, R., Yaono, R., and Yoshikawa, S. (1996) *Science* **269**, 1069–1074
14. Hobe, S., Förster, R., Klinger, J., and Paulsen, H. (1995) *Biochemistry* **34**, 10224–10228
15. Trémolières, A., Dainese, P., and Bassi, R. (1994) *Eur. J. Biochem.* **221**, 721–730
16. Cheng, L., Stys, D., and Allen, J. F. (1995) *Physiol. Plant.* **93**, 173–178
17. Burke, J. J., Ditto, C. L., and Arntzen, C. J. (1978) *Arch. Biochem. Biophys.* **187**, 252–263
18. Kühlbrandt, W., Thaler, T. H., and Wehrli, E. (1983) *J. Cell Biol.* **96**, 1414–1424
19. Yang, J. T., Wu, C. S., and Martinez, H. M. (1986) *Methods Enzymol.* **130**, 208–269
20. Hobe, S., Prytulla, S., Kühlbrandt, W., and Paulsen, H. (1994) *EMBO J.* **13**, 3423–3429
21. Bax, A., and Davis, D. G. (1985) *J. Magn. Reson.* **65**, 355–360
22. Bax, A., Griffey, R. H., and Hawkins, B. L. (1983) *J. Magn. Reson.* **55**, 301–307
23. Kumar, A., Hosur, R. V., and Chandrasekhar, K. (1984) *J. Magn. Reson.* **60**, 143–148
24. Wüthrich, K. (1986) *NMR of Proteins and Nucleic Acids*, Wiley Interscience, New York
25. Surewicz, W. K., Mantsch, H. H., and Chapman, D. (1993) *Biochemistry* **32**, 389–394
26. Krimm, S., and Bandekar, J. (1986) *Adv. Protein Chem.* **38**, 181–364
27. Wilder, C. L., Friedrich, A. D., Potts, R. O., Daumy, G. O., and Francoeur, M. L. (1992) *Biochemistry* **31**, 27–31
28. Byler, D. M., and Susi, H. (1986) *Biopolymers* **25**, 469–487
29. Jackson, M., and Mantsch, H. H. (1995) *Crit. Rev. Biochem. Mol. Biol.* **30**, 95–120
30. Torii, H., and Tasumi, M. (1992) *J. Chem. Phys.* **96**, 3379–3387
31. Venyaminov, S. Y., and Kalnin, N. N. (1990) *Biopolymers* **30**, 1243–1257
32. Venyaminov, S. Y., and Kalnin, N. N. (1990) *Biopolymers* **30**, 1259–1271
33. Kalnin, N. N., Baikalov, I. A., and Venyaminov, S. Y. (1990) *Biopolymers* **30**, 1273–1280
34. Giuffra, E., Cugini, D., Croce, R., and Bassi, R. (1996) *Eur. J. Biochem.* **238**, 112–120
35. Otvos, L., Jr., Thurin, J., Kollat, E., Urge, L., Mantsch, H. H., and Hollosi, M. (1991) *Int. J. Pept. Protein Res.* **38**, 476–482
36. Fabian, H., Otvos, L., Jr., Szendrei, G. I., Lang, E., and Mantsch, H. H. (1994) *J. Biomol. Struct. & Dyn.* **12**, 573–579
37. Augusteyn, R. C., Koretz, J. F., and Schurtenberger, P. (1989) *Biochim. Biophys. Acta* **999**, 293–299
38. Ramwani, J. J., Epand, R. M., and Moscarello, M. A. (1989) *Biochemistry* **28**, 6538–6543
39. Mortishire-Smith, R. J., Pitzenberger, S. M., Burke, C. J., Middaugh, C. R., Garsky, V. M., and Johnson, R. G. (1995) *Biochemistry* **34**, 7603–7613
40. Buelt, M. K., Xu, Z., Banaszak, L. J., and Bernlohr, D. A. (1992) *Biochemistry* **31**, 3493–3499
41. Rajagopal, P., Waygood, E. B., and Klevit, R. E. (1994) *Biochemistry* **33**, 15271–15282
42. Otvos, L., Jr., Hollosi, M., Perczel, A., Dietzschold, B., and Fasman, G. D. (1988) *J. Protein Chem.* **7**, 365–376
43. Croce, R., Breton, J., and Bassi, R. (1996) *Biochemistry* **35**, 11142–11148
44. Nussberger, S., Dörr, K., Wang, D. N., and Kühlbrandt, W. (1993) *J. Mol. Biol.* **234**, 347–356
45. Lindblom, G., and Rilfors, L. (1989) *Biochim. Biophys. Acta* **988**, 221–256
46. Paulsen, H., and Kuttkat, A. (1993) *Photochem. Photobiol.* **57**, 139–142
47. Barford, D., Hu, S.-H., and Johnson, L. N. (1991) *J. Mol. Biol.* **218**, 233–260
48. Pribic, R., van Stokkum, I. H., Chapman, D., Haris, P. I., and Bloemendal, M. (1993) *Anal. Biochem.* **214**, 366–378
49. Williams, K. A., and Deber, C. M. (1991) *Biochemistry* **30**, 8919–8923
50. Ludlam, C. F., Sonar, S., Lee, C. P., Coleman, M., Herzfeld, J., RajBhandary, U. L., and Rothschild, K. J. (1995) *Biochemistry* **34**, 2–6
51. Vanhoff, G., Goossens, F., De Meester, I., Hendriks, D., and Scharpé, S. (1995) *FASEB J.* **9**, 736–744
52. Barber, J. (1982) *Annu. Rev. Plant. Physiol.* **33**, 261–295
53. Wollman, F.-A., and Diner, B. (1980) *Arch. Biochem. Biophys.* **201**, 646–658
54. Kohorn, B. D., and Yakir, D. (1990) *J. Biol. Chem.* **265**, 2118–2123
55. Allen, J. F. (1992) *Trends Biochem. Sci.* **17**, 12–17
56. Stys, D. (1995) *Physiol. Plant.* **95**, 651–657
57. Wu, W.-G., and Huang, C.-H. (1981) *Lipids* **6**, 820–822
58. Matthews, B. W., Fenna, R. E., Bolognesi, M. C., Schmid, M. F., and Olson, J. M. (1979) *J. Mol. Biol.* **131**, 259–285
59. Dürring, M., Schmidt, G. B., and Huber, R. (1991) *J. Mol. Biol.* **217**, 577–592
60. McDermott, G., Prince, S. M., Freer, A. A., Hawthornwaite-Lawless, A. M., Papiz, M. Z., Cogdell, R. J., and Isaacs, N. W. (1995) *Nature* **374**, 517–521
61. Allen, J. P., Feher, G., Yeates, T. O., Komiya, H., and Rees, D. C. (1987) *Proc. Natl. Acad. Sci. U. S. A.* **84**, 6162–6166
62. Allen, J. P., Feher, G., Yeates, T. O., Komiya, H., and Rees, D. C. (1987) *Proc. Natl. Acad. Sci. U. S. A.* **84**, 5730–5734
63. Kraub, N., Schubert, W.-D., Klukas, O., Fromme, P., Witt, H. T., and Saenger, W. (1996) *Nat. Struct. Biol.* **3**, 965–973
64. Schreuder, H. A., Knight, S., Curmi, P. M., Andersson, I., Cascio, D., Sweet, R. M., Bränden, C. I., and Eisenberg, D. (1993) *Protein Sci.* **2**, 1136–1146
65. Schneider, G., Knight, S., Andersson, I., Bränden, C. I., Lindqvist, Y., and Lundqvist, T. (1990) *EMBO J.* **9**, 2045–2050
66. Kauppinen, J. K., Moffatt, D. J., Mantsch, H. H., and Cameron, D. G. (1981) *Appl. Spectrosc.* **35**, 271–276

PHOTOSYNTHETICA 37 (2): 325-334, 1999

The relation between changes in non-photochemical quenching, low temperature fluorescence emission, and membrane ultrastructure upon binding of polyionic compounds and fragments of light-harvesting complex 2

D. ŠTYS*,**, P. ŠIFFEL*,***, I. HUNALOVÁ*,***, and J. NEBESÁŘOVÁ*,****

*Laboratory of Biomembranes, Faculty of Biological Sciences, University of South Bohemia, Branišovská 31, CZ-370 05 České Budějovice, Czech Republic**
*Department of Autotrophic Microorganisms, Institute of Microbiology, Academy of Sciences of the Czech Republic, CZ-379 01 Třeboň, Opatovický mlýn, Czech Republic***
*Institute of Molecular Biology of Plants, Academy of Sciences of the Czech Republic, Branišovská 31, CZ-370 05 České Budějovice, Czech Republic****
*Institute of Parasitology, Academy of Sciences of the Czech Republic, Branišovská 31, CZ-370 05 České Budějovice, Czech Republic*****

Abstract

Experiments were performed to distinguish some of the proposed mechanisms by which thylakoid membranes regulate the performance of photosynthetic apparatus in relation to non-photochemical quenching, q_N. Aliphatic diamines were used as uncouplers of transmembrane H^+ gradient as they can be transported across the membrane at the expense of hydrogen cations. Diamines did not induce changes in low-temperature fluorescence emission but induced different changes in membrane ultrastructure. Positively charged peptides did not affect membrane ultrastructure but blocked q_N. In addition, they caused an increase of low temperature fluorescence emission between 710 and 720 nm. For control peptide, the maximal fluorescence increase was found at 715 nm. Fragments of light-harvesting complex 2 in their phosphorylated and non-phosphorylated form shifted the position of this increase. We believe that peptides bind to membrane surface and reduce the mobility of membrane components whose migration is needed for observation of q_N. Phosphorylated and non-phosphophorylated LHC2 fragments bind to different binding sites for corresponding forms of the protein.

Received 22 April 1999, *accepted* 30 August 1999.
Abbreviations: Chl - chlorophyll; LHC2 - light-harvesting complex 2; PS - photosystem; q_N - non-photochemical quenching of chlorophyll fluorescence.
Acknowledgement: Authors thank Prof. John F. Allen from the department of Plant Cell Biology, University of Lund, Sweden, for providing materials developed in his laboratory and for his steady interest and valuable discussions. This work was supported by grants GA 206/97/0325 of the Grant Agency of Czech Republic and VS 96085 of the Ministery of Education, Youth, and Sports of the Czech Republic.

Additional key words: decyldiamine; ethylenediamine; peptides; membrane fragments; phosphorylation; *Pisum sativum*.

Introduction

Non-photochemical quenching of chlorophyll (Chl) fluorescence (q_N) is a relatively easy-to-measure parameter related to the state of photosynthetic apparatus. Because it may be measured non-invasively (Schreiber 1983), many plant physiologists and biologists routinely use this parameter in experiments. Most of the fluorescence emission of photosynthetic apparatus at room temperature originates from photosystem (PS) 2 (Krause and Weis 1991) and its transients probably reflect changes in the efficiency of utilisation of energy captured by PS2 antennae.

Several mechanisms were proposed for q_N. Each of them was based on different lines of biochemical evidences. Quenching related to xantophyll cycle is supposed to be caused by excitation energy flow from Chl to zeaxanthin, a pigment whose concentration in the membrane increases with rising irradiance (Hager 1966, Gilmore 1997). Another line of evidence points out that proton gradient across the thylakoid membrane is necessary for q_N (Briantais *et al.* 1979). Lowering of solution pH in suspension of isolated PS2 membranes leads to a decrease in fluorescence yield (Krieger and Weis 1992). The analogy between the reduction of fluorescence emission in precipitated isolated LHC2 (Burke *et al.* 1978) and the decrease in fluorescence emission of leaves and thylakoid membranes has suggested the hypothesis (Ruban *et al.* 1992) relating the decrease in fluorescence yield with LHC2 aggregation. This hypothesis was recently modified and nowadays the minor antennae are considered to play crucial role in q_N (Crofts and Yerkes 1994, Ruban *et al.* 1996).

Another mechanism by which plants regulate the energy flow from antennae to reaction centres is phosphorylation of membrane proteins (first observed by Bennett 1977; reviewed by Allen 1992). This mechanism is probably directly related to state 1-state 2 transitions (reviewed by Allen 1992), *i.e.*, increase of absorption cross-section of PS1 at the expense of that of PS2 and *vice-versa*. According to Rintamäkki *et al.* (1997) the phosphorylation pattern of thylakoid membrane proteins *in vivo* varies with irradiance and length of irradiation. Similar observation was reported earlier (Stys *et al.* 1995) on isolated thylakoids. Main evidence between the low-irradiance and high-irradiance phosphorylation lies in the phosphorylation of LHC2 which is high at low irradiance and low at high irradiance—clearly, the role of LHC2 is different in each of these states and the original mechanism, suggesting that phospho-LHC2 leaves PS2 and binds to PS1, can hardly be employed (reviewed by Allen 1992).

In this article, we describe experiments aimed at distinguishing some of the proposed mechanisms for q_N. The low-pH induced quenching was blocked by diamines which are supposed to be transported across the membrane at the expense of protons (Portis and McCarty 1976). Similar changes in q_N were observed when positively charged peptides, which bind to charged surface but are not transported across the membrane, were added to the reaction medium in the absence of diamines. Changes in membrane ultrastructure were observed only in the presence of diamines and differed between ethylenediamine and decyldiamine. The phospho- and non-phospho-

LHC2 fragments induce a red or blue shift in emission of PS1, respectively, which indicates that the main influence of LHC2 may be sought in PS1 and its antennae.

Materials and methods

Isolation of thylakoids: Thylakoids were isolated from three-weeks-old pea (*Pisum sativum* L. cv. Tyrkys) seedlings grown on a perlite substrate in a heated greenhouse under supplementary irradiation with halide lamps (200 μmol m^{-2} s^{-1}). 3 g of leaves were crushed in 25 cm^3 of isolation medium (0.4 M sorbitol, 2.5 mM $MgCl_2$, 10 mM KCl, 1 mM $MnCl_2$, 50 mM Tricine, 1 % bovine serum albumine, pH 7.5) on ice and filtered through eight layers of cotton gaze. Chloroplasts were sedimented at 5000×*g* for 4 min at 4 °C. The pellet was resuspended in a shock medium (15 mM $MgCl_2$, 10 mM KCl, 1 mM $MnCl_2$, 50 mM tricine, pH 7.1) and stirred for 1 min. Thylakoids were sedimented at 5000×*g* for 4 min, resuspended in the shock medium with 0.33 M sorbitol, and stored on ice.

In all cases and for all experiments described except electron microscopy, the dependence of the observed effect on concentration of either diamine or peptide was tested to exclude a possible qualitative change at certain concentration. Finally, the concentration of 10 mM was chosen for diamines and 0:83 mM for peptides. The concentrations above these values either did not change the extent of observed effect (diamines) or caused precipitation (control peptide).

Fluorescence spectra: Thylakoids were diluted in resuspension medium supplemented with the desired concentration of polypeptides or polyamines to give final Chl concentration of 25 g m^{-3} and mixed with 10 cm^3 of 2 mM rhodamine B solution (internal fluorescence standard). The mixture was kept on ice for 5 min, pipetted into a shallow (0.4 mm) groove of a metal holder, and frozen in liquid nitrogen. Chl concentration in the sample was 1 g m^{-3}. Emission spectra were measured with a *Fluorolog* fluorimeter (*SPEX*) equipped with halogen lamp and double monochromators. Excitation wavelength was 480 nm. Spectral emission and excitation bandwiths were 2 and 4 nm, respectively.

Fluorescence yield: Influence of polypeptides and polyamines on the Chl fluorescence yield and its light-induced changes were assayed with a PAM fluorimeter (*Walz*, Germany). Thylakoids were diluted to 20 g(Chl) m^{-3} with the resuspension medium with 3 mM of sodium ascorbate in a cuvette, and tested compounds (reagents) of desired concentration were added. Changes in the fluorescence yield upon red actinic irradiation (λ >650 nm, 300 μmol m^{-2} s^{-1}) and Chl relaxation in the dark were recorded. The maximal fluorescence yield was determined using "white-light" saturation pulses (3000 μmol m^{-2} s^{-1} for 1 s). The fluorescence yield was measured at room temperature.

Peptide synthesis was performed as described earlier (Cheng *et al.* 1994, Stys *et al.* 1995) . In general, the t-Boc strategy was used (Barany and Merrifield 1980). In the place of phophothreonine, Thr[$OPO(OPh)_2$] was incorporated and deprotection was carried out as described by Grehn *et al.* (1987). Peptides were synthesized in the

laboratory of Dr. Ivo Bláha in the Institute of Organic Chemistry and Biochemistry of the Academy of Science of the Czech Republic in Prague (peptides SRPLSDQEKRKQISVRGLAGVENV, RKSATTKKVASSGSP) and in the laboratory of Dr. Henry Franzén at the Biomedical Unit at Lund University (RKSAT(PO_4)TKKVASSGSP).

Fixation and preparation of samples for electron microscopy: Samples for electron microscopy were prepared essentially as described in Wollenberger *et al.* (1995). Samples were fixed overnight with 1 % osmium tetroxide, dehydrated with acetone, and embedded in Spurr resin (*Polysciences*, USA). Thin sections were stained with uranyl acetate at room temperature and examined with a *Philips EM 420* electron microscope.

Calculation of fluorescence parameters was done generally as defined in Krause and Weis (1991). Non-photochemical quenching q_N was calculated according to the formula

$$q_N = \frac{F_m - F_m'}{F_m'}$$

Results and discussion

Influence of charged compounds on membrane ultrastructure: The influence of charged compounds on membrane ultrastructure was examined by electron microscopy of isolated thylakoids. Polyionic compounds such as ethylenediamine or nigericin are frequently used as uncouplers of the transmembrane H^+ gradient across thylakoid membranes (Portis and McCarty 1976). These compounds are probably transported across the thylakoid membrane in uncharged state while they lose H^+ ion on the side where the environment is deficient in H^+ (stroma) and accept it on opposite side (lumen). In this way the ion balance remains unaffected but the identity of ions is changed. To our knowledge, the influence of these positively charged ion compounds on membrane ultrastructure was not systematically examined although it is known that polyamines modify membrane surfaces and adhesion of membrane lamellae (see Gulbrand *et al.* 1984 for summary including discussion of mechanisms which cause this effect). The compounds used in our study are indicated in Table 1. Despite the fact that for both diamines the mechanism of membrane transport should be the same, the influence on membrane ultrastructure (Fig. 1*A* - free membranes in medium) was different—ethylenediamine induced formation of tight membrane stacks (Fig. 1*B*) while decyldiamine induced formation of elongated stacked regions (Fig. 1*C*) similar to that observed in presence of polylysine (Berg *et al.* 1974). Hence both compounds, apart from possible transport across the membrane, modify also the surface of the membrane and do it in different way. We believe that ethylenediamine, due to its shorter aliphatic chain, can link only membranes with flat surfaces, while decyldiamine is able to link even regions from which extend bulky and space occupying domains such as subunits on stromal side of PSI or ATP-synthase.

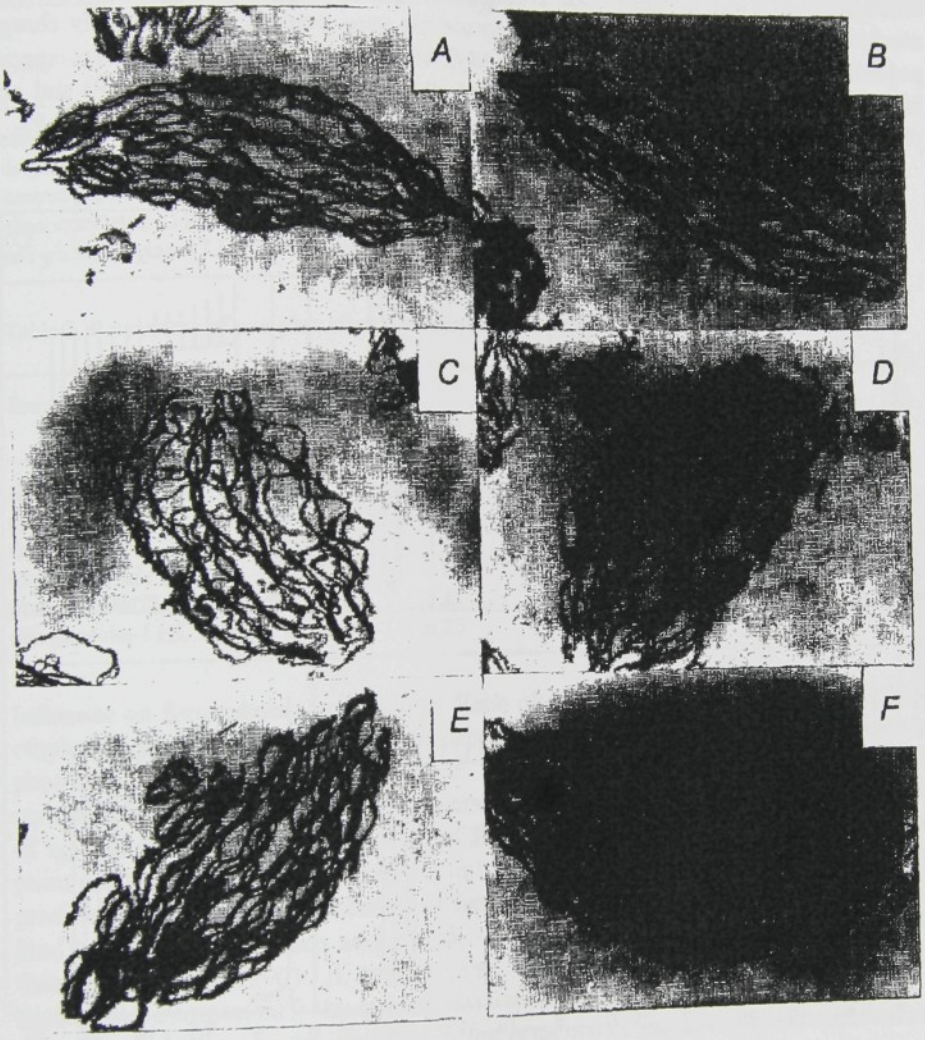

Fig. 1. Electron microscopic pictures of thin layer section of thylakoid membrane in the absence (*A*) and in presence of (*B*) ethylendiamine or (*C*) decyldiamine in the medium. The ultrastructural changes observed in the presence of diamines differ from each other (see text). Peptides caused irregular minor ultrastructural changes which were difficult to evaluate and were not statistically significant (*D* - P1, SRPLSDQEKRKQISVRGLAGVENV, *E* - P2, RKSAT(PO4)TKKVASSGSP, *F* - P3, RKSATTKKVASSGSP).

The effect of non-transportable polyions was examined using multiply charged peptides containing carboxylic and other acidic groups. Such compounds, although positively charged in neutral medium, cannot become completely uncharged at any conditions and thus cannot be transported across the membrane by the same mechanism as diamines. As control peptide we used peptide P1 (positively charged peptide with sequence SRPLSDQEKRKQISVRGLAGVENV). To examine specific binding of LHC2 we used phosphorylated (RKSAT(PO4)TKKVASSGSP) and non-phosphorylated (RKSATTKKVASSGSP) fragments of LHC2, denoted P2 and P3.

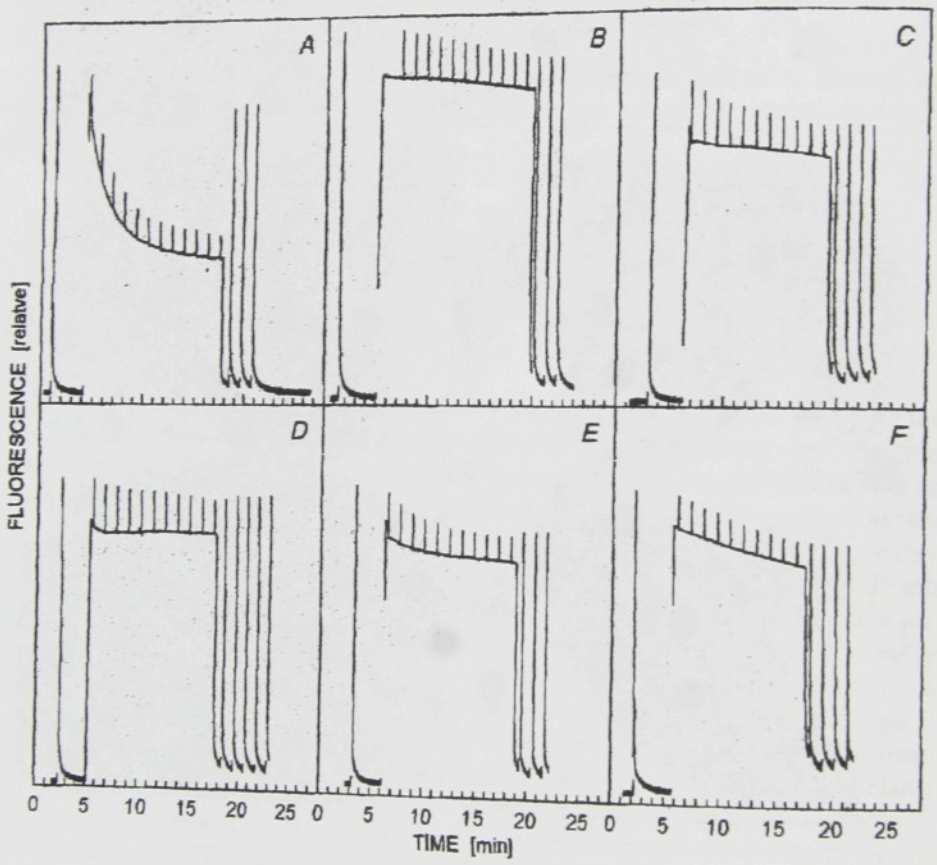

Fig. 2. Course of variable fluorescence of isolated thylakoids in suspension medium (*A*), in suspension medium with added 10 mM ethylenediamine (*B*), 10 mM decyldiamine, (*C*) 0.83 mM peptide fragment of phosphorylation site of glycogen dehydrogenase P1, SRPLSDQEKRKQISVRGLAGVENV (*D*), 0.83 mM phosphorylated fragment of LHC2 P2, RKSAT(PO4)TKKVASSGSP (*E*), and 0.83 mM unphosphorylated fragment of LHC2 P3, RKSATTKKVASSGSP. Both the presence of diamines (*B* and *C*), of the peptide from glycogen phosphorylase (*D*) and of the phophorylated LHC2 fragment (*E*) the non-photochemical quenching is inhibited. In the presence of non-phosphorylated LHC2 fragment (*F*) a steady linear decrease of fluorescence was observed.

The influence of peptides on membrane ultrastructure is depicted on Fig. 1*D-F*. No significant deviation of membrane morphology from the control sample (Fig. 1*A*) was found. This observation is rather surprising since generally peptides bind to membrane surface and this was supported also by our observations described below.

Table 1. Structures of compounds used in the study.

ethylenediamine	$NH_3(CH_2)_2\,NH_3$
decyldiamine	$NH_3(CH_2)_{10}\,NH_3$
control peptide (P1)	SRPLSDQEKRKQISVRGLAGVENV
phosphorylated LHC2 fragment (P2)	RKSAT(PO_4)TKKVASSGSP
non-phosphorylated LHC2 fragment (P3)	RKSATTKKVASSGSP

Table 2. Parameters of non-photochemical quenching as defined in Krause and Weiss (1991).

Sample	F_0/F_m		F_v/F_m		q_N
	dark adapted	light adapted	dark adapted	light adapted	
suspension medium	0.19	0.21	0.81	0.79	0.74
ethylenediamine	0.19	0.20	0.81	0.82	0.06
decyldiamine	0.27	0.29	0.80	0.79	0.05
control peptide (P1)	0.21	0.24	0.79	0.76	0.12
phospho-LHC2 (P2)	0.21	0.23	0.81	0.77	0.15
non-phospho-LHC2 (P3)	0.22	0.26	0.78	0.75	0.15

Influence on fluorescence parameters: Each of the compounds used in the study, *i.e.*, ethylenediamine, decyldiamine, and peptides P1, P2, and P3, was able to block non-photochemical quenching (Fig. 2*A-F* and Table 2). Upon addition of various compounds used in this study, we observed both quantitative differences in the extent of q_N and differences in the course of fluorescence decrease. Thus our experiments point out that q_N may be blocked not only by depletion of the trans-membrane proton gradient, but also by modification of membrane surface. Positively charged peptides bind to membrane surface and islands of membrane components are formed below them (Sackmann 1990). If nothing else, this leads to restriction in diffusion of membrane components. In principle, none of the experiments reported so far demonstrated that q_N was inhibited in the presence of diamines by elimination of H^+ gradient and not by binding of diamines to membrane surface. We believe, however, that the fact that diamines change membrane ultrastructure, while the peptides do not, is caused by transport of diamines to lumenal side of the membrane. Peptides most probably mainly restrict the lateral migration of some membranes components. This points out that lateral migration of membrane components (not necessarily proteins) is a second factor required for the formation of q_N.

Differences between effects of individual compounds were found in low-temperature fluorescence spectra. Since we assumed that majority of changes involve Chl *b*-containing antenna systems we used excitation wavelength 480 nm. Incubation of membranes in the dark did not lead to any spectral change in presence of any

compounds used. When the membranes were irradiated for 5 min at 300 μmol m^{-2} s^{-1} in the respective medium prior to low-temperature measurements, some changes appeared. The presence of peptides in the medium lead to increase in fluorescence emission between 710 and 720 nm (Fig. 3*B*). This effect was not observed in the presence of diamines (Fig. 3*A*). However, there were systematic differences between the influence of individual peptides. Control peptide induced maximal fluorescence increase at 715 nm. Phosphorylated fragment of LHC2, P2, induced maximal increase at 720 nm and the non-phosphorylated fragment, P3, induced maximal increase at 712 nm (Fig. 3*B*). Similar changes were observed earlier in experiments in the presence of ATP, *i.e.*, when phosphorylation of membrane proteins was observed (Stys *et al.* 1995).

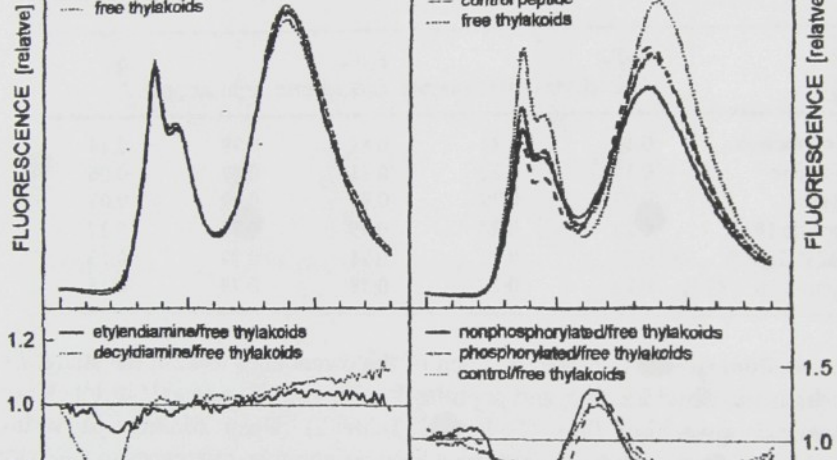

Fig. 3. 77 K fluorescence emission spectra of thylakoids frozen at high energy state after 10 min irradiation with 1000 μmol m^{-2} s^{-1} of "white light", at conditions when the non-photochemical quenching occurred in free membranes. *Upper panels* represents emission spectrum of free thylakoids (*dotted line*), thylakoids in the presence of (*A*) 10 mM ethylenediamine (*solid line*) and 10 mM decyldiamine (*dashed line*), or (*B*) in the presence of 0.83 mM peptide P1, SRPLSDQEKRKQISVRGLAGVENV (*short dashed line*), 0.83 mM peptide P2, RKSAT(PO4)TKKVASSGSP (*long dashed line*) and 0.83 mM peptide P3, RKSATTKKVASSGSP (*solid line*). *Lower panels*: ratio of the spectra recorded with and without (*A*) 10 mM ethylenediamine or (*B*) added peptides in the medium.

We believe that the fluorescence increase between 710 and 720 nm is an indication of restriction of lateral migration (perhaps it reflects inappropriate aggregation of photosystems or antenna systems). The LHC2 fragment occupied specific and different binding sites on the membrane which had became accessible

upon membrane irradiation. These observations indicate that LHC2 may be involved in fine tuning of PS1 antenna and that phosphorylated and non-phosphorylated LHC2 influence different sites.

In conclusion, we demonstrated that diamines known as ΔpH uncouplers have a paralell effect on membrane ultrastructure. The effect on ultrastructure depends on the length of the aliphatic chain. The differences in membrane ultrastructure cannot be put in relation to non-photochemical quenching. The mechanism of non-photochemical quenching involves probably also migration in the membrane plane. The low-temperature experiments indicate that there are specific binding sites for both phosphorylated and non-phosphorylated LHC2. It supports the results of Rintamäkki *et al.* (1997) and Stys *et al.* (1995) which indicate that there are two stages in the adaptation of thylakoid membranes to light—an early stage, in which LHC2 is the prominent phosphoprotein, and the late stage, when LHC2 is functional in non-phosphorylated form. It might be hypothesised that both non-phosphorylated and phosphorylated LHC2, in response to irradiation, physically migrate and bind to a specific binding site on outer antennae of PS1.

Question to be solved is to which extent the observation on isolated thylakoids may be applied to observations on intact leaves. The similarity of results on isolated thylakoids (Stys *et al.* 1995) and on intact leaves (Rintamäkki *et al.* 1997) shows that at least in the case of phosphorylation, results on isolated thylakoids and intact leaves are comparable. Isolated thylakoids inavoidably miss many enzyme components, products, and intermediates such as ribulose-1,5-bisphosphate carboxylase/-oxygenase, the terminal electron acceptor, the electron carriers such as $NADP^+$ and ferredoxin, substrates and products of the ATP synthase reaction to list just the components certainly related to the thylakoid membrane. In a combination of mild isolation methods, optimisation of isolation media, and addition of protective compounds such as ascorbate, similar behaviour of the signal of variable fluorescence to that observed in intact leaves may be preserved. We thus believe that the observations presented in this article reflect at least a part of the mechanisms which contribute to q_N quenching in intact leaves.

References

Allen, J.F.: Protein phosphorylation in regulation of photosynthesis. - Biochim. biophys. Acta **1098**: 275-335, 1992.

Barany, G., Merrifield, R.B.: Special methods in peptide synthesis. - In: Gross, E., Meienhofer, J. (ed.): The Peptides. Vol. 2. Pp. 1-284. Academic Press, New York 1980.

Bennett, J.: Phosphorylation of chloroplast membrane polypeptides. - Nature **269**: 344-346, 1977.

Berg, S., Dodge, S., Krogmann, D.W., Dilley, R.A.: Chloroplast grana membrane carboxyl groups. Their involvement in membrane association. - Plant Physiol. **53**: 619-627, 1974.

Briantais, J.-M., Vernotte, C., Picaud, M., Krause, G.H.: A quantitative study of the slow decline of chlorophyll *a* fluorescence in isolated chloroplasts. - Biochim. biophys. Acta **548**:128-138, 1979.

Burke, J.J., Ditto, C.L., Arntzen, C.J.: Involvement of the light-harvesting complex in cation regulation of excitation energy distribution in chloroplasts. - Arch. Biochem. Biophys. **187**: 252-263, 1978.

Cheng, L., Spangfort, M.D., Allen, J.F.: Substrate specificity and kinetics of thylakoid phosphoprotein phosphatase reaction. - Biochim. biophys. Acta **1188**: 151-157, 1994.

Crofts, A.R., Yerkes, C.T.: A molecular mechanism for q_E-quenching. - FEBS Lett. **352**: 265-270, 1994.

Gilmore, A.M.: Mechanistic aspects of xantophyll cycle-dependent photoprotection in higher plant chloroplasts and leaves. - Physiol. Plant. **99**: 197-200, 1997.

Grehn, I., Fransson, B., Ragnarsson, U.: Synthesis of substrates of cyclic AMP-dependent kinase and use of their precursors for convenient preparation of phosphoserine peptides. - J. chem. Soc. Perkin Elmer I **1987**: 529-535, 1987.

Gulbrand, L., Jönsson, B., Wennerström, H., Linse, P.: Electrical double layer forces. - J. chem. Phys. **80**: 2221-2228, 1984.

Hager, A.: Die Zusammenhänge zwischen lichtinduzierten Xanthophyll-Umwandlungen und Hill Reaktion. - Ber. deutsch. bot. Gesell. **79**: 94-107, 1966.

Krause, G.H., Weis, E.: Chlorophyll fluorescence and photosynthesis: the basics. - Annu. Rev. Plant Physiol. Plant mol. Biol. **42**: 313-349, 1991.

Krieger, A., Weis, E.: Energy-dependent quenching of chlorophyll-*a*-fluorescence: The involvement of proton-calcium exchange at photosystem 2. - Photosynthetica **27**: 89-98, 1992.

Portis, A.R., McCarty, R.E.: Quantitative relationships between phosphorylation, electron flow, and internal hydrogen ion concentrations in spinach chloroplasts. - J. biol. Chem. **251**: 1610-1617, 1976.

Rintamäkki, E., Salonen, M., Suoranta, U.M., Carlberg, I., Andersson, B., Aro, E.M.: Phosphorylation of light-harvesting complex II and photosystem II core proteins show different irradiance-dependent regulation *in vivo*. Application of phosphothreonine antibodies to analysis of thylakoid phosphoproteins. - J. biol. Chem. **272**: 30476-30482, 1997.

Ruban, A.V., Rees, D., Pascal, A.A., Horton, P.: Mechanism of ΔpH-dependent dissipation of absorbed excitation energy by photosynthetic membranes. II. The relationship between LHCII aggregation *in vitro* and qE in isolated thylakoids. - Biochim. biophys. Acta **1102**: 39-44, 1992.

Ruban, A.V., Young, A.J., Horton, P.: Dynamic properties of the minor chlorophyll *a/b* binding proteins of photosystem II, an *in vitro* model for photprotective energy dissipation in the photosynthetic membrane of green plants. - Biochemistry **35**: 674-678, 1996

Sackmann, E.: Molecular and global structure and dynamics of membranes and lipid bilayers. - Can. J. Phys. **68**: 999-1012, 1990.

Schreiber, U.: Chlorophyll fluorescence yield changes as a tool in plant physiology. I. The measuring system. - Photosynth. Res. **4**: 361-373, 1983.

Stys, D., Stancek, M., Cheng, L., Allen, J.F.: Complex formation in plant thylakoid membranes. Competition studies on membrane protein interactions using synthetic peptide fragments. - Photosynth. Res. **44**: 277-285, 1995.

Wollenberger, L., Weibull, C., Albertsson, P.-Å.: Further characterization of the chloroplast grana margins: the non-detergent preparation of granal Photosystem I cannot reduce ferredoxin in the absence of $NADP^+$ reduction. - Biochim. biophys. Acta **1230**: 10-22, 1995.

ELSEVIER

Journal of Molecular Structure 523 (2000) 281–287

Journal of
MOLECULAR
STRUCTURE

www.elsevier.nl/locate/molstruc

Studies of phospholipid binding to *N*-terminal domain of membrane protein light-harvesting complex II

V. Veverka[a,b,c,*], R. Hrabal[b,c], M. Durchan[c,d], D. Štys[c,e]

[a]*Department of Analytical Chemistry, Institute of Chemical Technology, Technická 5, CZ 166 28 Prague 6, Czech Republic*
[b]*Laboratory of NMR Spectroscopy, Institute of Chemical Technology, Technická 5, CZ 166 28 Prague 6, Czech Republic*
[c]*Laboratory of Biomembranes, University of South Bohemia Branišovská 31, CZ-370 05 České Budějovice, Czech Republic*
[d]*Department of Autotrophic Microorganism, Institute of Microbiology, Czech Academy of Science, 379 81 Trebon–Opatovický mlýn, Czech Republic*
[e]*Department of Photosynthesis, Institute of Molecular Biology of Plants, Czech Academy of Science, Branišovská 31, CZ-370 05 České Budějovice, Czech Republic*

Received 16 August 1999; received in revised form 22 October 1999; accepted 22 October 1999

Abstract

The peptide fragment of the light harvesting complex II comprising the trimerisation site binds strongly and selectively to phosphatidylglycerol while the affinity to the other LHCII-bound lipid digalactosyldiacylglycerol is negligible. Upon its binding, large aggregates of the lipid are formed which do not occur in the presence of other peptides, in particular the peptide comprising the phosphorylation site. Our observation supports a hypothesis that the trimerisation site of LHCII is also the specific binding site for phosphatidylglycerol and favors another hypothesis that the phosphorylation site is directly involved in the control of trimerisation. © 2000 Elsevier Science B.V. All rights reserved.

Keywords: Light-harvesting complex II; Trimerisation; Specific lipid binding

1. Introduction

Light harvesting complex II is the major protein of thylakoid membranes of plants [1]. Model of a three-dimensional structure of this membrane protein was published by Kühlbrandt et al. [2,3]. The model based on electron diffraction data shows mutual positions of all three monomeric units. The high sequential diversity among species and probably also a lack of order within the *N*-terminal region prevented more detailed analysis of the *N*-terminal domain of the protein.

It has been known for a long time that trimerisation of the light harvesting complex II depends on intactness of the *N*-terminal region of the protein, which may be cleaved by proteinases [4,5]. Furthermore, it has also been proved that phosphatidylglycerol is needed for the correct formation of trimers [6]. Hobe et al. [7] identified the amino acid sequence W16–R21 to form the site of the light-harvesting complex II responsible for the trimer formation and raised a hypothesis that the trimerisation site is identical with the phosphatidylglycerol binding site. However, it was also found that residue Ile 222 which is located within the *C*-terminal domain, is also essential for successful formation of trimers [8].

The *N*-terminal domain of LHCII is vitally important for understanding the regulation of the protein

*Corresponding author. Department of Analytical Chemistry, Institute of Chemical Technology, Technická 5, CZ 166 28 Prague 6, Czech Republic. Tel.: +42-2-2435-3805; fax: +42-2-2431-1082.
E-mail address: veverkav@vscht.cz (V. Veverka).

0022-2860/00/$ - see front matter © 2000 Elsevier Science B.V. All rights reserved.
PII: S0022-2860(00)00...

function, because it contains the phosphorylation site. The structural changes, which follow this modification were hypothesized for the first time by Allen [10] and later supported experimentally by Nilsson et al. [11]. However, Nilsson's experiments were performed in the absence of lipids.

In this contribution we report on a study of binding of phosphatidylglycerol to the peptide fragments derived from the *N*-terminal domain of LHCII. By the identification of amino acid residues involved in the binding we want to demonstrate the identity of the lipid binding and trimerisation sites of this protein.

2. Materials and methods

Three peptides P1 (H–RKSATTKKVYGSSP–OH), P5 (H–WYGPDRVKYLGPFSG–OH) and P6 (H–RKSATTKKVYGSSPWYGPDRVKYLGPFSG–OH) were synthesized using Fmoc strategy. Phosphatidylglycerol (PG), digalactosyldiacylglycerol (DGDG) and monogalactosyldiacylglycerol (MGDG) were purchased from Lipid Products (Surrey, UK). NMR samples of the free peptides were prepared as 0.5–2 mM solutions in a mixture of 90% H_2O and 10% D_2O. pH value was adjusted to 4.1 by adding small amounts of either HCl or NaOH. Complexes with phospholipids were prepared by adding the stock solutions of the particular peptide to colloidal solutions of phospholipids and homogenized by 30 min sonication. The concentration of the phospholipid was 0.5 mM and the peptide/lipid ratios were up to 1:5.

NMR experiments were carried out on a Bruker DRX-500 Avance spectrometer equipped with a 5-mm inverse, triple resonance gradient probe at 27°C.

CD spectra were measured on a modified Jasco J-715 spectrometer with the option of right-angle detection. Samples were prepared in the same way as described for the NMR spectroscopy and measured in 0.1 mm thick quartz cuvette.

3. Results

3.1. NMR spectroscopy

The samples consisted of a stable suspension of lipid vesicles, which was achieved by sonication of the lipid–peptide mixture. NMR spectra of the free lipids contained quite sharp lines corresponding to the aliphatic chains of lipid fatty acids (Fig. 1). It demonstrated that the size of the vesicles was sufficiently small to allow the recognition of a bound form of the peptide.

Sequences of the peptides used in the study and their location in the sequence of the intact LHCII are summarized in Table 1. Upon addition of the peptide P5, which comprises the trimerisation site but not the phosphorylation site, the signals of phosphatidylglycerol nonspecifically broadened due to an increase in the size of the vesicles and finally disappeared in the noise (Fig. 1, panel A). An analogous experiment when peptide P5 was added to the suspension of digalactosyldiacylglycerol (Fig. 1, panel B) did not lead to a complete disappearance of the lipid signals at any achievable peptide concentration. The signals of the lipid broadened negligibly even at high concentrations of the peptide. It is also worth mentioning that the NMR signals of the peptide P5 were much less intensive in the presence of PG than in the presence of DGDG (Fig. 1). This phenomenon can be explained by the existence of a certain fraction of the peptide that is tightly bound to the lipid vesicles and share their long rotational correlation time. This results in shortening T_2 relaxation times of the NMR resonances and therefore they become invisible in the spectrum. In an analogous experiment in which the binding of the positively charged phosphorylation-site fragment P1 to phosphatidylglycerol was examined (Fig. 1, panel C) the addition of the peptide did not lead to any changes in the NMR spectrum, leaving the size of the vesicles unchanged. Upon addition of the peptide P6 (Fig. 1, panel D) the signals of phosphatidylglycerol broadened in a similar way as in the case of peptide P5.

We have compared two-dimensional TOCSY spectra of the peptide P6 in the presence and absence of lipids (Fig. 2) and identified Gly 18, Asp 20, Arg 21

Table 1
N-terminal peptide fragments of LHCII. Phospholipid binding (trimerisation) site is marked

P1	RKSATTKKLLVASSGSP
P5	WYGPDRVKYLGPFSG
P6	RKSATTKKLLVASSGSPWYGPDRVKYLGPFSG

Fig. 1. Changes
LHCII. Panel A

and Gly 26
experienced
their proton
changes is o

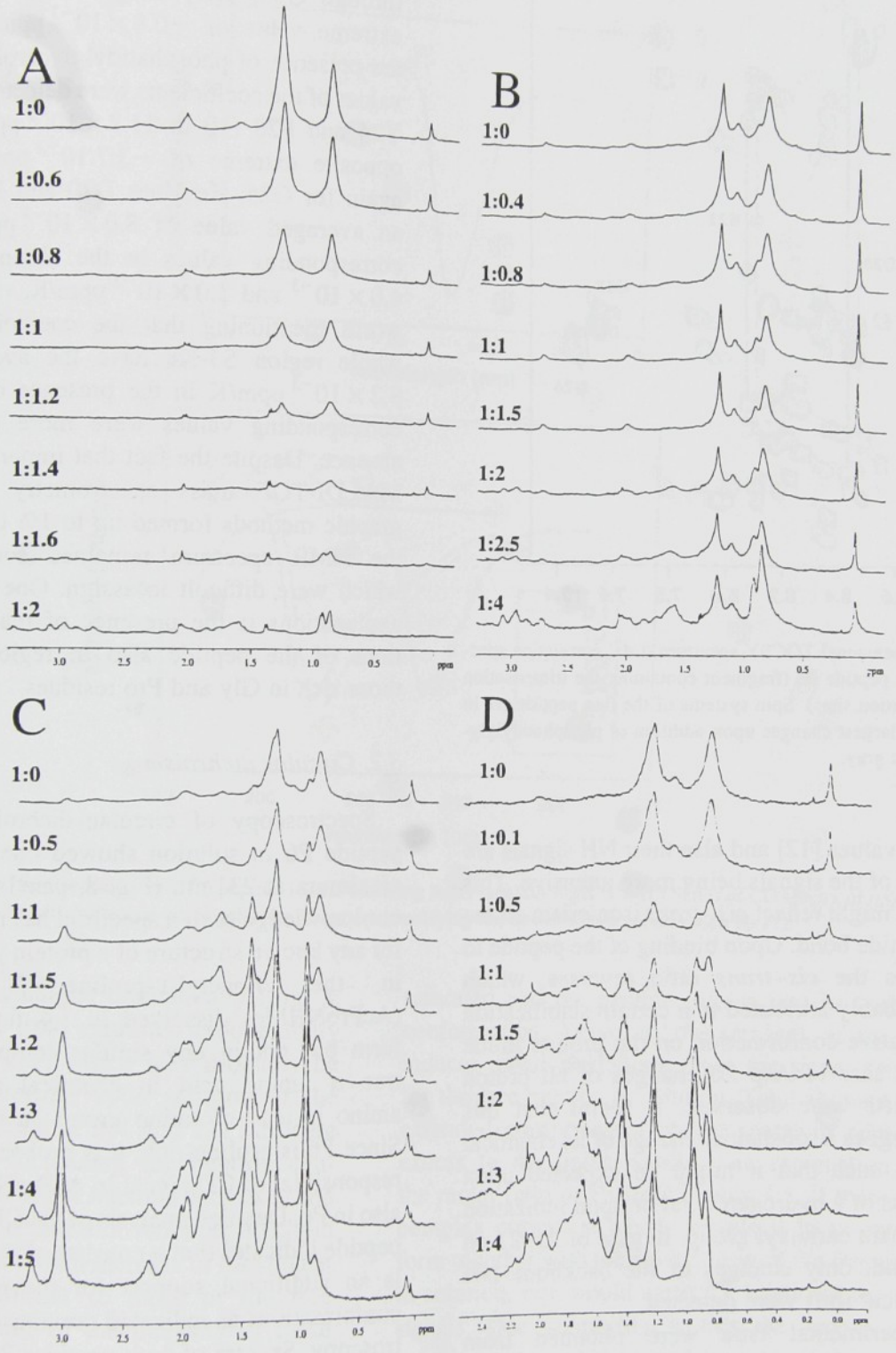

Fig. 1. Changes of the proton NMR spectra in the aliphatic region of a stable suspension of lipids in water upon addition of peptide fragments of LHCII. Panel A represents a mixture of PG and P5, panel B DGDG and P5, panel C PG and P1 and panel D PG and P6.

and Gly 26 to be the amino acid residues which experienced the largest changes of chemical shift of their proton resonances. However, each of these changes is of a different character. Residue Gly 18 is the first of two glycine residues followed by prolines. Both glycines have their NH protons shifted upfield significantly (Gly 18 by 0.83 ppm and Gly 26 by 0.90 ppm, respectively) when compared with their

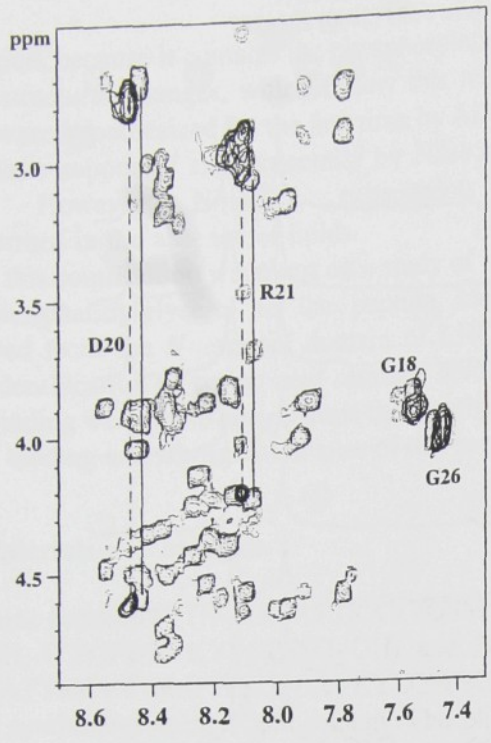

Fig. 2. Two-dimensional TOCSY spectrum (total correlation spectroscopy) of the peptide P6 (fragment containing the trimerisation and phosphorylation sites). Spin systems of the free peptide are in black and their largest changes upon addition of phosphatidylglycerol are in light gray.

random-coil values [12] and also their NH signals are doubled, one of the signals being more intensive. This phenomenon might reflect *cis–trans* isomerism on the Gly–Pro peptide bond. Upon binding of the peptide to lipid vesicles the *cis–trans* ratio reverses, which might be probably attributed to a certain stabilization of the alternative conformation on the proline imide bond. In the case of Asp 20 changes of all proton chemical shifts were observed. It seems that this residue undergoes a substantial change of its chemical environment, such that it might be expected upon formation/loss of a hydrogen bond or upon ionization of the side chain carboxyl group. In case of Arg21 on the other hand, only changes of the backbone NH proton chemical shift were detected.

More experimental data were obtained from temperature dependency of chemical shifts of amide protons of P6 in the absence and presence of phosphatidylglycerol. In the free peptide, the largest deviations from the averaged values of temperature coefficients ($7–9 \times 10^{-3}$ ppm/K) were found out for amino acid residues in the *C*-terminal region from S14 through G30. They ranged from 5.5×10^{-3} to an extreme value of -0.8×10^{-3} ppm/K for G26. In the presence of phosphatidylglycerol the most exotic values of the coefficients were detected for W16, K23, Y24 and F28 (10 to 11.8×10^{-3} ppm/K) while the opposite extreme of $-3.7.10^{-3}$ ppm/K was found again for G26. Residues D20 and R21 experienced an averaged value of 8.0×10^{-3} ppm/K while the corresponding values in the absence of PG were 4.0×10^{-3} and 3.0×10^{-3} ppm/K, respectively. It is worth mentioning that the coefficients within the whole region S3-K8 have the averaged value of 8.2×10^{-3} ppm/K in the presence of PG while the corresponding values were more dispersed in its absence. Despite the fact that impurities detected by MALDI-TOF mass spectrometry and chromatographic methods formed up to 1% of the sample, in the NMR spectrum remained some cross-peaks, which were difficult to assign. One of the plausible explanations is the presence of multiple conformations of the peptide also in regions distant from those rich in Gly and Pro residues.

3.2. Circular dichroism

Spectroscopy of circular dichroism of the free peptide P6 in solution showed one strong negative maximum at 231 nm (Fig. 3, panel a). According to our knowledge such a spectrum has not been reported for any known structure of a protein yet but was found in the *N*-acetyl-L-proline *N'* Methylamide (AcProNHMe) dissolved in 1,4-dioxane or chloroform but not in any similar compound containing true α amino acid in chemical sense—i.e. with amino instead of imino group on its α carbon [9]. Since P6 is proline-rich, it is probable that structures responsible for CD signal in AcProNHMe are present also in P6. Detailed analysis of the CD spectrum of the peptide indicates that it consists of two maxima which is an additional support for the existence of two conformations as indicated previously by NMR spectroscopy. Spectra of both peptides P1 and P5 showed maxima at 205 nm indicating a prevalence of an extended structure (data not shown). The spectra of P1 and P5 did not change upon addition of PG, DGDG or MG (data not shown).

Upon addition of the peptide P6 to the solution of

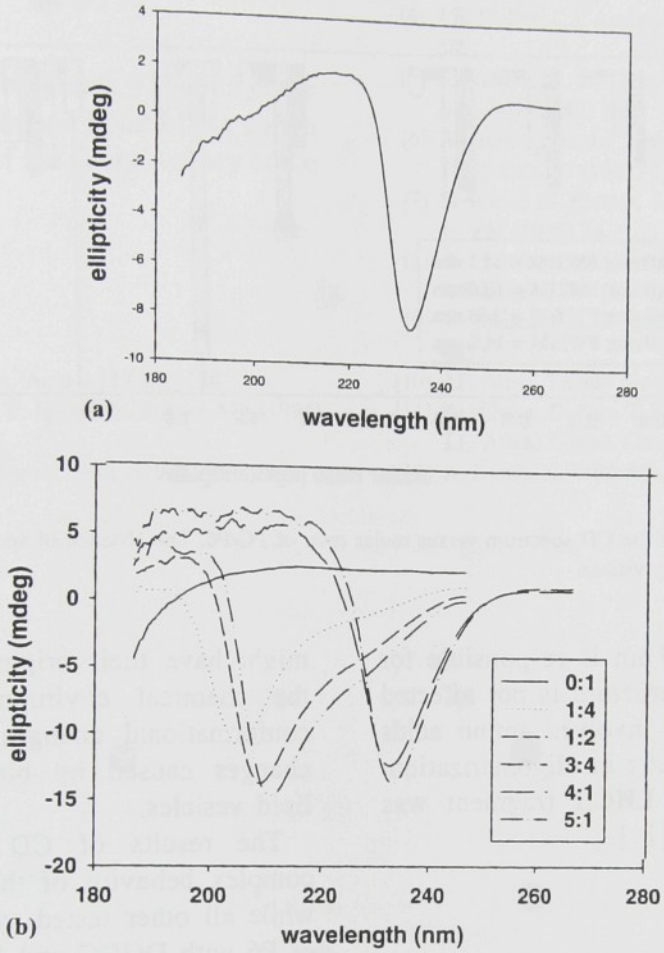

3. (a) CD spectrum of the free peptide 5 mM P6 peptide in self-buffering water solution at pH = 7. (b) Series of CD spectra of mixtures of sphatidylglycerol and P6 in self-buffering water solution. Numbers identifying the lines indicate molar ratios P6:PG.

the CD spectrum changed dramatically (Fig. 3, el b). While the free lipid exhibited exponentially aying signal in far UV, which may probably be ibuted to light scattering, upon addition of the tide mainly the maxima at 211 and 221 nm were ected (Fig. 4). On increasing the peptide con- ration, the intensity of these maxima decreased and nearly vanished at concentration ratios peptide:lipid e 4:1 when we observed an increase of maxima at 5 and 235.9 nm, similar to those of the free ide. The relative ratio of the intensity of these maxima was changing during the titration.

herefore, we propose, that at low peptide:lipid os the peptide is tightly bound to the surface of vesicles and adopts an extended conformation to interactions of its positively charged residues h negatively charged surface of the lipid. With easing peptide concentration the surface becomes saturated and the peptide refolds into its "original" conformation. However, the presence of the lipids induces small deviations from the signal observed for the free peptide in solution. Total absence of the extended conformation in the spectrum peptide in excess to the lipids needs some explanation since the molar ratio of P6:lipid is only 4:1. If there was a complex present in which peptide is in an extended form together with the folded form of the free peptide in solution, one would expect 3:1 ratio of these two signals. One possibility is that the excess of the peptide increases the k_{on} and k_{off} rates of the peptide-to-lipid binding and consequently the lifetime of the bound form to such extent that it becomes non-observable. It is, however, known that CD is capable to detect conformational changes with higher sensitivity than any other method. We, therefore, prefer the possibility that for CD

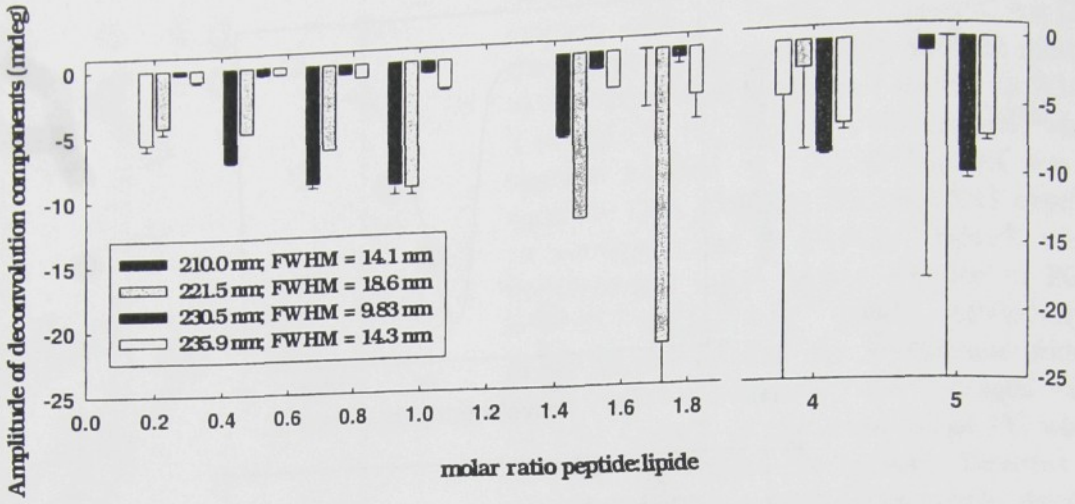

Fig. 4. Plot of major components of the CD spectrum versus molar ratio of PG/P6. The absence of spectral forms indicating an extende conformation of the peptide is clearly visible.

maxima at 230.5 and 235.9 nm is responsible for an oligomer of P6 whose structure is not affected by binding to lipids which involves amino acids outside the region participating in oligomerization. Oligomerization in shorter LHCII fragment was observed by Nilsson et al. [11].

4. Discussion

The involvement of Gly 18, Asp 20 and Arg 21 in the binding of the LHCII *N*-terminal domain to the lipid vesicles is one of the first experimental evidences of the identity of the lipid binding site and the trimerisation site which was originally proposed by Hobe et al. [7]. The experiments described here indicate that the region encompassing the trimerisation site strongly prefers binding to phosphatidylglycerol over digalactosyldiacylglycerol, the two major lipid components of plant cell membranes [5].

Our experimental results also indicate the existence of a certain prevalent structure of the peptide fragments P5 and P6 containing the trimerisation site. These peptides also contain two preserved dipeptide sequences, i.e. Gly–Pro, in which the chemical shifts of NH-protons of both glycines are far from their random coil values (Fig. 2). It is difficult to interpret the differences between the temperature coefficients in the presence and absence of PG since they might have their origins not only in changes o the chemical environment caused by possibl conformational changes of the peptide but als changes caused by binding the peptide to th lipid vesicles.

The results of CD spectroscopy indicate complex behavior of the mixture of PG and P while all other tested systems, including mixture of P6 with DGDG and MGDG proved no interac tion between the lipids and the peptide that migh promote a certain change in the peptide structure At low P6/PG ratio, when the negatively charge surface of the vesicles is not compensated by pos tively charged peptide, the CD signal has the cha acter corresponding to an extended or a turn-lik structure of the peptide with maxima at 210 an 221.5 nm. As the P6/PG ratio increases, the nega tive surface charge becomes saturated and th main signal is a combination of two maxim found in the free peptide which indicates tha the peptide eventually folds into its origina conformation which is not affected by th presence of lipids. We propose that binding o PG and oligomerization of LHCII which ma mediate adhesion of membrane lamellae are tw separate processes of adjacent regions of the N terminal domain of LHCII. In any case, our result favor a possibility that binding of PG to the N terminal domain of LHCII is part of the regulatio of higher levels of membrane organization.

Acknowledgements

This work was supported by grants VS96085 of the Ministry of Education, Youth and Sport of the Czech Republic and 206/97/0325 of the Grant Agency of the Czech Republic.

References

[1] S. Jansson, Biochim. Biophys. Acta 1 (1994) 1184.
[2] W. Kühlbrandt, D.N. Wang, Y. Fujiyoshi, Nature 614 (1994) 367.
[3] W. Kühlbrandt, Curr. Opin. Struct. Biol. 519 (1994) 4.
[4] J.E. Mullet, C.J. Arntzen, Biochim. Biophys. Acta 100 (1980) 589.
[5] S. Nußberger, K. Dörr, D.N. Wang, W. Kühlbrandt, J. Mol. Biol. 347 (1993) 234.
[6] A. Tremolieres, J.P. Dubacq, F. Ambard-Bretteville, R. Remy, FEBS Lett. 27 (1981) 130.
[7] S. Hobe, R. Förster, J. Klinger, H. Paulsen, Biochemistry 10 224 (1995) 34.
[8] A. Kuttkat, A. Hartmann, S. Hobe, H. Paulsen, Eur. J. Biochem. 288 (1996) 242.
[9] V. Madison, K.D. Kopple, J. Am. Chem. Soc. 120 (1980) 4855.
[10] J.F. Allen, Trends Biochem. Sci. 12 (1992) 17.
[11] A. Nilsson, D. Stys, T. Drakenberg, M.D. Spangfort, S. Forsén, J.F. Allen, J. Biol. Chem. 18350 (1997) 272.
[12] A. Bundi, K. Wuthrich, Biopolymers 285 (1979) 18.

PHOTOSYNTHETICA 41 (1): 1-7, 2003

REVIEW

The PsbH protein of photosystem 2

J. KOMENDA[*,**,***], D. ŠTYS[*,**], and L. LUPÍNKOVÁ[*,**]

Institute of Physical Biology, University of South Bohemia, 373 33 Nové Hrady, Czech Republic[*]
Laboratory of Photosynthesis, Institute of Microbiology, Academy of Sciences of the Czech Republic, 379 81 Třeboň, Czech Republic[**]

Abstract

The PsbH protein belongs to a group of small protein subunits of the photosystem 2 (PS2) complex and genes encoding PsbH homologues have been so far found in all studied oxygenic phototrophs. This single helix membrane protein is important for the proper function of the PS2 acceptor side and for stable assembly of PS2. Its hypothetical function as an analogue of the H subunit of the bacterial reaction centre as well as a putative role of its phosphorylation is evaluated.

Additional keywords: chloroplast; cyanobacterium; D1 protein; phosphorylation; photosynthesis.

Identification of the protein

Photosystem 2 (PS2) of higher plants, algae, and cyanobacteria is a membrane pigment-protein complex catalysing oxidation of water and reduction of plastoquinone. Its core consists of nearly 10 protein subunits of variable size. Two pairs of homologous polypeptides D1-D2 and CP47-CP43 represent the larger ones. The first pair binds redox-active functional groups of the reaction centre (like P680, pheophytin, and quinones Q_A and Q_B) performing charge separation while the second pair binds chlorophyll (Chl) molecules needed for energy transfer to the reaction center. There are also a number of low molecular mass proteins mostly with unknown function even though it is assumed that they are important for the optimisation of electron and energy transfer and for assembly of the complex (for review see Hankamer *et al.* 1997).

Bennett (1977, 1979) has originally found in thylakoids of higher plants the PsbH protein, the product of the psbH gene, as 10-kDa phosphoprotein. Its phosphorylation occurs on the threonine residue similarly to LHC2 proteins (Bennett 1977) and this phosphate group could be removed by trypsin (Bennett 1980). The protein has been initially considered as part of the ATP synthase due to its co-migration with the DCCD-reactive CFo subunit III (Alfonso *et al.* 1980), as a small subunit of the cytochrome b_6f complex (Süss 1981), or as the α-subunit of cytochrome *b*-559 (Metz *et al.* 1983, Widger *et al.* 1984). First information on its amino acid composition and partial N-terminal sequence (first 9 amino acid residues) has been obtained with the protein isolated and purified from spinach PS2 particles by Farchaus and Dilley (1986). These authors provided evidence for the unique character of the protein clearly distinct from the cytochrome *b*-559 and ATP synthase subunits. Later, Hird *et al.* (1991) determined the whole sequence of the protein by sequencing a region of wheat chloroplast DNA. Genes similar to that found in wheat have been also found in liverwort, tobacco, and rice (Ohyama *et al.* 1986, Shinozaki *et al.* 1986, Hiratsuka *et al.* 1989). Protein with a similar amino acid sequence has been also partially sequenced in *Chlamydomonas* (Dedner *et al.* 1988) and in the thermophilic cyanobacterium *Synechococcus vulcanus* (Koike *et al.* 1989). Gene encoding the PsbH protein from the cyanobacterium *Synechocystis* PCC 6803 has been cloned and sequenced by Abdel-Mawgood and

Received 25 November 2002, *accepted* 17 February 2003.
[***] Fax: +420-384-721246, e-mail: komenda@alga.cz
Abbreviations: Chl – chlorophyll; DMBQ – 2,5-dimethyl-*p*-benzoquinone; IC7 – *psb*H-deletion mutant of the cyanobacterium *Synechocystis PCC* 6803; PS1 and PS2 – photosystem 1 and photosystem 2; WT – wild-type strain of the cyanobacterium *Synechocystis PCC* 6803.
Acknowledgment: We thank Prof. J. Barber for providing the *psb*H deletion mutant of *Synechocystis PCC* 6803. This work was sponsored by project MSM 12310001 of the Ministery of Education, Youth, and Sports of the Czech Republic and by Institutional Research Concept no. AV0Z5020903.

Table 1. Aligned N-terminal sequences of psbH homologs in various organisms (according to SWISS PROT database, May 2002). S.P.a.n., SWISS PROT accession number; organisms *1-8* do not contain LHC2-type of the PS2 antenna, organisms *9-23* contain LHC2-type of the external PS2 antenna. Tentatively phosphorylable threonine residues are in bold. * Sequence determined from the direct N-terminal protein sequencing.

Organism	S.P.a.n.	Aligned N-terminal sequence
1 Prochlorothrix	P31095	----------GQKTALSNFLKPFNSNAGKVVPG
2 Cyanidium	O19925	----------ALKTRLGELLRPLNSQYGKVAPG
3 Cyanophora	P48105	----------PQRTALGNILRPLNSEYGKVAPG
4 Guillardia	O78514	----------ALRTRLGELLRPLNSEYGKVAPG
5 Odontella	P49475	----------ALRTRLGEI LRPLNAEYGKVAPG
6 Porphyra	P51325	----------ALRTRLGEILRPLNSEYGKVAPG
*7 Synechococcus**	P19052	----------ARRTWLGDILRPLNSEYGKV
8 Synechocystis	P14835	----------AQRTRLGDILRPLNSEYGKVVPG
9 Chlamydomonas	P22666	ATGT—SKAKPSKVNSDFQEPGLVTPLGTLLRPLNSEAGKVLPG
10 Chlorella	P56323	ATGTTSKVKVS----------GVSTPLGTLLKPLNSEYGKVAPG
11 Euglena	P31555	---T—TISKNKTSNSK----------GKTTTLGTI LKPLNSKYGKVLPG
12 Marchantia	P12160	ATQIIDDTPKTK----------GKKSGIGDI LKPLNSEYGKVAPG
13 Mesostigma	Q9MUV4	AD—TSQ----------GKRTVVGNFLKPLNSEYGKVAPG
14 Arabidopsis	P56780	ATQTVEDSSRSG----------PRSTTVGKLLKPLNSEYGKVAPG
15 Hordeum	P12363	ATQTVEDSSKPR----------PKRTGAGSLLKPL NSEYGKVAPG
16 Nicotiana	P06415	ATQTVENSSRSG----------PRRTAVGDLLKPLNSEYGKVAPG
17 Oenothera	P19820	ATQTAEESSRAR----------PKKTGLGGLLKPLNSEYGKVAPG
18 Oryza	P09449	ATQTVEDSSRPG----------PRQTRVGNLLKPLNSEYGKVAPG
19 Pinus	P41627	ATQTIDDTSKTT----------PKETLVGTTLKPLNSEYGKVAPG
20 Populus	Q36632	ATQSVEGSSRSG----------PRRTIVGDLLKPLNSEYGKVAPG
21 Spinacea	P05146	ATQTVESSSRSR----------PKPTTVGALLKPLNSKYGKVAPR
22 Triticum	P04965	ATQTVEDSSKPR----------PKRTGAGSLLKPLNSEYGKVAPG
23 Zea	P24993	ATQTVEDSSRPK----------PKRTGAGSLLKPLNSEYGKVAPG

Dilley (1990) and Mayes and Barber (1991). From that time genes encoding PsbH homologues have been identified and completely sequenced in more than 25 organisms showing that the PsbH protein is a common component of PS2 in all oxygenic photosynthetic organisms (Table 1).

Localisation and expression of the gene in chloroplasts and cyanobacteria

In plants the *psb*H gene exhibits a conservative location in the *psb*B-*psb*H-*pet*B-*pet*D operon. The order and orientation of these genes are highly conserved in plant chloroplast genomes (*e.g.* Westhoff *et al.* 1983, Ohyama *et al.* 1986, Shinozaki *et al.* 1986). A range of transcripts of various sizes containing the entire operon or its components can be detected in chloroplasts (Westhoff and Herrmann 1988, Westoff *et al.* 1991). This means that all genes in the operon are co-transcribed and afterwards the primary transcript is processed. In *Synechocystis* PCC 6803, the *psb*H gene is a component of a different gene cluster containing *psb*N, *psb*H, *pet*C, and *pet*A genes (Mayes and Barber 1991). However, in contrast to the situation in chloroplasts, the *psb*H is transcribed as monocistronic mRNA while *pet*C-*pet*A genes as a separate, dicistronic unit (Mayes *et al.* 1993). In both types of organisms, the *psb*H gene is localised in a vicinity of genes coding for components of the cytochrome b_6f complex. Functional importance of this association is possible, although it is challenged by the fact that in *Chlamydomonas reinhardtii* the genes encoding components of the cytochrome b_6f complex are localised elsewhere in the chloroplast genome, and that the *psb*H gene exists in the cluster with *psb*B and *psb*T genes that code for CP47 and a small PS2 subunit PsbT, respectively. On the basis of analysis of nuclear mutants with impaired accumulation of *psb*B, *psb*T, and *psb*H transcripts it has been assumed that these three genes are co-transcribed (Monod *et al.* 1992, Johnson and Schmidt 1993). However, no interdependence of *psb*B/*psb*T and *psb*H mRNA accumulation suggests that *psb*B/*psb*T and *psb*H have separate promoters and each can be transcribed independently (Summer *et al.* 1997).

Despite the ongoing transcription of *psb*B and *psb*H genes, only *psb*H gene product could be identified in membranes of etiolated plant seedlings while CP47, the product of *psb*B, is not accumulated (Hird *et al.* 1991). Therefore, the transcription of the *psb*H gene and accumulation of its translation product is light independent.

Functional and structural role of the protein in PS2

Based on a certain similarity with the sequence of a LHC2 protein, Allen and Holmes (1986) proposed that the PsbH protein may bind Chl and play a role in the distribution of energy between both photosystems, as a part of the LHC2 complex. However, the absence of histidine residues in this single transmembrane helix-containing protein (Fig. 1) raised doubts about its ability to bind-Chl. The hypothesis was also questioned after the discovery of PsbH in cyanobacteria lacking LHC2. A further negation of the hypothesis was brought about by the finding that the protein is present in etioplasts while known Chl-binding proteins, including CP47, are stabile incorporated into the membrane only after irradiation when Chl is synthesised and stabilises the apoproteins (Eichacker *et al.* 1990). Based on the correlation between the phosphorylation of the PS2 proteins (Hodges *et al.* 1985), particularly of the PsbH protein (Packham 1987), and the electron transfer rate from the primary to the secondary quinone acceptors Q_A and Q_B, it has been proposed that the re-oxidation rate of Q_A is dependent on the phosphorylation status of the PsbH protein. This could indicate a close proximity of the PsbH protein to the reaction centre of PS2. First more extensive characterisation of the protein role in PS2 has been allowed by the construction of the *psb*H-less mutant of *Synechocystis PCC* 6803 (Mayes *et al.* 1993). The PS2 complex of the mutant differed from the WT complex in several aspects. Compared to the WT, the mutant strain was able to grow autotrophically but more slowly and only under low irradiance. In the absence of the PsbH protein, PS2 remained functional, but electron transfer between Q_A and Q_B was significantly slower, as revealed by fluorescence measurements (Mayes *et al.* 1993; Fig. 2). Measurements of thermoluminescence and flash-induced oxygen evolution revealed modification of the Q_B binding site but the influence of the PsbH absence on the donor side of PS2 and on the oxygen evolving complex could not be excluded. Recently, a more extensive characterisation of the *psb*H deletion mutant revealed further features of the PsbH-deficient PS2 (Komenda *et al.* 2002). We have found that after removal of CO_2 from the medium, electron transport between Q_A and Q_B is further slowed down. However, this change can be easily reversed by the addition of bicarbonate. In contrast, in the wild type strain (WT) the rate of Q_A re-oxidation remains the same after CO_2 removal. Also the very fast inactivation of DMBQ-supported oxygen evolving activity under high irradiance, typical for the mutant (Komenda and Barber 1995), can be either accelerated by CO_2 removal or slowed down on the addition of bicarbonate immediately prior to irradiation. This result corroborates the results of Sundby *et al.* (1989) who showed a negative correlation between the phosphorylation of the PsbH protein and the concentration of bicarbonate in plant thylakoids. These data indicate that the PsbH protein is needed for the stable binding of bicarbonate on the PS2 acceptor side.

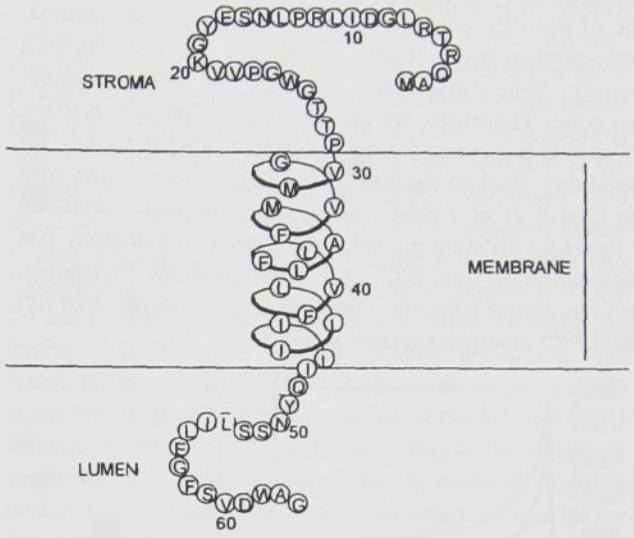

Fig. 1. Putative structure of the PsbH protein from the cyanobacterium *Synechocystis* PCC 6803.

After exposure of the mutant cells to high irradiance (1 000 μmol m^{-2} s^{-1}) formation of the D1-cytochrome *b*-559 adduct and formation of the D1 fragments has been identified (Komenda *et al.* 2002). At the same time, the oxygen-dependent shift of the D1 protein mobility in the electrophoretic gel and positive identification of the D1 band by an *Oxyblot* kit showed that increased oxidation of the D1 protein occurs in the mutant. As these features were unique for the mutant, and were not observed in the WT strain, it is assumed that in the absence of the PsbH protein, the impaired function of PS2 leads to increased probability of the formation of reactive oxygen species. These oxygen species oxidise the D1 protein which can be subsequently cross-linked with the α-subunit of cytochrome *b*-559 or fragmented.

A very important feature of the protein is its susceptibility to phosphorylation. This post-translational modification has been demonstrated in higher plants (Bennett 1977) and in the green alga *Chlamydomonas* (Dedner *et al.* 1988). The protein seems to be phosphorylated on two residues, one was identified as threonine 2 (Michel and Bennett 1987, Michel *et al.* 1988) while the other remains unknown (Vener *et al.* 2001). In line with this, a double band of phosphorylated PsbH in the PS2 of green algae *Chlamydomonas* and *Chlorella* has been identified with anti-phosphothreonine antibody (Hamel *et al.* 2000, Komenda *et al.* 2002, and Fig. 3). There is also a report on PsbH phosphorylation in *Synechocystis* (Race and Gounaris 1993) despite the absence of threonine in the

N-terminus segment of the protein in this organism. A recent Western blot analysis of threonine protein phosphoryla-tion in thylakoids and PS2 complexes in *Synechocystis* did not reveal any phosphoproteins (Fig. 3) and also la-belling with ^{33}P did not provide any evidence for the phosphorylation of the PsbH protein (Komenda *et al.* 2002). The aligned N-terminal sequences of PsbH (Table 1) show that all organisms not-containing LHC2-type of the PS2 antenna (prochlorophytes, cyanobacteria, rhodo-phytes, and diatoms) contain the PsbH protein with shor-ter N-terminal part without the phosphorylable threonine. Therefore, we believe that the phosphorylation of PsbH is important for the function of PS2 in the LHC2-containing stacked regions of the membrane. In line with this Giardi *et al.* (1994) showed that de-phosphorylation of PsbH by alkaline phosphatase causes an extremely fast inactivation of the PS2 in isolated spinach thylakoids, while in cyano-bacterial membranes the enzyme does not affect PS2 electron transfer activity.

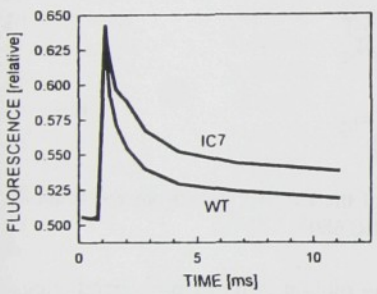

Fig. 2. Re-oxidation of the PS2 primary electron acceptor Q_A is slowed down in the absence of the PsbH protein. Re-oxidation of the PS2 primary electron acceptor Q_A in cells of the WT strain (*solid line*) and the psbH-deletion mutant IC7 (*dotted line*) was measured by the double modulated fluorimeter *P.S.I.* as decay of the variable component of fluorescence elicited by strong flash after 5-min dark adaptation.

Phosphorylation of the PsbH increases with irradiance in chloroplasts (Ebbert and Godde 1994) and also in plant leaves (Rintamäkki *et al.* 1997). In isolated plant thylakoids the phosphorylated PsbH is steadily accumulated during 60-min irradiation and no saturation has been observed (Štys *et al.* 1995). It is in contrast with phosphorylation of LHC2 that has its maximum at ambient irradiance but becomes inhibited at higher irradiance or after 30 min irradiation.

Besides its role in the function of the PS2 core complex, the PsbH protein is important also for the biogenesis and the structure of PS2. Deletion of the protein in *Chlamydomonas reinhardtii* leads to the disappearance of PS2 from the thylakoid membrane, documenting its role in the stable assembly of PS2 (Summer *et al.* 1997, O'Connor *et al.* 1998). Analysis of the PS2 assembly intermediates by radioactive pulse labelling showed that the synthesis of main protein components of the PS2 core D1, D2, CP43, and CP47 is not affected but their assembly into larger PS2 complexes is inhibited (Summer *et al.* 1997). In the PsbH-deletion mutant of *Synechocystis* the turnover

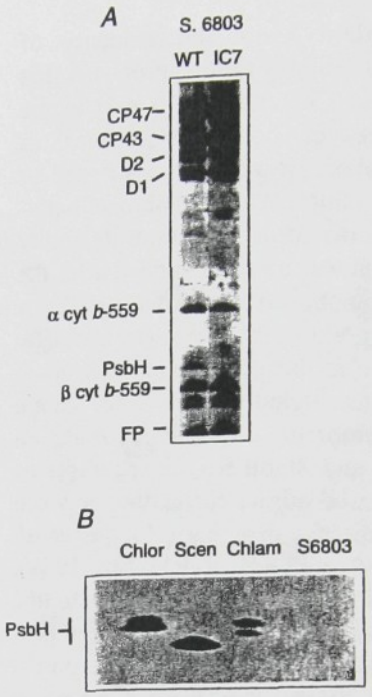

Fig. 3. (*A*) Identification of the PsbH protein in *Synechocystis* PS2 core complexes of WT and psbH deletion mutant IC7 and (*B*) its phosphorylation in PS2 core complexes of green algae *Chlorella* (Chlor), *Scenedesmus* (Scen), and *Chlamydomonas* (Chlam), and of the cyanobacterium *Synechocystis* (S6803). PS2 core complexes were obtained by *Deriphat*-PAGE of dodecylmaltoside solubilised thylakoids. Analysis was performed on 12-20 % polyacrylamide gel containing 7 M urea, gel was either stained by Coomassie Blue (*A*) or electroblotted, and phosphoproteins on the nitrocellulose membrane were detected by anti phosphothreonine antibodies (*Zymed*, USA; *B*).

of the D1 protein is slowed down and recovery from photoinhibition is also slower (Komenda and Barber 1995). This can be related to the effect described above, as the restoration of the PS2 activity occurs after the D1 replacement during which at least partial reassembly or rearrangement of PS2 subunits is required. As shown in the deletion mutant of *Chlamydomonas*, this process is exactly what is inhibited. A role of the PsbH protein in the stabilisation of PS2 has also been supported by our recent experimental data. We have isolated the PS2 core complex from the deletion mutant of *Synechocystis* and subjected it to *Deriphat* non-denaturing electrophoresis. In contrast to the isolated PS2 core from WT, a large amount of the reaction centre complex D1-D2-cytochrome *b*-559 appeared on the gel indicating that PsbH protein may stabilise the binding of CP47 to the D1-D2 heterodimer (Komenda *et al.* 2002). Such a role could also explain the instability of the PS2 core in *Chlamydo-*

monas, since weak binding of CP47 to the heterodimer could allow a fast proteolysis of PS2 subunits before the complex becomes fully assembled.

Recently, Zouni *et al.* (2001) published a model of PS2 of the thermophilic cyanobacterium *Synechococcus elongatus*, based on X-ray structural analysis at 35 nm resolution. In this model, the helix on the side of CP47 and D2, in the proximity of the Q_A-Q_B region, was tentatively ascribed to the PsbH protein. This position of the PsbH protein was chosen because of the apparent effect of PsbH phosphorylation (in higher plants) or the PsbH absence (in cyanobacteria) on the electron transfer between the PS2 quinone acceptors. This localisation is in agreement with our data since it can also explain the recently observed stabilisation effect on the binding of CP47 to the D1-D2 heterodimer (Komenda *et al.* 2002). Using Blue-Native Gel Electrophoresis, a mild electrophoretic method for separation of native membrane complexes according to their size, no PS2 dimers were identified in the *psb*H-deletion strain IC7 of *Synechocystis* (Fig. 4). This is again in agreement with position of the protein in the interface between the PS2 monomers. The proximity of the PsbH protein to the PS2 reaction centre is also suggested by results of Kuhn *et al.* (1988) and Chiaramonte *et al.* (1999). A parallel degradation of the D1 and the PsbH proteins and their tentative cross-linking during irradiation of isolated spinach thylakoids was found (Kuhn *et al.* 1988). Chiaramonte *et al.* (1999) suggested close structural interaction of the D1 and PsbH subunits in PS2 from *Synechocystis* due to the observed conformational modification of the Q_B herbicide binding pocket that is caused by the replacement of the native PsbH by the homologue from maize (see also Bergantino *et al.* 2002). These data taken together are not in contradiction with the hypothesis of Packham (1988) who considered the PsbH protein as a possible functional homologue of the H subunit in the reaction centre of photosynthetic bacteria.

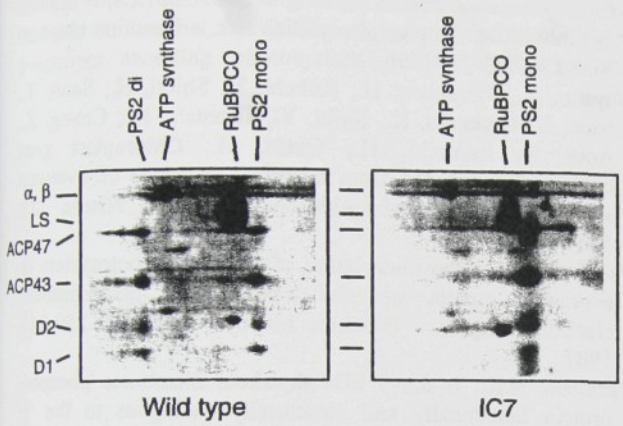

Fig. 4. The PS2 dimer is absent in the thylakoids of the *Synechocystis psb*H deletion mutant IC7. Thylakoids from the wild type (*left panel*) and IC7 mutant (*right panel*) were solubilised by dodecylmaltoside and complexes were analysed by Blue Native PAGE. Subunit composition of the complexes was determined by SDS-PAGE on 12-20 % acrylamide gel containing 7 M urea, and the 2-D gel was stained by Coomassie Blue. LS – large subunit of ribulose-1,5-bisphosphate carboxylase/oxygenase (RuBPCO); α, β – subunits of ATP synthase; PS2 di and mono – dimer and monomer of the PS2 core complex.

References

Abdel-Mawgood, A.L., Dilley, R.A.: Cloning and nucleotide sequence of the psbH gene from cyanobacterium *Synechocystis* 6803. – Plant mol. Biol. **14**: 445-446, 1990.

Alfonso, R., Nelson, N., Racker, E.: A light dependent protein kinase activity of chloroplasts. – Plant Physiol. **65**: 730-734, 1980.

Allen, J.F., Holmes, N.G.: A general model for regulation of photosynthetic unit function by protein phosphorylation. – FEBS Lett. **202**: 175-181, 1986.

Bennett, J.: Phosphorylation of chloroplast membrane polypeptides. – Nature **269**: 344-346, 1977.

Bennett, J.: Chloroplast phosphoproteins. The protein kinase of thylakoid membranes is light-dependent. – FEBS Lett. **103**: 342-344, 1979.

Bennett, J.: Chloroplasts phosphoproteins. Evidence for a thylakoid-bound phosphoprotein phosphatase. – Eur. J. Biochem. **104**: 85-89, 1980.

Bergantino, E., Brunetta, A., Segalla, A., Szabo, I., Carbonera, D., Bordignon, E., Rigoni, F., Giacometti, G.M.: Structural and functional role of the PsbH protein in resistance to light stress in *Synechocystis* PCC 6803. – Funct. Plant Biol. **29**: 1181-1187, 2002.

Chiaramonte, S., Giacometti, G.M., Bergantino, E.: Construction and characterization of a functional mutant of *Synechocystis* 6803 harbouring a eukaryotic PS2-H subunit. – Eur. J. Biochem. **260**: 833-843, 1999.

Dedner, N., Meyer, H.E., Ashton, C., Wildner, G.F.: N-terminal sequence analysis of the 8 kDa protein in *Chlamydomonas reinhardii*. Localization of the phosphothreonine. – FEBS Lett. **236**: 77-82, 1988.

Ebbert, V., Godde, D.: Regulation of thylakoid protein phosphorylation in intact chloroplasts by the activity of kinases and phosphatases. – Biochim. biophys. Acta **1187**: 335-346, 1994.

Eichacker, L.A., Soll, J., Lauterbach, P., Rüdiger, W., Klein, R.R., Mullet, J.E.: *In vitro* synthesis of chlorophyll *a* in the dark triggers accumulation of chlorophyll *a* apoproteins in barley etioplasts. – J. biol. Chem. **265**: 13566-13571, 1990.

Farchaus, J., Dilley, R.A.: Purification and partial sequence of the M_r 10,000 phosphoprotein from spinach thylakoids. – Arch. Biochem. Biophys. **244**: 94-101, 1986.

Giardi, M.T., Komenda, J., Masojidek, J.: Involvement of protein phosphorylation in the sensitivity of photosystem II to strong illumination. – Physiol. Plant. **92**: 181-187, 1994.

Hamel, P., Olive, J., Pierre, Y., Wollman, F.-A., De Vitry, C.: A new subunit of cytochrome b_6f complex undergoes reversible

phosphorylation upon state transition. – J. biol. Chem. **275:** 17072-17079, 2000.

Hankamer, B., Barber, J., Boekema, E.J.: Structure and membrane organization of photosystem-II in green plants. – Annu. Rev. Plant Physiol. Plant mol. Biol. **48**: 641-671, 1997.

Hiratsuka, J., Shimada, H., Whittier, R., Ishibashi, T., Sakamoto, M., Mori, M., Kondo, C., Honji, Y., Sun, C.-R., Meng, B.-Y., Li, Y.-Q., Kanno, A., Nishizawa, Y., Hirai, A., Shinozaki, K., Sigiura, M.: The complete sequence of the rice (*Oryza sativa*) chloroplast genome: intermolecular recombination between distinct tRNA genes accounts for a major plastid DNA inversion during the evolution of the cereals. – Mol. gen. Genet. **217**: 185-194, 1989.

Hird, S.M., Webber, A.N., Wilson, R.J., Dyer, T.A., Gray, J.C.: Differential expression of the *psb*B and *psb*H genes encoding the 47 kDa chlorophyll *a*-protein and the 10 kDa phosphoprotein of photosystem II during chloroplast development in wheat. – Curr. Sci. **19**: 199-206, 1991.

Hodges, M., Packham, N.K., Barber, J.: Modification of photosystem II activity by protein phosphorylation. – FEBS Lett. **181**: 83-87, 1985.

Johnson, C.H., Schmidt, G.W.: The *psb*B gene cluster of the *Chlamydomonas reinhardtii* chloroplast: sequence and transcriptional analyses of *psb*N and *psb*H. – Plant mol. Biol. **22**: 645-658, 1993.

Koike, H., Mamada, K., Ikeuchi, M., Inoue, Y.: Low-molecular-mass proteins in cyanobacterial photosystem II: identification of *psb*H and *psb*K gene products by N-terminal sequencing. – FEBS Lett. **244**: 391-396, 1989.

Komenda, J., Barber, J.: Comparison of *psb*O and *psb*H deletion mutants of *Synechocystis* PCC 6803 indicate that degradation of D1 protein is regulated by the Q_B site and is dependent on protein synthesis. – Biochemistry **34**: 9625-9631, 1995.

Komenda, J., Lupínková, L., Kopecký, J.: Absence of the *psb*H gene product destabilizes the Photosystem II complex and bicarbonate binding on its acceptor side in *Synechocystis* PCC 6803. – Eur. J. Biochem. **269**: 610-619, 2002.

Kuhn, M., Thiel, P., Böger, P.: The 9-kDa phosphoprotein involved in photoinhibition. – Z. Naturforsch. **43C**: 413-417, 1988.

Mayes, S.R., Barber, J.: Primary structure of the *psb*N-*psb*H-*pet*C-*pet*A gene cluster of the cyanobacterium *Synechocystis* PCC-6803. – Plant mol. Biol. **17**: 289-293, 1991.

Mayes, S.R., Dubbs, J.M., Vass, I., Hideg, É., Nagy, L., Barber, J.: Further characterization of the *psb*H locus of *Synechocystis* sp PCC 6803: Inactivation of *psb*H impairs Q_A to Q_B electron transport in photosystem 2. – Biochemistry **32**: 1454-1465, 1993.

Metz, J.G., Ulmer, G., Bricker, T.M., Miles, D.: Purification of cytochrome *b*-559 from oxygen-evolving Photosystem II preparations of spinach and maize. – Biochim. biophys. Acta **725**: 203-209, 1983.

Michel, H., Hunt, D.F., Shabanowitz, J., Bennett, J.: Tandem mass spectrometry reveals that three photosystem II proteins of spinach chloroplasts contain *N*-acetyl-*O*-phosphothreonine at their NH_2 termini. – J. biol. Chem. **263**: 1123-1130, 1988.

Michel, H.P., Bennett, J.: Identification of the phosphorylation site of an 8.3 kDa protein from photosystem II of spinach. – FEBS Lett. **212**: 103-108, 1987.

Monod, C., Goldschmidt-Clermont, M., Rochaix, J.-D.: Accumulation of chloroplast *psb*B RNA requires a nuclear factor in *Chlamydomonas reinhardtii*. – Mol. gen. Genet. **231**: 449-459, 1992.

O'Connor, H.E., Ruffle, S.V., Cain, A.J., Deak, Z., Vass, I., Nugent, J.H.A., Purton, S.: The 9-kDa phosphoprotein of photosystem II. Generation and characterisation of *Chlamydomonas* mutant lacking PSII-H and a site-directed mutant lacking the phosphorylation site. – Biochim. biophys. Acta **1364**: 63-72, 1998.

Ohyama, K., Fukuzawa, H., Kohchi, T., Shirai, H., Sano, T., Sano, S., Umesono, K., Shiki, Y., Takeuchi, M., Chang, Z., Aota, S., Inokuchi, H., Ozeki, H.: Chloroplast gene organization deduced from complete sequence of liverwort *Marchantia polymorpha* chloroplast DNA. – Nature **322**: 572-574, 1986.

Packham, N.K.: Phosphorylation of the 9 kDa Photosystem II-associated protein and the inhibition of photosynthetic electron transport. – Biochim. biophys. Acta **893**: 259-266, 1987.

Packham, N.K.: Is the 9 kDa thylakoid membrane phosphoprotein functionally and structurally analogous to the 'H' subunit of the bacterial reaction centres? – FEBS Lett. **231**: 284-290, 1988.

Race, H.L., Gounaris, K.: Identification of the *psb*H gene-product as a 6 kDa phosphoprotein in the cyanobacterium *Synechocystis* 6803. – FEBS Lett. **323**: 35-39, 1993.

Rintamäkki, E., Salonen, M., Suoranta, U.M., Carlberg, I., Andersson, B., Aro, E.M.: Phosphorylation of light-harvesting complex II and photosystem II core proteins shows different irradiance-dependent regulation in vivo - Application of phosphothreonine antibodies to analysis of thylakoid phosphoproteins. – J. biol. Chem. **272**: 30476-30482, 1997.

Shinozaki, K., Ohme, M., Tanaka, M., Wakasugi, T., Hayashida, N., Matsubayashi, T., Zaita, N., Chungwongse, J., Obokata, J., Yamagushi-Shinozaki, K., Ohto, C., Torazawa, K., Meng, B.Y., Sugita, M., Deno, H., Kamogashira, T., Yamada, K., Kusuda, J., Takaiwa, F., Kato, A., Tohdon, N., Shimada, H., Sugiura, M.: The complete nucleotide sequence of the tobacco chloroplast genome: its gene organization and expression. – EMBO J. **5**: 2043-2049, 1986.

Stys, D., Stancek, M., Cheng, L., Allen, J.F.: Complex formation in plant thylakoid membranes. Competition studies on membrane protein interactions using synthetic peptide fragments. – Photosynth. Res. **44**: 277-285, 1995.

Summer, E.J., Schmid, V.H.R., Bruns, B.U., Schmidt, G.W.: Requirement for the H phosphoprotein in Photosystem II of *Chlamydomonas reinhardtii*. – Plant Physiol. **113**: 1359-1368, 1997.

Sundby, C., Larsson, U.K., Henrysson, T.: Effects of bicarbonate on thylakoid protein phosphorylation. – Biochim. biophys. Acta **975**: 277-282, 1989.

Süss, K.-H.: Identification of chloroplast thylakoid phosphoproteins. Evidence for the absence of phosphoryl-polypeptide intermediates in the ATPase complex. – Biochem. biophys. Res. Commun. **102**: 724-729, 1981.

Vener, A.V., Harms, A., Sussman, M.R., Vierstra, R.D.: Mass spectrometric resolution of reversible protein phosphorylation in photosynthetic membranes of *Arabidopsis thaliana*. – J.

biol. Chem. **276:** 6959-66, 2001.

Westhoff, P., Alt, J., Herrmann, R.G.: Localization of the genes for the two chlorophyll *a*-conjugated polypeptides (mol. wt. 51 and 44 kd) of the photosystem II reaction centre on the spinach plastid chromosome. – EMBO J. **2**: 2229-2237, 1983.

Westhoff, P., Herrmann, R.G.: Complex RNA maturation in chloroplasts. The *psb*B operon from spinach. – Eur. J. Biochem. **171**: 551-564, 1988.

Westhoff, P., Offermann-Steinhard, K., Höfer, M., Eskins, K., Oswald, A., Streubel, M.: Differential accumulation of plastid transcripts encoding photosystem II components in the mesophyll and bundle-sheath cells of monocotyledonous NADP-malic enzyme-type-C_4 plants. – Planta **184**: 377-388, 1991.

Widger, W.R., Farchaus, J.W., Cramer, W.A., Dilley, R.A.: Studies on the relation of the M_r 9000 phosphoprotein to cytochrome *b*-559 in spinach thylakoid membranes. – Arch. Biochem. Biophys. **233**: 72-79, 1984.

Zouni, A., Witt, H.T., Kern, J., Fromme, P., Krauss, N., Saenger, W., Orth, P.: Crystal structure of photosystem II from *Synechococcus elongatus* at 3.8 Å resolution. – Nature **409**: 739-43, 2001.

Available online at www.sciencedirect.com
SCIENCE DIRECT®
Protein Expression and Purification 32 (2003) 18–27
Protein Expression & Purification
www.elsevier.com/locate/yprep

Overexpression and purification of recombinant membrane PsbH protein in *Escherichia coli*

Zbyněk Halbhuber,[a] Zdeňka Petrmichlová,[a] Kassimir Alexciev,[b] Eva Thulin,[c] and Dalibor Štys[a,d,*]

[a] *Photosynthesis Research Center, Institute of Physical Biology, University of South Bohemia, Zamek 136, 373 33 Nove Hrady, Czech Republic*
[b] *CanAg Diagnostics, 414 55 Gothenburg, Sweden*
[c] *Department of Biophysical Chemistry, Lund University, Box 124, 22100 Lund, Sweden*
[d] *Department of Autotrophic Microorganisms, Institute of Microbiology, CAS, 37901 Trebon—Opatovicky mlyn, Czech Republic*

Received 5 December 2002, and in revised form 25 May 2003

Abstract

In this work, we featured an expression system that enables the production of sufficient quantities (~mg) of low molecular weight membrane protein of photosystem II, PsbH protein, for solid-state NMR as well as other biophysical studies. *Psb*H gene from cyanobacterium *Synechocystis* sp. PCC 6803 was cloned into a plasmid expression vector, which allowed expression of the PsbH protein as a glutathione-*S* transferase (GST) fusion protein in *Escherichia coli* BL21(DE3) cells. A relatively large GST anchor overcomes foreseeable problems with the low solubility of membrane proteins and the toxicity caused by protein incorporation into the membrane of the host organism. As a result, the majority of fusion protein was obtained in a soluble state and could be purified from crude bacterial lysate by affinity chromatography on immobilized glutathione under non-denaturing conditions. The PsbH protein was cleaved from the carrier protein with Factor Xa protease and purified on DEAE–cellulose column with yields of up to 2.1 μg protein/ml of bacterial culture. The procedure as we optimized is applicable for isolation of small membrane proteins for structural studies.
© 2003 Elsevier Inc. All rights reserved.

Photosystem II (PSII)[1] is a membrane protein complex found in thylakoid membranes of higher plants, algae, and cyanobacteria, which catalyzes light-induced electron transfer and water-splitting reactions, leading to the formation of molecular oxygen. Structure of PSII was established by X-ray diffraction at 3.8 Å resolution [1]. It is a dimer composed of more than 25 subunits per monomer, organized as a reaction center complex surrounded by the so-called inner antenna proteins CP43 and CP47 and the extrinsic water-splitting complex. A number of small polypeptides of unknown function with molecular weight below 10 kDa are associated with PSII and these include the *psb*H, *psb*I, *psb*J, *psb*K, *psb*L, *psb*M, *psb*N, and *psb*R gene products. There are also proteins of size 9.12, 6.1, 5, and 4.1 kDa, which could not be located in the structure, and their function remains unknown.

The *psb*H gene product is localized close to the reaction center of PSII in higher plants, algae, and cyanobacteria. The *psb*H gene product was originally detected as a 10 kDa phosphoprotein in pea chloroplasts [2] and subsequently sequenced in a number of prokaryotic and eukaryotic organisms. The chloroplast *psb*H gene encodes protein of 72 amino acid residues in higher plants [3–5] and 87 amino acid residues in the green unicellular alga *Chlamydomonas reinhardtii* [6,7]. Interestingly, the sequencing of *psb*H gene from cyanobacteria has revealed

* Corresponding author. Fax: +420386361111.
E-mail address: stys@jcu.cz (D. Štys).

[1] *Abbreviations used:* GST, glutathione *S*-transferase; NMR, nuclear magnetic resonance; DEAE, diethylaminoethyl; PSII, Photosystem II; PSI, Photosystem I; CP47 protein, *psb*B gene product; D1 protein, *psb*A gene product; PCR, polymerase chain reaction; IPTG, isopropyl thiogalactoside; EDTA, ethylenediaminetetraacetic acid; PMSF, phenylmethylsulfonyl fluoride; OG, octyl glucoside; LDAO, lauryldimethylamine oxide; SDS, sodium dodecyl sulfate; MALDI-TOF MS, matrix-assisted laser desorption/ionization time of flight mass spectrometry; cmc, critical micelle concentration.

1046-5928/$ - see front matter © 2003 Elsevier Inc. All rights reserved.
doi:10.1016/S1046-5928(03)00188-8

The expression plasmid pGEX-3X was at first treated with *Bam*HI and purified and arised overhangs were blunt-ended using S1 nuclease. Further, the vector with the blunt-ends was treated with *Eco*RI and purified. The pretreated PCR product was cloned into this prearranged expression plasmid pGEX-3X. The structure of the plasmid was confirmed by DNA sequencing (Fig. 1). The obtained plasmid (designated pKAH25) allowed expression of the PsbH protein as a fusion protein with GST.

Strain and growth conditions

Escherichia coli strain BL21(DE3) was used for the GST–PsbH fusion protein expression. Cells containing the pKAH25 were grown overnight in LB (standard growth medium) supplemented with 100 μg/ml ampicillin and used as a 0.1% inoculum for 1 liter of the culture. Cells were grown at 37 °C with shaking at 210 rpm. The expression of the GST–PsbH fusion protein was induced at the late exponential phase of growth ($OD_{550} = 1$) by adding isopropyl thiogalactoside (IPTG) to a final concentration of 1 mM in the culture. Cells were collected by centrifugation (5000*g*, 15 min) 4 h after induction.

Purification of GST–PsbH fusion protein

Cells were suspended in 10 volumes of extraction buffer A (20 mM Tris, 100 mM NaCl, 1 mM EDTA,

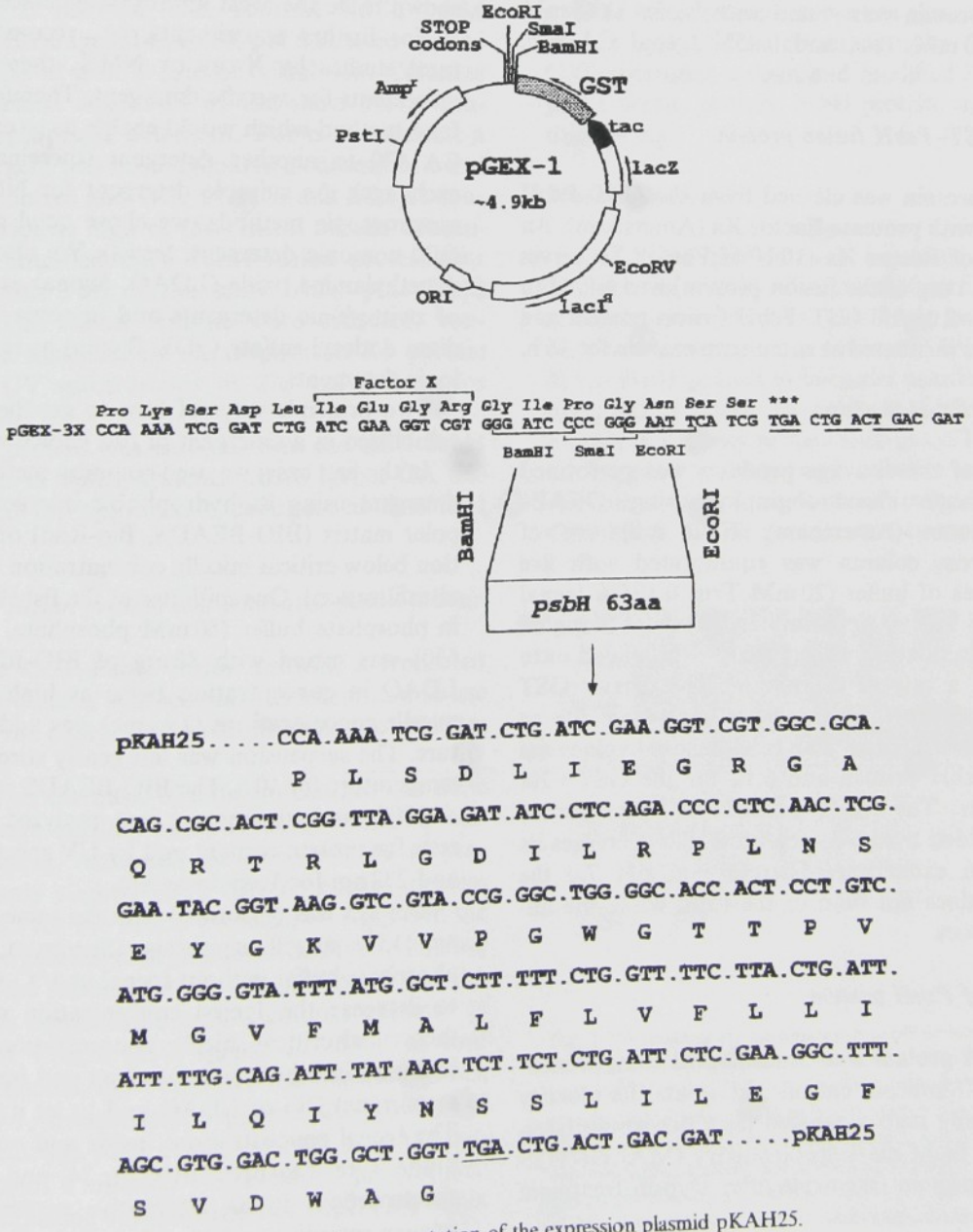

Fig. 1. Schematic representation of the expression plasmid pKAH25.

and 0.5% Igepal CA 630, pH 8.0, and 0.1 mM PMSF, 1% lysozyme) per gram of cell paste and stirred on ice for 10 min. The slurry was frozen and melted three times and then sonicated during intensive cooling (Dynatech Sonic disintegrator) to decrease its overheating. The extract was clarified by centrifugation (25,000*g*, 30 min, 4 °C). The supernatant was collected and purified using affinity chromatography. Ten milliliters of glutathione–agarose affinity column (Sigma) was equilibrated with five column volumes of buffer B (20 mM Tris, 100 mM NaCl, 1 mM EDTA, 0.5% Igepal CA 630, and 0.5% milk powder, pH 8.0). The supernatant was applied onto the column at 0.3 ml/min. The column was washed with 10 column volumes of buffer C (20 mM Tris, 100 mM NaCl, 1 mM EDTA, and 0.25% Igepal CA 630, pH 8.0) and the bounded GST–PsbH fusion protein was eluted with buffer D (5 mM glutathione, 50 mM Tris, and 0.25% Igepal CA 630, pH 8.0).

Cleavage of GST–PsbH fusion protein

The PsbH protein was cleaved from the GST–PsbH fusion protein with protease Factor Xa (Amersham). An equal volume of Factor Xa (10 U of Factor Xa serves for cleaving of 1 mg of the fusion protein) was added to a solution of 1–2 mg/ml GST–PsbH fusion protein and the mixture was incubated at room temperature for 16 h.

Purification of PsbH protein

Separation of the cleavage products was performed by ion exchange chromatography using DEAE–Sepharose column (Amersham). Four milliliters of DEAE–Sepharose column was equilibrated with five column volumes of buffer (20 mM Tris, 0.125% Igepal CA 630, pH 7.0). Approximately 1 ml of 1 mg/ml cleavage protein mixture was subsequently loaded onto the column at a rate of 0.3 ml/min. The carrier GST protein and the PsbH protein were separated due to differences in their charge. The calculated p*I* values are 6.43 for the PsbH protein and 6.12 for the GST + Xa anchor protein. The PsbH protein as a membrane protein is enfolded by the detergent, which decreases its binding to ion exchanger. Therefore at pH 7.0 the PsbH protein does not bind to the resin while the anchor protein does.

Identification of PsbH protein

Eluted PsbH protein was concentrated using Centricon filter units (Amicon, cut-off 3 kDa) and its identity was verified using matrix-assisted laser desorption/ionization time of flight mass spectrometry (MALDI-TOF MS) of PsbH protein fragments after trypsin treatment and by amino acid analysis.

Detergent exchange and cleavage of GST–PsbH fusion protein in OG and LDAO

Membrane proteins require lipids or lipid-like environment to prevent aggregation and folding. This was achieved by use of detergents during isolation procedure. Detergents enfold membrane domains and prevent protein precipitation. The expression system, when a short membrane protein is coupled to a relatively large soluble tag, was used to enhance solubility and to prevent protein precipitation. In this case, a mild detergent was sufficient to keep the protein in solution.

However, for the first isolation steps (cell disruption, clarification, and fusion protein purification) we had to use large volumes of buffers and therefore an inexpensive detergent was chosen. An Igepal CA 630 has been shown to be the most appropriate choice.

For further experiments, i.e., reconstitution, structural studies by X-ray or NMR, there are often requirements for specific detergent. Therefore, we looked for a method which would enable us to exchange Igepal CA 630 to another detergent (thereinafter detergent exchange). As suitable detergent for NMR and other spectroscopic methods, we chose octyl glucoside (OG, mild nonionic detergent, Serva). We also tested lauryldimethylamine oxide (LDAO, Sigma) as representative of zwitterionic detergents and in some experiment sodium dodecyl sulfate (SDS, Sigma) as representative of ionic detergents.

Two principle ways of how to get the PsbH protein solubilized in a detergent of our choice were used.

In the first case, we used common methods to remove detergent using its hydrophobic interaction with nonpolar matrix (BIO-BEADS, Bio-Rad) or stepwise dilution below critical micelle concentration (cmc) (dialysis, ultrafiltration). One milliliter of the PsbH protein (1 mg) in phosphate buffer (50 mM phosphate, 1% Igepal CA 630) was mixed with 80 mg of BIO-BEADS. OG or LDAO in concentration twice as high as the critical micelle concentrations (2× cmc) was added to this mixture. The suspension was left gently stirred at the room temperature for 10 h. The BIO-BEADS were centrifuged at 1000*g* and supernatant was analyzed by electrophoresis for protein content and by UV spectroscopy at 276 and 232 nm for Igepal content.

Dialysis was performed with the same protein sample on 3 kDa cut-off membrane (Spectrum, USA) against phosphate buffer without Igepal at 4 °C. Our layout was to decrease the Igepal concentration near above the theoretical critical micelle concentration (0.1 mM) and then add into both volumes (out and inside the dialysis membrane) OG or LDAO and to let it dialyze further. The Igepal concentrations inside and outside the membrane were measured after 10, 24, and 48 h using UV spectroscopy. In an alternative procedure, the same protein sample was diluted below the theoretical critical

micelle concentration of Igepal CA 630 with buffer (50 mM phosphate, 2× cmc OG or LDAO) and concentrated using Centricon filter units (Amicon) with membrane cut-off 3 kDa at 7000*g* at 4 °C until the decrease of volume to approximately 300 µl. The concentration of Igepal CA 630 was determined using UV spectroscopy in the filtrate, passed through the membrane and as well in concentrate, captured on the membrane.

In the second case, detergent exchange was performed on the fusion protein bounded to the glutathione–agarose affinity column. Igepal CA 630 was replaced by three types of detergents; OG (mild nonionic detergent), LDAO (zwitterionic detergent), and SDS (ionic detergent). For preliminary experiments, we used four small columns (0.5 ml of gel). Two milligrams of fusion protein in buffer C (20 mM Tris, 100 mM NaCl, 1 mM EDTA, and 0.25% Igepal CA 630, pH 8.0) were applied on each column at a flow rate of 0.5 ml/min. Columns were then washed with 2 ml of the same buffer containing an appropriate detergent. For each column, a different detergent was used: Igepal in a concentration of 0.125% as a control and OG, LDAO, and SDS in concentrations twice as high as the critical micelle concentration. The bounded GST–PsbH fusion protein was then eluted with 3 ml of the same buffer plus 5 mM glutathione. The eluted samples were collected, concentrated, and analyzed by electrophoresis for protein content and UV spectroscopy at 276 and 232 nm for Igepal content.

The PsbH protein was cleaved from the GST–PsbH fusion protein in buffer systems where Igepal CA 630 was exchanged for appropriate detergent as described above.

Separation of fusion protein and truncated fusion protein

Besides the GST–PsbH fusion protein, a truncated GST fusion protein is synthesized. We attempted to use differences of the charge and hydrophobicity to separate both proteins.

Separation on the basis of different charges was done by ion exchange chromatography using Mono Q column (Amersham). Although the calculated p*I* of proteins differs only slightly (6.12 for the anchor protein GST + Xa, 6.13 for the fusion protein), we supposed the additional decrease of charge due to detergent binding in the case of the fusion protein. Ten milliliters of Mono Q column was equilibrated with 5 column volumes of buffer (10 mM Tris, 0.125% Igepal CA 630). In four parallel experiments, the buffer pH was adjusted to 6.5, 7.0, 8.0, or 9.1, respectively. Approximately 500 µl of 1 mg/ml protein was subsequently loaded onto the column at a rate of 1 ml/min. The bounded protein was eluted with increasing concentration of NaCl (0–1 M) in the same buffer.

Separation on the basis of hydrophobicity was done using Phenyl–Sepharose column (Amersham). Small column (0.5 ml) was equilibrated with five column volumes of buffer (50 mM phosphate, 0.125% Igepal CA 630, and 1 M $(NH_4)_2SO_4$). Approximately 500 µl of 1 mg/ml protein was subsequently loaded onto the column at a rate of 1 ml/min. The bounded protein was eluted with decreasing concentration of $(NH_4)_2SO_4$ (1–0 M) in the same buffer.

Results and discussion

PsbH membrane protein is found in PSII complex with no apparent function ascribed as of now. The aim of this work was to isolate the GST–PsbH fusion protein and the PsbH membrane protein alone for 3D structure studies by NMR or crystallography. We adopted the GST expression system and modified it for production of membrane protein, PsbH protein, in sufficient quantities (~mg).

Protein expression

The PsbH protein was expressed in *E. coli* BL 21(DE3) as a GST C-terminal fusion protein. Initial attempts to overexpress the PsbH protein in *E. coli* without a carrier protein resulted in lethal accumulation of the PsbH protein in bacterial membranes (M. Tichy, unpublished data). In contrast, fusion of the PsbH protein to a carrier protein such as GST has been shown to improve stability and enhance solubility of recombinant protein in bacterial cells. Solubility of the GST–PsbH fusion protein was confirmed by the first

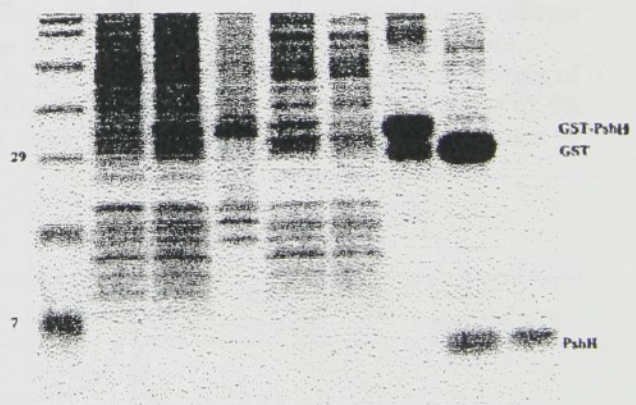

Fig. 2. Purification of cyanobacterial PsbH protein expressed in *E. coli*, 15% SDS–PAGE gel. Lane 1, molecular weight markers; lane 2, cells before IPTG induction; lane 3, cells overproducing GST–PsbH fusion protein; lane 4, sediment; lane 5, supernatant; lane 6, unbound fraction after passage over affinity column; lane 7, fraction eluted from affinity column; lane 8, eluted fraction cleaved by Factor Xa; and lane 9, PsbH protein purified using anex column (Fig. 3B, peak 3). Part of the fusion protein is integrated to membrane and appears in the sediment (lane 4).

overexpression experiment, when the majority of fusion protein was released into the cytoplasm of the cell (Fig. 2, lane 5 supernatant). Although no inclusion bodies were present in the transformed cells, a certain fraction of the fusion protein sedimented upon centrifugation at 25000*g*, which might be a consequence of a partial integration of the protein in bacterial membranes (Fig. 2, lane 4).

Fusion protein purification and its constitutive proteolytic cleavage

Crude bacterial protein extract of cells, after induction of overexpression by IPTG, was purified on an affinity column (chromatogram in Fig. 3A) (Fig. 2, lanes 6 and 7). Lane 7 in Fig. 2 (result of affinity purification) shows that two major proteins with an apparent molecular weight of about 30 kDa were copurified. One of them was characterized as a 35 kDa protein corresponding to the GST–PsbH fusion protein. The second was a 29 kDa protein corresponding to the GST–PsbH protein truncated by the PsbH part (truncated fusion protein). No glutathione-binding protein of similar molecular weight was found in the non-transformed strain (data not shown), which is in agreement with other reports on this expression system (for review see [28]).

One of our goals was to isolate the PsbH membrane protein for crystallization. The number of crystallized soluble proteins increases rapidly because of less methodic problems with purification and crystallization. Our expression system with large soluble anchor protein allowed us to overcome problems with overexpression of membrane proteins (as mentioned above) and it gives us a system where the less soluble PsbH protein can co-crystallize with the soluble GST anchor. Recently, successful crystallization of GST-fused with peptides was presented [29]. For the crystal growth, however, the uniformity and homogeneity of the sample are of prime importance. We either had to separate the fusion protein and truncated protein or to eliminate the presence of the truncated protein in the expression system.

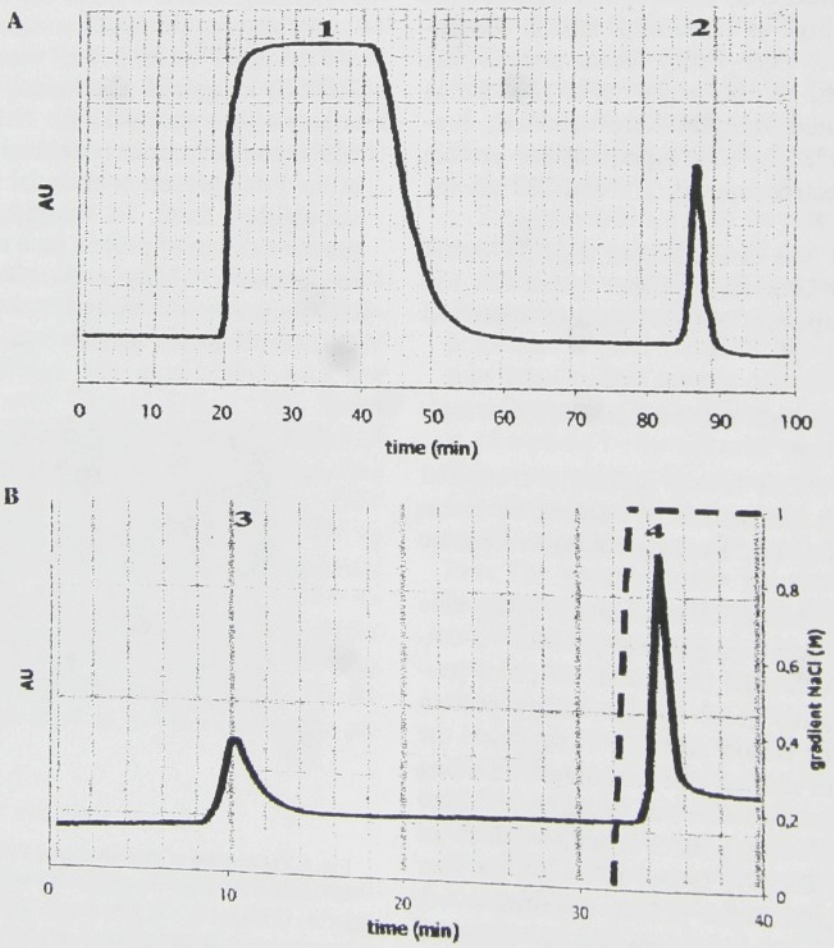

Fig. 3. Chart recorder chromatograms. (A) Purification of the GST–PsbH fusion protein. The clarified cell extract was loaded onto affinity column (peak 1). After column washing, the bounded protein was eluted (peak 2). (B) Purification of the PsbH protein. The cleaved fusion protein was loaded onto anex column. The PsbH protein passed through the column (peak 3) while the GST carrier was bound to the column and was eluted (peak 4) with increasing NaCl concentration (dashed line).

	235 nm	275 nm
Igepal	1,0389	1,4688
OG	0,1910	0,0672
SDS	0,2656	0,0665
LDAO	0,2481	0,0772

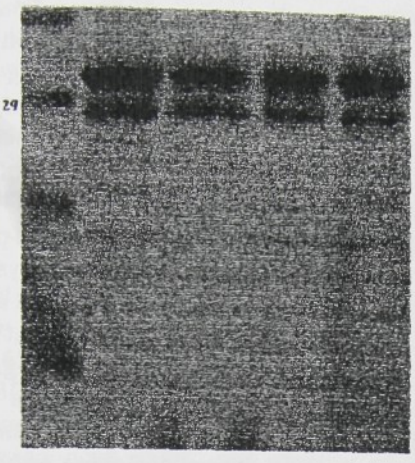

Fig. 5. Detergent replacement for NMR studies. The glutathione agarose column with bounded fusion protein was pre-washed by an alternative detergent. The same detergent was used in the elution buffer. The eluted fraction was analyzed by UV spectroscopy (presence of Igepal) and by electrophoresis (protein content). The gel shows the same content of protein in all detergents. Lane 1, molecular weight markers; lane 2, Igepal CA 630; lane 3, OG; lane 4, SDS, and lane 5, LDAO. Table inserted shows the rapid decrease of absorbance at wavelengths typical for Igepal CA 630 of the samples with exchanged detergents. The final detergent in the sample is mentioned in the left column. The decrease of the values shows the exchange of the Igepal CA 630 for the final detergent.

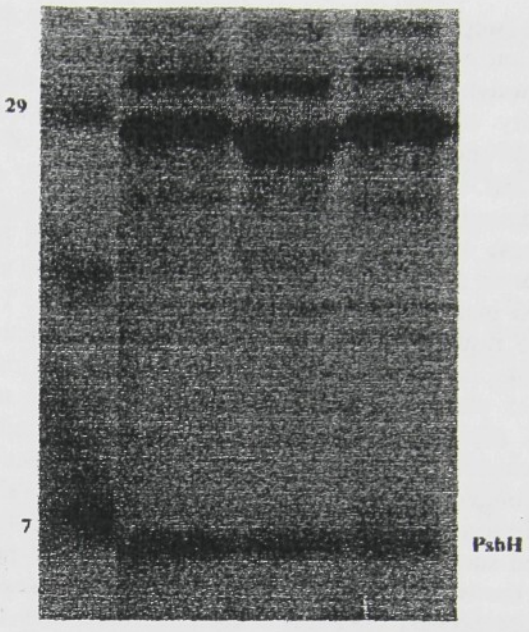

Fig. 6. Cleavage of GST–PsbH fusion protein by Factor Xa. The efficiency of cleavage by Factor Xa was evaluated in the presence of different detergents. Lane 1, molecular weight markers; lane 2, Igepal CA 630; lane 3, LDAO; and lane 4, OG.

Consequently, we tested detergent exchange on the fusion protein bound to the affinity column.

We tested mild nonionic detergent OG, zwitterionic detergent LDAO, and ionic detergent SDS. The table in Fig. 5 shows the disappearance of absorbance at 276 and 232 nm typical for Igepal in all three cases upon elution of the column by alternative detergents. The gel (Fig. 5) shows approximately the same content of protein in all eluents with different exchanged detergents, suggesting that the fusion protein was completely solubilized in each of them.

In the next step, cleavage of the fusion protein by factor Xa was tested in the presence of the alternative detergents. OG and LDAO did not denature Factor Xa, while SDS was excluded as a denaturing agent. Fig. 6 shows that both detergents allow clear cleavage comparable to that achieved in Igepal.

The concentration of the fusion protein GST–PsbH was estimated by the method of Peterson [31] with the yield of 16 mg GST–PsbH fusion protein from 1 liter of cell culture (3.86 mg fusion protein per gram of wet biomass) (Table 1). Factor Xa cleaved the GST–PsbH fusion protein after 16 h, resulting in fragments of the size of 6 kDa (PsbH protein) and 29 kDa (anchor protein) (Fig. 2, lane 8), which were subsequently separated on a DEAE–cellulose column (chromatogram in Fig. 3B) (Fig. 2, lane 9). As a result, the GST carrier was bound to the column while the PsbH protein passed through the column.

The final yield of the PsbH protein from the 16 mg of purified GST–PsbH was 2.1 mg, giving a value of 67.5% with respect to the theoretical yield. The results of

Table 1
Purification of PsbH protein from 1 liter *E. coli* culture

Parameter	Value	PsbH protein fraction of total protein	Fold purification
Optical density	2.63 g	—	—
Wet biomass	4.15 g	—	—
Whole protein concentration in whole wet biomass	0.83 g[a]	0.00396	1
GST–PsbH protein after affinity chromatography	16 mg[a] (>95% yield of the affinity chromatography step)[b]	0.196	49.5
PsbH protein after DEAE chromatography	2.1 mg[a] (67.5% yield of the Xa protease cleavage and DEAE chromatography)	1	252.5

[a] The protein concentration was estimated according to Peterson [31].
[b] Determined by densitometry of gel.

There were several likely explanations for the co-production of the two proteins with an apparent molecular weight of about 30 kDa. (i) We considered the possibility of the presence of the plasmid mixture (pKAH25 and pGEX-3X) used for transformation of *E. coli* BL21(DE3). To test this possibility, an *Eco*RV restriction analysis was performed. *Eco*RV restriction endonuclease recognizes only one site on pGEX-3X but two sites on pKAH25, due to the second recognized site localized inside the inserted *psb*H gene sequence. The cleavage resulted, as expected, in only two restriction fragments, which confirmed the existence of only pKAH25 plasmid in the transformed cells (data not shown). (ii) We considered a putative weak terminal codon exists at the beginning of *psb*H coding sequence, which could cause premature termination of GST–PsbH transcription. The examination of the codon content excluded such a possibility. (iii) The possibility of producing the bacterial GST in comparable amounts with the overexpressed GST–PsbH fusion protein was unequivocally excluded, since no protein of appropriate molecular weight was found in cells without inserted plasmid (data not shown). (iv) The plasmid pKAH25 was used for transformation of another *E. coli* strain, MN 522. The purification, however, resulted in presence of two bands after elution. (v) Finally, we compared (Fig. 4) the ratio of the fusion protein and its truncated version prior to the induction (constitutive production) and after the induction of overexpression by IPTG. The truncated protein prevailed in non-induced cells and the full-length fusion protein in induced material. Moreover, the abundance of the truncated fusion protein increased with prolonged time of cell harvesting (data not shown).

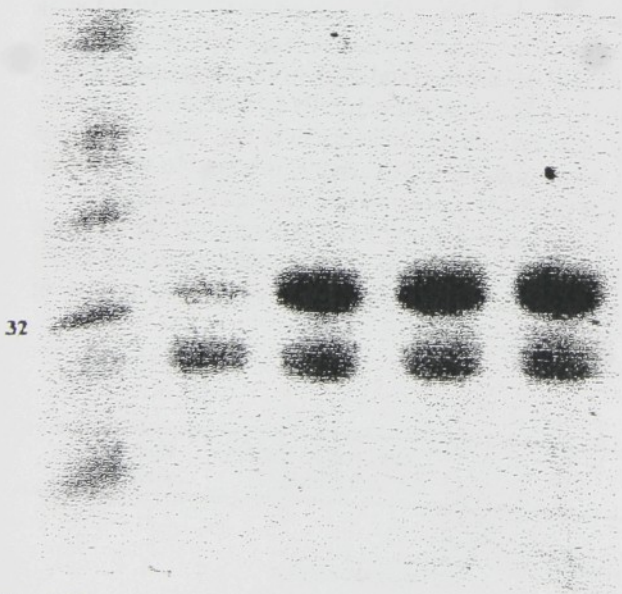

Fig. 4. Ratio of the GST–PsbH fusion protein and truncated GST protein after induction of overexpression. The overexpression of the fusion protein was induced by adding IPTG. With increasing concentration of IPTG was raised amount of the fusion GST–PsbH protein was raised while concentration of the truncated protein did not change. Lane 1, molecular weight markers; lane 2, non-IPTG; lane 3, 0.1 mM IPTG; lane 4, 0.5 mM IPTG; and lane 5, 1 mM IPTG.

As the most probable explanation, we propose that there is a constitutive proteolytic process common to all *E. coli* strains, which cleaves the fusion protein. It seems that there are fragments of the GST–PsbH fusion protein truncated by the transmembrane part produced as it is seen from the electrophoretic analysis (Fig. 2, lane 5). However, we were not able to detect any protein with a molecular weight comparable to that of the PsbH protein in the membrane fraction (Fig. 2, lane 4). The corresponding protease could play a role in protection of the cell against integration of misassembled membrane proteins. There are some enzymes, which could cause this cleavage (for review see [30]).

Although we proposed a possible mechanism of the fusion protein truncation, we were not able to eliminate the presence of the truncated protein in the expression system. To produce homogeneous sample of fusion protein for crystallization, we attempted to remove the 29 kDa protein. Using Mono-Q we were not able to separate the GST–PsbH fusion protein from the truncated fusion protein. Some degree of separation was achieved when hydrophobic chromatography (phenyl-Sepharose) was used. However, the resolution of the GST–PsbH fusion and the truncated fusion protein peaks was very weak, resulting in substantial dilution of the protein and a loss of the considerable part of product (data not shown). Better resolution of the separation method will be the matter of further studies. The partially purified GST–PsbH protein is now the subject of crystallization experiments.

To reach the goal of isolation of the PsbH protein itself, the separation of the fusion protein from the truncated form is not required.

Detergent exchange and sample optimization

Igepal CA 630 is a nonionic detergent suitable for isolation at nondenaturing conditions; it preserves the protein in a form close to the native state. For NMR, crystallization, and many spectroscopic methods, this detergent is often unsuitable. None of the known methods of detergent exchange (hydrophobic adsorption on BIO-BEADS (Bio-Rad), dialysis, and ultrafiltration) were successful in removing the detergent after purification of the PsbH protein. The adsorption kinetics of our protein on hydrophobic BIO BEADS was similar to that of Igepal (or whole micelles absorbed) and no enrichment was observed. Dialysis and ultrafiltration using 3 kDa filters/membranes resulted in unchanged detergent to protein ratio, indicating that micelles did not penetrate the membrane. The dilution of protein solution below the cmc did not interrupt Igepal binding to the protein.

purification are summarized in Table 1. The identity of the resulting protein product was confirmed by trypsin fragmentation followed by MALDI-TOF MS analysis. Two detected fragments of trypsine cleavage were characterized as 5–20 and 7–20 fragments of the PsbH protein. These correspond to the two possible trypsin cleavage sites in position four and six on N-terminus of the PsbH protein.

The amino acid analysis revealed the ratio of amino acid concentration (nmol) in the purified PsbH protein Ala/Arg/Thr (0.865/0.866/0.824), which confirms the theoretical ratio 3/3/3 derived from the amino acid sequence. Since these amino acids are spread along the whole protein amino acid chain, the identity of the protein was unequivocally proven.

Conclusions

The original goal of the project, the preparation of a low molecular weight membrane protein in sufficient amount for structural studies by NMR and protein crystallography, was achieved. Overexpression in the form of fusion protein with large soluble tag proved to be a proper method to obtain high yield of the protein and facilitated relatively easy isolation. Compared to the other membrane-protein expression systems, the major problem, which had to be overcome, was the detergent exchange due to the similarity of the size of protein-containing and protein-free detergent micelle. An alternative strategy for the detergent exchange was introduced. The cleavage of the GST–PsbH fusion protein in the exchanged detergent followed by concentration was shown as the optimal isolation procedure.

Acknowledgments

We would like to specially honor to Prof. John F. Allen, Department of Plant Biochemistry, Lund University, for inspiration of this project and funding its initial steps. We particularly wish to thank Dr. J. Zbrožek at the Institute of Molecular Genetics in Prague for his assistance with the amino acid analysis, Mgr. P. Novak at the Institute of Microbiology in Prague for performing MALDI-TOF MS fragmentation analysis, and Dr. F. Vacha for critical reading of the manuscript. This work was funded by the Project Grants FRVS 1290 and MSM12310001 of the Ministry of Education, Youth and Sports of the Czech Republic.

References

[1] A. Zouni, H.T. Witt, J. Kern, P. Fromme, N. Krauss, W. Saenger, P. Orth, Crystal structure of photosystem II from *Synechococcus elongatus* at 3.8 angstrom resolution, Nature 409 (6821) (2001) 739–743.

[2] J. Bennet, Phosphorylation of chloroplast membrane polypeptides, Nature 269 (1977) 344–346.

[3] J. Farchaus, R.A. Dilley, Purification and partial sequence of the M_r 10000 phosphoprotein from spinach thylakoids, Arch. Biochem. Biophys. 244 (1986) 94–101.

[4] K. Shinozaki, M. Ohme, M. Tanaka, T. Wakasugi, N. Hayashida, T. Matsubayashi, N. Zaita, J. Chungwongse, J. Obokata, K. Yamagushishinozaki, C. Ohto, K. Torazawa, Meng-By, M. Sugita, H. Deno, T. Kamogashira, K. Yamada, J. Kusuda, F. Takaiwa, A. Kato, N. Tohdon, H. Shimada, M. Sugiura, The complete nucleotide sequence of the tobacco chloroplast genome—its gene organization and expression, EMBO J. 5 (1986) 2043–2049.

[5] K. Ohyama, H. Fukuzawa, T. Kohchi, H. Shirai, T. Sano, S. Sano, K. Umesono, Y. Shiki, M. Takeuchi, Z. Chang, S. Aota, H. Inokuchi, H. Ozeki, Chloroplast gene organization deduced from complete sequence of liverwort *Marchantia-polymorpha* chloroplast DNA, Nature 322 (1986) 572–574.

[6] N. Dedner, H.E. Meyer, C. Ashton, G.F. Wildner, N-terminal sequence analysis of the 8 kDa protein in *Chlamydomonas reinhardii*. Localization of the phosphothreonine, FEBS Lett. 236 (1988) 77–82.

[7] C. Johnson, G.W. Schmidt, The *psb*B gene cluster of the *Chlamydomonas reinhardtii* chloroplast-sequence and transcriptional analyses of *psb*N and *psb*H, Plant Mol. Biol. 22 (1993) 645–658.

[8] H. Koike, K. Mamada, M. Ikeuchi, Y. Inoue, Low-molecular-mass proteins in cyanobacterial photosystem II—identification of *psb*H and *psb*K gene products by N-terminal sequencing, FEBS Lett. 244 (1989) 391–396.

[9] S.R. Mayes, J. Barber, Primary structure of the *psb*N-*psb*H-*pet*C-*pet*A gene cluster of the cyanobacterium *Synechocystis* PCC-6803, Plant Mol. Biol. 17 (1991) 289–293.

[10] A.L. Abdel-Mangood, R.A. Dilley, Cloning and nucleotide-sequence of the *psb*H gene from cyanobacterium *Synechocystis* 6803, Plant Mol. Biol. 14 (1990) 445–446.

[11] M. Ikeuchi, F.G. Plumley, Y. Inoue, G.W. Schmidt, Phophorylation of photosystem II components, CP 43 apoprotein, D1, D2, and 10 to 11 kilodalton protein in chloroplast thylakoids of higher plants, Plant Physiol. 85 (1987) 638–642.

[12] M. Ikeuchi, Y. Inoue, A new 4.8 kDa polypeptide intrinsic to the PS II reaction center, as revealed by modified SDS–PAGE with improved resolution of low molecular weight proteins, Plant Cell Physiol. 29 (1988) 1233–1239.

[13] C. Büchel, E. Morris, E. Orlova, J. Barber, Localisation of the PsbH subunit in photosystem II: a new approach using labelling of His-tags with a Ni^{2+}/-NTA gold cluster and single particle analysis, J. Mol. Biol. 312 (2001) 371–379.

[14] C. De Vitry, B.A. Diner, J.L. Popot, Photosystem II particles from *Chlamydomonas reinhardtii*—purification, molecular weight, small subunit composition, and protein-phosphorylation, J. Biol. Chem. 266 (1991) 16614–16621.

[15] J.F. Allen, Protein-phosphorylation in regulation of photosynthesis, Biochim. Biophys. Acta 1098 (1992) 275–335.

[16] H.P. Michel, J. Bennett, Identification of the phosphorylation site of an 8.3 kDa protein from photosystem II of spinach, FEBS Lett. 212 (1987) 1123–1130.

[17] D. Štys, M. Stancek, L. Cheng, J.F. Allen, Complex formation in plant thylakoid membranes. Competition studies on membrane–protein interactions using synthetic peptide fragments, Photosynth. Res. 44 (1995) 277–285.

[18] H.L. Race, K. Gounaris, Identification of the *psb*H gene product as a 6 kDa phosphoprotein in the cyanobacterium *Synechocystis* 6803, FEBS Lett. 323 (1993) 35–39.

19] S.R. Mayes, J.M. Dubbs, I. Vass, E. Hideg, L. Nagy, J. Barber, Further characterization of the *psb*H locus of *Synechocystis* sp. PCC 6803—inactivation of *psb*H impairs Q(A) to Q(B) electron-transport in photosystem 2, Biochemistry 32 (1993) 1454–1465.

20] J. Komenda, J. Barber, Comparison of *psb*O and *psb*H deletion mutants of *Synechocystis* PCC 6803 indicates that degradation of D1 protein is regulated by the Q_B site and dependent on protein-synthesis, Biochemistry 29 (1995) 9625–9631.

21] C. Sundby, U.K. Larsson, T. Henrysson, Effects of bicarbonate on thylakoid protein phosphorylation, Biochim. Biophys. Acta 975 (1989) 277–282.

22] J. Komenda, L. Lupínková, J. Kopecký, Absence of the *psb*H gene product destabilizes photosystem II complex and bicarbonate binding on its acceptor side in *Synechocystis* PCC 6803, Eur. J. Biochem. 269 (2002) 610–619.

23] E.J. Summer, V.H.R. Schmid, B.U. Bruns, G.W. Schmidt, Requirement for the H phosphoprotein in photosystem II of *Chlamydomonas reinhardtii*, Plant Physiol. 113 (1997) 1359–1368.

24] H.E. O'Connor, S.V. Ruffle, A.J. Cain, Z. Deak, I. Vass, J.H.A. Nugent, S. Purton, The 9-kDa phosphoprotein of photosystem II. Generation and characterisation of *Chlamydomonas* mutants lacking PSII-H and a site-directed mutant lacking the phosphorylation site, Biochim. Biophys. Acta 1364 (1998) 63–72.

[25] M. Kuhn, P. Thiel, P. Böger, The 9 kDa phosphoprotein involved in photoinhibition, Z. Naturforch. 43C (1988) 413–417.

[26] M.T. Giardi, J. Komenda, J. Masojidek, Involvement of protein phosphorylation in the sensitivity of photosystem II to strong illumination, Physiol. Plantarum 92 (1994) 181–187.

[27] Y. Takahashi, H. Matsumoto, M. Goldschmidt-Clermont, J.D. Rochaix, Directed disruption of the *Chlamydomonas* chloroplast *psb*K gene destabilizes the photosystem II reaction center complex, Plant Mol. Biol. 24 (1994) 779–788.

[28] M. Uhlen, T. Moks, Gene fusion for purpose of expression: an introduction, Methods Enzymol. 185 (1990) 129–143.

[29] Y.H. Han, Y.H. Chung, T.Y. Kim, S.J. Hong, J.D. Choi, Y.J. Chung, Crystallization of *Clonorchis sinensis* 26 kDa glutathione *S*-transferase and its fusion proteins with peptides of different lengths, Acta Cryst. D 57 (2001) 579–581.

[30] S. Gottesman, Proteases and their targets in *Escherichia coli*, Annu. Rev. Genet. 30 (1996) 465–506.

[31] G.L. Peterson, A simplification of the protein assay method of Lowry et al. which is more generally applicable, Anal. Biochem. 83 (1977) 346–356.

PHOTOSYNTHETICA 43 (3): 421-424, 2005

BRIEF COMMUNICATION

Secondary structure estimation of recombinant *psbH*, encoding a photosynthetic membrane protein of cyanobacterium *Synechocystis* sp. PCC 6803

D. ŠTYS*, W. SCHOEFBERGER*, Z. HALBHUBER*, J. RISTVEJOVA*, N. MÜLLER**, and R. ETTRICH*,***

*Laboratories of High Performance Computing and Biomembranes, Institute of Physical Biology of the University of South Bohemia, and Institute of Systems Biology and Ecology, Academy of Sciences of the Czech Republic, Zámek 136, 373 33 Nové Hrady, Czech Republic**
*Johannes Kepler Universität, Altenbergerstrasse 69, Linz, Austria***

Abstract

The PsbH protein of cyanobacterium *Synechocystis* sp. PCC 6803 was expressed as a fusion protein with glutathione-S transferase (GST) in *E. coli* grown on a mineral medium enriched in ^{15}N isotope. After enzymatic cleavage of the fusion protein, the ^{1}H-^{15}N-HSQC spectrum of PsbH protein in presence of the detergent β-D-octyl-glucopyranoside (OG) was recorded on a *Bruker DRX* 500 MHz NMR spectrometer equipped with a 5 mm TXI cryoprobe to enhance the sensitivity and resolution. Non-labelled protein was used for secondary structure estimation by de-convolution from circular dichroism (CD) spectra. Experimental results were compared with our results from a structural model of PsbH using a restraint-based comparative modelling approach combined with molecular dynamics and energetic modelling. We found that PsbH shows 34–38 % α-helical structure (Thr36-Ser60), a maximum of around 15 % of β-sheet, and 12–19 % of β-turn.

Additional key words: CD spectroscopy; molecular dynamics calculations; NMR spectroscopy; photosystem 2; protein folding.

The PsbH protein is one of the small protein subunits of photosystem 2 (PS2), a membrane pigment-protein complex that catalyzes the light-induced electron transfer and water-splitting reactions. The PsbH protein was originally found in thylakoids of higher plants and detected as a 10 kDa phosphoprotein (Bennett 1977, Allen 1992). Genes encoding PsbH homologues have so far been identified in all oxygenic phototrophs studied (for review see Komenda *et al.* 2003) and its deduced amino acid sequence predicts a single transmembrane helix. In higher plants and green algae the PsbH protein undergoes reversible phosphorylation at two threonine residues close to the N-terminus (Michel and Bennett 1987, Vener *et al.* 2001). The cyanobacterial PsbH protein is truncated at the N-terminus and misses these phosphorylation sites (Koike *et al.* 1989). The function of PsbH in PS2 has been associated with control of the electron flow from Q_A to Q_B (Mayes *et al.* 1993), protection from photoinhibition (Komenda and Barber 1995), bicarbonate binding on its acceptor site (Komenda *et al.* 2002), or chaperon-like function in the assembly of the PS2 core and of small stress-induced chlorophyll (Chl) binding proteins (Komenda 2005). In *Chlamydomonas reinhardtii*, disruption of the PsbH subunit led to a rapid degradation of D2 protein and mutants lacking PsbH were unable to assemble any functional PS2 (Summer *et al.* 1997).

Three-dimensional structures of the PS2 core complex have been solved by electron microscopy (for review see

Received 22 February 2005, *accepted* 23 May 2005.
***Corresponding author; fax: +420386361279, e-mail: ettrich@greentech
Acknowledgement: We specially thank Prof. J.F. Allen, Department of Plant Biochemistry, Lund University, for inspiration of this project and funding its initial steps. We thank Dr. K. Bezouška (Faculty of Science, Charles University, Prague) for providing additional computing facilities. This research was supported by AKTION Austria-Czech Republic (No. 40p2), by the Ministry of Education, Youth, and Sports of the Czech Republic (MSM6007665808), and by the Academy of Sciences of the Czech Republic (Institutional research concept AVOZ60870520) and by the Austrian Science Fund (FWF-Project P15380).

Bumba and Vácha 2003) and X-ray crystallography (Zouni *et al.* 2001, Kamiya and Shen 2003, Ferreira *et al.* 2004). Apart from the major PS2 subunits (CP47, CP43, D1, and D2 protein) and components of cyt b_{559} (PsbE and PsbF proteins), identification and localization of the other small protein subunits has been contradictory concerning the crystal structures (see Shi and Schröder 2004). Recently, the location of PsbH subunit within the PS2 complex from electron microscopy and single particle analysis was identified (Bumba, unpublished), in good agreement with the crystal structure of the PS2 complex of cyanobacterium *Thermosynechococcus elongatus* (Ferreira *et al.* 2004). The location of the PsbH subunit close to the CP47 protein is also supported by the fact that the PsbH protein stabilizes the binding of CP47 to the D1-D2 heterodimer (Komenda *et al.* 2002) and thus supports the assembly of the PS2 core (Summer *et al.* 1997). PsbH is predicted to have a single transmembrane helix, a small C-terminal domain in the lumen, and a larger N-terminal domain in the stroma (Komenda *et al.* 2002). PsbH is one of the proteins expressed in etiolated and irradiated leaves in higher plants on the same level, which indicates that its function may be considered separately from the rest of the multiprotein complex.

The PsbH protein of cyanobacterium *Synechocystis* sp. PCC 6803 *psbH* gene (locuss12598) was over-expressed as a fusion protein with glutathione-S transferase (GST) in *E. coli* and the PsbH-GST fusion protein was enzymatically cleaved and purified according to the procedure given by Halbhuber *et al.* (2003).

We isolated non-labelled PsbH protein for circular dichroism (CD) spectrometry. CD spectra of the sample were recorded on a *Jasco*-instrument, controlled by PC-based *ISA OMA* software at 20 °C in 1-mm quartz cuvettes, after 15 min of temperature equilibration. Five scans were accumulated for each spectrum with a response time of 2 s, a bandwidth of 2 nm, and a scan speed of 10 nm min^{-1} from 190 to 250 nm. Background spectra without protein were subtracted. The protein concentration was 20 μM.

To study the structure of PsbH protein we performed uniform isotope labelling of the PsbH protein according the procedures using minimal media (M9) (Rhee *et al.* 1997, Halbhuber *et al.* 2003). We isolated and purified the ^{15}N labelled protein to a concentration of 1.1 kg m^{-3} in presence of non-ionic β-D-octyl-glucopyranoside. ^{1}H-^{15}N HSQC spectra were recorded on a *Bruker DRX* 500 MHz NMR spectrometer equipped with a 5 mm *TXI* cryoprobe to enhance sensitivity and resolution. The dialysed protein sample was mixed with D_2O (H_2O/D_2O 1 : 20) to perform the NMR experiments. The standard *Bruker* pulse sequence for these experiments was the *hsqc-etf3-gpsi2* pulse program.

A model of the the PsbH protein of cyanobacterium *Synechocystis* sp. PCC 6803 was generated by analogy to the crystal structure at 0.35 nm resolution of the PS2 complex of cyanobacterium *Thermosynechococcus elongatus* (Ferreira *et al.* 2004) (PDB code 1S5L). Bumba *et al.* (unpublished) recently showed the position of the PsbH in this structure to be correct, however, 22 amino acids at the N-terminal end of the protein are missing in the crystal structure. Therefore the suggested structure for these amino acids is not based on homology with the crystal but generated from a loop database. The three-dimensional model constituted by all non-hydrogen atoms was built and examined by the *MODELLER7* package (Sali and Blundell 1993). As the crystal structure has a very low resolution and large parts of the protein were not resolved, we decided to refine the homology model by running a 1.2 ns molecular dynamics simulation in aqueous solution using the *YAMBER2* force field (Krieger *et al.* 2004) to induce better folding of the protein. The protein structure was placed into a box of 7.3×8.2×9.6 nm size, which was 1 nm larger than the protein along all three axes. The box was filled with TIP3P water, sodium ions were iteratively placed at the coordinates with the lowest electrostatic potential until the cell was neutral. Molecular dynamics simulations

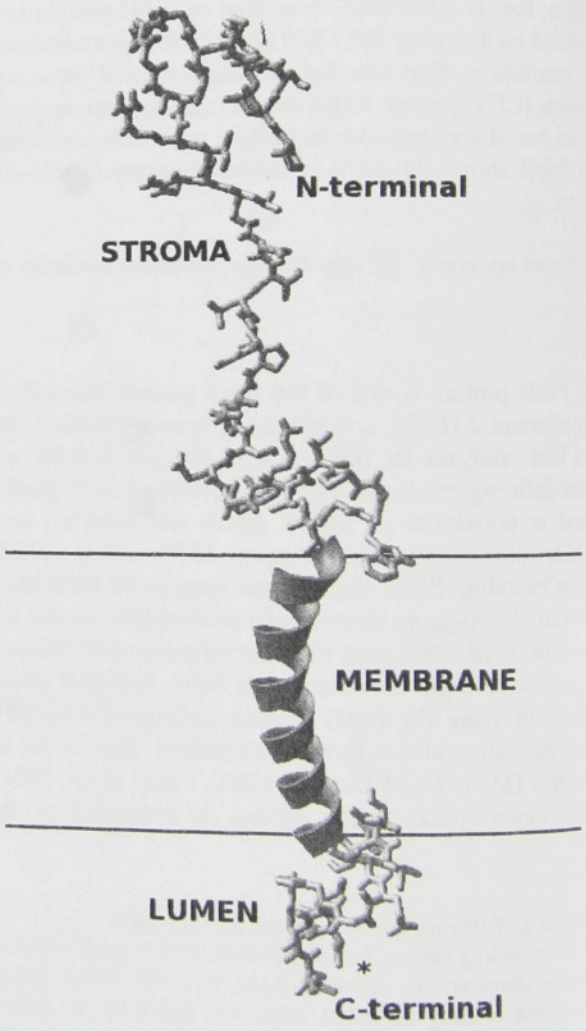

Fig. 1. Three-dimensional representation of the calculated structure of PsbH from *Synechocystis* sp. PCC 6803. The possible ion binding site in the lumen is marked *.

were run with *YASARA* (www.yasara.org), using a multiple time step of 1 fs for intra-molecular and 2 fs for intermolecular forces. A 1.2 nm cut-off was taken for Lennard Jones forces and the direct space portion of the electrostatic forces, which were calculated using the Particle Mesh Ewald method (Essman *et al.* 1995) with a grid spacing 0.1 nm, 4th order B-splines, and a tolerance of 10^{-4} for the direct space sum. The simulation of the homology model was then run at 298 K and constant přessure (NPT ensemble) to account for volume changes due to fluctuations of homology models in solution. Residues 37–59 in the trans-membrane helix were restrained during the simulation to mimic the stabilization of this part by the membrane. Root mean square deviation for C_α and the total energy of the systems indicated that the protein structure arrive at an equilibrium state after 750 ps. The resulting structure was minimized to convergence of the energy gradient to less than 0.02 kJ mol^{-1} nm^{-1} using the *TRIPOS* force field included in the *MAXIMIN2* module of *SYBYL* (*TRIPOS Associates*). The minimization included electrostatic interactions based on Gasteiger Hückel partial charge distributions using a dielectric constant with a distance-dependent function $\varepsilon = 4\,r$ and a non-bonded interaction cut-off of 1.2 nm. The final model (Fig. 1) had 98.3 % of residues in the two most favoured regions of the Ramachandran plot and an acceptable overall geometry, both determined with the *ProCheck* program (Laskowski *et al.* 1993). No residues were found in disallowed regions. The overall *g*-factor of the structure obtained showed a value of –0.16. The *g*-factor should be above –0.5 and values below –1.0 may need investigation. Amino acids from Thr36-Ser60 adopted an α-helical fold, which corresponds to 34.2 % of the total secondary structure, and 12.3 % of the amino acids were found in a β-turn conformation. No stable β-sheet structure was found in the model. This has been confronted with the estimation of secondary structure from the experimental far-UV CD by deconvolution using the method of *VARSELEC* (variable selection method) included in the *Dicroprot V2.5* program (Deléage and Geourjon 1993) with 33 reference spectra. The calculation yielded a 38 % helical structure, 15–19 % sheet and 19 % β-turn. In our opinion, the deconvolution is reliable mostly for α-helix and to a lower extent for β-sheet and other structures. The distinction between anti-parallel and parallel β-sheets looks very difficult and is not very reliable, so that we summarized the overall β-sheet content.

Additionally, we used the *K2D* program based on neural network theory (Andrade *et al.* 1993). Calculations from CD spectra using the *K2d* software gave 37 % helical structure, 14 % sheet, and 49 % random coil. We can summarize the results of the quantitative analysis of the far-UV CD spectra in the following way: Both methods showed an α-helical content between 37 and 38 % and thus completely agreed with the model. Most critical and unreliable is the estimation of the β-structure from CD-spectra, which is an intrinsic limitation of the method.

Certainly, we can state that the CD spectra of the protein/detergent mixture indicate that the protein adopts a mixture of secondary structures, including helix, sheet, and random coil. As CD shows the average of all structures present in the sample, it is not possible to suggest from a CD spectrum if a protein is proper folded or if it is a mixture of different folds or aggregates. Therefore the 1H-15N-HSQC spectrum of PsbH protein in OG was recorded and, as shown in Fig. 2*B*, it has 70 resolved amino acid signals within the range of 7.0–9.0 mg kg^{-1}. Thus, we can clearly state that we have a properly folded protein and in future it will be promising to perform NMR structural assignments of doubly labelled ^{15}N-^{13}C protein/detergent system.

Pure unlabelled and ^{15}N labelled PsbH protein was prepared to study the secondary structure content of properly folded membrane protein PsbH. CD-spectra and two-dimensional ^{1}H-^{15}N-HSQC NMR experiments revealed that psbH protein in the detergent OG has a proper fold that fully corresponds to theoretical

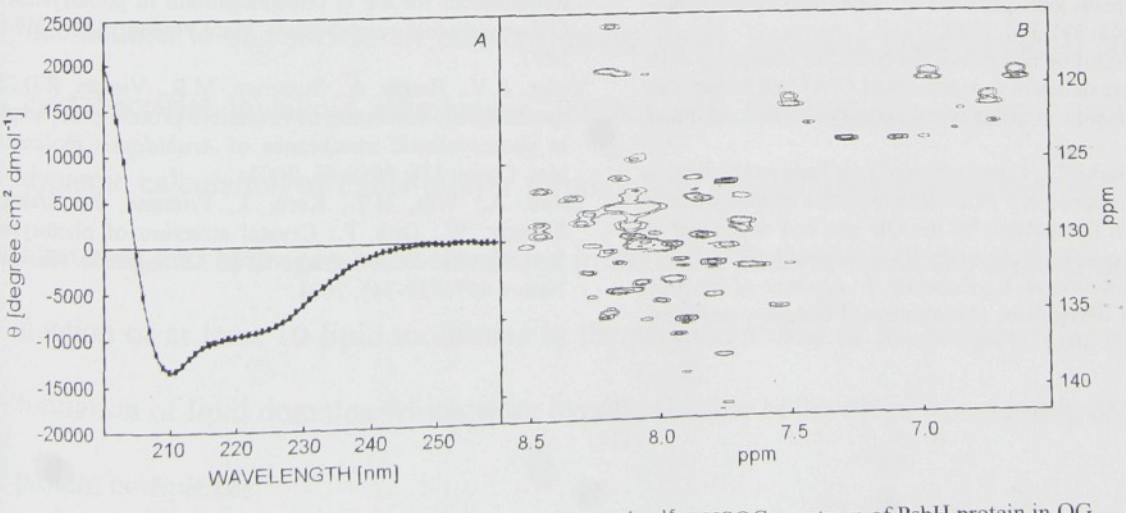

Fig. 2. *A*: Circular dichroism spectra of PsbH protein in OG. *B*: ^{1}H-^{15}N-HSQC spectrum of PsbH protein in OG.

calculations from molecular dynamics. The transmembrane helix from the structural model gives 34.2 % of the total secondary structure content, which corresponds to the helical structure measured by CD. This fact excludes the existence of additional helical structure in the stroma or lumen. Regarding the β-sheet content, the structural model does not show sheet structure, however, the β-turn from Glu7-Gly10 suggests a possible sheet structure at the N-terminus of the protein. Additionally, the fold adopted from Ser25-Gly35 shows Ψ-Φ values in the β-sheet region of the Ramachandran plot. In connection with the β-turn just before the helix this might lead to a β-structure under certain circumstances. The part of the protein in the lumen seems to adopt only a random coil structure. Interestingly, we find a high affinity for ions in the region formed by Glu65, Ser68, Asp70, and the C-terminal (Gly73) oxygen (marked * in Fig. 1). The possible ability of the C-terminal domain in the lumen to bind ions has to be explored further.

References

Allen, J.F.: Protein phosphorylation in regulation of photosynthesis. – Biochim. biophys. Acta **1098**: 275-335, 1992.

Andrade, M.A., Chacón, P., Merelo, J.J., Morán, F.: Evaluation of secondary structure of proteins from UV circular dichroism using an unsupervised learning neural network. – Prot. Eng. **6**: 383-390, 1993.

Bennett, J.: Phosphorylation of chloroplast membrane polypeptides. – Nature **269**: 344-346, 1977.

Bumba, L., Vácha, F.: Electron microscopy in structural studies of Photosystem II. – Photosynth. Res. **77**: 1-19, 2003.

Deléage, G., Geourjon, C.: An interactive graphic program for calculating the secondary structure content of proteins from circular-dichroism spectrum. – Comp. appl. Biosci. **9**: 197-199, 1993.

Essman, U., Perera, L., Berkowitz, M.L., Darden, T., Lee, H.., Pedersen, L.G.: A smooth particle mesh Ewald method. – J. chem. Phys. **103**: 8577-8593, 1995.

Ferreira, K.N., Iverson, T.M., Maghlaoui, K., Barber, J., Iwata, S.: Architecture of the photosynthetic oxygen-evolving center. – Science, in press, 2004.

Halbhuber, Z., Petrmichlová, Z., Alexciev, K., Thulin, E., Štys, D.: Overexpression and purification of recombinant membrane PsbH protein in *Escherichia coli*. – Protein Exp. Purif. **32**: 18-27, 2003.

Kamiya, N., Shen, J.R.: Crystal structure of oxygen-evolving Photosystem II from *Thermosynechococcus vulcanus* at 3.7 Angstrom resolution. – Proc. nat. Acad. Sci. USA **100**: 98-103, 2003.

Koike, H., Mamada, K., Ikeuchi, M., Inoue, Y.: Low-molecular-mass proteins in cyanobacterial photosystem II: identification of *psb*H and *psb*K gene products by N-terminal sequencing. – FEBS Lett. **244**: 391-396, 1989.

Komenda, J.: Autotrophic cells of the *Synechocystis psbH* deletion mutant are deficient in synthesis of CP47 and accumulate inactive PSII core complexes. – Photosynth. Res. in press, 2005.

Komenda, J., Barber, J., Comparison of *psbO* and *psbH* deletion mutants of *Synechocystis* PCC 6803 indicates that degradation of D1 protein is regulated by the QB site and dependent on protein synthesis. – Biochemistry **29**: 9625-9631, 1995.

Komenda, J., Lupínková, L., Kopecký, J.: Absence of the *psb*H gene product destabilizes photosystem II complex and bicarbonate binding on its acceptor side in *Synechocystis* PCC 6803. – Eur. J. Biochem. **269**: 610-619, 2002.

Komenda, J., Štys, D., Lupínková, L.: The PsbH protein in photosystem 2. – Photosynthetica **41**: 1-7, 2003.

Krieger, E., Darden, T., Nabuurs, S., Finkelstein, B.A., Vriend, G.: Making optimal use of empirical energy functions: force-field parameterization in crystal space. – Proteins: Struct. Funct. Bioinform. **57**: 678-683, 2004.

Laskowski, R.A., MacArthur, M.W., Moss, D.S., Thornton, J.M.: Procheck – a program to check the stereochemical quality of protein structures. – J. appl. Cryst. **26**: 283-291, 1993.

Mayes, S.R., Dubbs, J.M., Vass, I., Hideg, É., Nagy, L., Barber, J.: Further characterization of the *psb*H locus of *Synechocystis* sp. PCC 6803 inactivation of *psb*H impairs Q_A to Q_B electron-transport in photosystem 2. – Biochemistry **32**: 1454-1465, 1993.

Michel, H.P., Bennett, J.: Identification of the phosphorylation site of an 8.3 kDa protein from photosystem II of spinach. – FEBS Lett. **212**: 103-108, 1987.

Rhee, J., II, Rode, J., Diaz-Ricci, J.C., Poock, D., Weigel, B., Kretzmer, G., Schügerl, K.: Influence of the medium composition and plasmid combination on the growth of recombinant *Escherichia coli* JM109 and on the production of the fusion protein EcoRI::SPA. – J. Biotechnol. **55**: 69-83, 1997.

Sali, A., Blundell, T.L.: Comparative modelling by satisfaction of spatial restraints. – J. mol. Biol. **234**: 779-815, 1993.

Shi, L.X., Schröder, W.P.: The low molecular mass subunits of the photosynthetic supracomplex, photosystem II. – Biochim. biophys. Acta **1608**: 75-96, 2004.

Summer, E.J., Schmid, V.H.R., Bruns, B.U., Schmidt, G.W.: Requirement for the H phosphoprotein in photosystem II of *Chlamydomonas reinhardtii*. – Plant Physiol. **113**: 1359-1368, 1997.

Vener, A.V., Harms, A., Sussman, M.R., Viersta, R.D.: Mass spectrometric resolution of reversible protein phosphorylation in photosynthetic membranes of *Arabidopsis thaliana*. – J. biol. Chem. **276**: 6959-66, 2001.

Zouni, A., Witt, H.T., Kern, J., Fromme, P., Krauss, N., Saenger, W., Orth, P.: Crystal structure of photosystem II from *Synechococcus elongatus* at 3.8 angstrom resolution. – Nature **409**: 739-743, 2001.

Molecular basis of a lipid-PsbH protein interaction: a structural and computational study.

Dalibor Stys*,[#], Žofie Sovová*, Zbyněk Halbhuber*, Michal Green**, Wolfgang Schoefberger*,[+], Josef Komenda [#,++], Jaroslava Ristvejova*, Norbert Müller[+] and Rüdiger Ettrich*,[$]

**Laboratories of High Performance Computing and Biomembranes, Institute of Physical Biology of the University of South Bohemia, and Institute of Systems Biology and Ecology, Academy of Sciences of the Czech Republic, Zámek 136, 373 33 Nové Hrady, Czech Republic*

[#]*Department of Autotrophic Microorganisms, Institute of Microbiology CAS, 37901 Trebon - Opatovicky mlyn, Czech Republic*

***The College of New Jersey, Ewing NJ, United States of America*

[+]*Johannes Kepler Universität, Altenbergerstrasse 69, Linz, Austria*

[++]*Department of ecophysiology of autotrophic microorganisms, , Institute of Physical Biology of the University of South Bohemia, Zámek 136, 373 33 Nové Hrady, Czech Republic*

[$]corresponding author

Abstract

Interaction of the PsbH protein of photosystem II was analysed by combination of CD and NMR spectroscopy and computer modeling. CD and NMR spectroscopy indicated that interactions to of PsbH to all bilayer-forming lipids, including those extracted directly from cyanobacterial thylakoid membranes, interact with PsbH non-specifically. The molecular dynamic calculation of PsbH-bilayer forming lipid interactions indicates that both salt-bridge formation and hydrogen bond formation in the lipid-water interface are feasible and stabilize fraction of at least 10 lipid molecules in the neighbourhood of the protein. This may lead to formation of lipid domains which were hypothesized to be involved in assembly of membrane protein complexes.

Seznam zkratek

Introduction

The fact that interactions between certain proteins and lipids in thylakoid membranes is accompanied by formation of large-scale chiral domains detectable in the chlorophyll region of the spectrum has been reported long time ago (for a review see Páli et al., 2003). Recently we have reported that this function may be localised to the N-terminal domain of the protein LHCII of plants (Veverka et al. 2000). Alongside with LHCII, the PsbH protein is the second protein the function of which is regulated by phosphorylation in higher plants (Allen 1992). It has also been reported that the course of regulation of the PsbH protein and the LHCII by phosphorylation are different thus probably having different functions (Stys et al., 1995, Rintamakki et. al. 1997).

The molecular biology, biochemical and low-resolution structural analyses exemplified that the PsbH protein seems have specific and key role in function of thylakoid membranes of all organisms of green photosynthesis (Komenda et al., 2003). It is an integral, well localized, part of the Photosystem II core complex (Bumba et al. 2005) and it seems to have key role in the Photosystem II complex assembly and in other processes associated with in the maintenance of the thylakoid membrane functionality (Komenda et al., 2005). It is also quite obvious that the PsbH protein in the thylakoid membrane does not occur only in the Photosystem II complex but that it exists either in the free form or in complexes with other proteins (Komenda et al. 2005).

In attempts to understand the function of the thylakoid membrane, the understanding of the function of the PsbH protein has prominent position. The fact that it is a 7 kDa protein with a single transmembrane helix does not give much hope for obtaining high-resolution structures of free form of the protein at atomic resolution by any method. The protein as such is necessarily highly affected by the lipid environment and any structure information without consideration of lipids has little relevance. The existence of singular protein in detergent micelles using NMR spectroscopy was reported (Stys et al., 2005), however, the data which

we could obtain in this system did not bring any information specific to structure of the protein. The attempts to examine the protein-lipid complex unambiguously led to formation of aggregates nonobservable by NMR spectroscopy.

The structure of bound from of the PsbH protein was reported in the structure of photosystem II core described by Loll et al. (2005). In this structure model, psbH is tightly bound to the CP47 antenna and serves merely as a subunit of this complex. This is reflected also in the structure of the psbH N-terminal domain which forms a helix pointing inside the complex.

This article reports the observation of formation large scale chiral structures in the PsbH-bilayer forming lipid system which are observable by circular dichroism and analogous to those which were observed in presence of LHCII N-terminal domain. In the absence of the exchange between the bound form and the free form of the protein, which allowed assignment of interacting residues, the only way how to obtain any information on the molecular basis of the interaction was ab-initio modeling which is being reported in this article. The pattern of lipid-protein interactions as well as the structure of the protein in presence of lipids is building up very quickly, is stable and unambiguous.

Materials and methods

The PsbH protein of cyanobacterium *Synechocystis* sp. PCC 6803 *psbH* gene (locuss12598) was over-expressed as a fusion protein with a glutathione-S transferase (GST) in *E. coli* and the PsbH-GST fusion protein was enzymatically cleaved and purified according to the procedure given by Halbhuber et al. (2003).

We isolated non-labelled PsbH protein for circular dichroism (CD) spectrometry. CD spectra of the sample were recorded on a *Jasco*-J715 spectropolarimeter, controlled by PC-based *ISA OMA* software at 20 °C in 1-mm quartz cuvettes, after 15 min of temperature equilibration. Five scans were accumulated for each spectrum with a response time of 2 s, a bandwidth of 2 nm, and a scan speed of 10 nm min^{-1} from 190 to 250 nm. Background spectra

without protein were subtracted. The protein was diluted to final concentration of 20 μM using a phosphate buffer (K_2HPO_4 20mM, KCl 100mM, pH 6.8) with presence of a non-ionic detergent β-D-octylglucopyranoside (OG) (2%v/w). The cuvette position was next to the photomultiplier to decline light scattering.

To study the structure of the PsbH protein we performed uniform isotope labelling of the PsbH protein according the procedures using minimal media (M9) (Halbhuber et al. 2003, Rhee et al. 1997). We isolated and purified the ^{15}N labelled protein to a concentration of 1.1 kg m^{-3} in phosphate buffer (K_2HPO_4 20mM, KCl 100mM, pH 6.8) with presence of OG. ^{1}H-^{15}N HSQC spectra were recorded on a *Bruker DRX* 500 MHz NMR spectrometer equipped with a 5 mm *TXI* cryoprobe to enhance sensitivity and resolution. The protein sample was mixed with D_2O (H_2O/D_2O 1 : 20) to perform the NMR experiments. We recorded spectra of the PsbH protein in OG and then divided sample into four parts and added the liposomes of different lipid classes (sulphoquinovosysldiacylglycerol – SQDG, monogalactosyldiacyl glycerol – MGDG, digalactosysldiacylglycerol – DGDG, phosphatidylglycerol – PG and extract from the thylakoid membrane) to achieve lipid concentration 1% w/w. The standard *Bruker* pulse sequence for these experiments was the *hsqc-etf3-gpsi2* pulse program.

For titration experiments we used liposomes prepared by reversed phase evaporation method according to Rigaud et al. (1983). We used isolated lipids donated by Lipid Products (Nutfield, UK) and also the hexan-isopropanol extracts of the thylakoid membrane prepared according to Hara and Radin (1978).

A model of the the PsbH protein of cyanobacterium *Synechocystis* sp. PCC 6803 was generated by analogy to the crystal structure at 0.35 nm resolution of the Photosystem II complex of cyanobacterium *Thermosynechococcus elongatus* (Ferreira et al. 2004) (PDB code 1S5L). Bumba et al. (2005) recently showed the position of the PsbH protein in this structure to be correct, however, 22 amino acids at the N-terminal end of the protein are missing in most of the crystal structure except that of Loll et al (2005). The later model, howevere,

indicates strong dependency of the structure of the N-terminus on the protein-protein interactions which is not be expected upon insertion of the protein into the bilayer. Therefore the suggested structure for these amino acids is not based on homology with the crystal but generated from a loop database. The three-dimensional model constituted by all non-hydrogen atoms was built and examined by the *MODELLER7* package (Sali and Blundell 1993). As the crystal structure has a very low resolution and large parts of the protein were not resolved, we decided to refine the homology model by running a 1.2 ns molecular dynamics simulation in aqueous solution using the *YAMBER2* force field (Krieger et al. 2004) to induce better folding of the protein. The protein structure was placed into a box of 7.3×8.2×9.6 nm size, which was 1 nm larger than the protein along all three axes. The box was filled with TIP3P water, sodium ions were iteratively placed at the coordinates with the lowest electrostatic potential until the cell was neutral. Molecular dynamics simulations were run with *YASARA* (www.yasara.org), using a multiple time step of 1 fs for intra-molecular and 2 fs for intermolecular forces. A 1.2 nm cut-off was taken for Lennard Jones forces and the direct space portion of the electrostatic forces, which were calculated using the Particle Mesh Ewald method (Essman et al. 1995) with a grid spacing 0.1 nm, 4^{th} order B-splines, and a tolerance of 10^{-4} for the direct space sum. The simulation of the homology model was then run at 298 K and constant pressure (NPT ensemble) to account for volume changes due to fluctuations of homology models in solution. The resulting structure was minimized to convergence of the energy gradient to less than 0.05 kcal·mol^{-1}·Ĺ$^{-1}$ using the *TRIPOS* force field included in the *MAXIMIN2* module of *SYBYL* (*TRIPOS Associates Inc.*). The minimization included electrostatic interactions based on Gasteiger Hückel partial charge distributions using a dielectric constant with a distance-dependent function $\varepsilon = 4\,r$ and a non-bonded interaction cut-off of 1.2 nm.

A preequilibrated POPC bilayer of 128 lipids (kindly provided by Peter Tieleman (Tieleman et al., 1999)) was used as a model of the biological membrane. Lipids were removed to

generate a hole in the center of the bilayer. In a short simulation using the procedure of Faraldo-Gomez et al. (2002), remaining lipids were removed from the hole to generate a cylindrical-shaped cavity. The protein was inserted into the cavity. The entire system was then resolvated. The system was equilibrated for 250 ps with positional restraints applied on the protein atoms to allow the solvent to relax. The production runs, without any restraints, were 20 ns long. The simulation was run with GROMACS (Berendsen et al. 1995, Lindahl et al. 2001) using the ffG43a2 forcefield with a 2-fs time step. SETTLE (for water) and LINCS (Hess et al. 1997, Miyamoto and Kollman 1992) were used to constrain covalent bond lengths. Long range electrostatic interactions were computed with the Particle-Mesh Ewald method (Darden et al. 1993). The temperature was kept at 300 K by separately coupling the protein, lipids, and solvent to an external temperature bath (τ=0.1 ps) (Berendsen et al. 1984). The pressure was kept constant at 1 bar by weak coupling (τ =1.0 ps) to a pressure bath (Berendsen et al. 1984) in the z-dimension with constant area. The protein proved to be stable during both simulations. Molecular graphics were made using VMD (Humphrey et al. 1996).

Results

Structural measurements:

Circular dichroism spectroscopy was performed by titration of the PsbH protein in OG micelles by specific lipids of the thylakoid membrane. In the presence of non-bilayer forming lipid MGDG the structure remained in the same conformation as free in the detergent. All the three bilayer forming lipids, PG, DGDG as well as SQDG unanimously induced formation of long-wavelength component with apparent maximum at 235 nm (figure 1). Similarly, also the reconstitution with the original lipid-phase extract led to formation of the long-wavelength domain (figure 2). The lipid mixture itself has tendency to formation of separate phases which was exemplified by induction of CD bands in the chlorophyll part of the spectrum upon extraction of lipids by detergent. This signal was not observed in presence of the PsbH protein

(data not. shown). No indications of formation of specific pigment – PsbH protein interactions were observed.

In our previous paper we have demonstrated that the peptide with specific lipid binding site exhibits spectrum with strong component at 235 nm (Veverka et al., 2000). In the case of 30 amino acids of LHCII (Veverka et al., 2000), the anomalous signal was observed already in the free peptide, during the interactions with lipids it initially disappeared and built up again when peptide became in excess. Contribution of the PsbH protein in octylglucoside solution, although it was not so prominent due to contribution of secondary structures from other parts of the molecule. In excess of any bilayers-forming lipid, the long-wavelength signal became prominent in the PsbH protein spectrum.

The major difference between the LHCII and the PsbH experiments was thus the specificity of interaction – in LHCII N-terminal domain interacts specifically with PG- which was exemplified also in other studies (i.e. Nussberger et al. 1993) which showed that PG and DGDG interactions are specific and localized to different parts of the molecule. The result on the PsbH protein thus shows that interaction of the protein to lipid has strong non-specific component dependent only on the tendency of lipids towards formation of the bilayer.

NMR measurements:

The attempts to achieve more detailed information on involvement of individual groups in PG, DGDG and SQDG - protein binding resulted in depletion of the PsbH protein signal upon titration by lipids. Our results (figure 3) indicate disappearance of the protein signal upon addition of lipids when the decrease of the protein signal was depleted which indicates formation of large ensembles relaxing too quickly for the signal to be observed, and, apparently, a fraction of protein molecules remained in the solution unaffected by the presence of lipids. This is again in contrast to behaviour observed in LHCII N-terminal fragment where specific chemical shifts changes were observed upon specific binding to PG.

We believe that the correct interpretation of this observation is that there is a fraction of large liposomes to which is bound fraction of the PsbH protein and fraction of the free, lipid unbound, PsbH protein which remains in detergent micelles. This again supports the hypothesis that the interaction between the PsbH protein and lipids is a non-specific one and occurs only if there is a some bilayer formed.

Molecular modeling of the PsbH protein in the lipid bilayer

In case that the interaction is unspecific, the only method which enables any details of the nature of interactions at high resolution level is the molecular dynamics calculation. This method became recently available for membrane-protein systems thanks to development of computer technology. There have been developed three major types of membranes which correspond to the major lipid classes of animal membranes. Most of the calculations of lipid-protein interactions is now performed using these model membranes. The only alternative reported so far was the paper by Venturoli et al. (2005) who utilized unified atom approach. This approach does not treat each atom explicitly and would not bring the type of information which is necessary to interpret our experimental findings.

The molecular modeling has to be divided into several steps. The first step is the search for non-specific interactions. This may be done, similarly as in the case of experiment by examining of the interaction with lipid which does not occur in the protein natural environment. This was also the easiest first step since such lipid bilayers are already available for introduction of protein molecules. This first step is matter of this report. In further, future steps, we shall model first the bilayers containing both other headgroups (PG, DGDG, SQDG) as well as different fatty acid chains.

The final model (Fig. 1) had 98.3 % of residues in the two most favoured regions of the Ramachandran plot and an acceptable overall geometry, both determined with the *ProCheck*

program (Laskowski et al. 1993). No residues were found in disallowed regions. The overall *g*-factor of the structure obtained showed a value of –0.16. The *g*-factor should be above –0.5 and values below –1.0 may need investigation. Amino acids from Thr36-Ser60 adopted an α-helical fold, which corresponds to 34.2 % of the total secondary structure, and 12.3 % of the amino acids were found in a β-turn conformation. One stable β-sheet structure was found in the model. This has been confronted with the estimation of secondary structure from the experimental far-UV CD by deconvolution using the method of *VARSELEC* (variable selection method) included in the *Dicroprot V2.5* program (Deléage and Geourjon 1993) with 33 reference spectra. The calculation yielded a 38 % helical structure, 15–19 % sheet and 19 % β-turn. In our opinion, the deconvolution is reliable mostly for α-helix and to a lower extent for β-sheet and other structures. The distinction between anti-parallel and parallel β-sheet looks very difficult and are not very reliable, so that we summarized the overall β-sheet content.

Upon the 20 ns molecular dynamics run there were observed two main movements of the protein: the extra membrane domains sunk into the lipid-protein interface in two steps and the transmembrane helix tilted. During this folding process the forming of a beta bridge between in the N-terminal domain seems to be a key event, speeding up the formation of additional beta bridges with the phosholipid headgroups. First question which we asked was whether there is a detectable change in the conformation of proline residues that would build a basis of an anomalous CD signal. No such structure was found, throughout the molecular dynamic run the ratio of *cis:trans* conformation of the proline residue remained in the range found in any protein structure.

Second question was the nature of interactions in the lipid-water interface as well as in hydrophobic regions. The intention to examine the non-specific interactions brings about the necessity to distinguish between interactions accessible in all bilayer-forming lipid classes and

those which should be considered specific to the lipid used for calculation, the Phosphatidylcholin (POPC). The later interactions should be abandoned. We found that there are two specific salt bridges and 24 hydrogen bonds representing interactions to eight lipid molecules at the N-terminal end of the protein – stromal side of the membrane and three lipid molecules at the C-terminal end - lumenal side residing in the neighbourhood of a protein for the last 10 ns of simulation (tab. 1). The salt bridges were, naturally, observed between the lipid phosphate group and the sidechain of asparagine and arginine residues in the protein N-terminus. Alongside with these salt bridges, hydrogen bonds were created by R12 and K20 (tab. 2) indicating that these interactions are difficult to distinguish from each other. Furthermore hydrogen bonds to phosphate groups are formed by sidechains of Q3, S16 and S59 and by mainchain NH of L14. Majority of the hydrogen bonds is formed between sidechain (Y18, W27, W28, Q56) and mainchain (G24, W28, S68) atoms of aminoacid residues is and the glycerol or palmitic acid oxygen atoms. I this way, small domain of twelve lipid residues is maintained close to the protein. All these interactions were observed to the same lipid molecule throughout the calculation.

Conclusions:

Our results represent attempt towards understanding of molecular details of the role of the protein PsbH in the formation of lipid domains in the thylakoid membranes. The only experimental data available to us were that of CD and NMR spectroscopy, neither of them, however, giving specific answer. On top of that, all the experiments indicated that the interaction of the PsbH protein with the lipid bilayer is only partly specific. It was thus necessary to approach the computational method of molecular dynamics to examine the question whether (a) the structure of the PsbH protein is stable in the lipid bilayer in absence of other proteins of the Photosystem II complex and (b) whether there are lipid molecules which are forming interactions with the PsbH protein which seem to be persistent on a long

time scale, in another words whether there is a population of lipids which, when bound to the protein, keeps this binding at least on a timescale of the computer experiment. The answer was positive in both cases. We thus may conclude that there is a fair basis for the hypothesis that the PsbH protein organizes a lipid domain in the thylakoid membrane which may be one of the bases for specific incorporation of other proteins in the particular position in the complex.

In the course of this study, the structural model of psbH bound to CP47 antenna complex was published. The comparison of the two structures, free and bound, indicates the potential of psbH N-terminus structural switch in formation of Photosystem II structure and its regulation. It is not only the energetics of protein-protein binding but also the entropy change in the lipid bilayer that accompanies the change which should be considered in this process. Assessment of extent to which individual factors contribute to this process, however, is based on new metodological developments which are in progress in our laboratory.

Acknowledgement:

This research was supported by AKTION Austria-Czech Republic (No. 40p2), by the Ministry of Education, Youth and Sports of the Czech Republic (MSM6007665808, MSM0021620835, LC06010), by the Academy of Sciences of the Czech Republic (Institutional research concept AVOZ60870520) and the Grant Agency of the Czech Republic (grant No. 206/03/D082)

References:

Allen, J.F.: Protein-phosphorylation in regulation of photosynthesis - Biochimica et Biophysica Acta **1098**: 275-335, 1992.

Andrade, M.A., Chacón, P., Merelo, J.J., Morán, F.: Evaluation of secondary structure of proteins from UV circular dichroism using an unsupervised learning neural network. – Prot. Eng. **6**: 383-390, 1993.

Bennett, J.: Phosphorylation of chloroplast membrane polypeptides. – Nature **269**: 344-346, 1977.

Berendsen, H. J. C., Postma, J. P. M., van Gunsteren, W. F., DiNola, A., Haak, J. R.: Molecular-dynamics with coupling to an external bath. - J. Chem. Phys. **81:** 3684–3690, 1984.

Berendsen, H. J. C., van der Spoel, D., van Drunen, R.: GROMACS - a message-passing parallel molecular-dynamics implementation. - Comput. Phys. Commun. **91:** 43–56, 1995.

Bumba, L., Tichy, M., Dobakova, M., Komenda, J., Vacha, F.: Localization of the PsbH subunit in photosystem II from the Synechocystis 6803 using the His-tagged Ni-NTA Nanogold labeling - Journal of Structural Biology **152**: 28-35, 2005.

Bumba, L., Vácha, F.: Electron microscopy in structural studies of Photosystem II. – Photosynth. Res. **77**: 1-19, 2003.

Darden, T., York, D., Pedersen, L.: Particle-Mesh Ewald - an n.log(n) method for ewald sums in large systems. - J. Chem. Phys. **98,** 10089–10092, 1993.

Deléage, G., Geourjon, C.: An interactive graphic program for calculating the secondary structure content of proteins from circular-dichroism spectrum. – Comp. appl. Biosci. **9**: 197-199, 1993.

Essman, U., Perera, L., Berkowitz, M.L., Darden, T., Lee, H.., Pedersen, L.G.: A smooth particle mesh Ewald method. – J. chem. Phys. **103**: 8577-8593, 1995.

Faraldo-Gomez, J. D., Smith, G. R., Sansom, M. S. P.: Setting up and optimization of membrane protein simulations. - Eur. Biophys.J. **31:** 217–227, 2002.

Ferreira, K.N., Iverson, T.M., Maghlaoui, K., Barber, J., Iwata, S.: Architecture of the photosynthetic oxygen-evolving center. – Science, **303**: 1831-1838, 2004.

Halbhuber, Z., Petrmichlova, Z., Alexciev, K., Thulin, E., Stys, D.: Overexpression and purification of recombinant membrane PsbH protein in Escherichia coli. - Protein Expression and Purification **32**: 18-27, 2003.

Hara, A., Radin, N.S.: Lipid extraction of tissues with a low toxicity solvent. Analyt. Biochem. **90**: 420-426, 1978.

Hess, B., Bekker, H., Berendsen, H. J. C., Fraaije, J.: LINCS: A linear constraint solver for molecular simulations. - J. Comput.Chem. **18:** 1463–1472, 1997.

Humphrey, W., Dalke, A., Schulten, K.: VMD: Visual molecular dynamics.- J. Mol. Graphics **14:** 33–38, 1996.

Kamiya, N., Shen, J.R.: Crystal structure of oxygen-evolving Photosystem II from Thermosynechococcus vulcanus at 3.7 Angstrom resolution. – Proc. nat. Acad. Sci. USA **100**: 98-103, 2003.

Koike, H., Mamada, K., Ikeuchi, M., Inoue, Y.: Low-molecular-mass proteins in cyanobacterial photosystem II: identification of *psb*H and *psb*K gene products by N-terminal sequencing. – FEBS Lett. **244**: 391-396, 1989.

Komenda, J., Barber, J.: Comparison of psbO and psbH deletion mutants of Synechocystis PCC 6803 indicates that degradation of D1 protein is regulated by the QB site and dependent on protein synthesis. – Biochemistry **29**: 9625-9631, 1995.

Komenda, J., Lupínková, L., Kopecký, J.: Absence of the *psb*H gene product destabilizes photosystem II complex and bicarbonate binding on its acceptor side in *Synechocystis* PCC 6803. – Eur. J. Biochem. **269**: 610-619, 2002.

Komenda, J., Stys, D., Lupinkova, L.: The PsbH protein of photosystem 2 - Photosynthetica **41**: 1-7, 2003.

Komenda, J., Tichy, M., Eichacker, L.A.: The PsbH protein is associated with the inner antenna CP47 and facilitates D1 processing and incorporation into PSII in the cyanobacterium Synechocystis PCC 6803. - Plant and Cell Physiology **46**: 1477-1483, 2005.

Komenda, J.: Autotrophic cells of the *Synechocystis* psbH deletion mutant are deficient in synthesis of CP47 and accumulate inactive PSII core complexes. – Photosynth. Res. **85**: 161-167 , 2005.

Krieger, E., Darden, T., Nabuurs, S., Finkelstein, B, A., Vriend, G.: Making optimal use of empirical energy functions: force-field parameterization in crystal space. – Proteins: Struct. Funct. Bioinform. **57**: 678-683, 2004.

Laskowski, R.A., MacArthur, M.W., Moss, D.S., Thornton, J.M.: Procheck – a program to check the stereochemical quality of protein structures. – J. appl. Cryst. **26**: 283-291, 1993.

Lindahl, E., Hess, B., van der Spoel, D.: GROMACS 3.0: a package for molecular simulation and trajectory analysis. - J. Mol. Model. **7:** 306–317, 2001.

Loll, B., Kern, J., Saenger, W., Zouni, A., Biesiadka, J.: Towards complete cofactor arrangement in the 3.0 angstrom resolution structure of photosystem II. - Nature **438**: 1040-1044, 2005.

Mayes, S.R., Dubbs, J.M., Vass, I., Hideg, É., Nagy, L., Barber, J.: Further characterization of the *psb*H locus of *Synechocystis* sp. PCC 6803 inactivation of *psb*H impairs Q_A to Q_B electron-transport in photosystem 2. – Biochemistry **32**: 1454-1465, 1993.

Michel, H.P., Bennett, J.: Identification of the phosphorylation site of an 8.3 kDa protein from photosystem II of spinach. – FEBS Lett. **212**: 103-108, 1987.

Miyamoto, S., Kollman, P. A.: SETTLE - an analytical version of the shake and rattle algorithm for rigid water models. - J. Comput. Chem. **13:** 952–962, 1992.

Nussberger, S., Dorr, K., Wang, D.N., Kuhlbrandt, W.: Lipid-protein interactions in crystals of plant light-harvesting complex. - Journal of Molecular Biology **234**: 347-356, 1993.

Pali, T., Garab, G., Horvath, L.I., Kota, Z.: Functional significance of the lipid-protein interface in photosynthetic membranes. Cellular and Molecular Life Sciences **60**: 1591-1606, 2003.

Rhee, J.I., Bode, J., Diaz-Ricci, J.C., Poock, D., Weigel, B., Kretzmer, G., Schügerl, K.: Influence of the medium composition and plasmid combination on the growth of recombinant Escherichia coli JM109 and on the production of the fusion protein EcoRI::SPA. – J. Biotechnol. **55**: 69-83, 1997.

Rigaud, J.L., Bluzat, A., Buschen, S.: Incorporation of bacteriorhodopsin into large unilamellar liposomes by reverse phase. - Biophys. Biochem. Res. Commun. **111**: 373-382, 1983.

Rintamaki, E., Salonen, M., Suoranta, U.M., Carlberg, I., Andersson, B., Aro, E.M.: Phosphorylation of light-harvesting complex II and photosystem II core proteins shows different irradiance-dependent regulation in vivo - Application of phosphothreonine antibodies to analysis of thylakoid phosphoproteins. - Journal of Biological Chemistry **272**: 30476-30482, 1997.

Sali, A., Blundell, T.L.: Comparative modelling by satisfaction of spatial restraints. – J. mol. Biol. **234**: 779 -815, 1993.

Shi, L.X., Schröder, W.P.: The low molecular mass subunits of the photosynthetic supracomplex, photosystem II. – Biochim. biophys. Acta **1608**: 75-96, 2004.

Stys, D., Schoefberger, W., Halbhuber, Z., Ristvejova, J., Muller, N., Ettrich, R.: Secondary structure estimation of recombinant psbH, encoding a photosynthetic membrane protein of cyanobacterium Synechocystis sp PCC 6803. - Photosynthetica **43**: 421-424, 2005.

Stys, D., Stancek, M., Cheng, L.L., Allen, J.F.:. Complex-formation in plant thylakoid membranes - competition studies on membrane-protein interactions using synthetic peptide-fragments. - Photosynthesis Research **44**: 277-285, 1995.

Summer, E.J., Schmid, V.H.R., Bruns, B.U., Schmidt, G.W.: Requirement for the H phosphoprotein in photosystem II of *Chlamydomonas reinhardtii*. – Plant Physiol. **113**: 1359-1368, 1997.

Tieleman, D. P., Berendsen, H. J. C., Sansom, M. S. P.: Surface binding of alamethicin stabilizes its helical structure: molecular dynamics simulations. Biophys. J. **76**: 3186–3191, 1999.

Vener, A.V., Harms, A., Sussman, M. R., Viersta, R.D.: Mass spectrometric resolution of reversible protein phosphorylation in photosynthetic membranes of *Arabidopsis thaliana*. – J. biol. Chem. **276**: 6959-66, 2001.

Venturoli, M., Smit, B., Sperotto, M. M.: Simulation studies of protein-induced bilayer deformations, and lipid-induced protein tilting, on a mesoscopic model for lipid bilayers with embedded proteins. - Biophysical Journal **88**: 1778-1798, 2005.

Veverka, V., Hrabal, R., Durchan, M., Stys, D.: Studies of phospholipid binding to N-terminal domain of membrane protein light-harvesting complex II. - Journal of Molecular Structure **523**: 281-287, 2000.

Zouni, A., Witt, H. T., Kern, J., Fromme, P., Krauss, N., Saenger, W., Orth, P.: Crystal structure of photosystem II from *Synechococcus elongatus* at 3.8 angstrom resolution. – Nature **409**: 739-743, 2001.

Figure legends:

Figure 1.

Formation of long-wavelength component with apparent maximum at 235 nm upon titration of the PsbH protein by thylakoid membrane lipids. All the three bilayer forming lipids, PG, DGDG as well as SQDG unanimously induced formation of long-wavelength component with apparent maximum at 235 nm which indicates that all bilayer-forming lipids are involved in similar, most probably non-specific, interaction with lipid molecules.

Figure 2.

Reconstitution of the PsbH protein with complete thylakoid membrane extract. The formation of long-wavelength signal in CD spectrum was observed as in the case of all individual lipid classes.

Figure 3

^{1}H-^{15}N HSQC spectra of the uniformly labeled PsbH protein. (a) Spectrum of the protein in presence of detergent micelles and (b) spectrum after addition of lipids in the molecular ratio protein to lipids 1:15. Even after careful analysis of the spectrum there were not found indices of specific protein-lipid interactions such as specific changes in chemical shifts. The only observation was decrease in intensity of all signals. We conclude that the most probable explanation is that the PsbH protein exists in the experiment (b) in two forms – bound to the liposome and free in detergent micelles while the former is not observable by NMR.

Figure 4.

Structure of the PsbH protein in the lipid bilayer at the beginning of the simulation (a) and at its end (b). Both N- and C- termini submerge in the interface region and the helix is tilted in order to match the hydrophobic regions. The course of the simulation illustrates the fact that

the simulation environment is capable to incorporate the membrane protein in conformity with accepted hypotheses on protein-lipid interactions. Details on individual interacting atoms and types of interactions are summarized in part in tables 1 and 2.

Figure 5. Calculation of RMSD (a) and of the number of hydrogen bonds formed between protein and lipid (b) in the course of simulation of the structure of PsbH submerged in the lipid bilayer. Significant increase in the number of hydrogen bonds was observed between 17 and 20ns of the simulation which indicates that stability of the lipid-protein interaction increases steadily. Since these hydrogen bonds were observed to the same lipid molecule throughout the calculation, the hypothesis that PsbH may constrain the mobility of certain lipid molecules appears feasible.

Figure 6.

Molecule of the lipid POPC illustrating the notation of atoms used throughout the discussion in the article.

Tab. 1 List of short-distance salt bridges formed between the PsbH protein and lipid molecules.

residue	lipid	average distance (last 10 ns)(nm)	final distance (nm)
ARG6	POPC169	0,157467658	0,16435
ASP9	POPC90	0,173498542	0,180036

Tab. 2 List of stable hydrogen bonds formed between the PsbH protein and the lipid molecules within 15 and 20 ns of the simulation.

Hydrogen Bond Analysis

Residue GLN 3 : Atom NE2 GLN 3 donates a bond to O7 POP 118 , H -O distance is 1.57 A. 1 bonds, 0 accepted, 1 donated.
Residue ARG 6 : Atom NE ARG 6 donates a bond to O7 POP 81 , H -O distance is 1.49 A. Atom NH1 ARG 6 donates a bond to O11 POP 169 , H -O distance is 1.45 A. Atom NH2 ARG 6 donates a bond to O11 POP 81 , H -O distance is 1.73 A. Atom NH2 ARG 6 donates a bond to O16 POP 144 , H -O distance is 1.94 A. 4 bonds, 0 accepted, 4 donated.
Residue ASP 9 : Atom N ASP 9 donates a bond to O10 POP 81 , H -O distance is 2.05 A. Atom O ASP 9 accepts a bond from N4 POP 118 , O -H distance is 2.42 A. 2 bonds, 1 accepted, 1 donated.
Residue TYR 18 : Atom OH TYR 18 donates a bond to O16 POP 90 , H -O distance is 1.81 A. 1 bonds, 0 accepted, 1 donated.

Residue LYS 20 : Atom NZ LYS 20 donates a bond to O14 POP 90 , H -O distance is 1.61 A. Atom NZ LYS 20 donates a bond to O14 POP 118 , H -O distance is 2.29 A. 2 bonds, 0 accepted, 2 donated.
Residue GLY 24 : Atom N GLY 24 donates a bond to O7 POP 111 , H -O distance is 2.13 A. 1 bonds, 0 accepted, 1 donated.
Residue TRP 25 : Atom N TRP 25 donates a bond to O35 POP 110 , H -O distance is 1.84 A. Atom NE1 TRP 25 donates a bond to O35 POP 111 , H -O distance is 2.21 A. 2 bonds, 0 accepted, 2 donated.
Residue GLY 26 : Atom N GLY 26 donates a bond to O35 POP 110 , H -O distance is 1.97 A. 1 bonds, 0 accepted, 1 donated.
Residue THR 27 : Atom OG1 THR 27 accepts a bond from O16 POP 114 , O -H distance is 2.20 A. Atom OG1 THR 27 donates a bond to O16 POP 114 , H -O distance is 1.61 A. 2 bonds, 1 accepted, 1 donated.

Residue THR 28 :

Atom OG1 THR 28 accepts a bond from O33 POP 114 , O -H distance is 2.23 A.

Atom OG1 THR 28 donates a bond to O33 POP 114 , H -O distance is 2.18 A.

2 bonds, 1 accepted, 1 donated.

Residue TYR 49 :

Atom OH TYR 49 donates a bond to O35 POP 70 , H -O distance is 1.68 A.

1 bonds, 0 accepted, 1 donated.

Residue ASN 50 :

Atom ND2 ASN 50 donates a bond to O14 POP 71 , H -O distance is 1.99 A.

Atom ND2 ASN 50 donates a bond to O33 POP 71 , H -O distance is 2.37 A.

2 bonds, 0 accepted, 2 donated.

Residue SER 51 :

Atom OG SER 51 accepts a bond from O7 POP 72 , O -H distance is 1.79 A.

Atom OG SER 51 donates a bond to O7 POP 72 , H -O distance is 1.62 A.

2 bonds, 1 accepted, 1 donated.

Residue GLU 56 :

Atom N GLU 56 donates a bond to O33 POP 168 , H -O distance is 1.80 A.

Atom O GLU 56 accepts a bond from O35 POP 124 , O -H distance is 1.96 A.

2 bonds, 1 accepted, 1 donated.

Residue SER 59 : Atom OG SER 59 donates a bond to O7 POP 76 , H -O distance is 1.47 A. 1 bonds, 0 accepted, 1 donated.
Residue ALA 63 : Atom N ALA 63 donates a bond to O11 POP 74 , H -O distance is 1.71 A. 1 bonds, 0 accepted, 1 donated.

Figure 1.

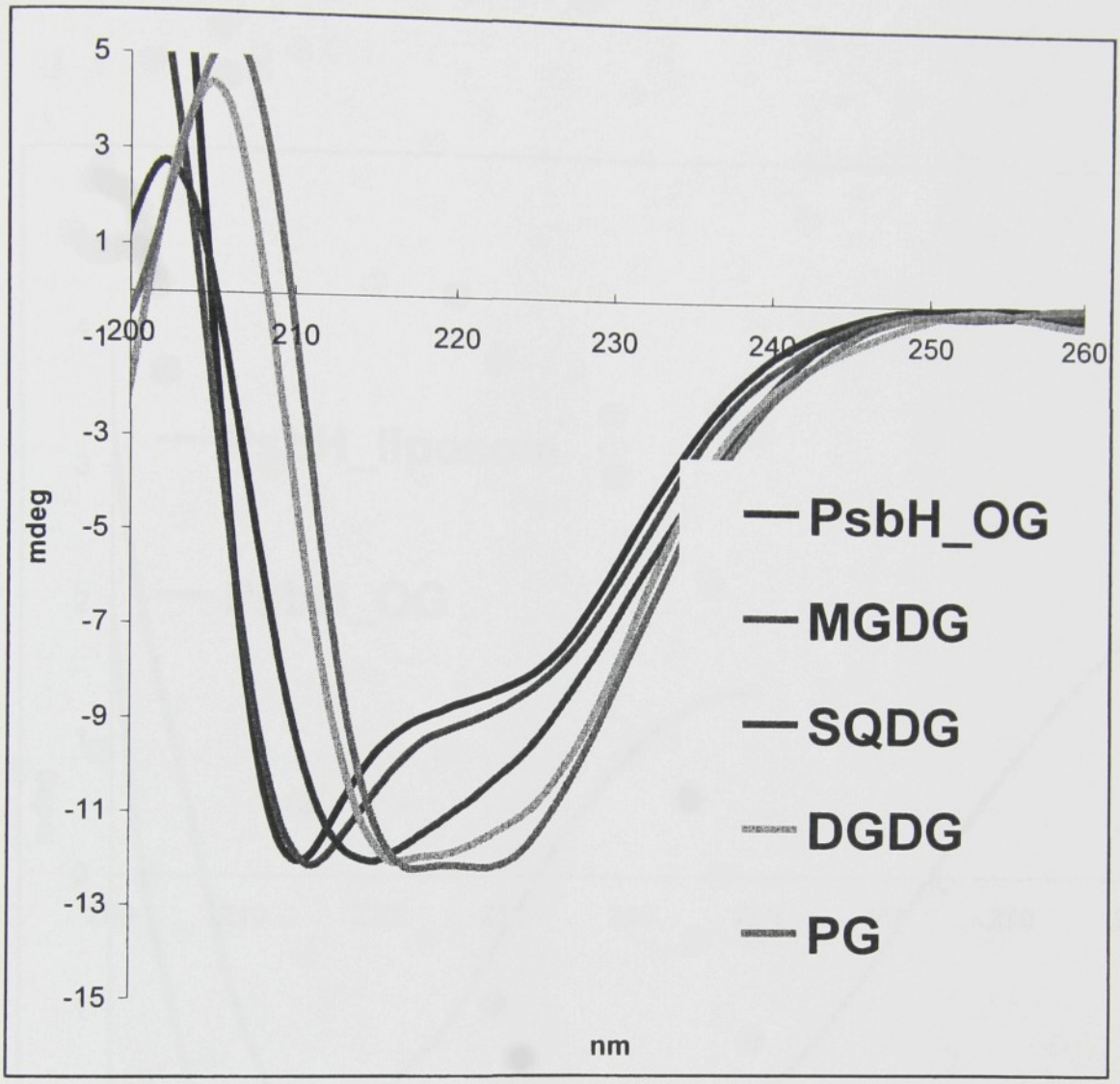
5
3
1
-1
-3
-5
-7
-9
-11
-13
-15
200
210
220
230
240
250
260
mdeg
nm
PsbH_OG
MGDG
SQDG
DGDG
PG

Figure 2

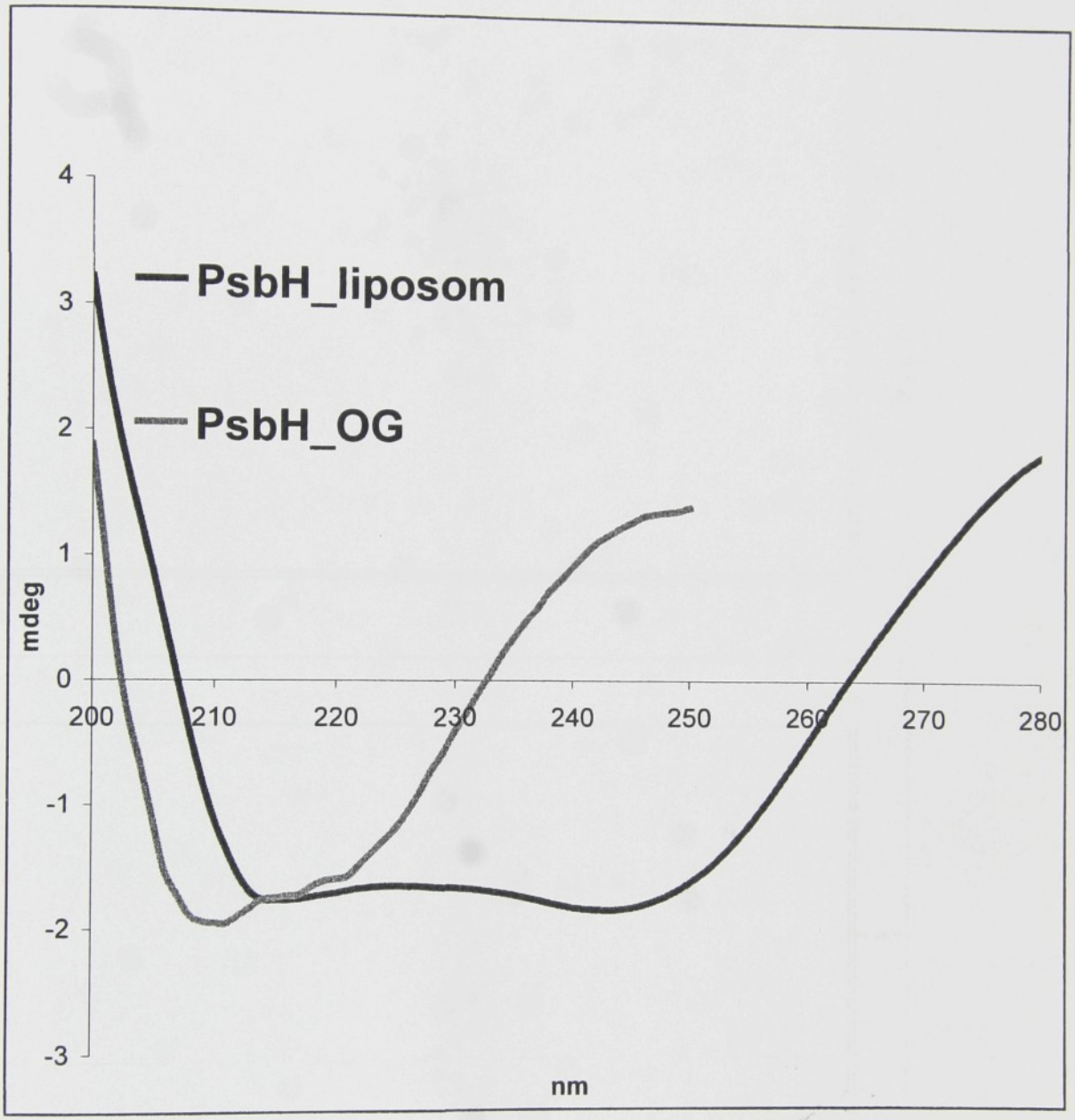
PsbH_liposom
PsbH_OG
mdeg
nm
4
3
2
1
0
-1
-2
-3
200
210
220
230
240
250
260
270
280

Figure 3

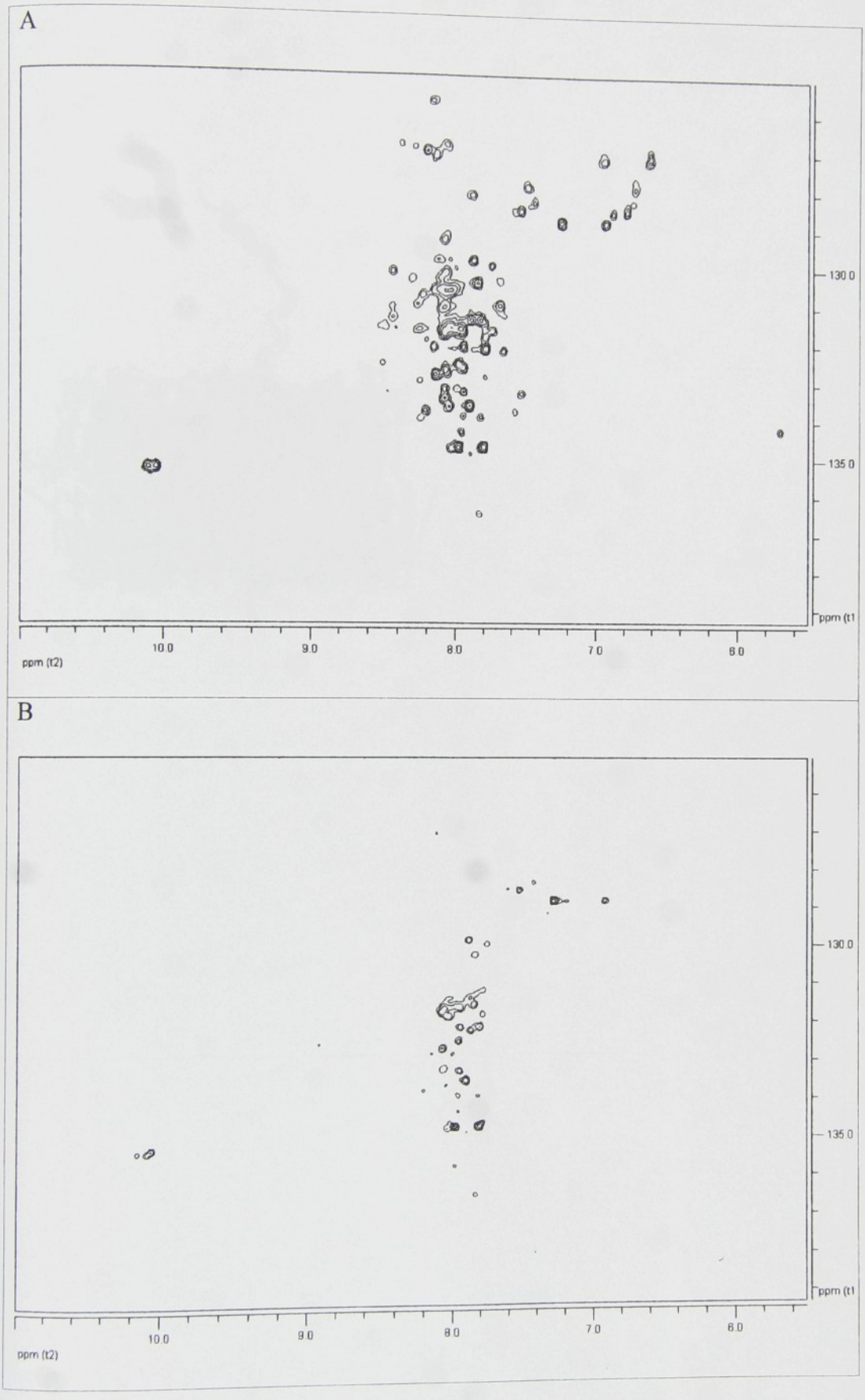
A
130.0
135.0
ppm (t1
10.0
9.0
8.0
7.0
6.0
ppm (t2)
B
130.0
135.0
ppm (t1
10.0
9.0
8.0
7.0
6.0
ppm (t2)

Figure 4a

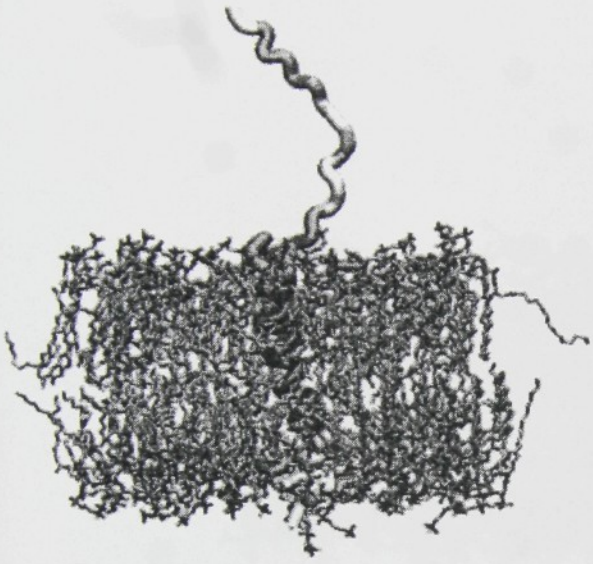

Figure 4b

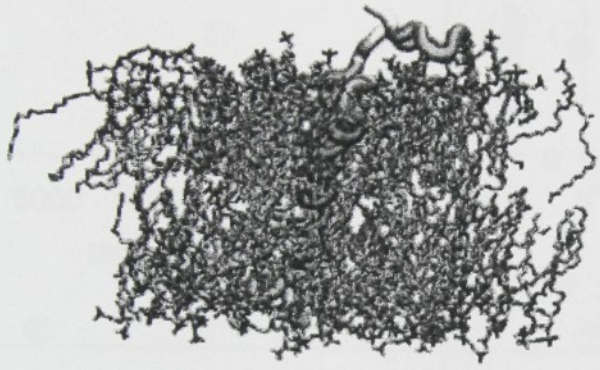

Figure 5a

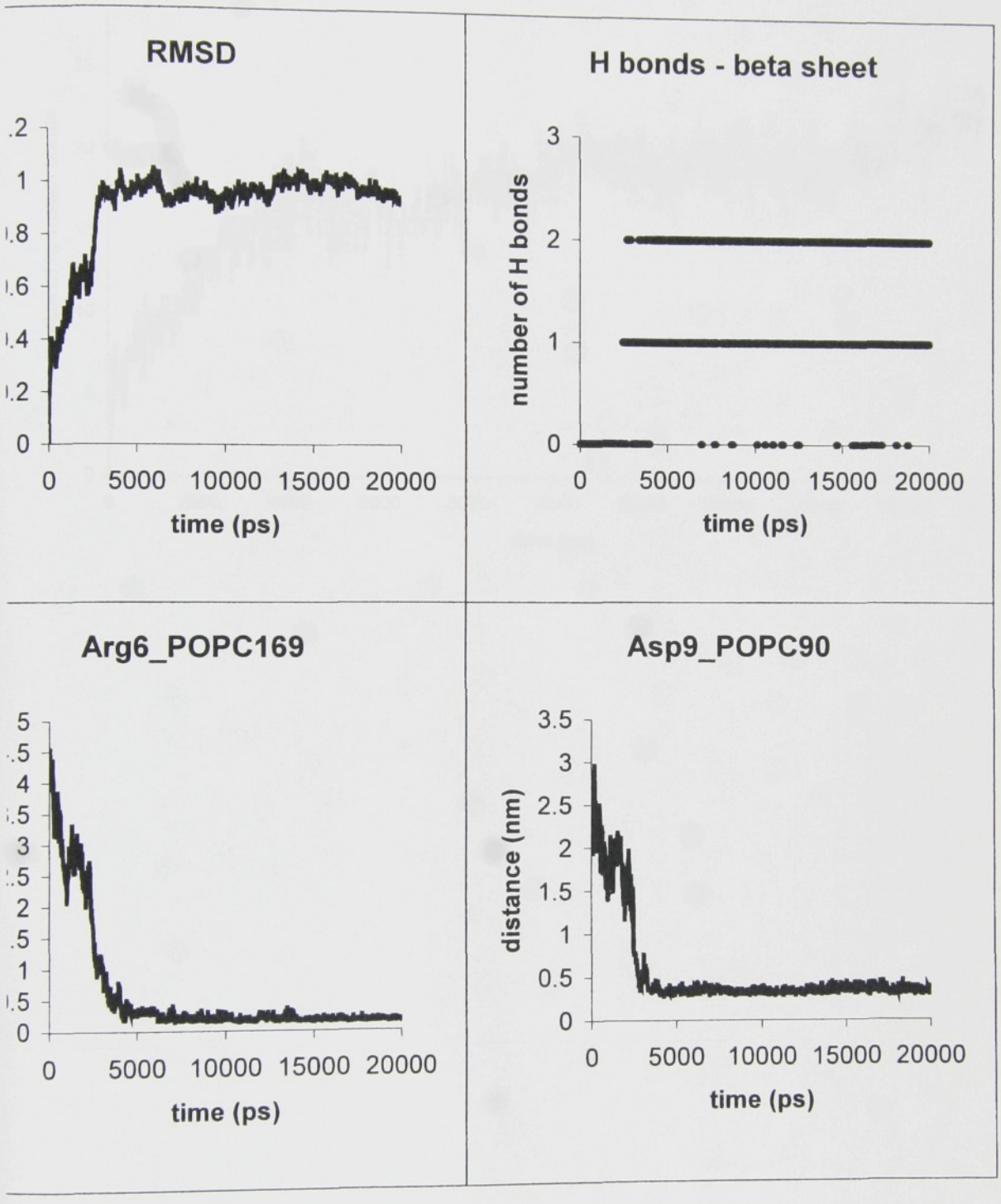
RMSD
.2
1
.8
.6
.4
.2
0
0
5000
10000
15000
20000
time (ps)
H bonds - beta sheet
number of H bonds
3
2
1
0
0
5000
10000
15000
20000
time (ps)
Arg6_POPC169
5
.5
4
.5
3
.5
2
.5
1
.5
0
0
5000
10000
15000
20000
time (ps)
Asp9_POPC90
distance (nm)
3.5
3
2.5
2
1.5
1
0.5
0
0
5000
10000
15000
20000
time (ps)

Figure 5b

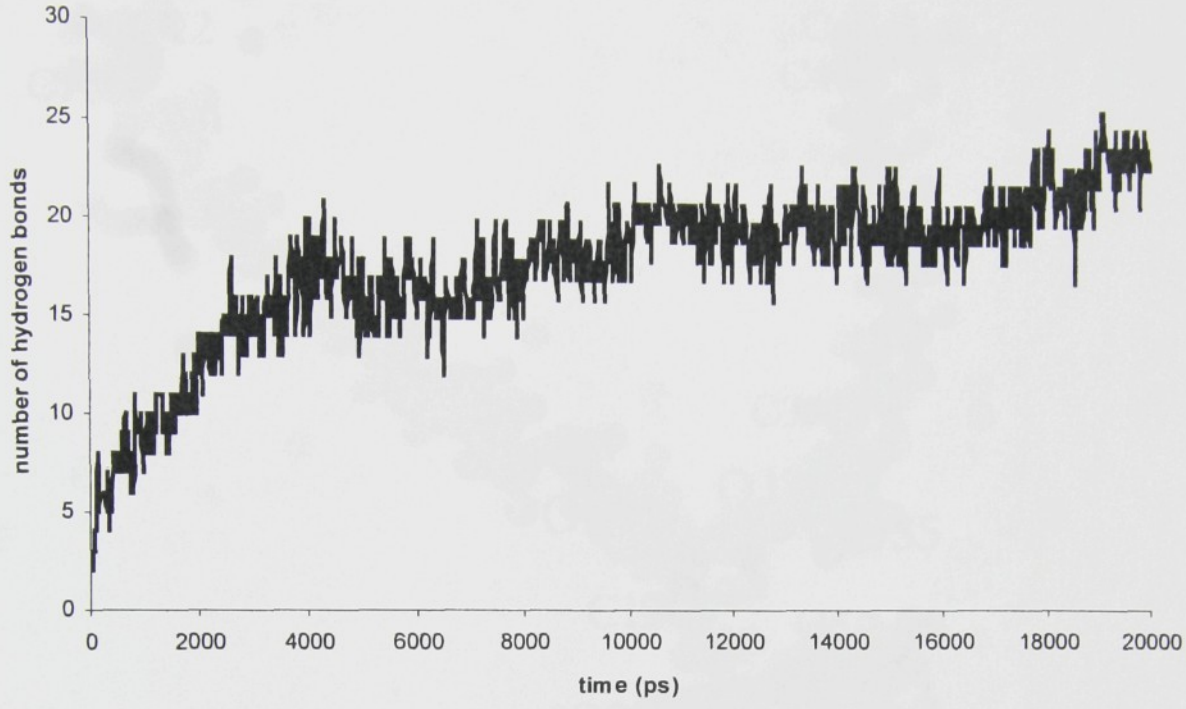
number of hydrogen bonds
0
5
10
15
20
25
30
0
2000
4000
6000
8000
10000
12000
14000
16000
18000
20000
time (ps)

Fig. 6